

主論文

**Palladium-Catalyzed Direct Arylation of C–H and O–H Bonds with
Aryl Halides**

(パラジウム触媒とアリールハライドを用いた C–H/O–H 結合直接
アリール化反応の開発)

Hiroyuki Kitano
Nagoya University
2024 年 3 月

Preface

The studies presented in this thesis have been carried out under the direction of Professor Kenichiro Itami at Institute of Transformative Bio-Molecules (WPI-ITbM), Nagoya University between July 2016 and June 2018. The studies are concerned with the development of Palladium-Catalyzed Direct Arylation of C–H and O–H Bonds with Aryl Halides.

First and foremost, I would like to express my heartfelt and utmost gratitude to Professor Kenichiro Itami for providing great opportunity, excellent support, valuable suggestions, and encouragement throughout this work. I would like to express my sincerest appreciation to Associate Professor Hideto Ito for his kind guidance, constructive advice, technical assistance, and enthusiasm.

I am deeply grateful to Team Leader Shinya Hagihara (RIKEN) for his guidance, daily discussions, precious support. I also show my significant acknowledgement to Associate Professor Kei Murakami (Kwansei Gakuin University), Associate Professor Ayato Sato, Associate Professor Yasutomo Segawa (Institute for Molecular Science), Associate Professor Akiko Yagi, Research Associate Takehisa Maekawa (Academia Sinica) for their insightful comments, helpful discussions, and encouragements.

I would like to express my sincere thanks also to Professor Hirokazu Kawagishi (Shizuoka University), Associate Professor Jae-Hoon Choe (Shizuoka University), Professor Toshiyuki Kan (University of Shizuoka) for wonderful collaboration on the fairy chemical project.

I cannot express much thanks enough to Dr. Shuya Yamada, Dr. Wataru Matsuoka, Dr. Ayaka Ueda, Dr. Shusei Fujiki, Dr. Kou P. Kawahara, Dr. Ryosuke Takise, Dr. Shin Suzuki for all experimental supports and beneficial suggestion. This thesis cannot exist without their contribution.

My especial appreciation goes to Ms. Yui Ueyama, Ms. Rika Kato, Ms. Nanako Kato for their kind support and great hospitality throughout my long-term laboratory life.

I would like to offer my special gratitude to Mr. Toshiaki Noda, Ms. Hideko Natsume and Mr.

Hisakazu Okamoto for their excellent work on fixing and devising scientific glasswares.

I am deeply grateful to Professor Susumu Saito, Professor Shigehiro Yamaguchi and Professor Hiroshi Shinokubo for their guidance and encouragement.

I heartily thank

Dr. Takahiro Uehara	Mr. Jumpei Suzuki	Ms. Sojung Kim
Dr. Tetsushi Yoshidomi	Ms. Wakana Hayashi	Dr. Yuanming Li
Dr. Takao Fujikawa	Dr. Yip Shu Jan (Alicia)	Mr. Ryan Fan
Dr. Hiroki Kondo	Mr. Kaoru Arisue	Mr. Matthew Robinson
Dr. Yutaro Saito	Dr. Atsushi Kinoshita	Dr. Phillippa Cooper
Dr. Masahiko Yoshimura	Mr. Motonobu Kuwayama	Dr. Chaolumen
Dr. Tsuyoshi Oshima	Mr. Kazuya Kawai	Dr. Maciej Krzeszewski
Dr. Kenta Kato	Ms. Akari Saito	Dr. Takayuki Nakamuro
Dr. Shun Yamashita	Dr. Yota Sakakibara	Dr. Philip Steib
Dr. Kakishi Uno	Mr. Taito Hiraga	Ms. Mizuho Uryu
Dr. Jiao Jiao	Ms. Ayana Mashimo	Ms. Mai Nagase
Dr. Asraa Ziadi	Dr. Michihisa Toya	Mr. Bumpei Maeda
Ms. Mari Shibata	Dr. Tomohiro Fukushima	Ms. Eri Makino
Mr. Keishu Okada	Dr. Levine David Robert	Ms. Kaho Matsushima
Ms. Masako Fushimi	Mr. Ryo Okude	Mr. Hiroki Shudo
Dr. Guillaume Povie	Ms. Leticia Sarah	Mr. Shingo Aoki
Dr. Ryotaro Yamada	Mr. Sho Ishida	Mr. Jake Wilson
Mr. Keiichiro Murai	Dr. Gregory Perry	Dr. Louis Evans
Ms. Eri Suzuki (Eri Ito)	Mr. Motoaki Usui	Dr. Takayuki Nakamuro
Mr. Kazushi Kumazawa	Dr. Satoshi Matsubara	
Mr. Yoshito Koga	Ms. Sakura Miyauchi	

and all alumni of Itami group.

I am deeply grateful to Dr. Yoshiaki Isobe, Dr. Takeo Ishiyama, Dr. Hiroshi Noguchi (Sumitomo Dainippon Pharma Co., Ltd, now at Sumitomo Pharma Co., Ltd) for providing the opportunity to conduct this research. I would also express my heartfelt gratitude to Dr. Katsunori Tsuboi, Dr. Kozo Yoshida, Dr. Shiro Tomoya, Dr. Nobuhisa Fukuda, Dr. Kyoji Ishida, Dr. Yuta Funakoshi, Dr. Yuki Mizukami (Sumitomo Dainippon Pharma Co., Ltd) for their support and encouragements.

Finally, I would like to express my deepest gratitude to my family, Mr. Kissho Kitano, Ms. Haruko Kitano, Ms. Maki Kitano, Mr. Kiichi Kitano, Ms. Anna Kitano for their constant assistance and encouragement.

Hiroyuki Kitano

Institute of Transformative Bio-Molecules (WPI-ITbM)

Nagoya University 2024

Contents

List of Abbreviations	1
General Introduction	4
Chapter 1	27
Discovery of Plant Growth Stimulants by C–H Arylation of 2-Azahypoxanthine	
Chapter 2	83
Annulative π -extension of indoles and pyrroles with diiodobiaryl by palladium catalysis: rapid synthesis of nitrogen-embedded polycyclic aromatic compounds	
Chapter 3	133
Palladium-Catalyzed Esterification of Carboxylic Acids with Aryl Iodides	
Conclusion of this thesis	165
List of Publications	167

Abbreviations

AHX	2-azahypoxanthine
AICA	5-aminoimidazole-4-carboxamide
AOH	2-aza-8-oxohypoxanthine
APEX	annulative π -extension
aq	aqueous solution
Ar	aryl
Ar	aryl
Bn	benzyl
Boc	<i>tert</i> -butoxycarbonyl
Boc	<i>tert</i> -butoxycarbonyl
br	broad
Bz	benzoyl
CAN	ceric ammonium nitrate
cat	catalyst/catalytic
CMD	concerted metallation deprotection
COX	cyclooxygenase
Cy	cyclohexane
d	doublet
dd	doublet of doublets
DFT	density functional theory
DGAT	diacylglycerol acyltransferase1
DMA	dimethylformamide
DMB	2,4-dimethoxybenzyl
DMF	dimethylformamide
DMSO	dimethylsulfoxide
equiv	equivalent(s)
ESI	electrospray ionization
Et	ethyl
FCs	fairly chemicals
GPC	gel permeation chromatography

h	hour(s)
HFIP	hexafluoroisopropanol
HMBC	heteronuclear multiple bond coherence
HMDS	hexamethyldisilazane
HMQC	heteronuclear multiple quantum correlation
HOMO	highest occupied molecular orbital
HRMS	high-resolution mass spectra
HX	hypoxanthine
Hz	hertz
IBn^F	[1,3-bis{(pentafluorophenyl)methyl}- imidazole-2-ylidene)]
ICA	imidazole-4-carboxamide
IMes	1,3-bis(2,4,6-trimethylphenyl)imidazole-2- ylidene
IPr	1,3-bis(2,6-diisopropylphenyl)imidazole-2- ylidene
LUMO	lowest unoccupied molecular orbital
<i>m</i>	meta
m	multiplet
M	molar (mol/L)
Me	methyl
min	minute(s)
MPLC	medium pressure liquid chromatography
MS	molecular sieves
NHC	N-heterocyclic carbene
NMR	nuclear magnetic resonance
Nu	nucleophiles
<i>o</i>	ortho
<i>p</i>	para
Pd/C	Palladium-activated carbon
Ph	phenyl
PivOH	Pivalic acid

PPh₃	triphenylphosphine
ppy	2-phenylpyridinato
PTLC	Preparative thin-layer chromatography
s	singlet
t	triplet
tBu	tert-butyl
td	triplet of doublets
TD-DFT	time-dependent density functional theory
TFE	tetrafluoroethanol
TfOH	trifluoromethanesulfonic acid
THF	tetrahydrofuran
TLC	thin-layer chromatography
UV	ultraviolet
vis	visible
Xan	xanthine
δ	chemical shift (NMR)

General Introduction

Palladium-catalyzed arylation reaction of aryl halides and its applications

An aromatic ring is a general structural motif ubiquitously found in the field of organic electronics, pharmaceuticals, natural products and chemical biology (Figure 1).¹ Generally, introducing aromatic rings into organic molecules can greatly influence their physical properties through elongation of π -conjugated systems, introduction of planarity, and enhancement of intra- and intermolecular CH- π and π - π interactions. These attractive features consequently have prompted a large number of synthetic chemists to discover novel functional aromatic molecules. In fact, the 2014 Orange Book published by Food and Drug Administration (FDA) in the United States reported that a benzene ring is the most frequently contained cyclic structure in the approved drugs.²

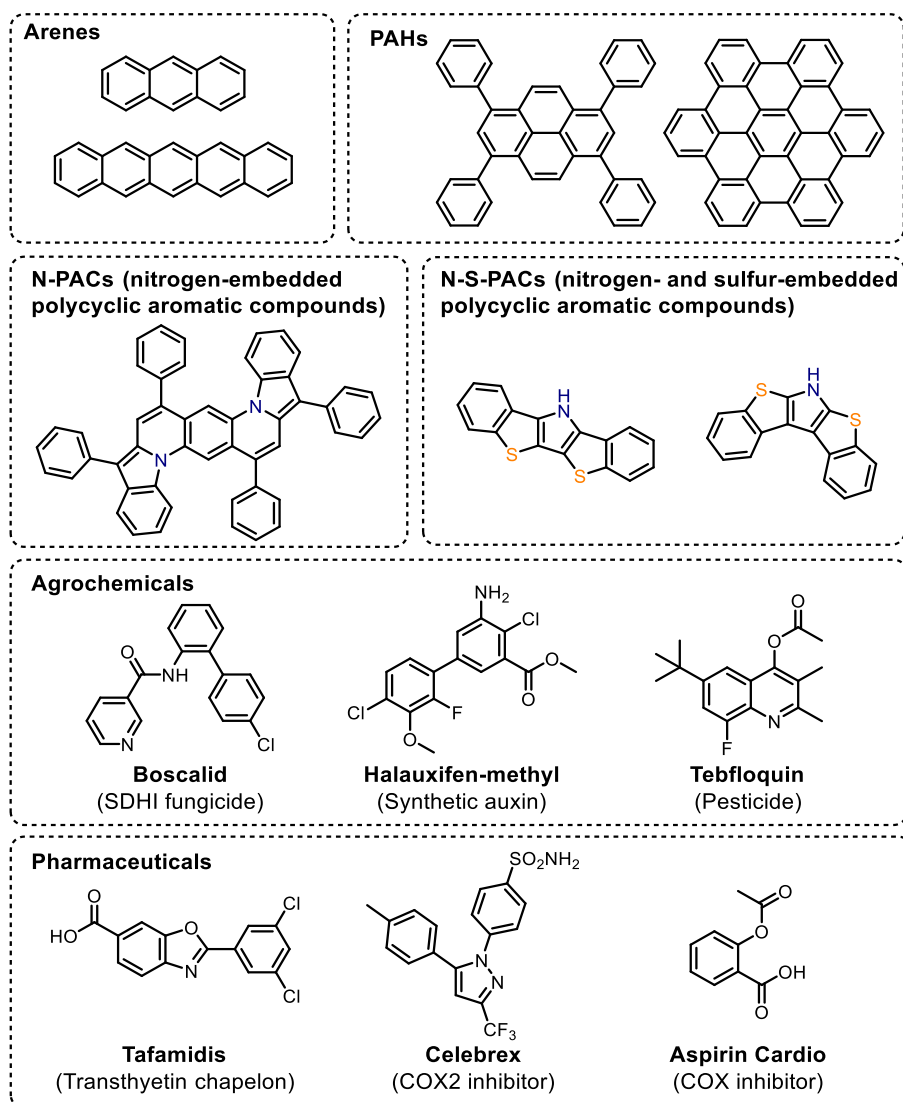


Figure 1. Representative functional aromatic compounds.

Along with the discovery and development of novel functional compounds, the synthetic methodologies for aromatic ring-containing molecules have also been sophisticated with the aim of constructing the desired aromatic rings in a regioselective fashion. As one of pioneering studies, a cross-coupling reaction between aryl Grignard reagents and aryl halides by nickel and palladium catalysts was developed by Kumada, Tamao and Corriu.³ This simple and efficient reaction has encouraged many researchers to apply various nucleophiles into this cross-coupling manifold (Figure 2). Later, catalytic systems applicable to various aryl halides and aryl nucleophiles such as aryl zinc (Negishi coupling),⁴ aryl tin (Migita–Kosugi–Stille coupling),⁵ aryl borane (Suzuki–Miyaura coupling)⁶ and aryl silane (Hiyama coupling)⁷ have been developed by many researchers.⁸

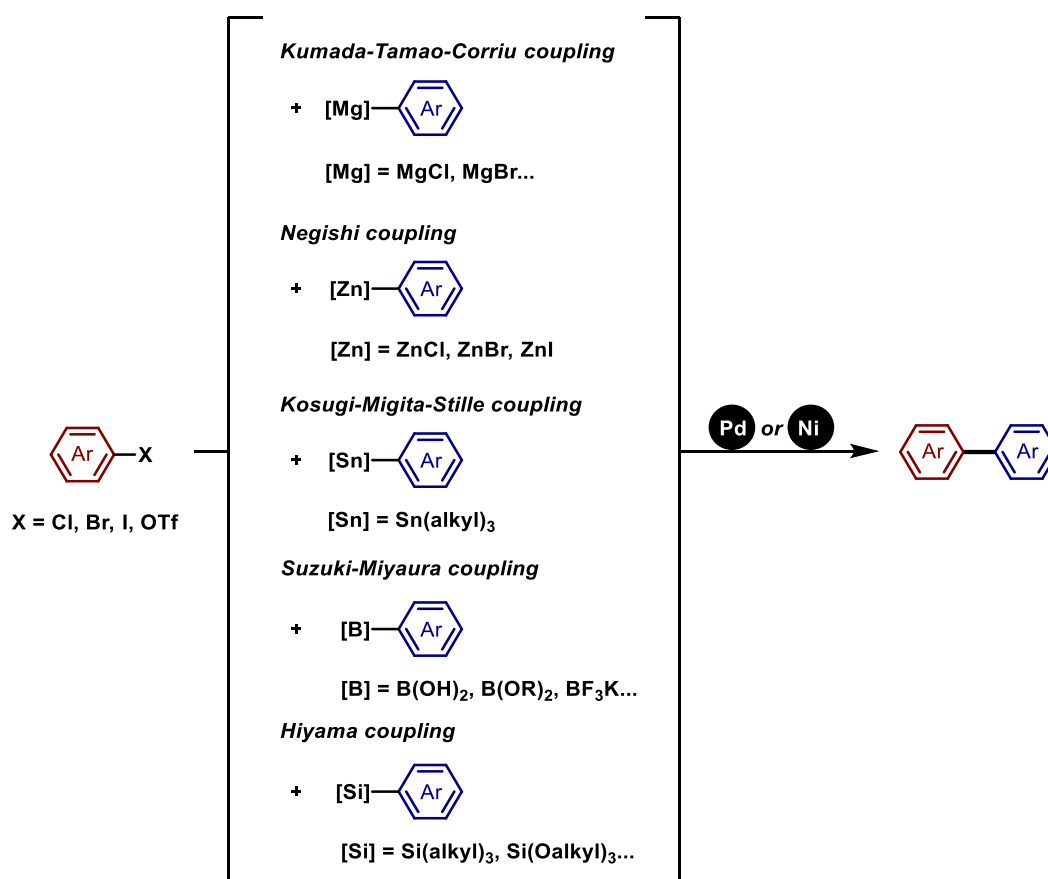


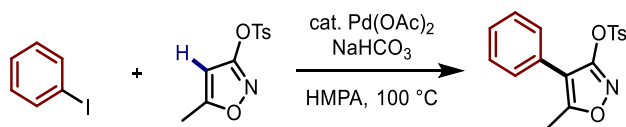
Figure 2. Representative Pd/Ni-catalyzed cross-coupling.

Various modes of transformation that have built up in this trend have contributed significantly in the area of pharmaceutical synthesis, as evidenced by the analysis of reactions used in the process chemistry routes of 128 drug candidate molecules from AstraZeneca, GlaxoSmithKline, and Pfizer.⁹ The number of reactions used for the synthesis of 128 compounds was 1039, of which

116 (11%) were related to C–C bond formation. This is the fourth most classified reaction after "alkylation and allylation of heteroatoms", "deprotection" and "acylation". In addition, 22% of the reactions of C–C bond formation are reactions using palladium catalyst, most of which are Suzuki couplings and related reactions such as Heck reactions and Sonogashira couplings. This statistical analysis shows the importance of palladium-catalyzed C–C bond formation reaction in drug manufacturing. Moreover, it is not hard to imagine that palladium-catalyzed coupling reactions are more important in early drug discovery, as convergent synthetic methods are preferred for structure-activity relationship studies.¹⁰

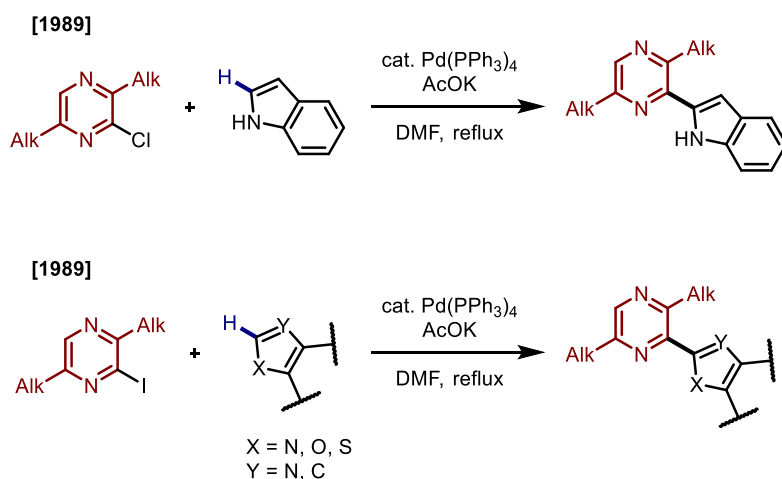
Emergence of C–H arylation

In recent decades, palladium-catalyzed C–H arylation reaction with aryl halides has been actively studied as a more straightforward reaction with less waste. One of early examples in palladium-catalyzed C–H arylation of aryl halide was disclosed by Nakamura *et al.* in 1982, where intermolecular C–H phenylation of 5-methylisoxazole with iodobenzene preferentially proceeded at C4-position in the presence of Pd(OAc)₂ as a catalyst (Scheme 1).¹¹



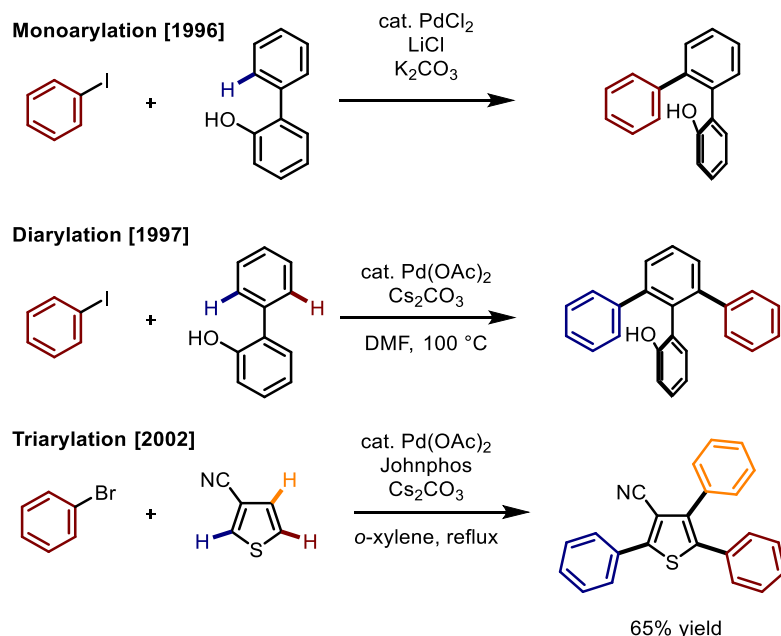
Scheme 1. Pd-catalyzed C–H arylation reaction reported by Nakamura *et al.*

In 1985, Ohta *et al.* discovered palladium-catalyzed C–H arylation of chloropyrazines with indoles (Scheme 2).¹² Starting with the reaction with indole, they demonstrated that the reaction can be applied to substrates such as furan, thiophene, pyrrole, benzofuran, benzothiophene, oxazole, thiazole, imidazole, benzooxazole, and benzothiazole.¹³



Scheme 2. Pd-catalyzed C–H arylation reaction reported by Ohta *et al.*

In 1996, Miura and co-workers reported the observation of a palladium-catalyzed C–H arylation reaction between 2-phenylphenol and iodobenzene (Scheme 3).¹⁴ Inspired by this transformation, they reported the regioselective mono-, di-arylation of 2-phenylphenol in the presence of catalytic Pd(OAc)₂ and Cs₂CO₃ as a base.¹⁵ Later on, they reported the triarylation of mono-substituted thiophenes.¹⁶



Scheme 3. Pd-catalyzed C–H mono-, di-, tri-arylation reaction reported by Miura *et al.*

Recently, it has become possible to perform the C–H arylation of electron deficient arenes. Fagnou and co-workers reported C–H arylation of electron-deficient perfluorobenzenes with aryl

halides through palladium catalysis (Figure 3a).¹⁷ It was a great surprise that perfluoroarene with no particular directing group reacts easily. Based on the results of a series of studies, they proposed that this reaction occurs by a concerted reaction mechanism in which the deprotonation of C–H occurs through abstracting by the coordinating carboxylate ligand on the palladium along with simultaneous metalation (Figure 3b). This reaction mechanism via concerted six-membered ring transition state was also proposed by Echavarren¹⁸ and now named as Concerted Metallation-Depronation (CMD) mechanism.¹⁹ Owing to the significant dedication to expand possible aromatic substrates in the palladium-catalyzed C–H arylation chemistry, current methodologies tolerate not only electronically biased arenes but also simple benzene derivatives as applicable substrates (Figure 3c).²⁰

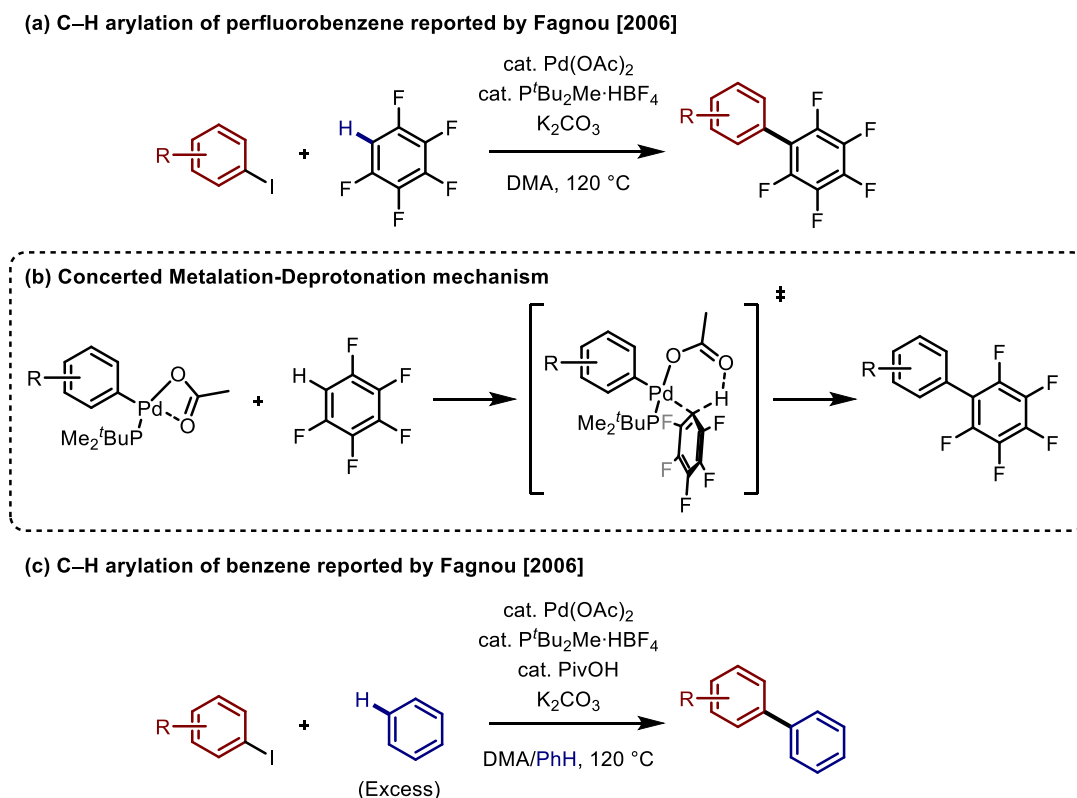
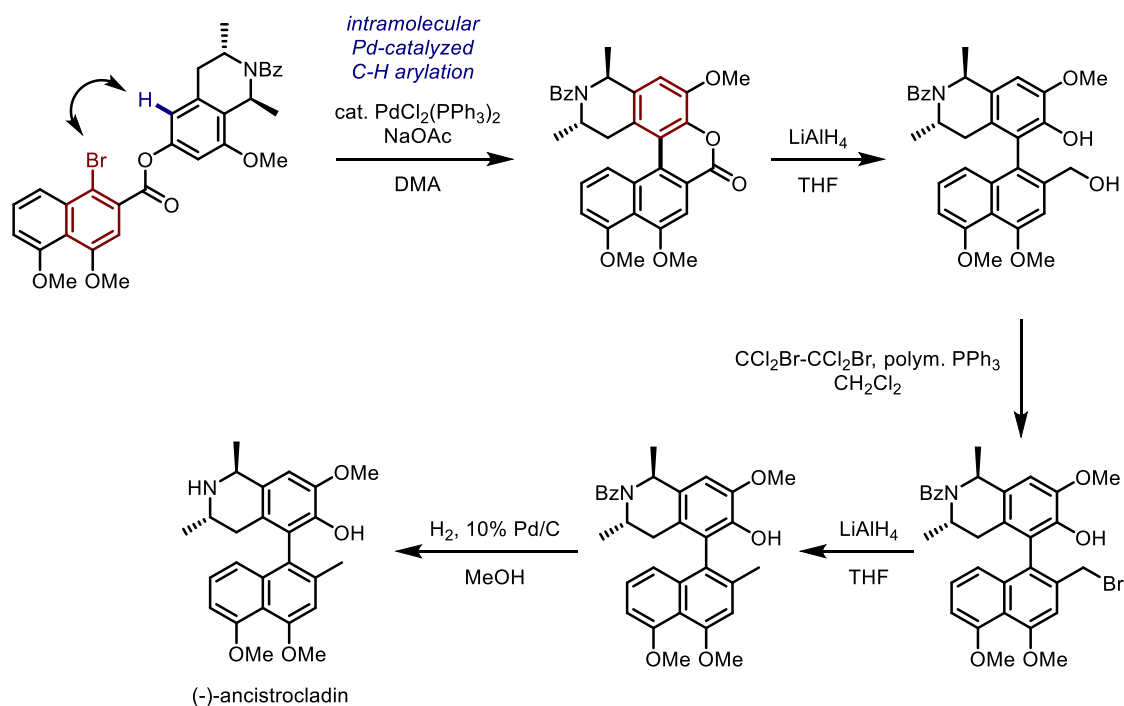


Figure 3. (a) C–H arylation of perfluorobenzene. (b) Reaction mechanism of concerted metalation-deprotonation mechanism. (c) C–H arylation of benzene.

A representative application of palladium-catalyzed direct arylation method is the natural product synthesis.²¹ As an early example, Bringmann and co-workers reported the total synthesis of (–)-ancistrocladin employing palladium-catalyzed intramolecular C–H arylation as a key

reaction (Scheme 4).²² The precisely designed coupling precursor bearing bromonaphthalene moiety underwent the intramolecular ring-closing C–H arylation in the presence of PdCl₂(PPh₃)₂ catalyst and stoichiometric NaOAc in dimethylacetamide (DMA) to afford the corresponding lactone derivative. Then, the obtained lactone intermediate was converted to the target (–)-ancistrocladin through four-step reactions.



There is also a large benefit using C–H arylation reactions in the phase searching for physiologically active substances. For example, in 2015, Itami, Yoshimura, Irle and co-workers reported the synthesis of molecules that modulate mammalian circadian clock by late-stage Pd-catalyzed C–H arylations (Figure 4).²³ The molecule KL001 was initially found as a period lengthening molecule for mammalian circadian clock that stabilizes CRY protein. Subsequently, SAR studies revealed that GO061, a derivative where the furan moiety was converted to a thiophene retained the activity. Then, by employing palladium-catalyzed C–H arylation with iodoarenes or arylboronic acids, successful conversion of GO061 into various thiophene-terminus-arylated derivatives was achieved. Interestingly, the regioselectivity of C4- and C5-positions on thiophene was completely switched by the choice of arylating agents. As a result, the structure-activity relationship of period lengthening and shortening was thoroughly investigated with diverse arylated derivatives, which was enabled by nature of late-stage functionalization of

C–H arylation.

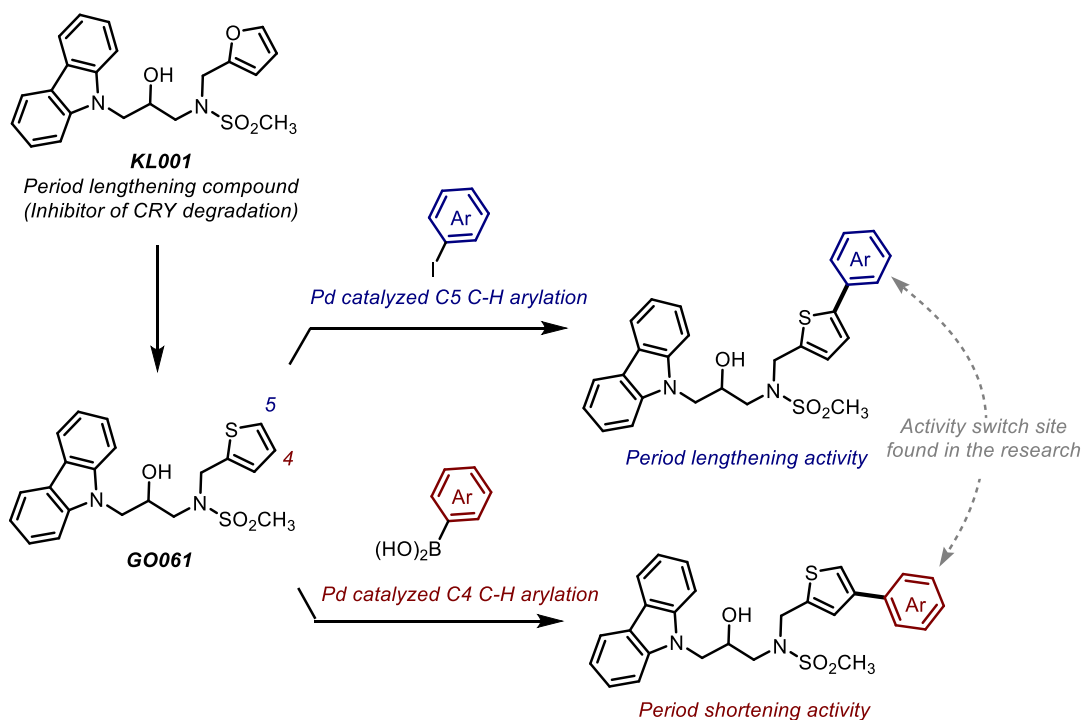
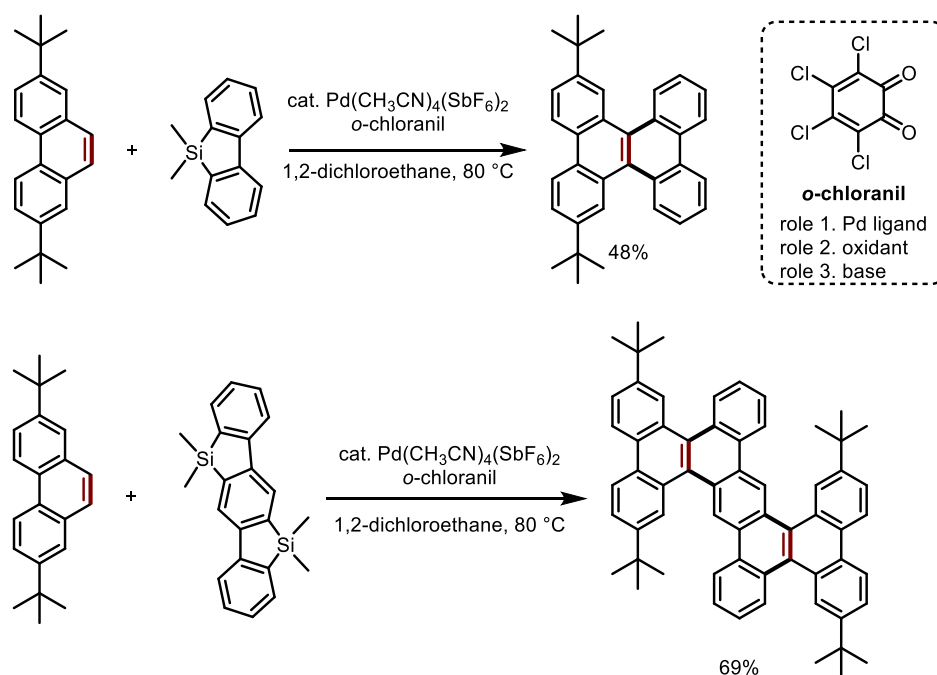


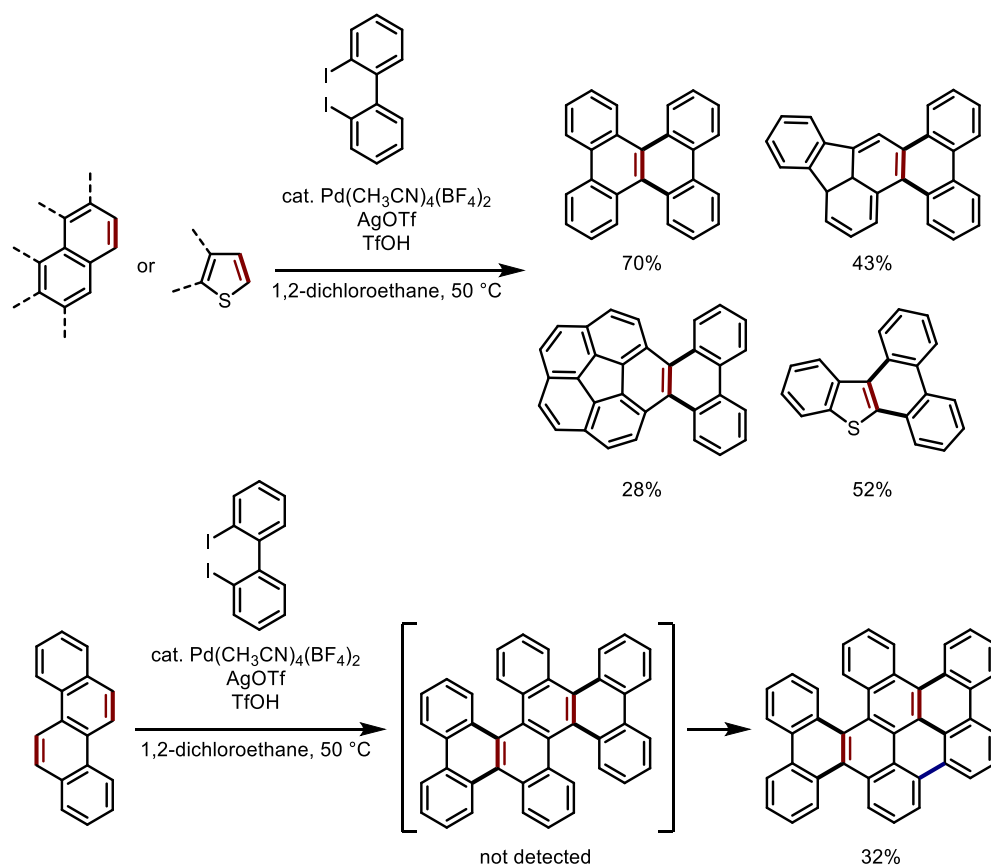
Figure 4. Derivatization of KL001 by late-stage Pd-catalyzed C–H arylations.

As another example that utilizes palladium-catalyzed C–H arylation in the synthesis of useful compounds, annulative π -extension (APEX) reaction has recently emerged for synthesizing polycyclic aromatic system.²⁴ APEX reaction is one of reaction concepts that implements one-step or stepwise aromatic ring extension from unfunctionalized arene substrate to further π -extended fused aromatic ring. Therefore, the APEX reaction involves inter- and intramolecular C–H bond functionalizations. For example, Itami, Ito and co-workers disclosed the first example of *K*-region (a convex armchair edge of PAH)-selective single step APEX reaction of PAHs using dibenzosiloles as π -extending agents under palladium catalysis (Scheme 5).²⁵ The Pd(CH₃CN)₄(SbF₆)₂/*o*-chloranil catalytic system is essential to facilitate APEX reaction of phenanthrenes to afford the corresponding dibenzo[*g,p*]chrysenes. This APEX reaction proceeds with exclusive *K*-region selectivity, and the following mechanistic investigation with computational DFT calculations elucidated the mechanism of C–H arylation, origin of regioselectivity and the three roles of *o*-chloranil as a ligand, stoichiometric oxidant and base through the transformation.²⁶



Scheme 5. *K*-region selective single-step APEX reaction of phenanthrene using dibenzosiloles.

Later, Itami, Ito and co-workers also developed an alternative palladium-catalyzed APEX reaction using diiodobiaryl compound as the π -extending reagent (Scheme 7).²⁷ The extensive conditions screening revealed that the combination of cationic $\text{Pd}(\text{CH}_3\text{CN})_4(\text{BF}_4)_2$, silver pivalate and triflic acid realized double C–H arylation of various unfunctionalized polycyclic aromatics such as phenanthrene, corannulene, fluoranthene and thiophene derivatives to afford π -extended molecules efficiently. Furthermore, when chrysene was used as a template PAH, two-fold APEX followed by Scholl-type cyclodehydrogenation occurred, yielding highly fused helical nanographene.



Scheme 6. Single-step APEX reaction of various polycyclic compounds using diiodobiphenyl.

Palladium-catalyzed multiple C–H arylations of nitrogen-containing heteroarenes with aryl halides

As mentioned earlier, the multiple C–H arylation of thiophenes, *i.e.* Pd-catalyzed APEX reaction at C2 and C3 positions has been developed so far (Schemes 3 and 6), but multiple C–H arylation (APEX reaction) of pyrroles and indoles in a single step was difficult. The reason for the difficulty is that the C2 and C3 positions of indole and pyrrole have different electronic characters, and thus it is difficult to achieve simultaneous arylations at C2 and C3 positions under same reaction conditions.

In 2007, a Pd-catalyzed C2-selective C–H arylation of indoles with aryl iodides was reported by Sames and co-workers (Figure 5).²⁸ The reaction of indole and iodobenzene with Pd(OAc)₂, PPh₃, and CsOAc selectively occurs at the C2 position of indoles. In this report, C2-arylated indole was preferentially formed rather than C3-arylated indole, and diarylated product was not reported. These facts imply that this catalytic system is not appropriate for C3-arylation nor double arylation such as APEX reaction. At about a same time of report by Sames, a C3-selective

C–H arylation of indoles with aryl bromides was reported in 2007 by He, Zhang and co-workers (Figure 6).²⁹ The reaction conditions reported by He, which employs aryl bromide and potassium carbonate as a base, are different from those in Sames' reaction. The results also showed a decrease in the yield of C3-arylated product when an electron-withdrawing group was introduced on the benzene ring of indole. From these facts and other mechanistic investigations, He, Zhang and co-workers inferred that the reaction can proceed through electrophilic substitution. In addition, there was no information about formation of diarylated product at C2 and C3 positions, which suggests that the catalytic system is also not suitable for double arylation and APEX reaction.

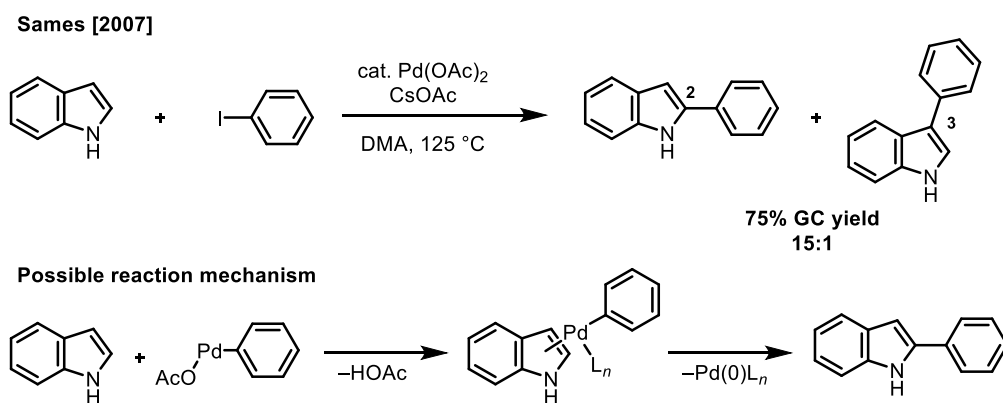


Figure 5. Pd-catalyzed C2-selective C–H arylation of indole reported by Sames.

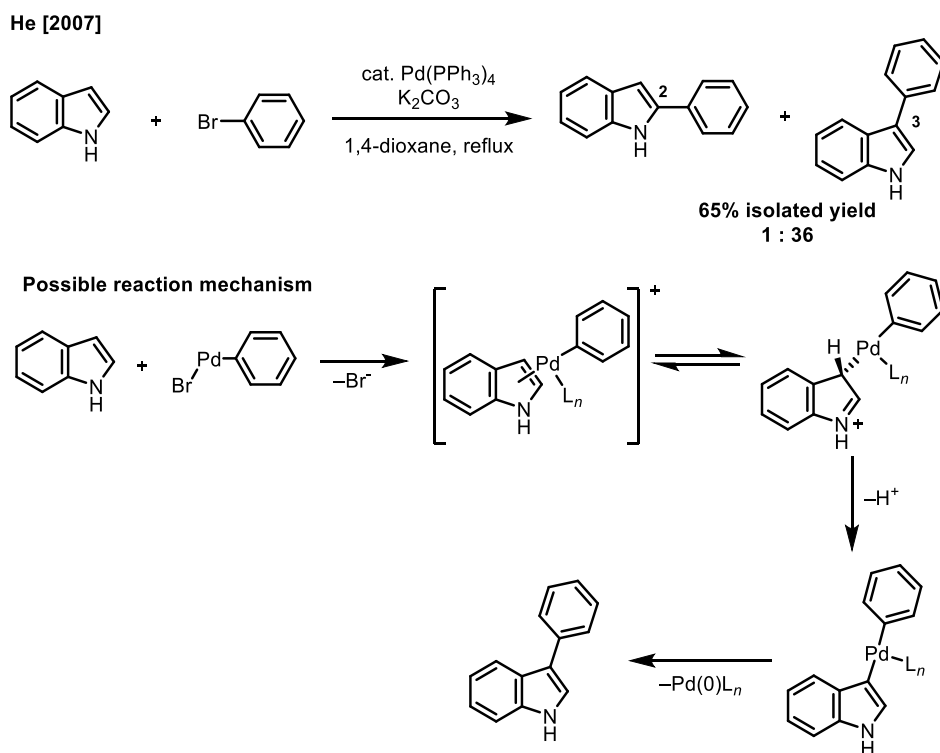
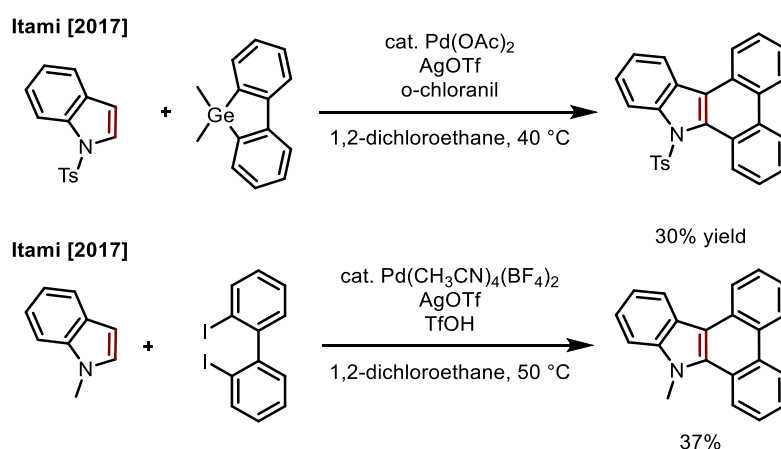


Figure 6. Pd-catalyzed C3-selective C–H arylation of indole reported by He.

To achieve diarylation at the C2 and C3 positions of indoles, development of a novel catalytic system as well as reaction conditions is needed. In particular, the choice of base and ligand on palladium would be important to overcome reactivity barriers and steric hindrance. A part from this, developing an annulative arylation reagent is also one of effective strategies for obtaining multi-arylated heteroarenes because once C–H arylation occurs at C2 or C3 positions of indoles/pyrroles, successive intramolecular C–H arylations at C3 or C2 positions are thought to be easily achieved. From these viewpoints, the APEX reaction is one of the few methods that can efficiently perform multi-arylation of pyrroles/indoles. In fact, the palladium-catalyzed APEX reactions of *N*-tosylindole and *N*-methylindole were demonstrated using dibenzogermole and diiodobiphenyl in the author's laboratory as peripheral demonstrations in APEX reaction of PAHs (Scheme 7).^{27,30} However, the reaction efficiency was not sufficient and reaction conditions were also not modified for heteroarenes, thus resulting in low yields of products and only three successful substrate examples. It could be attributed to decomposition of electron-rich heteroarenes by highly oxidative and/or acidic conditions using Pd/*o*-chloranil or Pd/AgOTf/TfOH. Thus, more mild reaction conditions and catalytic system will be needed for achieving APEX reaction of electron-rich heteroarenes such as indoles and pyrroles.



Scheme 7. Single-step APEX reaction of indoles using dibenzogermole and diiodobiphenyl.

Palladium-catalyzed C–H arylations of azoles with aryl halides

The difficulty of C–H arylation reaction varies greatly depending on the kind of heteroarenes. 1,3-Azoles such as *N*-methylbenzimidazole, benzothiazole, benzoxazole, and benzothiophene exhibit different reactivities toward direct arylation when these substrates are subjected to typical C–H arylation conditions with Pd catalyst and iodobenzene (Figure 7).³¹ The reactions proceed well with benzoxazole and benzothiophene. On the other hand, the reactions with benzothiophenes and benzimidazoles do not proceed well. These differences are caused by the different acidities of the C2 hydrogen atoms which are highly affected by surrounding heteroatoms.

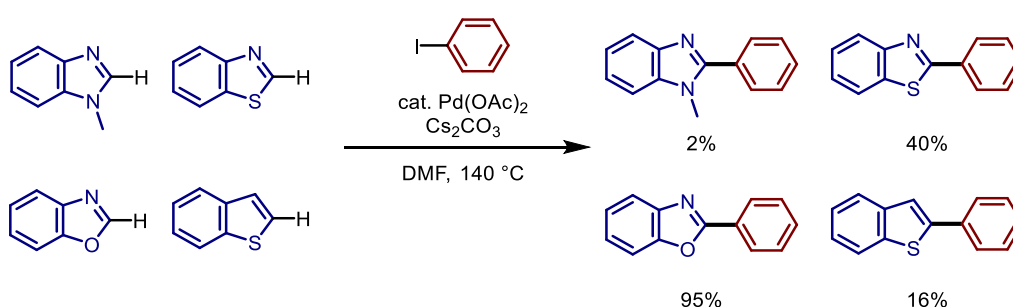


Figure 7. Pd-catalyzed C–H arylation of benzoazoles with iodobenzene.

To achieve direct arylation of benzothiophenes and benzimidazoles, Miura and co-workers found that the addition of copper salts is effective. The reactions of benzimidazole and benzothiazole, which give only 2% and 40% of the desired product under the conditions shown in Figure 8, were improved by the addition of a copper salt (Figure 8). Miura and co-workers

hypothesized that the copper cation of the salt coordinates to the heteroatoms on azoles can reduce the electron density of azoles, and thus resulting in increased acidities at C2 positions. The activation of C–H bonds by copper cation was also suggested by Gorlesky with DFT calculations (Figure 9).³² Calculating the activation free energy for the reaction through CMD mechanism with palladium without copper salts, the most reactive C–H bond to deprotonate is found to be the C5 position. On the other hand, when a copper salt is included in the calculation, the activation free energy of deprotonation of the C2 position decreases and becomes the most reactive site for deprotonative palladation.

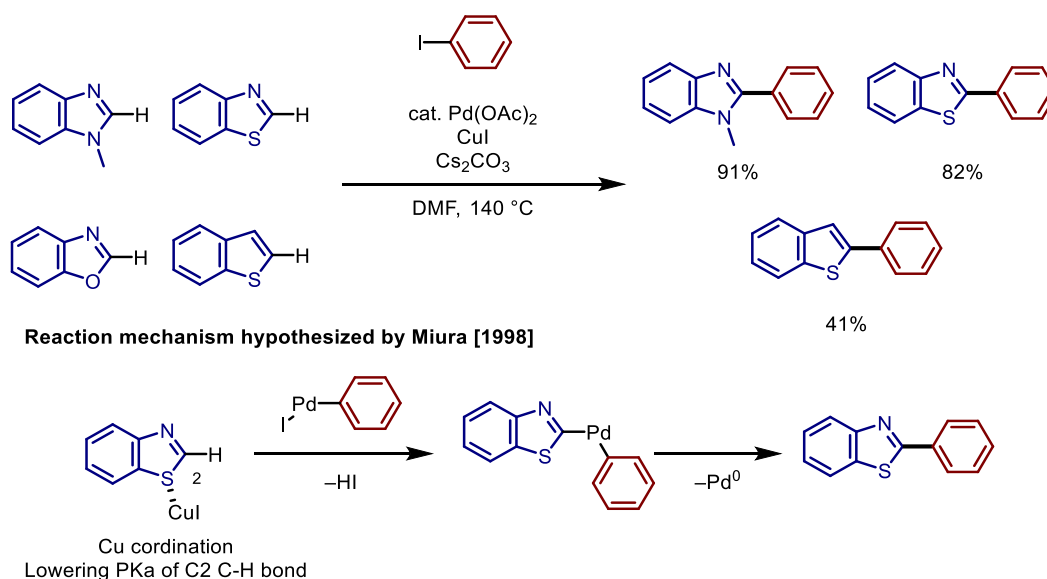


Figure 8. The use of copper iodide in Pd-catalyzed C–H arylation of benzoazoles with iodobenzene.

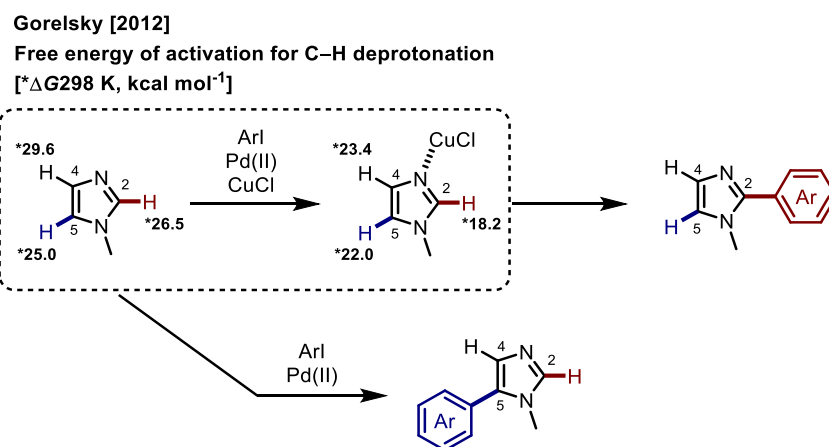


Figure 9. Free energy of activation for deprotonation of the C2 position on *N*-methylimidazole.

Functional group tolerability must also be considered for achieving efficient direct arylation of azoles. For example, C2 arylation reactions of imidazoles containing amide/imide/urea in their structures are very rare and difficult to perform. In addition to the inherent low reactivity in the C2 positions of imidazoles, coordination of electron-rich amide moiety to palladium catalyst can inhibit catalytic activity and turnover. Furthermore, relatively high temperature is required for the direct arylation of functional imidazole derivatives, which can degrade the substrate.³³ An example of C2 arylation reactions of imidazoles using Pd/Cu catalysis to complex structures is the synthesis of arylated xanthine derivatives by Hong *et al.*³⁴ At that time, the arylation reaction, under typical reaction conditions using Pd(OAc)₂, PivOH, and K₂CO₃ in DMF, the reaction did not proceed (Table 1, Entry 1). However, in the presence of a copper salt, the reaction progressed (Entry 2). Although several direct arylations of imidazoles with CuI have been achieved, substrates are still limited to simple structures having less or no functional group. There is still high demand to expand the applicable substrate scope having various functional groups which are very important for preparing complex molecules such as natural products and pharmaceuticals.

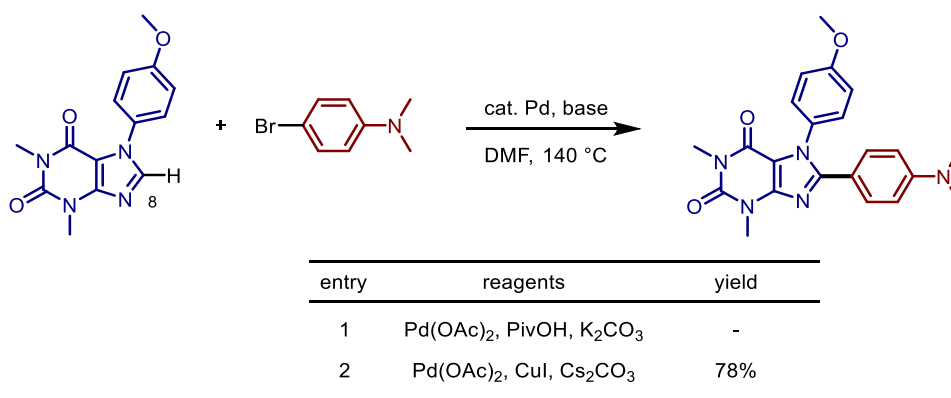


Table 1. Direct C–H arylation of xanthine

Palladium-catalyzed arylations of carboxylic acids with aryl halides

Next to the development of palladium chemistry toward C–C bond formation, arylation of N–H and O–H bonds with aryl halides has also been well studied. In 1995, Buchwald and Hartwig independently found the palladium-catalyzed intermolecular arylation of amine N–H bonds with aryl bromides in the presence of alkoxide or silylamide as a base (Figure 10).³⁵ While Ullmann–Goldberg reaction³⁶ using copper reagents was widely used for amination of aryl halides before 1995, the newly discovered palladium-catalyzed amination rapidly became popular because of its wider substrate scope even under milder conditions.³⁷

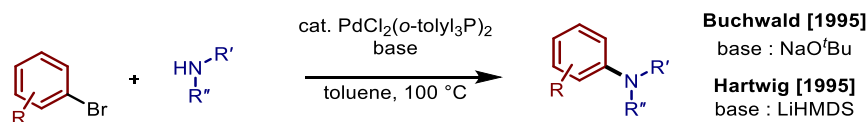


Figure 10. Pd-catalyzed N–H arylation reaction reported by Buchwald and Hartwig.

The discovery of new transformation has opened chemists' eyes and gave rational insights into the construction of catalytic systems that enable the heteroatom-arylation of amide, sulfonamides, alcohols, thiols and so on (Figure 11).³⁸⁻⁴⁰ Each coupling reaction is accomplished by finding the optimal conditions in terms of solvent, reaction temperature and especially ligands. The monodentate biarylphosphines (Buchwald ligands)⁴¹ with various substituents found in a series of studies allow a wide variety of couplings regardless of the nucleophilicity of the heteroatom.

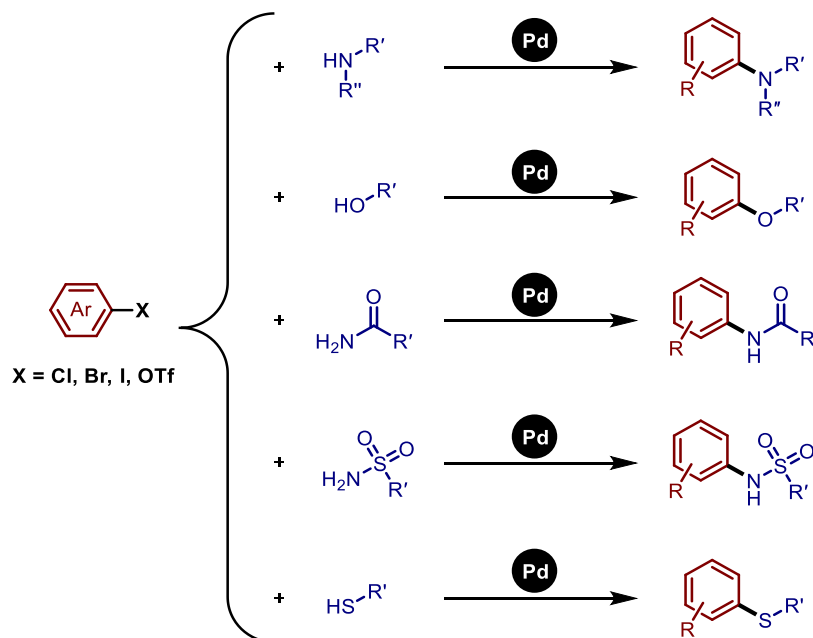


Figure 11. Representative Pd-catalyzed heteroatom-arylation.

However, in the palladium-catalyzed cross-coupling reactions, there are still challenging transformations that have still remained undeveloped. One of them represents the cross-coupling between aryl halides and carboxylic acids as nucleophiles to affect C_{aryl}–O_{acyl} bond formation affording aryl esters (Figure 12a). From a synthetic aspect, this transformation is complemented by O_{aryl}–C_{acyl} bond formation such as the condensation reaction of carboxyl acids and those derivatives with arens⁴², but the transformation involved in C_{aryl}–O_{acyl} bond formation has hardly been investigated in terms of both synthetic chemistry and organometallic chemistry. This is easily rationalized by following two assumptions: 1) carboxylate has a low nucleophilicity so that

it tends to deviate from Pd even if its coordinated (Figure 12b), 2) reductive elimination of Ar-OCOR from Ar-Pd-OCOR is less likely to occur in the Pd-complex having cation-coordinated κ^1 -carboxylate.⁴³ In addition, the aryl-palladium-carboxylate (Ar-Pd-OCOR) intermediate is known to act as an active species, and preferentially induces the C-H activation through CMD pathway rather than the reductive elimination of aryl carboxylate (Ar-OCOR), affording diaryl Pd species (Ar-Pd-Ar') followed by biaryls (Ar-Ar') (Figure 12c).¹⁹ Even in the related metal-catalyzed reactions *in situ*-forming aryl metal carboxylate (Ar-M-OCOR), C_{aryl}-O_{acyl} bond in Ar-OCOR is easily cleaved by oxidative addition of electron-rich low-valent metal such as nickel(0) (Figure 12d).⁴⁴ This implies the reductive elimination forming Ar-OCOR is quite challenging compared to other elementary steps. In fact, there are only few reports achieving Ar-OCOR formation through reductive elimination.⁴⁵ However, simple palladium-catalyzed O-H arylation of carboxylic acids with aryl halides has remained undeveloped, when we started the research in 2016 (Figure 12a).⁴⁶ Therefore, the novel synthetic strategy including reasonable design or selection of catalysts and ligands are demanded toward achieving such a transformation.

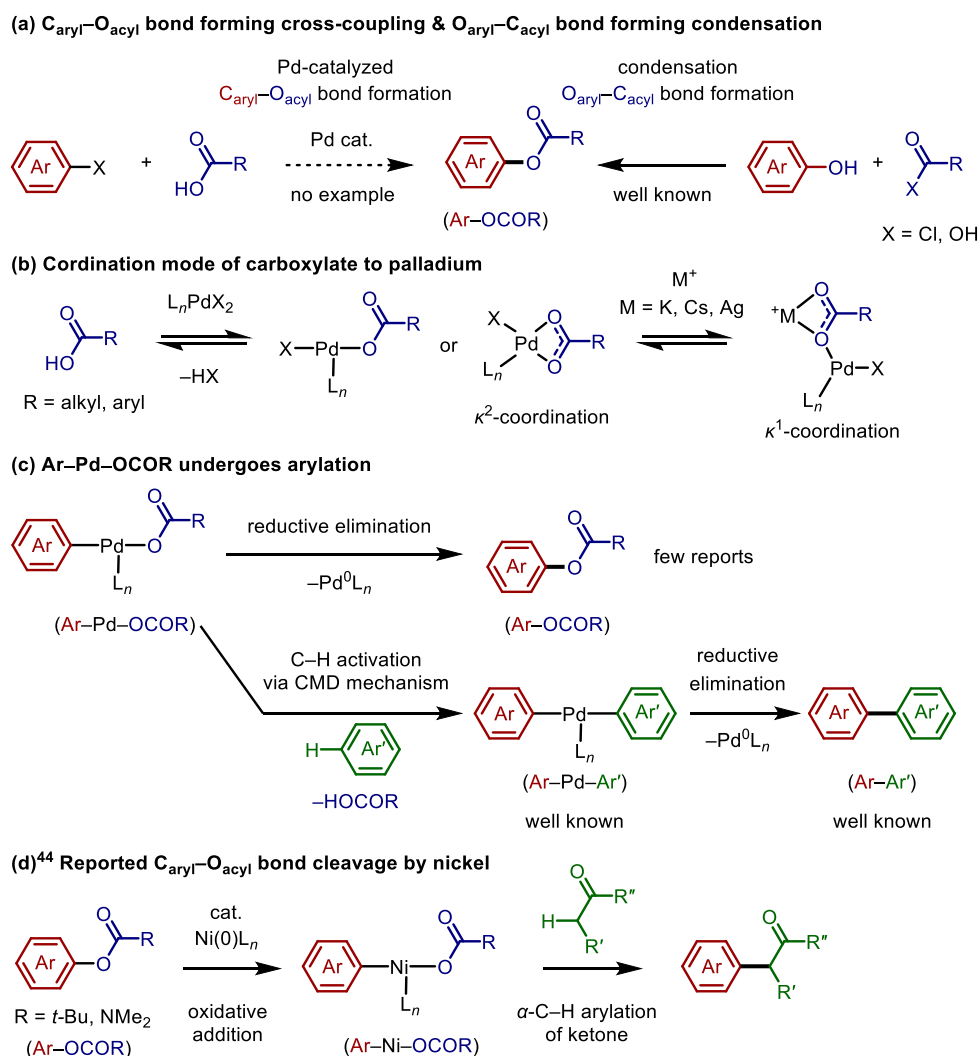


Figure 12. (a) $C_{\text{aryl}}-O_{\text{acyl}}$ bond formation and $O_{\text{aryl}}-C_{\text{acyl}}$ bond formation. (b) Coordination mode of carboxylate to palladium. (c) $Ar-Pd-OCOR$ undergoes arylation. (d) Example of $C_{\text{aryl}}-O_{\text{acyl}}$ bond cleavage by nickel.⁴⁴

Overview of this thesis

As described above, the development of Pd-catalyzed arylation reactions has advanced significantly in the recent decades for exploring arene-based functional molecules. Through improvements and optimizations of these reactions, the scope of nucleophiles that react with aryl palladium species has been widely expanded. Currently, the reactions utilizing nucleophiles generated from heteroatom-H and C-H bonds are now practically applicable, greatly contributing to the development of arene-based functional molecules. However, several challenging Pd-catalyzed reactions still remain difficult to achieve, such as the multi-arylation and/or APEX reaction of unfunctionalized heteroles, C-H arylation of azoles with highly functionalized

structures, and arylation of O–H bond in carboxylic acids. In this thesis, the development of novel Pd-catalyzed arylations of inactive O–H and C–H bonds is described. Newly designed electron-deficient *N*-heterocyclic carbene (NHC) ligands, palladium-catalytic system as well as reaction conditions with aryl halides enable a series of novel O–H/C–H arylations reaction of carboxylic acids, electron-rich heteroarenes and highly functionalized heteroarenes. Synthesis and bioactivity of novel plant-growth stimulant compounds possessing unusual imidazole core by the newly developed C–H arylation reaction is also described.

Chapter 1 describes a series of new arylated 2-azahypoxanthine (AHX) derivatives which were synthesized by Pd-catalyzed C–H arylation of AHX derivatives (Figure 13). The rice-growth-promoting activity of the arylated AHX synthesized in this study was evaluated. Among the synthesized compounds, C8-phenyl-substituted AHX derivative showed remarkable growth-promoting activity on rice.

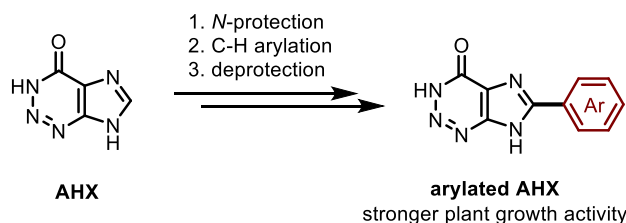


Figure 13. C–H arylation of 2-azahypoxanthine.

Chapter 2 describes a Pd-catalyzed APEX reaction of indoles and pyrroles (Figure 14). In the presence of palladium pivalate and silver carbonate, diverse indoles or pyrroles were coupled with diiodobiaryls in a double direct C–H arylation manner to afford corresponding π -extended heteroarenes in a single step. This catalytic system enables to provide structurally complicated and largely π -extended nitrogen-containing polycyclic aromatic compounds that are otherwise difficult to synthesize by classical coupling reactions.

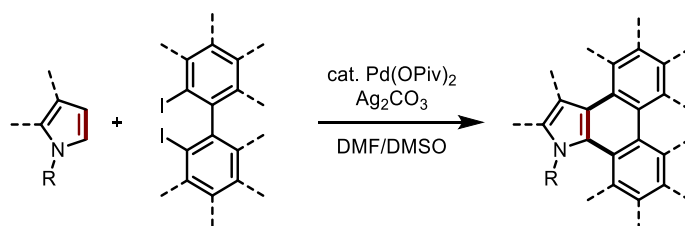


Figure 14. Pd-catalyzed APEX reaction of indoles and pyrroles with diiodobiaryls.

In Chapter 3, the first Pd-catalyzed arylation of O–H bond of carboxylic acids, so-called esterification, with aryl iodides is described (Figure 15). A Pd-based catalytic system consisting of electron-deficient NHC ligands such as IBn^F [1,3-bis{(pentafluorophenyl)methyl}-imidazole-2-ylidene)] was found to significantly accelerate the C_{aryl}–O bond-forming esterification reaction. A series of aryl iodides and carboxylic acids undergoes a cross-coupling reaction to provide the corresponding aryl esters in moderate to good yields.

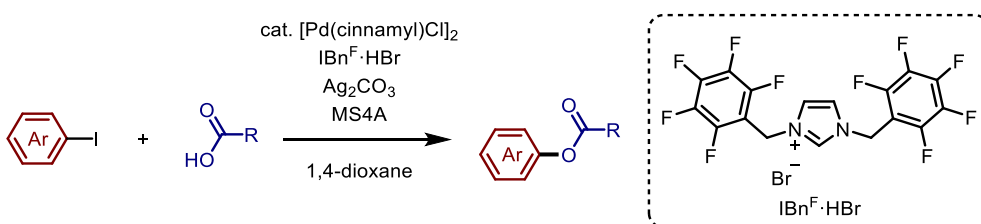


Figure 15. C_{aryl}–O_{acy} bond forming Pd-catalyzed cross-coupling reaction.

References and notes

1. Selected reviews for organic electronics: (a) Wu, J.; Pisula, W.; Müllen, K. *Chem. Rev.* **2007**, *107*, 718–747. (b) Beaujuge, P. M.; Reynolds, J. R. *Chem. Rev.* **2010**, *110*, 268–320. (c) Figueira-Duarte, T. M.; Müllen, K. *Chem. Rev.* **2011**, *111*, 7260–7314. (d) Wang, C.; Dong, H.; Hu, W.; Liu, Y.; Zhu, D. *Chem. Rev.* **2012**, *112*, 2208–2267. (e) Lee, E. K.; Lee, M. Y.; Park, C. H.; Lee, H. R.; Oh, J. H. *Advanced Materials* **2017**, *29*, 1703638. Selected reviews for biologically active compounds: (f) Patani, G. A.; LaVoie, E. J. *Chem. Rev.* **1996**, *96*, 3147–3176. (g) Butler, M. S. *J. Nat. Prod.* **2004**, *67*, 2141–2153. (h) Newman, D. J.; Cragg, G. M. *J. Nat. Prod.* **2012**, *75*, 311–335. (i) Thirumurugan, P.; Matosiuk, D.; Jozwiak, K. *Chem. Rev.* **2013**, *113*, 4905–4979. (j) Devendar, P.; Qu, R.-Y.; Kang, W.-M.; He, B.; Yang, G.-F. *J. Agric. Food Chem.* **2018**, *66*, 8914–8934.
2. Taylor, R. D.; MacCoss, M.; Lawson, A. D. G. *J. Med. Chem.* **2014**, *57*, 5845–5859.
3. Juhász, K.; Magyar, Á.; Hell, Z. *Synthesis* **2021**, *53*, 983–1002.
4. (a) Negishi, E. *ACC. Chem. Res.* **1982**, *15*, 340–348. (b) Milne, J. E.; Buchwald, S. L. *J. Am. Chem. Soc.* **2004**, *126*, 13028–13032.
5. (a) Kosugi, M.; Fugami, K. *Journal of Organometallic Chemistry* **2002**, *653*, 50–53. (b) Espinet, P.; Echavarren, A. M. *Angew Chem Int Ed* **2004**, *43*, 4704–4734. (c) Cordovilla, C.; Bartolomé, C.; Martínez-Ilarduya, J. M.; Espinet, P. *ACS Catal.* **2015**, *5*, 3040–3053. (d) Heravi, M. M.; Mohammadkhani, L. *Journal of Organometallic Chemistry* **2018**, *869*, 106–200.
6. (a) Kotha, S.; Lahiri, K.; Kashinath, D. *Tetrahedron* **2002**, *58*, 9633–9695. (b) Suzuki, A. *Journal of Organometallic Chemistry* **2002**, *653*, 50–53. (c) Suzuki, A. *Angew Chem Int Ed* **2011**, *50*, 6722–6737. (e) Lennox, A.J.J.; Lloyd-Jones, G.C. *Chem. Soc. Rev.* **2014**, *43*, 412–443.
7. (a) Hiyama, T. *Journal of Organometallic Chemistry* **2002**, *653*, 58–61. (b) Nakao, Y.; Hiyama, T. *Chem. Soc. Rev.* **2011**, *40*, 4893–4901. (c) Komiyama, T.; Minami, Y.; Hiyama, T. *Synlett* **2017**, *28*, 1873–1884. (d) Noor, R.; Zahoor, A. F.; Irfan, M.; Hussain, S. M.; Ahmad, S.; Irfan, A.; Kotwica-Mojzych, K.; Mojzych, M. *Molecules* **2022**, *27*, 5654.
8. (a) Hassan, J.; Sévignon, M.; Gozzi, C.; Schulz, E.; Lemaire, M. *Chem. Rev.* **2002**, *102*, 1359–1470. (b) Nicolaou, K. C.; Bulger, P. G.; Sarlah, D. *Angew Chem Int Ed* **2005**, *44*, 4442–4489. (c) Torborg, C.; Beller, M. *Adv Synth Catal* **2009**, *351*, 3027–3043. (d) Johansson Seechurn, C. C. C.; Kitching, M. O.; Colacot, T. J.; Snieckus, V. *Angew Chem Int Ed* **2012**, *51*, 5062–5085. (e) Pérez Sestelo, J.; Sarandeses, L. A. *Molecules* **2020**, *25*, 4500.

9. Carey, J. S.; Laffan, D.; Thomson, C.; Williams, M. T. *Org. Biomol. Chem.* **2006**, *4*, 2337.
10. (a) Brown, D. G.; Boström, J. *J. Med. Chem.* **2016**, *59*, 4443–4458. (b) Roughley, S. D.; Jordan, A. M. *J. Med. Chem.* **2011**, *54*, 3451–3479.
11. Nakamura, N.; Tajima, Y.; Sakai, K. *Heterocycles* **1982**, *17*, 235–245.
12. Akita, Y.; Inoue, A.; Yamamoto, K.; Ohta, A. *Heterocycles* **1985**, *9*, 2327–2333
13. Aoyagi, Y.; Inoue, A.; Koizumi, I.; Hashimoto, R.; Tokunaga, K.; Gohma, K.; Komatsu, J.; Sekine, K.; Miyafuji, A.; Kunoh, J.; Honma, R.; Akita, Y.; Ohta, A. *Heterocycles* **1992**, *33*, 257–272
14. Satoh, T.; Itaya, T.; Miura, M.; Nomura, M. *Chem. Lett.* **1996**, 823.
15. Satoh, T.; Kawamura, Y.; Miura, M.; Nomura, M. *Angew. Chem. Int. Ed. Engl.* **1997**, *36*, 1740–1742.
16. Okazawa, T.; Satoh, T.; Miura, M.; Nomura, M. *J. Am. Chem. Soc.* **2002**, *124*, 5286–5287.
17. Lafrance, M.; Rowley, C. N.; Woo, T. K.; Fagnou, K. *J. Am. Chem. Soc.* **2006**, *128*, 8754–8756.
18. (a) Garcia-Cuadrado, D.; Braga, A. A. C.; Maseras, F.; Echavarren, A. M. *J. Am. Chem. Soc.* **2006**, *128*, 1066–1067. (b) Garcia-Cuadrado, D.; de Mendoza, P.; Braga, A. A. C.; Maseras, F.; Echavarren, A. M. *J. Am. Chem. Soc.* **2007**, *129*, 6880–6886.
19. (a) Gorelsky, S. I.; Lapointe, D.; Fagnou, K. *J. Am. Chem. Soc.* **2008**, *130*, 10848–10849. (b) Lapointe, D.; Fagnou, K. *Chem. Lett.* **2010**, *39*, 1118–1126. (c) Ackermann, L. *Chem. Rev.* **2011**, *111*, 1315–1345. (d) Gorelsky, S. I. *Coordination Chemistry Reviews* **2013**, *257*, 153–164.
20. (a) Lafrance, M.; Fagnou, K. *J. Am. Chem. Soc.* **2006**, *128*, 16496–16497. (b) Tan, Y.; Hartwig, J. F. *J. Am. Chem. Soc.* **2011**, *133*, 3308–3311. (c) Kim, D.; Choi, G.; Kim, W.; Kim, D.; Kang, Y. K.; Hong, S. H. *Chem. Sci.* **2021**, *12*, 363–373.
21. Yamaguchi, J.; Yamaguchi, A. D.; Itami, K. *Angew Chem Int Ed* **2012**, *51*, 8960–9009.
22. Bringmann, G.; Jansen, J. R.; Rink, H. *Angew. Chem. Int. Ed. Engl.* **1986**, *25*, 913–915.
23. Oshima, T.; Yamanaka, I.; Kumar, A.; Yamaguchi, J.; Nishiwaki-Ohkawa, T.; Muto, K.; Kawamura, R.; Hirota, T.; Yagita, K.; Irle, S.; Kay, S. A.; Yoshimura, T.; Itami, K. *Angew Chem Int Ed* **2015**, *54*, 7193–7197.
24. (a) Ito, H.; Ozaki, K.; Itami, K. *Angew Chem Int Ed* **2017**, *56*, 11144–11164. (b) Ito, H.; Segawa, Y.; Murakami, K.; Itami, K. *J. Am. Chem. Soc.* **2019**, *141*, 3–10. (c) Ito, H.; Kawahara, K. P.; Itami, K. *Synthesis* **2023**, a-2169-4078.
25. Ozaki, K.; Murai, K.; Matsuoka, W.; Kawasumi, K.; Ito, H.; Itami, K. *Angew Chem Int*

- Ed* **2017**, *56*, 1361–1364.
26. Shibata, M.; Ito, H.; Itami, K. *J. Am. Chem. Soc.* **2018**, *140*, 2196–2205.
 27. Matsuoka, W.; Ito, H.; Itami, K. *Angew Chem Int Ed* **2017**, *56*, 12224–12228.
 28. Wang, X.; Gribkov, D. V.; Sames, D. *J. Org. Chem.* **2007**, *72*, 1476–1479.
 29. Zhang, Z.; Hu, Z.; Yu, Z.; Lei, P.; Chi, H.; Wang, Y.; He, R. *Tetrahedron Letters* **2007**, *48*, 2415–2419.
 30. Ozaki, K.; Matsuoka, W.; Ito, H.; Itami, K. *Org. Lett.* **2017**, *19*, 1930–1933.
 31. Pivsa-Art, S.; Satoh, T.; Kawamura, Y.; Miura, M.; Nomura, M. *BCSJ* **1998**, *71*, 467–473.
 32. Gorelsky, S. I. *Organometallics* **2012**, *31*, 794–797.
 33. (a) Macdonald, J.; Oldfield, V.; Bavetsias, V.; Blagg, J. *Org. Biomol. Chem.* **2013**, *11*, 2335. (b) Mahindra, A.; Jain, R. *Org. Biomol. Chem.* **2014**, *12*, 3792–3796.
 34. Kim, D.; Jun, H.; Lee, H.; Hong, S.-S.; Hong, S. *Org. Lett.* **2010**, *12*, 1212–1215.
 35. (a) Guram, A. S.; Rennels, R. A.; Buchwald, S. L. *Angew. Chem. Int. Ed. Engl.* **1995**, *34*, 1348–1350. (b) Louie, J.; Hartwig, J. F. *Tetrahedron Letters* **1995**, *36*, 3609–3612.
 36. (a) Kunz, K.; Scholz, U.; Ganzer, D. *Synlett* **2003**, No. 15, 2428–2439. (b) Beletskaya, I. P.; Cheprakov, A. V. *Coordination Chemistry Reviews* **2004**, *248*, 2337–2364. (c) Monnier, F.; Taillefer, M. *Angew Chem Int Ed* **2009**, *48*, 6954–6971. (d) Sambigiato, C.; Marsden, S. P.; Blacker, A. J.; McGowan, P. C. *Chem. Soc. Rev.* **2014**, *43*, 3525–3550. (e) Yang, Q.; Zhao, Y.; Ma, D. *Org. Process Res. Dev.* **2022**, *26*, 1690–1750.
 37. (a) Hartwig, J. F. *Angewandte Chemie International Edition* **1998**, *3*, 2046–2067. (b) Ruiz-Castillo, P.; Buchwald, S. L. *Chem. Rev.* **2016**, *116*, 12564–12649. (c) Heravi, M. M.; Kheilkordi, Z.; Zadsirjan, V.; Heydari, M.; Malmir, M. *Journal of Organometallic Chemistry* **2018**, *861*, 17–104. (c) Forero-Cortés, P. A.; Haydl, A. M. *Org. Process Res. Dev.* **2019**, *23*, 1478–1483.
 38. Selected examples for Pd-catalyzed etherification see: (a) Mann, G.; Hartwig, J. F. *J. Am. Chem. Soc.* **1996**, *118*, 13109. (b) Palucki, M.; Wolfe, J. P.; Buchwald, S. L. *J. Am. Chem. Soc.* **1997**, *119*, 3395. (c) Mann, G.; Hartwig, J. F. *J. Org. Chem.* **1997**, *62*, 5413. (d) Mann, G.; Hartwig, J. F. *Tetrahedron Lett.* **1997**, *38*, 8005. (e) Mann, G.; Incarvito, C.; Rheingold, A. L.; Hartwig, J. F. *J. Am. Chem. Soc.* **1999**, *121*, 3224.
 39. Selected examples for Pd-catalyzed amidation and sulfonamidation see : (a) Wolfe, J. P.; Rennels, R. A.; Buchwald, S. L. *Tetrahedron* **1996**, *52*, 7525–7546. (b) Shakespeare, W. C. *Tetrahedron Letters* **1999**, *40*, 2035–2038. (c) Hartwig, J. F.; Kawatsura, M.; Hauck, S. I.; Shaughnessy, K. H.; Alcazar-Roman, L. M. *J. Org. Chem.* **1999**, *64*, 5575–5580. (e) Hartwig,

- J. F.; Kawatsura, M.; Hauck, S. I.; Shaughnessy, K. H.; Alcazar-Roman, L. M. *J. Org. Chem.* **1999**, *64*, 5575–5580. (f) Yin, J.; Buchwald, S. L. *Org. Lett.* **2000**, *2*, 1101–1104. (g) Yin, J.; Buchwald, S. L. *J. Am. Chem. Soc.* **2002**, *124*, 6043–6048. (h) Burton, G.; Cao, P.; Li, G.; Rivero, R. *Org. Lett.* **2003**, *5*, 4373–4376. (i) Fujita, K.; Yamashita, M.; Puschmann, F.; Alvarez-Falcon, M. M.; Incarvito, C. D.; Hartwig, J. F. *J. Am. Chem. Soc.* **2006**, *128*, 9044–9045.
40. Selected examples for Pd-catalyzed thioetherification see : (a) Kosugi, M.; Shimizu, T.; Migita, *Chem. Lett.* **1978**, *7*, 13–14. (b) Kondo, T.; Mitsudo, T. *Chem. Rev.* **2000**, *100* (8), 3205–3220. (c) Li, G. Y. *Angew. Chem. Int. Ed.* **2001**, *40*, 1513–1516. (d) Li, G. Y.; Zheng, G.; Noonan, A. F. *J. Org. Chem.* **2001**, *66*, 8677–8681. (e) Li, G. Y. *J. Org. Chem.* **2002**, *67*, 3643–3650.
41. Surry, D. S.; Buchwald, S. L. *Angew Chem Int Ed* **2008**, *47*, 6338–6361.
42. For reviews, see: (a) Otera, J. *Chem. Rev.* **1993**, *93*, 1449–1470. (b) Ishihara, K. *Tetrahedron* **2009**, *65*, 1085–1109. For selected examples, see: (c) Chakraborti, A. K.; Shivani. *J. Org. Chem.* **2006**, *71*, 5785–5788. (d) Carle, M. S.; Shimokura, G. K.; Murphy, G. K. *Eur J Org Chem* **2016**, *2016*, 3930–3933.
43. (a) Shi, G.; Zhang, Y. *Adv Synth Catal* **2014**, *356*, 1419–1442. (b) Dutta, S.; Bhattacharya, T.; Geffers, F. J.; Bürger, M.; Maiti, D.; Werz, D. B. *Chem. Sci.* **2022**, *13*, 2551–2573.
44. (a) Guan, B.-T.; Wang, Y.; Li, B.-J.; Yu, D.-G.; Shi, Z.-J. *J. Am. Chem. Soc.* **2008**, *130*, 14468–14470. (b) Quasdorf, K. W.; Tian, X.; Garg, N. K. *J. Am. Chem. Soc.* **2008**, *130*, 14422–14423. (c) Li, B.; Li, Y.; Lu, X.; Liu, J.; Guan, B.; Shi, Z. *Angew Chem Int Ed* **2008**, *47*, 10124–10127. (d) Takise, R.; Muto, K.; Yamaguchi, J.; Itami, K. *Angew Chem Int Ed* **2014**, *53*, 6791–6794.
45. (a) Krylov, I. B.; Vil', V. A.; Terent'ev, A. O. *Beilstein J. Org. Chem.* **2015**, *11*, 92–146. (b) Moghimi, S.; Mahdavi, M.; Shafiee, A.; Foroumadi, A. *Eur J Org Chem* **2016**, *2016*, 3282–3299.
46. (a) Welin, E. R.; Le, C.; Arias-Rotondo, D. M.; McCusker, J. K.; MacMillan, D. W. C. *Science* **2017**, *355*, 380–385. (b) Liang, J.-Y.; Shen, S.-J.; Xu, X.-H.; Fu, Y.-L. *Org. Lett.* **2018**, *2*, 6627–6631. (c) Li, L.; Song, F.; Zhong, X.; Wu, Y.; Zhang, X.; Chen, J.; Huang, Y. *Adv Synth Catal* **2020**, *362*, 126–132.

**Discovery of Plant Growth Stimulants by
C–H Arylation of 2-Azahypoxanthine**

Abstract

A series of new AHX derivatives were synthesized by Pd-catalyzed C–H arylation. Their rice growth-promoting activity was evaluated *in vivo*. Among the synthesized compounds, C8 phenyl-substituted AHX showed remarkable growth-promoting activity on rice. The present study shows the power and significant opportunity of C–H functionalization chemistry to rapidly transform biologically active natural products into more active compounds.

1. Introduction

“Fairy ring” is naturally-occurring ring-shaped thick growth or necrotic spot of grasses, which are commonly seen on the lawn (Figure 1). Occasionally, fruiting bodies of fungi are also seen in the fairy rings. The term “fairy rings” originates from the myths and superstitions associated with their occurrence in the Middle Ages. The first scientific article discussing this phenomenon dates back in 1675.¹ In 1995, Couch proposed that this mysterious ring is a result of the interaction between a fairy-ring-forming fungus and a plant.²



Figure 1. Fairy ring on the turfgrass field, University of Shizuoka, Japan. Reprinted with permission by Dr. Makoto Inai. Copyright Dr. Makoto Inai.

More recently, Kawagishi and co-workers disclosed that the key molecular players of this interaction are plant-growth stimulating compound 2-azahypoxanthine (AHX) and plant-growth inhibitor imidazole-4-carboxamide (ICA) identified from one of the fairy-ring-forming fungi, *Lepista sordida*.³ These compounds have been termed “fairy chemicals” (FCs).⁴ The regulation of plant growth by FCs has been observed in all the plants tested, regardless of their species, demonstrating their broad effectiveness. Furthermore, treatment of FCs increased the yields of rice, wheat, and other various types of crops in greenhouse and/or field experiments.^{3,5} Furthermore, Kawagishi and co-workers also reported that AHX and its metabolite 2-aza-8-oxohypoxanthine (AOH) are endogenously produced in plants by a new purine metabolic pathway.^{3b,6} Based on the findings, Kawagishi and co-workers have hypothesized that FCs are a new family of plant hormone.⁷

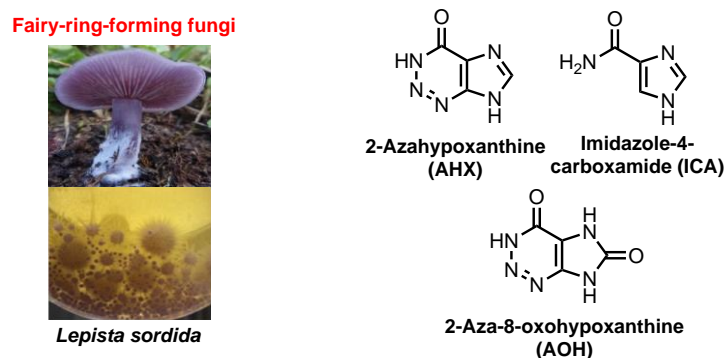


Figure 2. Fairy chemicals isolated from fairy-ring-forming fungi, *Lepista sordida*.

Despite the intriguing plant-growth activity of AHX, the mechanism of how AHX enhances plant growth remains poorly understood. Furthermore, the structure-activity relationship (SAR) of AHX derivatives has not yet been defined due to the challenges associated with chemically modifying AHX. There are two main reasons for the difficulty in synthesis of AHX derivatives. Firstly, AHX has a rare 1,2,3-triazin-4(3*H*)-one structure that is uncommon among natural products. The unique structure limits the availability of suitable chemical reactions and synthetic methods for modifying AHX. Secondly, AHX has only three hydrogen atoms available for substitution (Figure 3a). The limited number of substitution site further complicates the synthesis of AHX derivatives. Initially, synthesis of *N,N'*-dialkyl AHXs and *N*-alkyl AHX through a simple alkylation reaction and evaluation of their effects were performed to find molecules that show an enhanced plant growth-promoting activity (Figure 3b). While various alkyl AHXs **5–8**, **5'** and **8'** having benzyl, 4-methoxybenzyl and 2-trimethylsilylethoxyl groups were synthesized and tested, all the compounds did not show significant growth activity on both shoot and root comparing to AHX (Figures 4a and 4b). Conversely, compounds **5**, **6** and **7** showed slight plant growth inhibition on root.

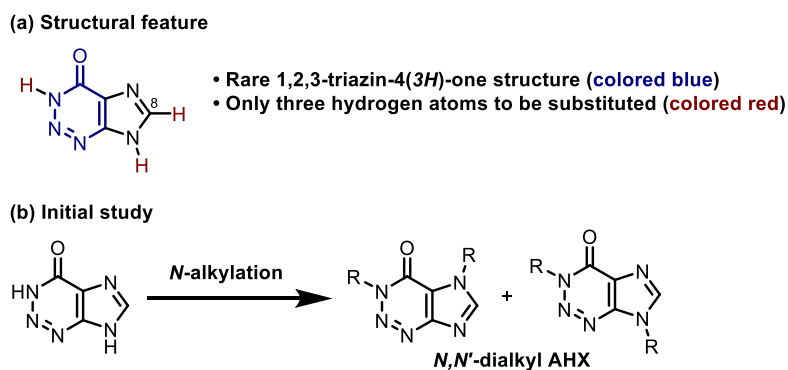


Figure 3. (a) Structural features of AHX. (b) Initial synthesis of AHX derivatives.

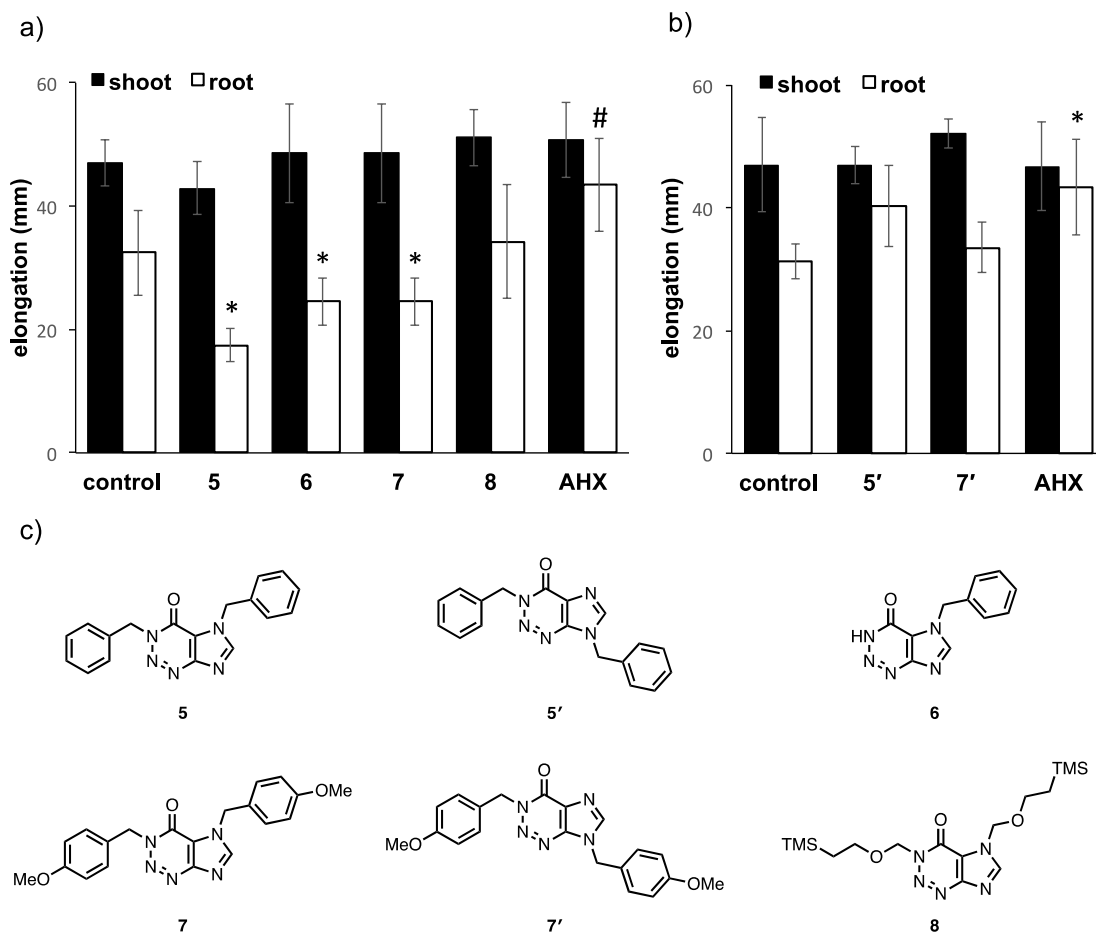
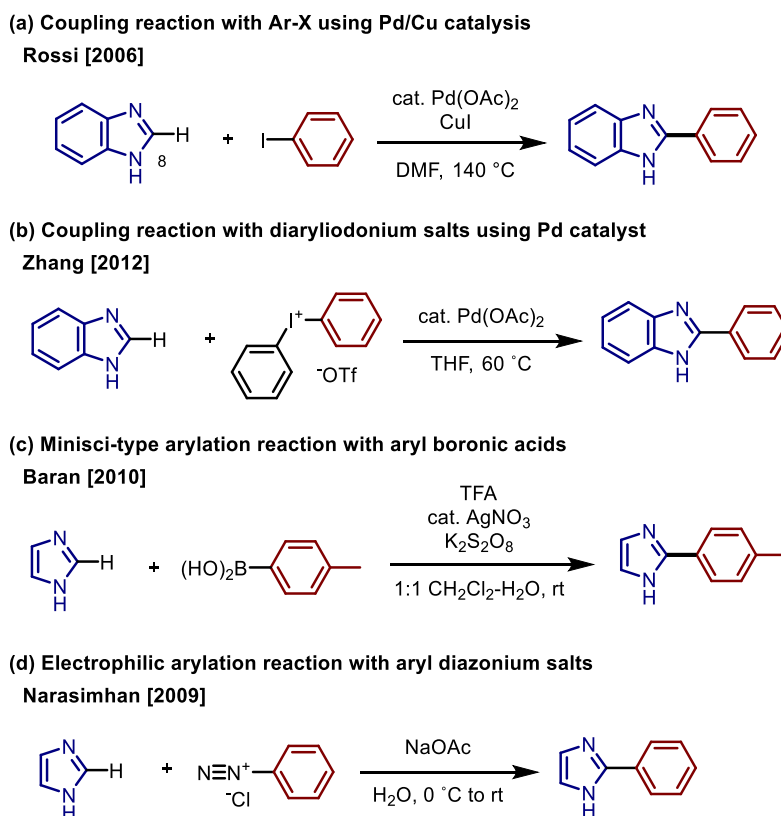


Figure 4. Structure-activity relationship of **5**, **5'**, **6**, **7**, **7'** and **8** on the growth of rice. (a) Effect of compounds **5**, **6**, **7** and **8** on the growth of shoot and root in rice. (b) Effect of compound **5'** and **7'** on the growth of shoot and root in rice. (c) Chemical structures of the compounds **5**, **5'**, **6**, **7**, **7'** and **8**. Germinated seeds were treated with 0.1 mM solution of **5**, **5'**, **6**, **7**, **7'**, **8** and AHX. Results are the mean \pm standard deviation ($n = 4$). Asterisk indicates a value that is significantly different from the control (Student's t -test, $p < 0.05$). Number sign indicates a value that is significantly different from the AHX treated group (Student's t -test, $p < 0.1$).

Then, functionalization of remaining C–H bond on imidazole ring in AHX and SAR study of obtained AHX derivatives were investigated. There are several known methods for introducing an aryl group directly at the C2 position of NH imidazole: 1) coupling reaction with haloarenes using Pd/Cu catalysis (Scheme 1a),⁸ 2) coupling reaction with diaryliodonium salts using Pd catalyst (Scheme 1b),⁹ 3) Minisci-type arylation reaction with aryl boronic acids (Scheme 1c),¹⁰ 4) electrophilic arylation reaction with aryl diazonium salts (Scheme 1d),¹¹ and also reaction using transition metal catalysts such as rhodium.¹² For arylation of C8 position of AHX, several

preliminary attempts, including halogenation and direct arylation, were conducted. However, these attempts encountered challenges due to the instability of the AHX skeleton and the lower reactivity observed at the C8 position. Therefore, an alternative appropriate synthetic method was required for obtaining C8-arylated AHX derivatives.



Scheme 1. Brief summary of reported direct C–H arylation of NH imidazoles.

In this chapter, the application of C–H arylation chemistry to synthesize AHX derivatives and the evaluation of their plant growth-promoting activity is described.¹³ The easy access to these derivatives allowed to rapidly discover a novel plant-growth stimulator that shows stronger activity than the original AHX (Figure 5). Owing to the general synthetic difficulty of C8-functionalized AHX derivatives, the AHX derivatives synthesized by the newly established method can possess an unexpected activity toward plant growth-regulation and an potential for identifying the target protein of AHX.

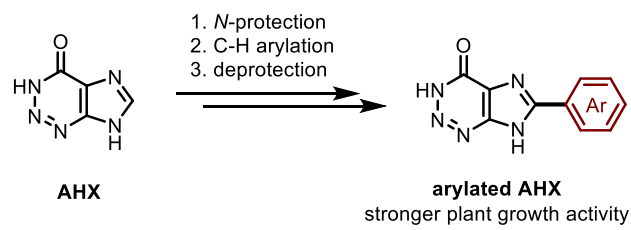


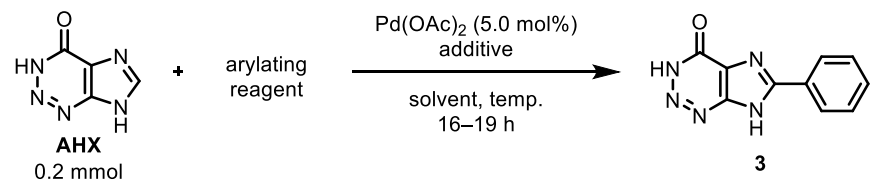
Figure 5. Brief summary of this chapter.

2. Results and Discussion

2-1. One step synthesis toward C8-substituted AHX derivatives

Extensive screening of reaction conditions was conducted to synthesize C8-arylated AHX in one step by C–H arylation. Initially, Pd/Cu-catalyzed direct C–H arylations of AHX were examined based on the reaction reported by Rossi (Table 1).⁸ However, no production of desired compound **3** was observed regardless of the equivalent of copper (entries 1 and 2) or the equivalent of base (entries 3 and 4). Although the direct C–H arylation of AHX using diphenyliodonium triflate as an arylating reagent was performed based on Zhang's report,⁹ desired compound **3** was not obtained under all conditions shown in entries 5–8.

Table 1. Pd-catalyzed direct C–H arylation of AHX.

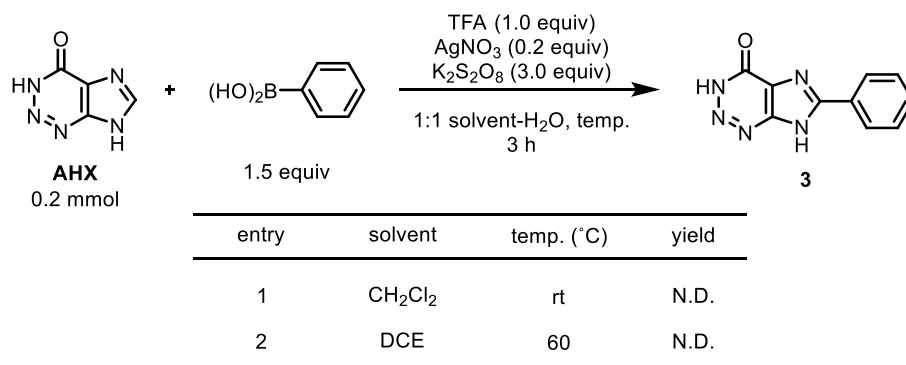


entry	arylating reagent	additive	solvent	temp. (°C)	yield
1	PhI (2.0 eq.)	CuI (2.0 eq.)	DMF	140	N.D.
2	PhI (2.0 eq.)	CuI (3.0 eq.)	DMF	140	N.D.
3	PhI (2.0 eq.)	CuI (2.0 eq.), K ₃ PO ₄ (3.0 eq.)	DMF	140	N.D.
4	PhI (2.0 eq.)	CuI (3.0 eq.), K ₃ PO ₄ (3.0 eq.)	DMF	140	N.D.
5	Ph ₂ I ⁺ OTf ⁻ (1.2 eq.)	-	THF	60	N.D.
6	Ph ₂ I ⁺ OTf ⁻ (1.2 eq.)	-	DMF	60	N.D.
7	Ph ₂ I ⁺ OTf ⁻ (1.2 eq.)	-	DMF	100	N.D.
8	Ph ₂ I ⁺ OTf ⁻ (1.2 eq.)	-	1,4-dioxane	100	N.D.

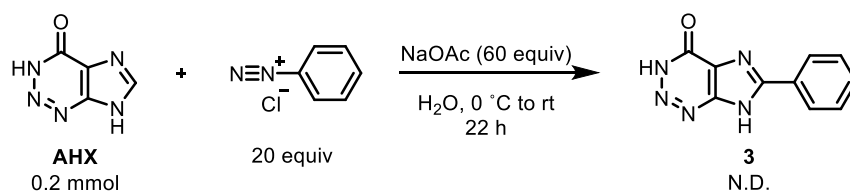
The lack of success in obtaining compound **3** through established Pd-catalyzed direct C–H arylation methods suggests that the highly polar nature of AHX renders it incompatible with Pd-catalytic reaction conditions. In order to overcome this obstacle, alternative reactions that do not depend on Pd catalysts were explored. Subsequently, the direct C–H arylation of AHX with phenylboronic acid was investigated according to the silver-catalyzed reaction reported by Baran (Scheme 2a).¹⁰ However, desired compound **3** was not obtained under any of the tested conditions (entries 1 and 2). In addition, the direct C–H arylation of AHX was demonstrated using

Narasimhan's conditions with phenyldiazonium chloride as an arylating reagent (Scheme 2b),¹¹ but no formation of compound **3** was observed.

(a) Direct C–H arylation of AHX with phenylboronic acid with silver salt



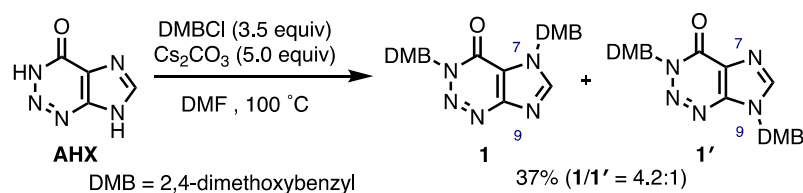
(b) Direct C–H arylation of AHX with phenyldiazonium chloride



Scheme 2. Non Pd-catalytic direct C–H arylation of AHX.

2-2. Synthesis of C8-substituted AHX derivatives from *N*-protected AHX

Thus, the introduction of a protecting group for the N–H moieties on AHX was employed in order to increase a tolerance of AHX toward various catalytic reaction conditions (Scheme 3). For this purpose, 2,4-dimethoxybenzyl group (DMB) was chosen as the protecting group for two nitrogen atoms due to its easy removability under mild oxidative conditions.¹⁴ First, the two nitrogen atoms on AHX was protected with the DMB group using 2,4-dimethoxybenzyl chloride (DMBCl) and Cs₂CO₃, affording a separable mixture of regioisomers **1** and **1'** in a ratio of 4.2:1. The structures of these isomers were identified by the heteronuclear multiple bond coherence (HMBC) and heteronuclear multiple quantum correlation (HMQC) in NMR spectroscopy (see Experimental Section for details). The low yield of **1/1'** would be attributed to the lower stabilities of both protecting group-free AHX and DMBCl.

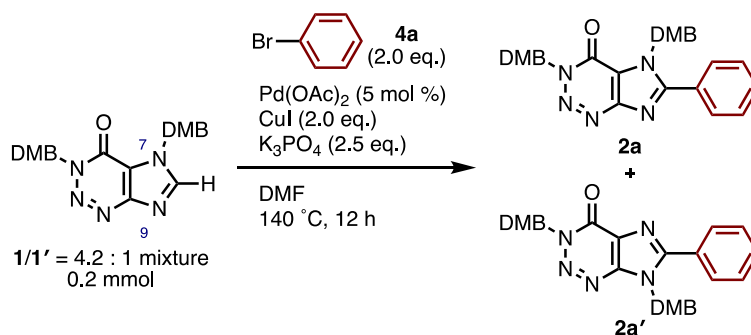


Scheme 3. Protection of AHX with a DMB group.

Next, the palladium-catalyzed C–H arylation of DMB-protected AHX (**1** and **1'**) was investigated with bromoarenes as arylating agents. Through extensive screening of the C–H arylation reactions conditions for related imidazole substrates reported by Miura¹⁵ and Rossi,⁸ suitable reaction conditions using Pd/Cu catalytic system with bromoarenes was finally found for efficient and unprecedented direct C–H arylation of DMB-protected AHX. The effects of various parameters in the Pd-catalyzed C–H arylation of DMB-protected AHX are summarized in Table 2. For example, treatment of DMB-protected AHX (**1/1'** = 4.2:1) with bromobenzene (2.0 equiv) in the presence of Pd(OAc)₂ (5 mol%), CuI (2.0 equiv), and K₃PO₄ (2.5 equiv) in DMF at 140 °C for 12 h afforded the expected C–H arylation products (**2a/2a'** = 1.4:1) in 50% yield (entry 1). The addition of ligands such as PCy₃, P^tBu₃, and BINAP had no beneficial effect on the yield of **2a/2a'** (43–52% yield; entries 2–4). The product yields depend on the base employed, increasing in the order of K₂CO₃ < Cs₂CO₃ < Na₂CO₃ < K₃PO₄ (entries 1, 5, 6, and 7). The polarity of solvents is also important. While DMF and DMA resulted in moderate yields (50% and 43% yields; entries 1 and 8), the reactions in 1,4-dioxane and toluene showed significant decrease in yield (entries 9

and 10). The use of iodobenzene instead of bromobenzene resulted in a lower yield of **2a/2a'** (37% yield; entry 11). While the absence of CuI almost shut down the reaction (entry 12), the absence of Pd(OAc)₂ still gave the target material in 11% yield (entry 13), suggesting that copper-mediated (non-palladium-catalyzed) C–H arylation is also occurring in this reaction. Notably, scaling up the reaction led to an increased yield (71% yield; entry 14).

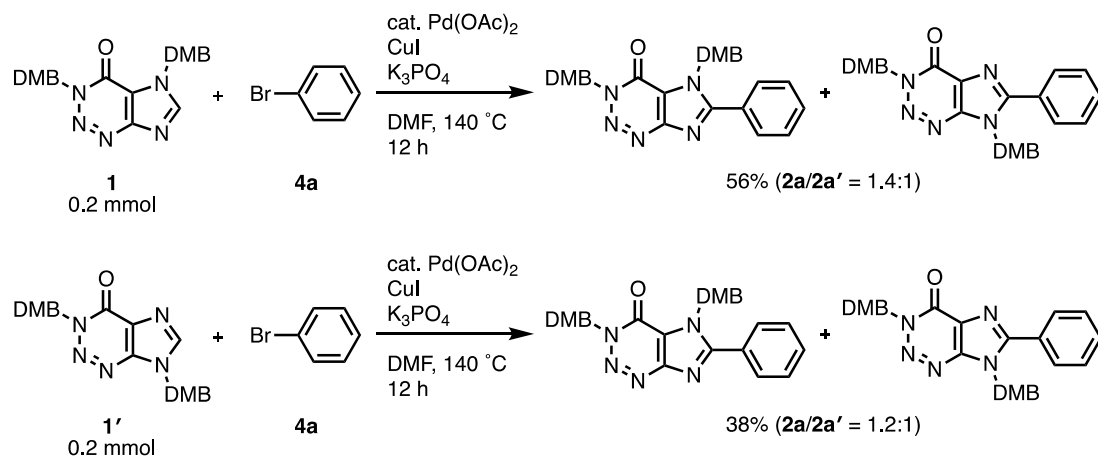
Table 2. Pd/Cu-mediated C–H phenylation of DMB protected AHX.



entry	deviation from standard conditions	yield ^a
1		50, 2a/2a' = 1.4:1
2	PCy ₃ ·HBF ₄ (10 mol%) was added	52, 2a/2a' = 1.4:1
3	P ^t Bu ₃ ·HBF ₄ (10 mol%) was added	49, 2a/2a' = 1.1:1
4	BINAP (5 mol%) was added	43, 2a/2a' = 1.4:1
5	Na ₂ CO ₃ instead of K ₃ PO ₄	46, 2a/2a' = 1.3:1
6	K ₂ CO ₃ instead of K ₃ PO ₄	21, 2a/2a' = 2.5:1
7	Cs ₂ CO ₃ instead of K ₃ PO ₄	44, 2a/2a' = 1.9:1
8	DMA instead of DMF	43, 2a/2a' = 1.7:1
9	1,4-dioxane instead of DMF	17, 2a/2a' = 3.3:1
10	toluene instead of DMF	17, 2a/2a' = 2.4:1
11	iodobenzene instead of 4a	37, 2a/2a' = 1.3:1
12	without CuI	1, 2a
13	without Pd(OAc) ₂	11, 2a/2a' = 1.8:1
14	1.1 mmol scale, reaction time 15 h	71 ^b , 2a/2a' = 2.6:1

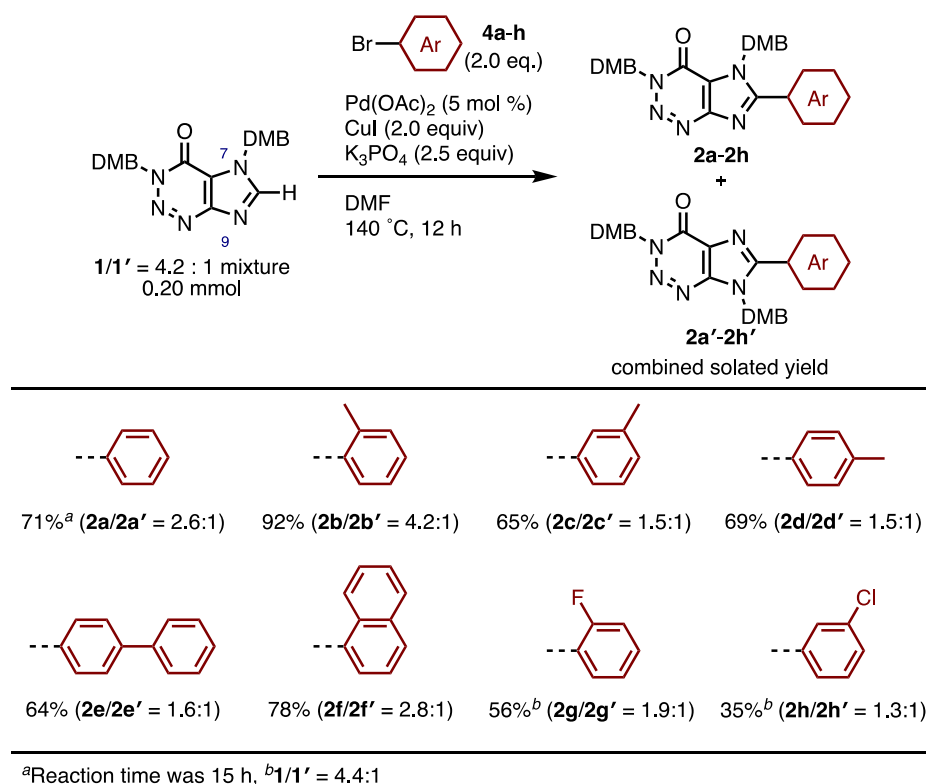
^aDetermined by gas chromatography by using CH₂Br₂ as an internal standard. ^bIsolated yield.

During the course of the reaction, the ratio of DMB regioisomers changed (Scheme 4). Conducting independent reactions using isomerically pure **1** and **1'** revealed that both isomers exhibited similar reactivity, resulting in a mixture of **2a** and **2a'** (**1**: 56% yield (**2a/2a'** = 1.4:1), **1'**: 38% yield (**2a/2a'** = 1.2:1)). These results suggest that migration of DMB group between N7 and N9 positions occurs during the reaction.

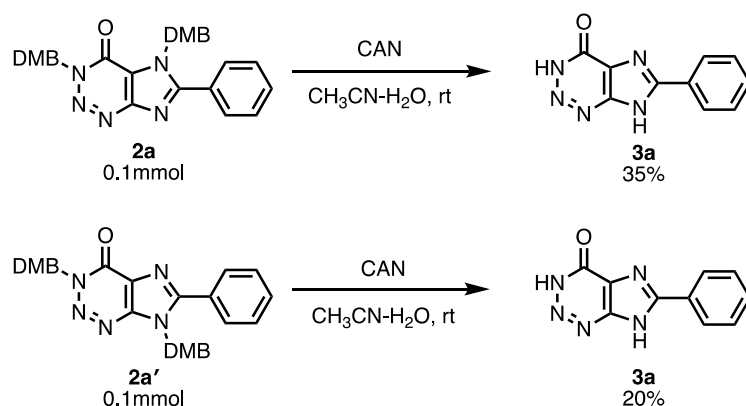


Scheme 4. Pd/Cu-mediated direct C–H arylation using isomerically pure **1** and **1'** with bromobenzene.

Using the optimized conditions, a range of arylated AHX derivatives **2/2'** were synthesized via Pd-catalyzed arylation with bromoarenes **4a–h** (Scheme 5). The reactions with sterically hindered bromoarenes, such as 2-bromotoluene (**4b**) and 1-bromonaphthalene (**4f**), gave the corresponding products **2b/2b'** and **2f/2f'** in good yields (92% and 78% yields). The reactions with bromobenzene (**4a**), 3-bromotoluene (**4c**), 4-bromotoluene (**4d**), 4-bromobiphenyl (**4e**), 1-bromo-2-fluorobenzene (**4g**) and 1-bromo-3-chlorobenzene (**4h**) resulted in moderate yields of C–H arylation products (**2a/2a'**, **2c/2c'**, **2d/2d'**, **2e/2e'**, **2g/2g'**, **2h/2h'**; 35–71%). The each regioisomer ratio of arylated AHX **2/2'** (1.3:1 to 4.2:1) varied compared to those of starting DMB-protected AHX **1/1'** (4.2:1), which suggests that the steric hindrance on arylating agents **4** could affect the reactivity toward DMB-protected AHX **1/1'**.



Scheme 5. Pd/Cu-mediated direct C–H arylation with different aryl bromides.



Scheme 7. Deprotection of DMB group using isomerically pure **2a** or **2a'**.

2-3. Biological study of AHX related compounds and 8-arylated AHX 3

With the newly synthesized compounds **3a–h** in hand, the SAR of AHX analogues and derivatives to the growth-promoting activity was examined. The growth-promoting activity was investigated using rice (*Oryza sativa* L. cv. Nipponbare). The activities of reported AHX-related compounds (Figure 6a) showed good agreement with the previously reported results (Figure 6b).¹⁶ Xanthine (Xan), hypoxanthine (HX), imidazole (IMI), ethyl imidazole-4-carboxylate (EtC) and 5-aminoimidazole-4-carboxamide (AICA) did not exhibit noticeable shoot or root growth-regulating activity. ICA exhibited growth-inhibitory activity in both shoot and root, and AHX and 2-aza-8-oxohypoxanthine (AOH) showed growth-promoting activity in root (Figure 6b).

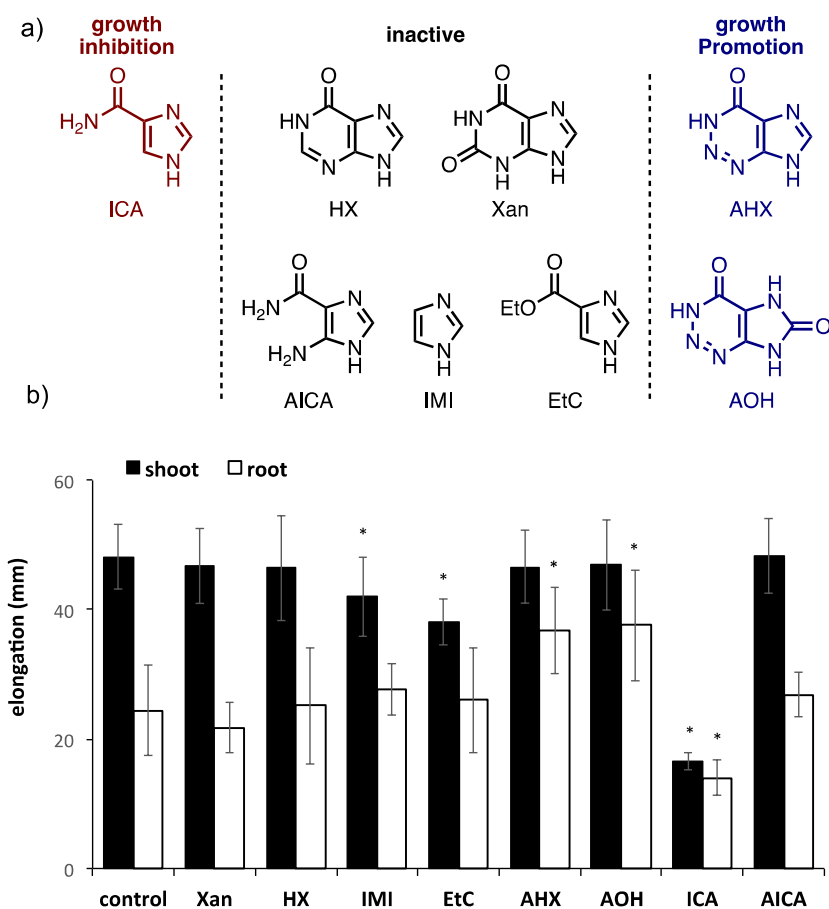


Figure 6. Plant growth-regulating activities of AHX-related compounds. a) Chemical structures of the reported AHX-related compounds. b) Effect of Xan, HX, IMI, EtC, AHX, AOH, ICA and AICA on the growth of rice. Germinated seeds were treated with 0.1 mM solution of Xan, HX, IMI, EtC, AHX, AOH, ICA, AICA and incubated for a week in a test tube. Results are the mean \pm standard deviation ($n = 12$). Asterisk indicates a value that is significantly different from the control (Student's t -test, $p < 0.05$).

The plant growth-regulating activities of the arylated AHX derivatives **3**, which were synthesized in this study, are summarized in Figures 7 and 8. All the arylated AHXs showed a tendency to exhibit stronger root growth-promoting activity than the original AHX. In particular, the introduction of phenyl (**3a**), *o*-methylphenyl (**3b**), 4-biphenyl (**3e**), 1-naphthyl (**3f**) or *m*-chlorophenyl (**3h**) moiety at the C8-position of AHX was found to be highly effective for the rice root growth activity. Substituting the phenyl group with an *m*-methyl (**3c**), *p*-methyl (**3d**) or *o*-fluoro (**3g**) group resulted in weaker activity compared to **3a**.

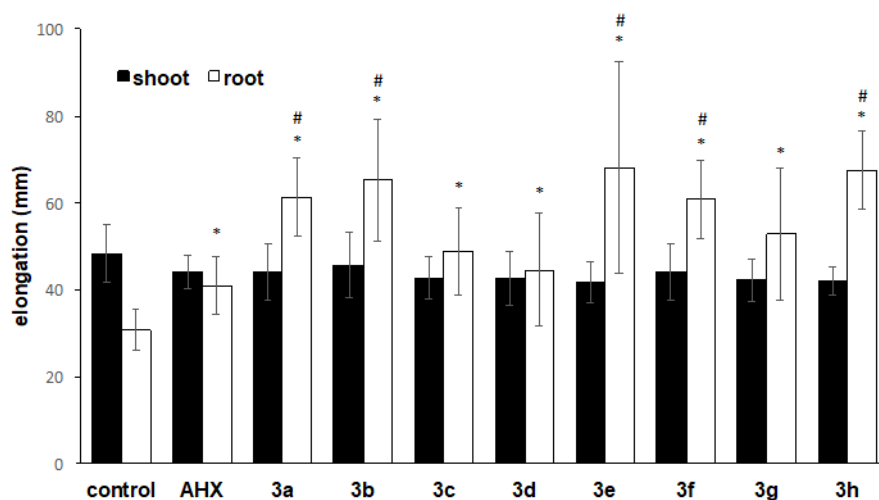


Figure 7. Effect of arylated AHXs **3a-h** on the growth of rice. Germinated seeds were treated with 0.1 mM solution of AHX, **3a-h** and incubated for a week in a test tube. Results are the mean \pm standard deviation ($n = 12$). Asterisk indicates a value that is significantly different from the control (Student's t -test, $p < 0.05$). Number sign indicates a value that is significantly different from the AHX treated group (Student's t -test, $p < 0.05$).



Figure 8. Images of rice seedlings after the growth-promotion assay. Germinated seeds were treated with 0.1 mM solution of compounds.

Then the dose effect of **3a** on the growth of shoot and root in rice was also evaluated (Figure 9). As a result, elongation of root was significantly elevated at the concentrations of 0.1, 0.2, 0.4 mM.

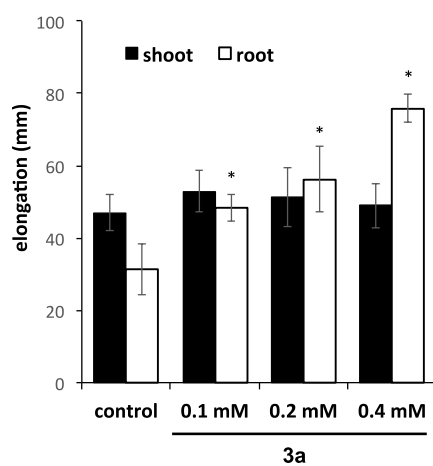


Figure 9. Dose-response curve for **3a** in shoot/root growth assay. Results are the mean \pm standard deviation ($n = 4$). Asterisk indicates a value that is significantly different from the control (Student's t -test, $p < 0.05$).

3. Conclusion

In summary, the C–H arylation reaction of DMB-protected AHX has facilitated the discovery of novel plant growth-promoting compounds. These newly synthesized arylated AHX derivatives showed stronger growth-promoting activity compared to the natural plant growth promoter AHX. These series of compounds have immense potential for agricultural applications. Future identification of target(s) of AHX and its arylated derivatives may provide the molecular basis of their interesting plant-growth activity including fairy-ring formation. Moreover, the present work emphasizes that, with the recent advent of game-changing C–H functionalization chemistry,¹⁷ there are significant opportunities to use these technologies to accelerate agricultural science.

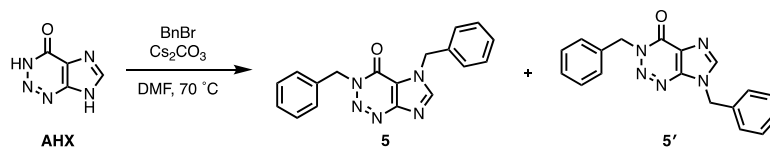
Experimental Section

1. General

Unless otherwise noted, all reactants or reagents including dry solvents were obtained from commercial suppliers and used as received. AHX was provided from Ushio Chemix Co. Ltd.. Pd(OAc)₂ was purchased from WAKO. Unless otherwise noted, all reactions were performed with dry solvents under an atmosphere of N₂ in dried glassware using standard vacuum-line techniques. All work-up and purification procedures were carried out with reagent-grade solvents in air. Analytical thin-layer chromatography (TLC) was performed using E. Merck silica gel 60 F₂₅₄ precoated plates (0.25 mm). The developed chromatogram was analyzed by UV lamp (254 nm). Medium Pressure liquid chromatography (MPLC) was performed using Yamazen W-prep 2XY or Biotage Isolera[®] equipped with WAKO Presep[®]. Preparative thin-layer chromatography (PTLC) was performed using Wakogel B5-F silica coated plates (0.75 mm) prepared in our laboratory. High-resolution mass spectra (HRMS) were conducted on Thermo Fisher Scientific Exactive. Nuclear magnetic resonance (NMR) spectra were recorded on a JEOL JNM-ECA-600 (¹H 600 MHz, ¹³C 150 MHz) and a JEOL JNM-ECA-600II with Ultra COOL[™]probe (¹H 600 MHz, ¹³C 150 MHz) spectrometer. Chemical shifts for ¹H NMR are expressed in parts per million (ppm) relative to tetramethylsilane (δ 0.00 ppm) or residual peak of CD₃OD (δ 3.31 ppm) or DMSO (δ 2.50 ppm). Chemical shifts for ¹³C NMR are expressed in ppm relative to CDCl₃ (δ 77.0 ppm), CD₃OD (δ 49.0 ppm) or DMSO (δ 39.52 ppm). Data are reported as follows: chemical shift, multiplicity (s = singlet, d = doublet, dd = doublet of doublets, t = triplet, td = triplet of doublets, m = multiplet, br = broad), coupling constant (Hz), and integration.

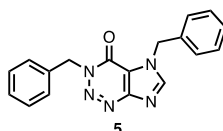
2. Synthesis of AHX derivatives

2-1. Synthesis of dibenzyl AHXs (5 and 5')



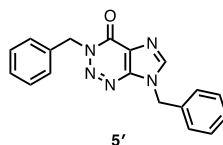
To a round-bottom flask containing a magnetic stirring bar, AHX (1.5 g, 11 mmol), benzyl bromide (3.8 g, 22 mmol) and DMF (50 mL) were added. Then, Cs₂CO₃ (11 g, 33 mmol) was added. The resultant mixture was stirred at 70 °C for 6 h. After cooling the reaction mixture to room temperature, the mixture was poured into water and extracted with EtOAc. The organic layer was washed with water, brine and dried over Na₂SO₄. After filtration, solvent was removed by evaporation. To the crude residue was added MeOH and then the mixture was sonicated. Resulting precipitation was then filtrated to afford the titled compound **5/5'** (5.6:1 mixture) as a white solid (1.2 g, 48% yield). These regioisomers can be separated by MPLC (chloroform/EtOAc = chloroform only to 4:1).

3,5-Dibenzyl-3,5-dihydro-4H-imidazo[4,5-*d*][1,2,3]triazin-4-one (5)



¹H NMR (600 MHz, CDCl₃) δ 7.94 (s, 1H), 7.50 (d, *J* = 7.2 Hz, 2H), 7.40–7.28 (m, 8H), 5.66 (s, 2H), 5.60 (s, 2H). ¹³C NMR (150 MHz, CDCl₃) δ 154.2, 151.3, 144.1, 135.5, 134.5, 129.3, 129.0, 128.8, 128.7, 128.3, 128.2, 116.9, 53.2, 51.2. HRMS (ESI⁺) *m/z* calcd for C₁₈H₁₆N₅O [M+H]⁺: 318.1349, found: 318.1349.

3,7-Dibenzyl-3,5-dihydro-4H-imidazo[4,5-*d*][1,2,3]triazin-4-one (5')

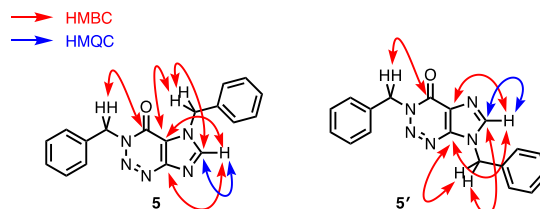


¹H NMR (600 MHz, CDCl₃) δ 7.91 (s, 1H), 7.53 (d, *J* = 6.6 Hz, 2H), 7.42–7.25 (m, 8H), 5.69 (s, 2H), 5.49 (s, 2H). ¹³C NMR (150 MHz, CDCl₃) δ 153.7, 145.0, 142.7, 135.6, 134.0, 129.3, 129.1,

128.7, 128.3, 128.2, 126.7, 53.4, 48.7 (one carbon peak was not observed because of overlapping).

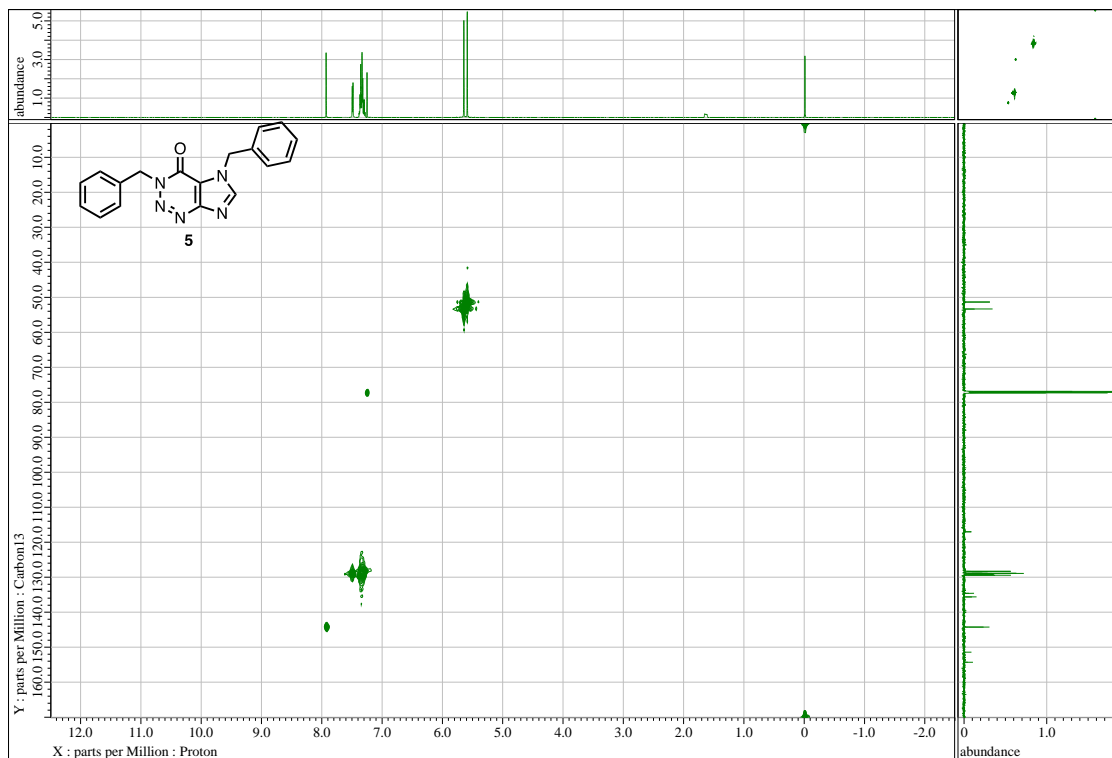
HRMS (ESI⁺) *m/z* calcd for C₁₈H₁₆N₅O [M+H]⁺: 318.1349, found: 318.1351.

HMBC/HMQC

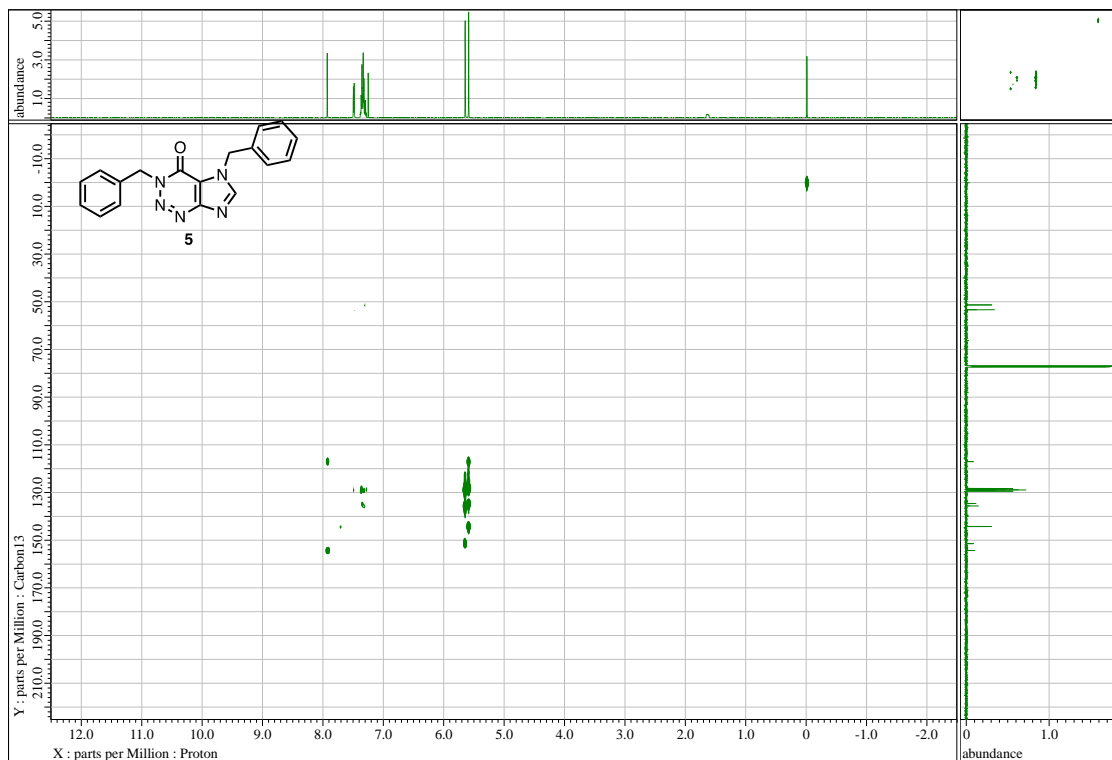


3,5-Dibenzyl-3,5-dihydro-4H-imidazo[4,5-d][1,2,3]triazin-4-one (5)

HMQC

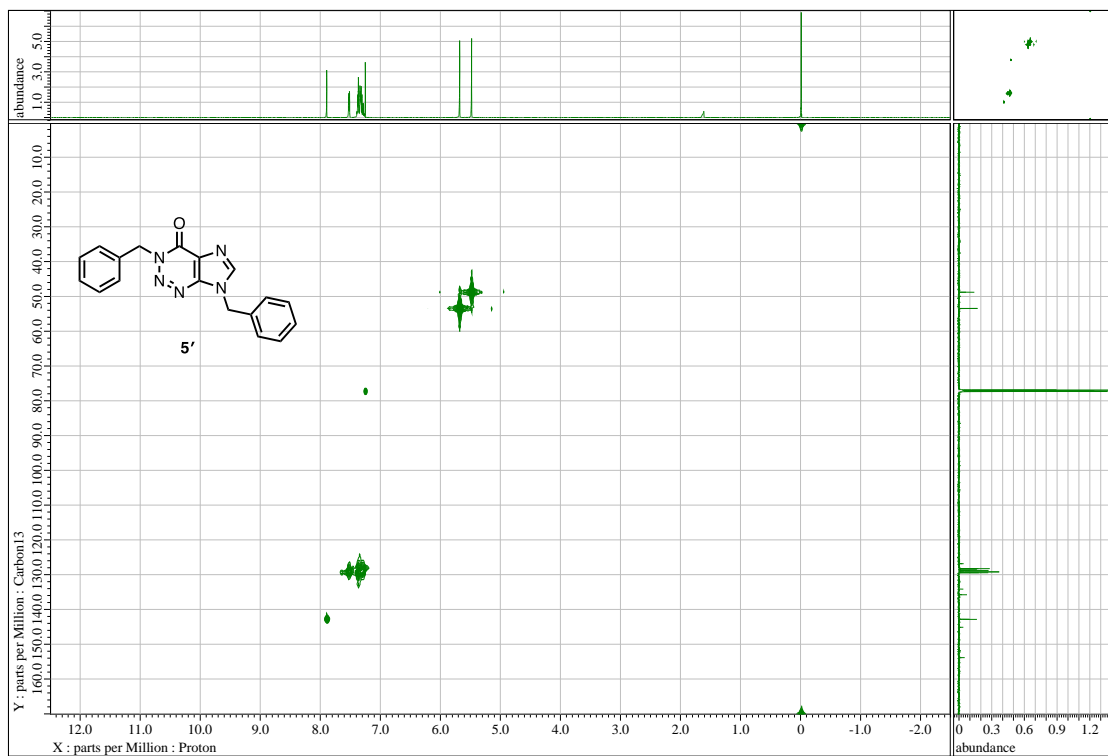


HMBC

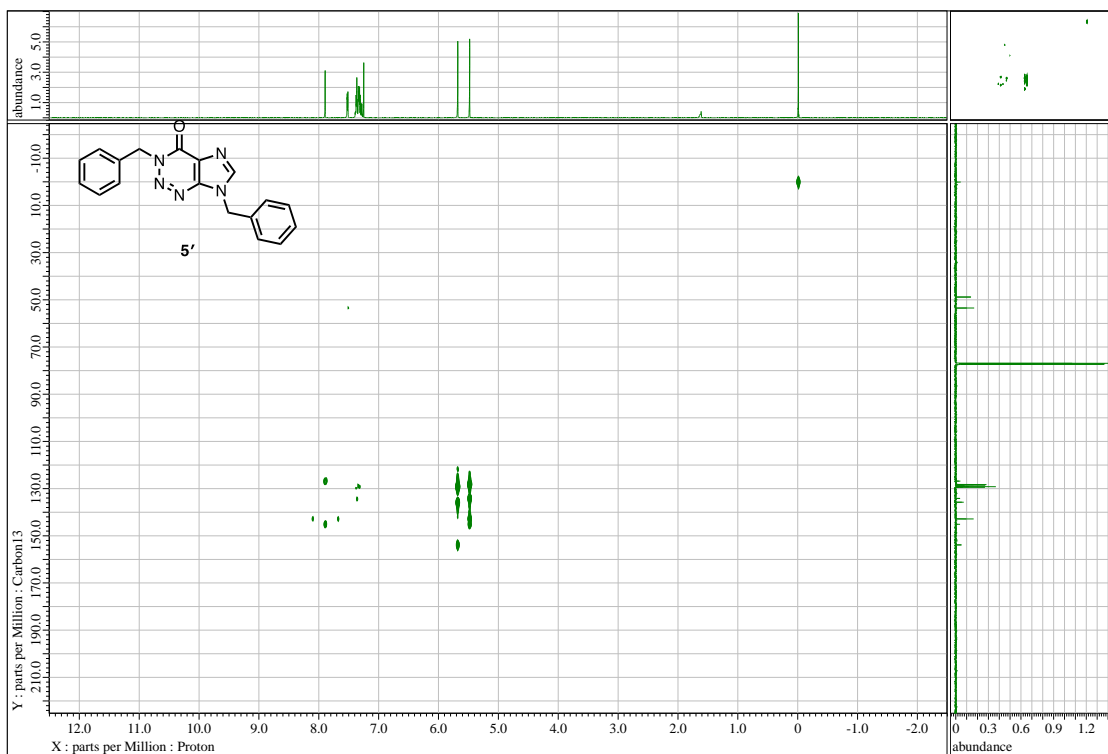


3,7-Dibenzyl-3,5-dihydro-4*H*-imidazo[4,5-*d*][1,2,3]triazin-4-one (5')

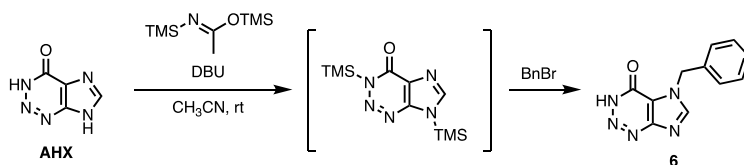
HMQC



HMBC

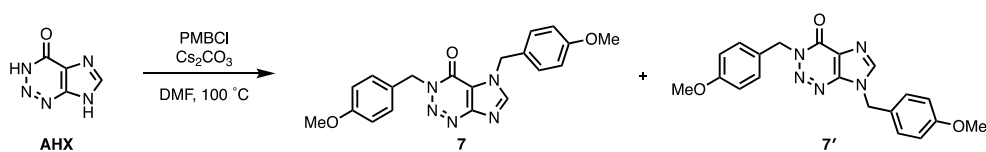


2-2. Synthesis of 5-benzyl-3,5-dihydro-4*H*-imidazo[4,5-*d*][1,2,3]triazin-4-one (6)



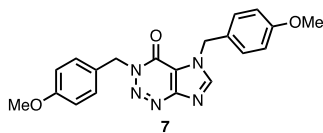
To a stirred suspension of AHX (50 mg, 0.36 mmol) in CH₃CN (2.0 mL) were added DBU (32 μL, 0.22 mmol) and *N,O*-bis(trimethylsilyl)acetamide (BSA, 89 μL, 0.36 mmol) at room temperature under an argon atmosphere. After being stirred for 30 min, benzyl bromide (48 μL, 0.40 mmol) was added to the reaction mixture. The resulting mixture was stirred at room temperature for 2 h. Then, MeOH was added and the mixture was concentrated under reduced pressure. The crude residue was purified by MPLC (chloroform/EtOAc = chloroform only to 3:2) to afford **6** as a white solid (26 mg, 31% yield). A single crystal of **6** was obtained from a THF solution through vapor diffusion method with pentane at room temperature, and the structure of **6** was determined by X-ray crystallographic analysis (see Table 3 and Figure 10 for detail). ¹H NMR (600 MHz, CD₃OD) δ 8.49 (s, 1H), 7.43 (d, *J* = 7.2 Hz, 2H), 7.38–7.30 (m, 3H), 5.67 (s, 2H). ¹³C NMR (150 MHz, CD₃OD) δ 155.6, 153.6, 146.5, 137.3, 130.1, 129.7, 129.1, 118.3, 52.0. HRMS (ESI⁺) *m/z* calcd for C₁₁H₉N₃ONa [M+Na]⁺: 250.0699, found: 250.0694.

2-3. Synthesis of di-*p*-methoxybenzyl AHXs (7 and 7')



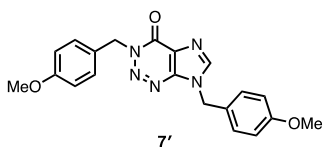
To a round-bottom flask containing a magnetic stirring bar, AHX (1.0 g, 7.3 mmol), *p*-methoxybenzyl chloride (2.4 g, 15 mmol) and DMF (30 mL) were added. Then, Cs₂CO₃ (7.1 g, 22 mmol) was added. The resultant mixture was stirred at 100 °C for 24 h. After cooling the reaction mixture to room temperature, the mixture was poured into water and extracted with EtOAc. The organic layer was washed with water, brine and dried over Na₂SO₄. After filtration, solvent was removed by evaporation. To the crude residue was added to Et₂O and then the mixture was sonicated. Resulting precipitation was then filtrated to afford the titled compound **7/7'** (2.8/1 mixture) as a white solid (2.0 g, 73% yield). These regioisomers can be separated by MPLC (chloroform/EtOAc = chloroform only to 4:1).

3,5-Bis(4-methoxybenzyl)-3,5-dihydro-4*H*-imidazo[4,5-*d*][1,2,3]triazin-4-one (7)



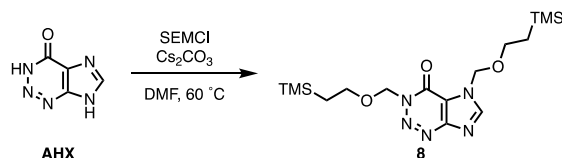
¹H NMR (600 MHz, CDCl₃) δ 7.90 (s, 1H), 7.47 (d, *J* = 9.0 Hz, 2H), 7.30 (d, *J* = 9.0 Hz, 2H), 6.89 (d, *J* = 9.0 Hz, 2H), 6.87 (d, *J* = 9.0 Hz, 2H), 5.60 (s, 2H), 5.53 (s, 2H), 3.80 (s, 3H), 3.78 (s, 3H). ¹³C NMR (150 MHz, CDCl₃) δ 160.0, 159.5, 154.2, 151.3, 143.9, 130.3, 129.8, 127.7, 126.5, 116.8, 114.6, 114.0, 55.3, 55.2, 52.8, 50.8. HRMS (ESI⁺) *m/z* calcd for C₂₀H₁₉N₅O₃Na [M+Na]⁺: 400.1380, found: 400.1377.

3,7-Bis(4-methoxybenzyl)-3,7-dihydro-4*H*-imidazo[4,5-*d*][1,2,3]triazin-4-one (7')



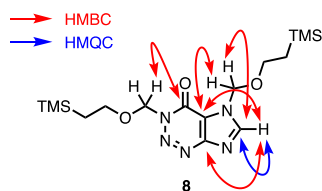
¹H NMR (600 MHz, CDCl₃) δ 7.87 (s, 1H), 7.49 (d, *J* = 9.0 Hz, 2H), 7.30 (d, *J* = 9.0 Hz, 2H), 6.89 (d, *J* = 9.0 Hz, 2H), 6.85 (d, *J* = 9.0 Hz, 2H), 5.63 (s, 2H), 5.41 (s, 2H), 3.80 (s, 3H), 3.77 (s, 3H). ¹³C NMR (150 MHz, CDCl₃) δ 160.1, 159.5, 153.7, 145.0, 142.6, 130.6, 129.8, 127.9, 126.7, 126.0, 114.6, 114.0, 55.3, 55.2, 52.9, 48.3. HRMS (ESI⁺) *m/z* calcd for C₂₀H₁₉N₅O₃Na [M+Na]⁺: 400.1380, found: 400.1377.

2-4. Synthesis of 3,5-bis((2-(trimethylsilyl)ethoxy)methyl)-3,5-dihydro-4*H*-imidazo[4,5-*d*][1,2,3]triazin-4-one (**8**)



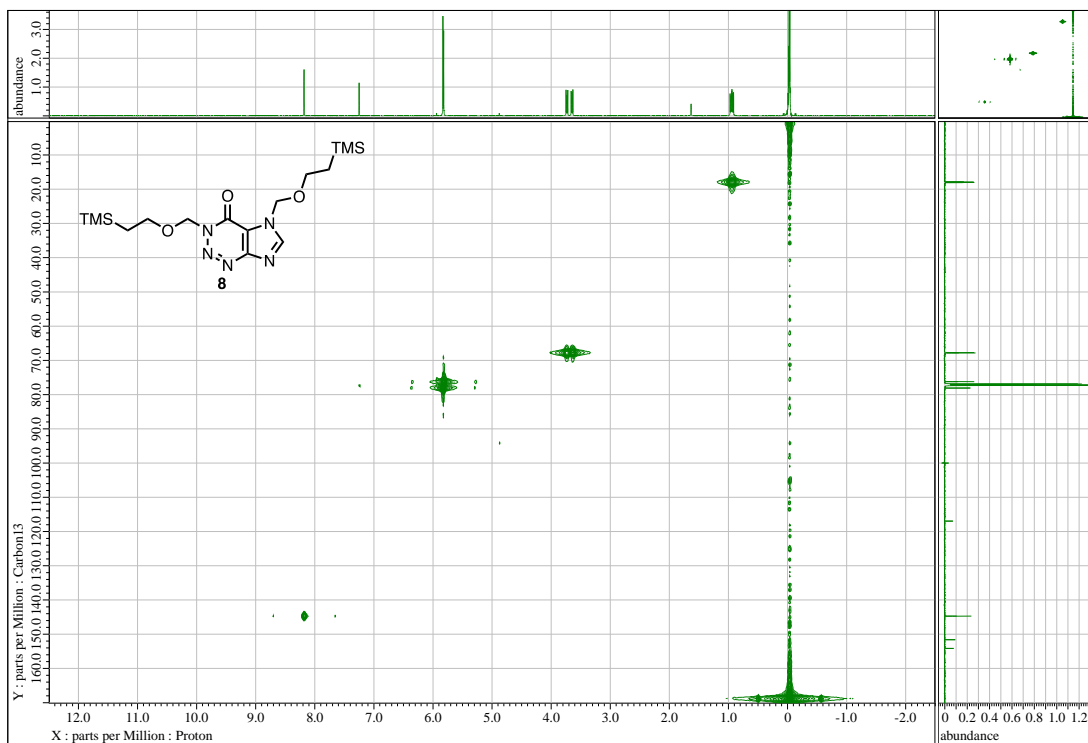
To a round-bottom flask containing a magnetic stirring bar, AHX (1.0 g, 7.3 mmol), 2-(chloromethoxy)ethyltrimethylsilane (2.5 g, 15 mmol) and DMF (50 mL) were added. Then, Cs₂CO₃ (7.1 g, 22 mmol) was added. The resultant mixture was stirred at 60 °C for 5 h. After cooling the reaction mixture to room temperature, the mixture was poured into water and extracted with EtOAc. The organic layer was washed with water, brine and dried over Na₂SO₄. After filtration, solvent was removed by evaporation. Then, the crude mixture was purified by MPLC (chloroform/EtOAc = 49:1 to 3:2) to afford **8** as a white solid (1.2 g, 40%). ¹H NMR (600 MHz, CDCl₃) δ 8.19 (s, 1H), 5.84 (s, 2H), 5.83 (s, 2H), 3.76–3.72 (m, 2H), 3.67–3.64 (m, 2H), 0.99–0.91 (m, 4H), –0.02 (s, 9H), –0.03 (s, 9H). ¹³C NMR (150 MHz, CDCl₃) δ 154.0, 151.5, 144.6, 116.8, 78.0, 76.1, 67.7, 67.6, 17.9, 17.7, –1.5 (2C). HRMS (ESI⁺) *m/z* calcd for C₁₆H₃₁N₅O₃Si₂Na [M+Na]⁺: 420.1858, found: 420.1853.

HMBC/HMQC

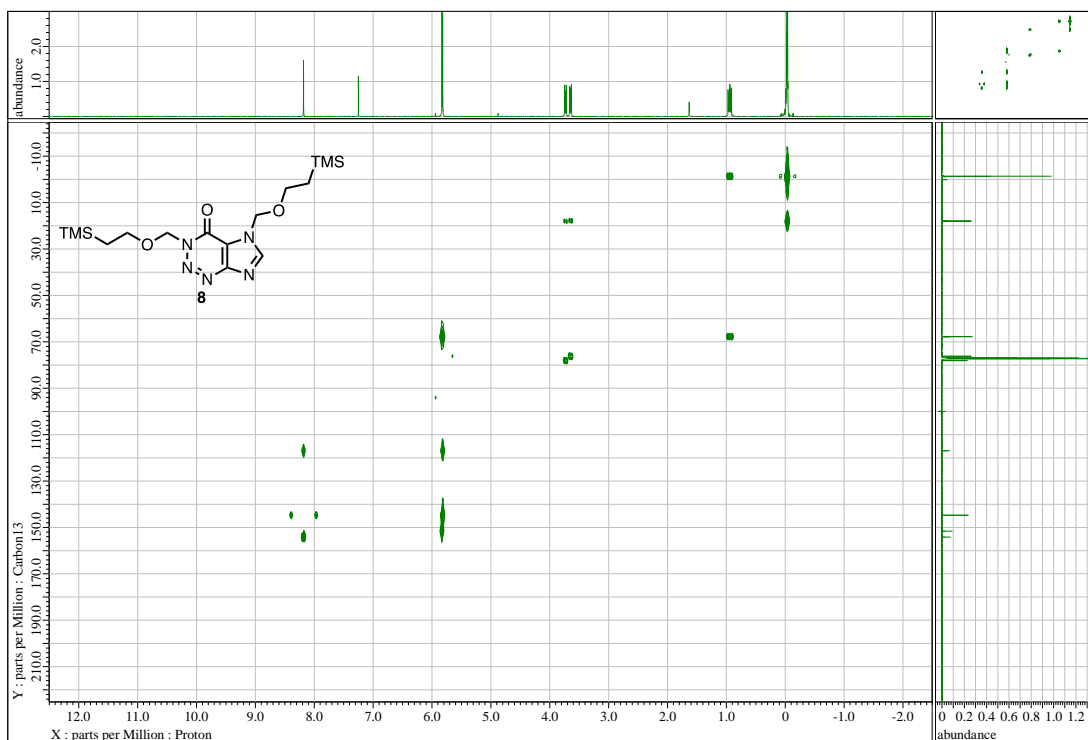


3,5-Bis((2-(trimethylsilyl)ethoxy)methyl)-3,5-dihydro-4H-imidazo[4,5-d][1,2,3]triazin-4-one (8)

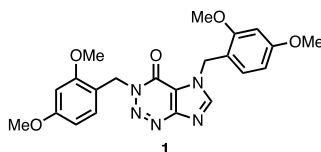
HMQC



HMBC

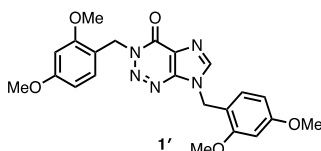


3,5-Bis(2,4-dimethoxybenzyl)-3,5-dihydro-4H-imidazo[4,5-d][1,2,3]triazin-4-one (1)



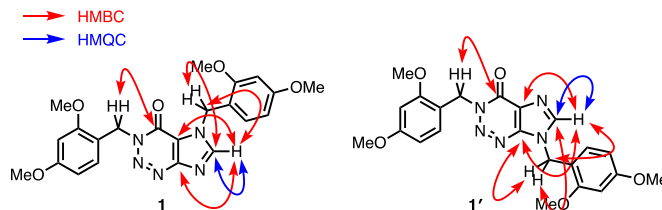
^1H NMR (600 MHz, CDCl_3) δ 8.04 (s, 1H), 7.49 (d, $J = 8.4$ Hz, 1H), 7.13 (d, $J = 8.4$ Hz, 1H), 6.48–6.41 (m, 4H), 5.64 (s, 2H), 5.53 (s, 2H), 3.83 (s, 3H), 3.82 (s, 3H), 3.79 (s, 3H), 3.78 (s, 3H). ^{13}C NMR (150 MHz, CDCl_3) δ 161.8, 160.8, 158.5, 158.4, 153.9, 151.5, 144.9, 132.1, 130.3, 116.7, 116.6, 115.6, 104.5, 104.1, 98.6, 98.5, 55.5, 55.4, 55.3 (2C), 47.9, 46.1. HRMS (ESI $^+$) m/z calcd for $\text{C}_{22}\text{H}_{23}\text{N}_5\text{O}_5\text{Na}$ $[\text{M}+\text{Na}]^+$: 460.1591, found: 460.1591.

3,7-Bis(2,4-dimethoxybenzyl)-3,7-dihydro-4H-imidazo[4,5-d][1,2,3]triazin-4-one (1')



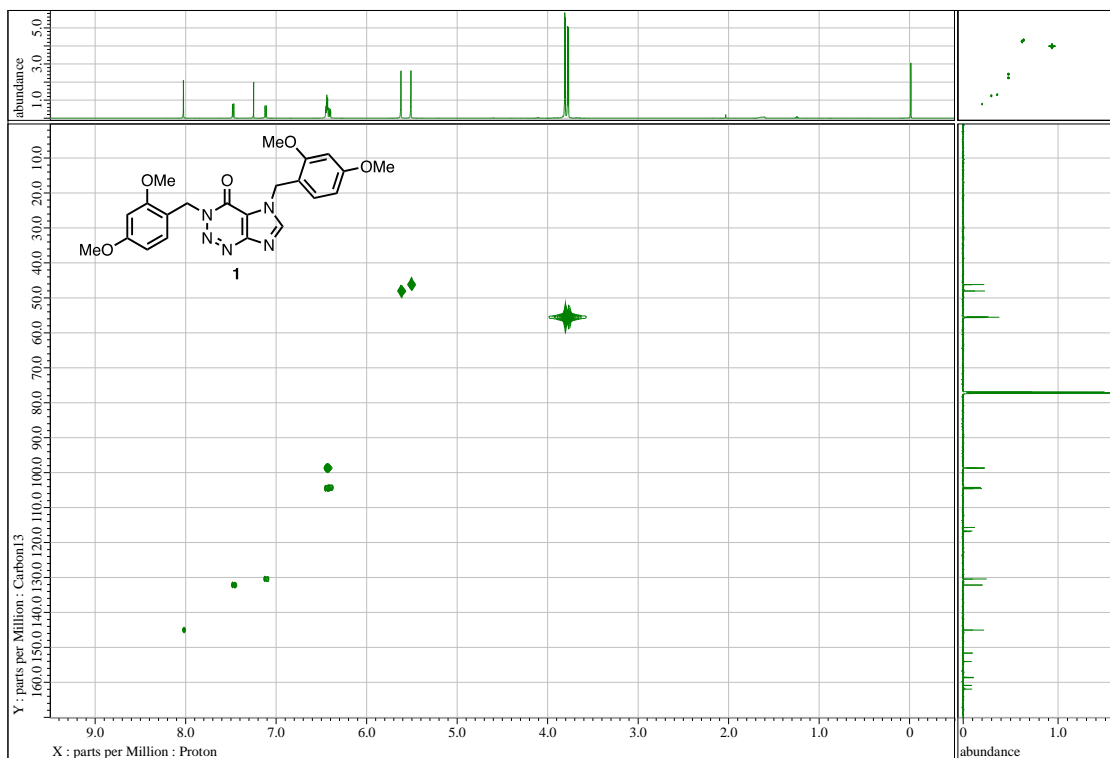
^1H NMR (600 MHz, CDCl_3) δ 7.97 (s, 1H), 7.38 (d, $J = 9.0$ Hz, 1H), 7.21 (d, $J = 9.0$ Hz, 1H), 6.48–6.39 (m, 4H), 5.65 (s, 2H), 5.40 (s, 2H), 3.83 (s, 3H), 3.82 (s, 3H), 3.80 (s, 3H), 3.77 (s, 3H). ^{13}C NMR (150 MHz, CDCl_3) δ 161.8, 160.8, 158.5 (2C), 154.1, 144.9, 143.4, 131.9, 131.0, 126.4, 116.8, 114.9, 104.4, 104.1, 98.7, 98.5, 55.55, 55.45, 55.4, 55.3, 47.9, 43.8. HRMS (ESI $^+$) m/z calcd for $\text{C}_{22}\text{H}_{23}\text{N}_5\text{O}_5\text{Na}$ $[\text{M}+\text{Na}]^+$: 460.1591, found: 460.1593.

HMBC/HMQC

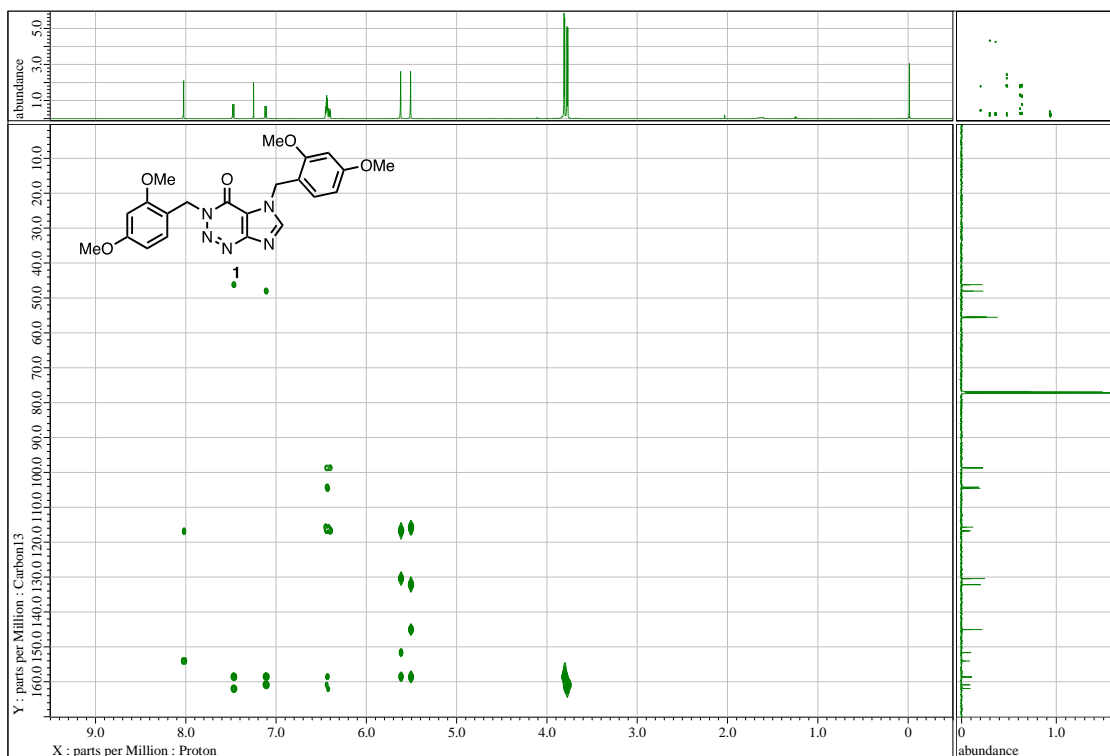


3,5-Bis(2,4-dimethoxybenzyl)-3,5-dihydro-4H-imidazo[4,5-d][1,2,3]triazin-4-one (1)

HMQC

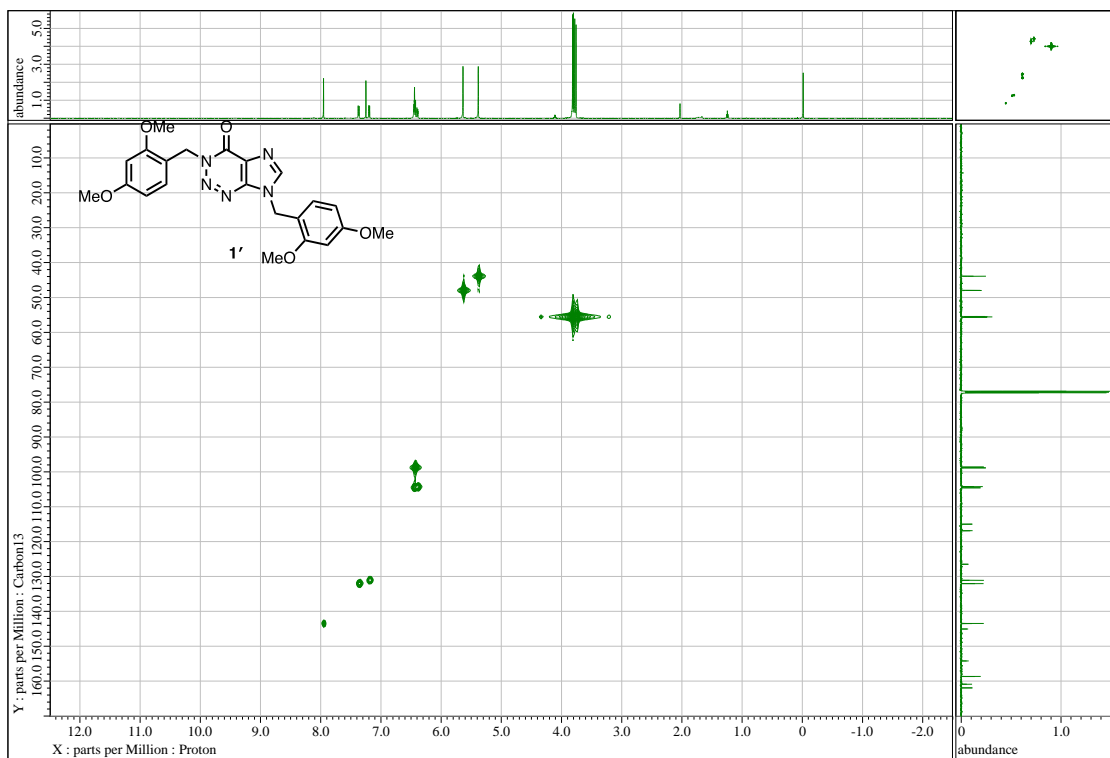


HMBC

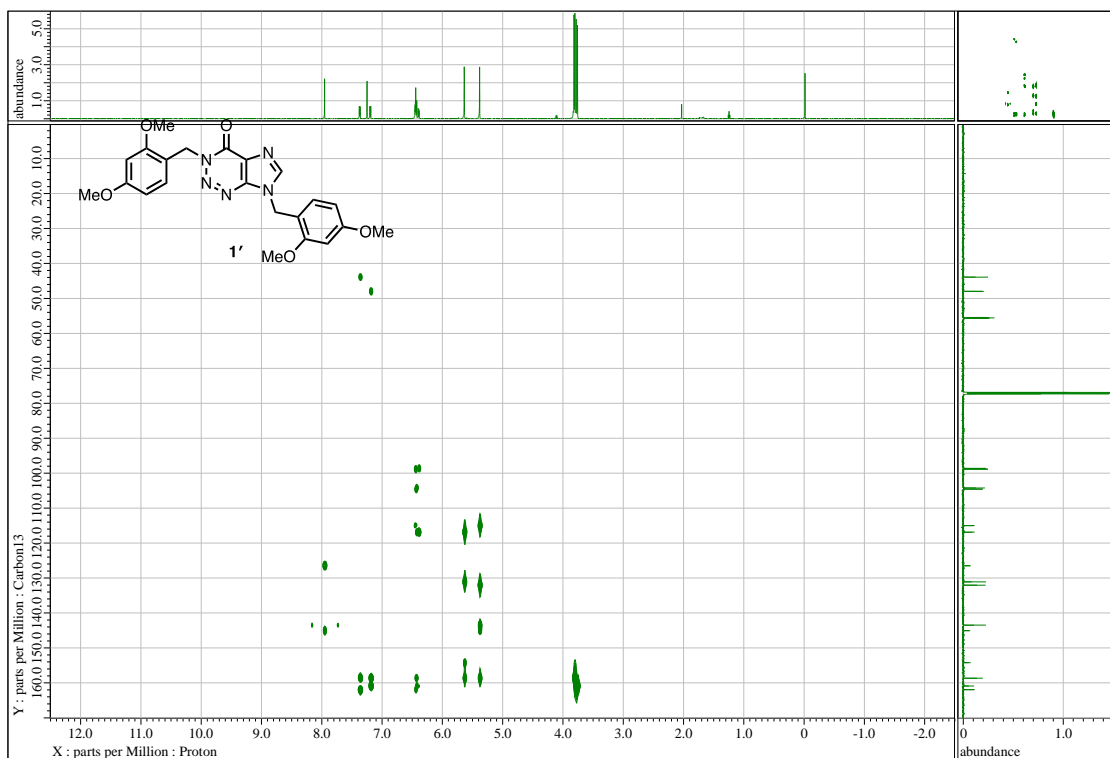


3,7-Bis(2,4-dimethoxybenzyl)-3,7-dihydro-4*H*-imidazo[4,5-*d*][1,2,3]triazin-4-one (1')

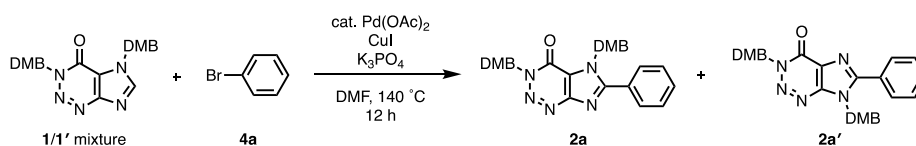
HMQC



HMBC

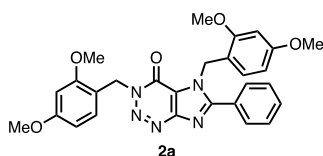


2-6. Synthesis of DMB-protected phenyl-AHXs (**2a** and **2a'**)



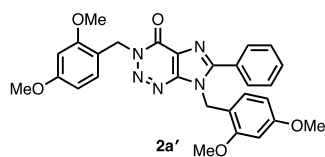
A Schlenk tube containing a magnetic stirring bar and K₃PO₄ (600 mg, 2.9 mmol) was dried with a heat gun for 3 min *in vacuo* and refilled with N₂ after cooling to room temperature. To this vessel were added the mixture of **1** and **1'** (500 mg, 1.1 mmol, **1/1'** = 4.2:1), CuI (435 mg, 2.3 mmol), Pd(OAc)₂ (13 mg, 0.057 mmol), bromobenzene (239 μ L, 2.3 mmol) and DMF (5.0 mL). The resultant mixture was stirred at 140 °C for 15 h under N₂ atmosphere. The reaction mixture was then cooled to room temperature, passed through a pad of Celite[®] with CHCl₃ as the eluent. The filtrate was washed with saturated NH₄Cl aq., water and brine. The organic extracts were dried over Na₂SO₄. After filtration, solvent was removed by evaporation. The resulting residue was purified by MPLC (chloroform/EtOAc = chloroform only to 3:1) to afford mixture of **2a** and **2a'** as a pale yellow amorphous solid (419 mg, 71%, **2a/2a'** = 2.6:1). For the NMR analyses, analytical amount of each isomer was isolated by PTLC (hexane/EtOAc = 4:1).

3,5-Bis(2,4-dimethoxybenzyl)-6-phenyl-3,5-dihydro-4*H*-imidazo[4,5-*d*][1,2,3]triazin-4-one (**2a**)



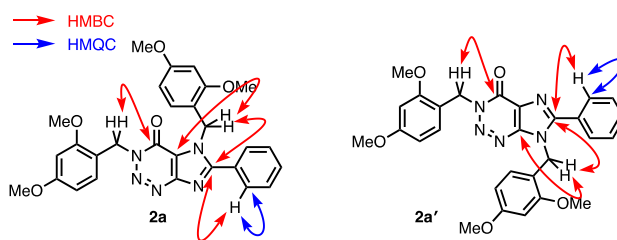
¹H NMR (600 MHz, CDCl₃) δ 7.65 (d, J = 8.4 Hz, 2H), 7.52–7.48 (m, 1H), 7.47–7.43 (m, 2H), 7.14 (d, J = 8.4 Hz, 1H), 6.72 (d, J = 8.4 Hz, 1H), 6.44 (d, J = 2.4 Hz, 1H), 6.41 (dd, J = 8.4, 2.4 Hz, 1H), 6.34 (d, J = 2.4 Hz, 1H), 6.29 (dd, J = 8.4, 2.4 Hz, 1H), 5.68 (s, 2H), 5.64 (s, 2H), 3.80 (s, 3H), 3.77 (s, 3H), 3.74 (s, 3H), 3.54 (s, 3H). ¹³C NMR (150 MHz, CDCl₃) δ 160.72, 160.70, 158.4, 157.4, 155.9, 153.4, 151.2, 130.6, 130.4, 129.3, 128.64, 128.61, 128.3, 118.6, 116.9, 116.7, 104.1, 104.0, 98.4, 98.2, 55.5, 55.3, 55.2, 55.0, 47.9, 45.9. HRMS (ESI⁺) m/z calcd for C₂₈H₂₇N₅O₅Na [M+Na]⁺: 536.1904, found: 536.1909.

3,7-Bis(2,4-dimethoxybenzyl)-6-phenyl-3,7-dihydro-4*H*-imidazo[4,5-*d*][1,2,3]triazin-4-one (**2a'**)



^1H NMR (600 MHz, CDCl_3) δ 7.73–7.70 (m, 2H), 7.52–7.48 (m, 1H), 7.47–7.43 (m, 2H), 7.24 (d, $J = 8.4$ Hz, 1H), 6.82 (d, $J = 8.4$ Hz, 1H), 6.45 (d, $J = 2.4$ Hz, 1H), 6.42 (dd, $J = 8.4, 2.4$ Hz, 1H), 6.39 (d, $J = 2.4$ Hz, 1H), 6.34 (dd, $J = 8.4, 2.4$ Hz, 1H), 5.69 (s, 2H), 5.57 (s, 2H), 3.81 (s, 3H), 3.77 (s, 3H), 3.75 (s, 3H), 3.62 (s, 3H). ^{13}C NMR (150 MHz, CDCl_3) δ 160.9, 160.7, 158.5, 157.4, 154.2, 154.1, 146.7, 131.0, 130.5, 129.2, 128.7, 128.6, 126.4, 116.8, 115.9, 104.1, 104.0, 98.5, 98.4, 55.5, 55.3 (2C), 55.1, 47.8, 43.7 (one carbon peak was not observed because of overlapping around 130 ppm). HRMS (ESI $^+$) m/z calcd for $\text{C}_{28}\text{H}_{28}\text{N}_5\text{O}_5$ $[\text{M}+\text{H}]^+$: 514.2085, found: 514.2086.

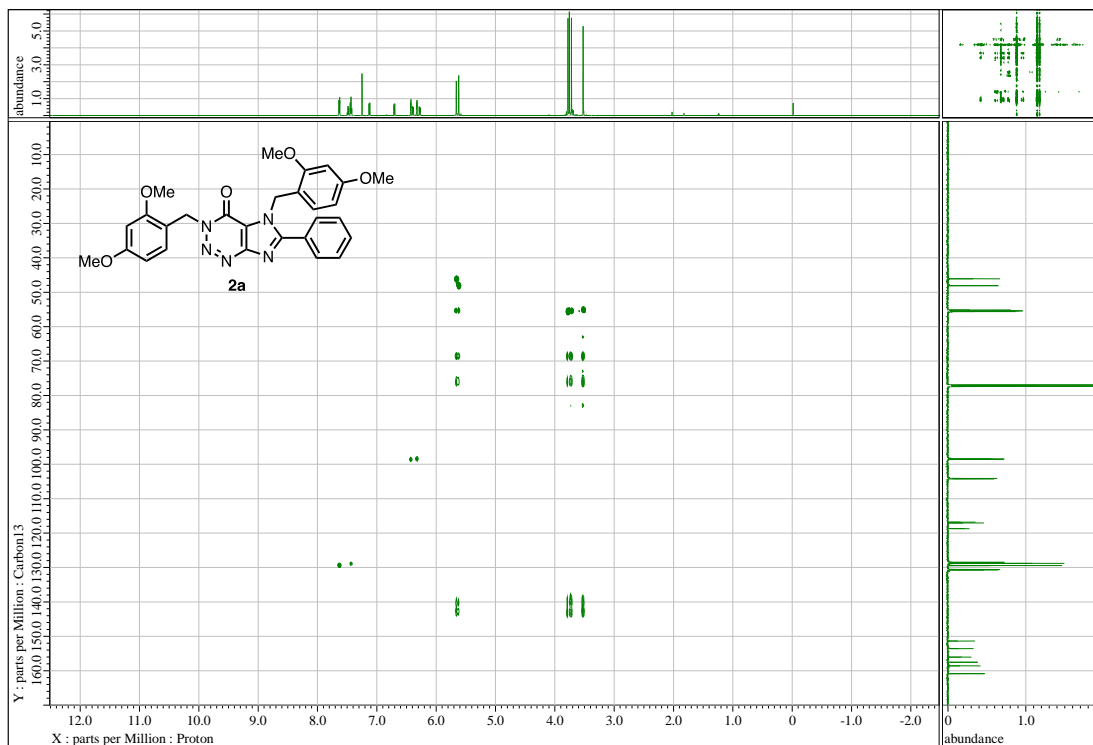
HMBC/HMQC



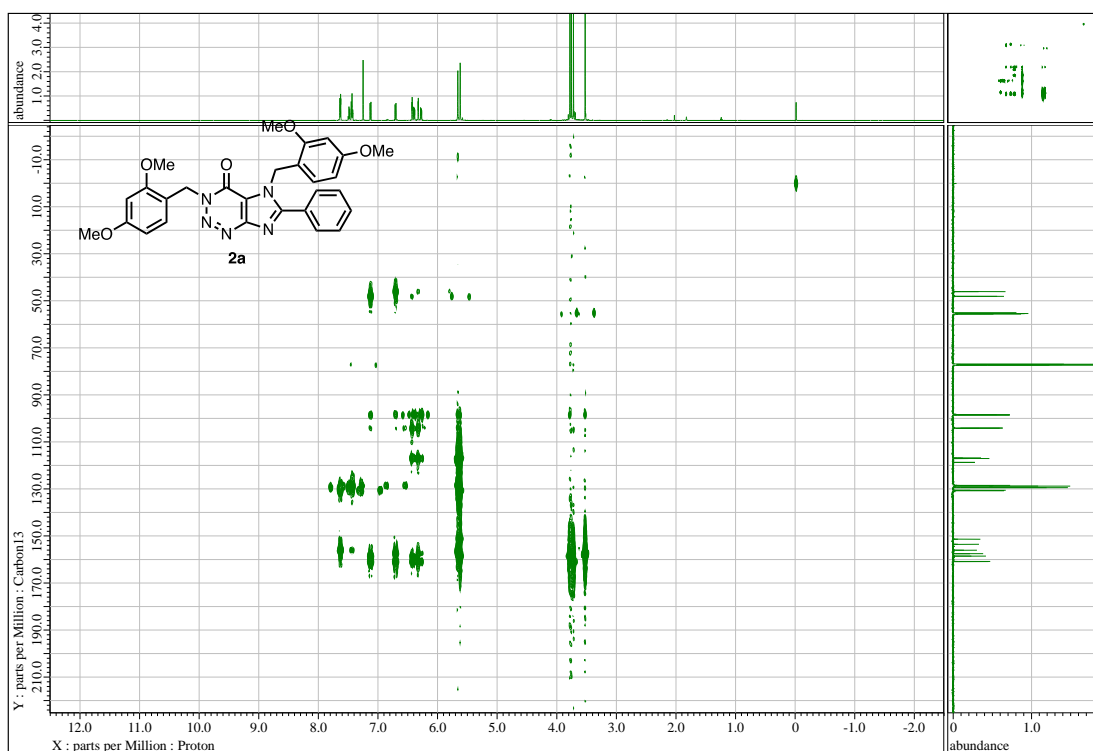
3,5-Bis(2,4-dimethoxybenzyl)-6-phenyl-3,5-dihydro-4*H*-imidazo[4,5-*d*][1,2,3]triazin-4-one

(2a)

HMQC

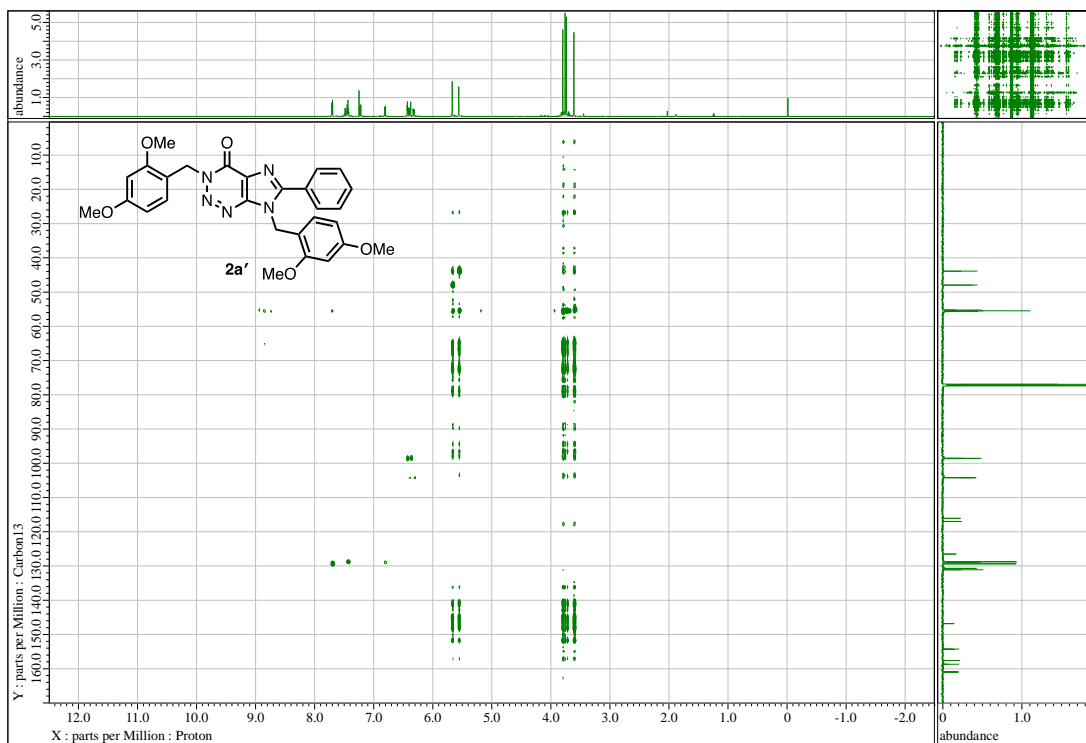


HMBC

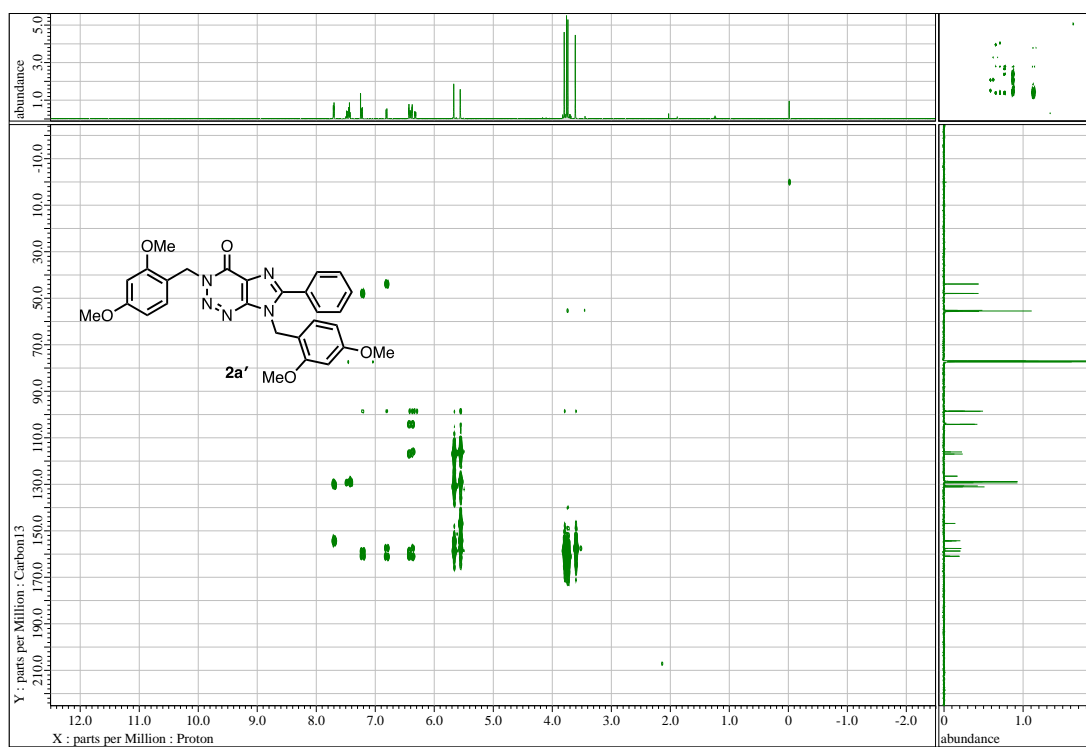


3,7-Bis(2,4-dimethoxybenzyl)-6-phenyl-3,7-dihydro-4*H*-imidazo[4,5-*d*][1,2,3]triazin-4-one
(2a')

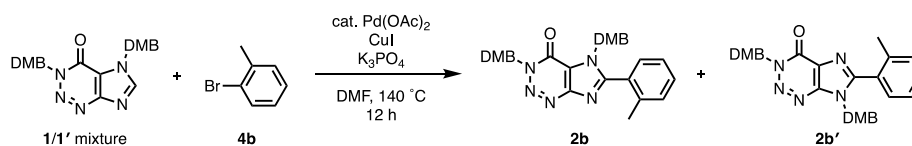
HMQC



HMBC

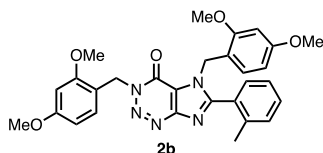


2-7. Synthesis of DMB-protected *o*-tolyl-AHXs (**2b** and **2b'**)



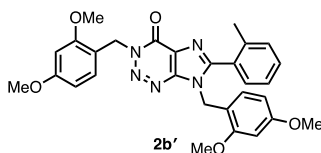
A Schlenk tube containing a magnetic stirring bar and K₃PO₄ (121 mg, 0.57 mmol) was dried with a heat gun for 3 min *in vacuo* and refilled with N₂ after cooling to room temperature. To this vessel were added the mixture of **1** and **1'** (100 mg, 0.23 mmol, **1/1'** = 4.2:1), CuI (87 mg, 0.46 mmol), Pd(OAc)₂ (2.6 mg, 0.011 mmol), 2-bromotoluene (55 μL, 0.46 mmol) and DMF (1.0 mL). The resultant mixture was stirred at 140 °C for 12 h under N₂ atmosphere. The reaction mixture was then cooled to room temperature, passed through a pad of Celite[®] with CHCl₃ as the eluent. The filtrate was washed with saturated NH₄Cl aq., water and brine. The organic extracts were dried over Na₂SO₄. After filtration, solvent was removed by evaporation. The resulting residue was purified by MPLC (chloroform/EtOAc = chloroform only to 3:1) to afford mixture of **2b** and **2b'** as a pale yellow amorphous solid (111 mg, 92%, **2b/2b'** = 4.2:1). For the NMR analyses, analytical amount of each isomer was isolated by PTLC (hexane/EtOAc = 4:1).

3,5-Bis(2,4-dimethoxybenzyl)-6-(*o*-tolyl)-3,5-dihydro-4*H*-imidazo[4,5-*d*][1,2,3]triazin-4-one (**2b**)



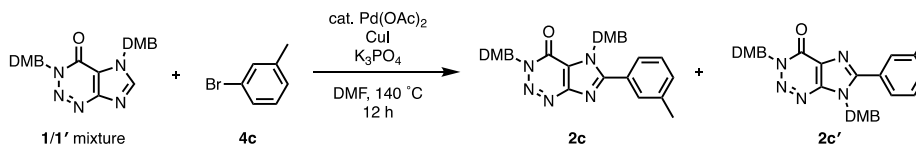
¹H NMR (600 MHz, CDCl₃) δ 7.38 (td, *J* = 7.8, 1.2 Hz, 1H), 7.26–7.20 (m, 3H), 7.17 (dd, *J* = 8.1, 0.9 Hz, 1H), 6.50–6.46 (m, 2H), 6.44 (dd, *J* = 9.0, 2.4 Hz, 1H), 6.21 (d, *J* = 2.4 Hz, 1H), 6.18 (dd, *J* = 8.4, 2.4 Hz, 1H), 5.69 (s, 2H), 5.49 (s, 2H), 3.84 (s, 3H), 3.79 (s, 3H), 3.72 (s, 3H), 3.35 (s, 3H), 1.96 (s, 3H). ¹³C NMR (150 MHz, CDCl₃) δ 160.9, 160.8, 158.6, 157.9, 155.7, 153.1, 151.4, 138.4, 130.6, 130.5, 130.3, 129.9, 129.6, 128.5, 125.6, 118.0, 116.7, 116.2, 104.1, 103.8, 98.5, 97.9, 55.6, 55.4, 55.3, 54.9, 48.1, 45.2, 19.4. HRMS (ESI⁺) *m/z* calcd for C₂₉H₃₀N₅O₅ [M+H]⁺: 528.2241, found: 528.2241.

3,7-Bis(2,4-dimethoxybenzyl)-6-(*o*-tolyl)-3,7-dihydro-4*H*-imidazo[4,5-*d*][1,2,3]triazin-4-one (2b')



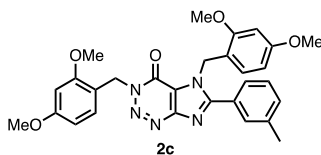
^1H NMR (600 MHz, CDCl_3) δ 7.39 (td, $J = 7.2, 1.8$ Hz, 1H), 7.28–7.20 (m, 4H), 6.76 (d, $J = 8.4$ Hz, 1H), 6.46 (d, $J = 2.4$ Hz, 1H), 6.44 (dd, $J = 7.8, 2.4$ Hz, 1H), 6.27–6.24 (m, 2H), 5.70 (s, 2H), 5.34 (s, 2H), 3.84 (s, 3H), 3.79 (s, 3H), 3.74 (s, 3H), 3.47 (s, 3H), 2.05 (s, 3H). ^{13}C NMR (150 MHz, CDCl_3) δ 161.0, 160.8, 158.6, 157.9, 154.13, 154.08, 146.0, 138.4, 131.0, 130.5, 130.4, 130.2, 129.8, 128.7, 125.9, 125.5, 116.9, 115.5, 104.1, 103.9, 98.5, 98.0, 55.6, 55.4, 55.3, 55.0, 47.9, 42.9, 19.6. HRMS (ESI $^+$) m/z calcd for $\text{C}_{29}\text{H}_{30}\text{N}_5\text{O}_5$ $[\text{M}+\text{H}]^+$: 528.2241, found: 528.2244.

2-8. Synthesis of DMB-protected *m*-tolyl-AHXs (2c and 2c')



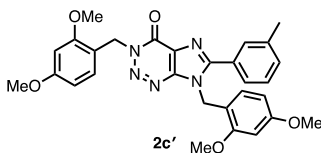
A Schlenk tube containing a magnetic stirring bar and K_3PO_4 (121 mg, 0.57 mmol) was dried with a heat gun for 3 min *in vacuo* and refilled with N_2 after cooling to room temperature. To this vessel, were added the mixture of **1** and **1'** (100 mg, 0.23 mmol, **1/1'** = 4.2:1), CuI (87 mg, 0.46 mmol), $\text{Pd}(\text{OAc})_2$ (2.6 mg, 0.011 mmol), 3-bromotoluene (55 μL , 0.46 mmol) and DMF (1.0 mL). The resultant mixture was stirred at 140 $^\circ\text{C}$ for 12 h under N_2 atmosphere. The reaction mixture was then cooled to room temperature, passed through a pad of Celite $^{\text{®}}$ with CHCl_3 as the eluent. The filtrate was washed with saturated NH_4Cl aq., water and brine. The organic extracts were dried over Na_2SO_4 . After filtration, solvent was removed by evaporation. The resulting residue was purified by MPLC (chloroform/EtOAc = chloroform only to 3:1) to afford mixture of **2c** and **2c'** as a pale yellow amorphous solid (79 mg, 65%, **2c/2c'** = 1.5:1). For the NMR analyses, analytical amount of each isomer was isolated by PTLC (hexane/EtOAc = 4:1).

3,5-Bis(2,4-dimethoxybenzyl)-6-(*m*-tolyl)-3,5-dihydro-4*H*-imidazo[4,5-*d*][1,2,3]triazin-4-one (2c)



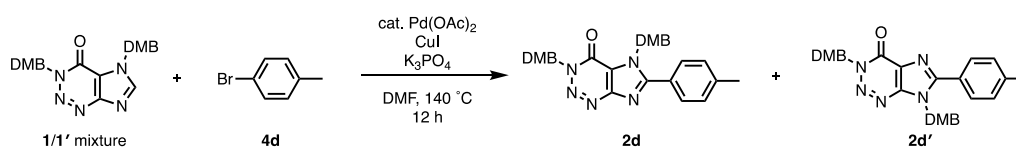
^1H NMR (600 MHz, CDCl_3) δ 7.49 (s, 1H), 7.40 (d, $J = 6.6$ Hz, 1H), 7.35–7.29 (m, 2H), 7.15 (d, $J = 8.4$ Hz, 2H), 6.72 (d, $J = 8.4$ Hz, 1H), 6.45 (d, $J = 2.4$ Hz, 2H), 6.41 (dd, $J = 8.4, 2.4$ Hz, 1H), 6.35 (d, $J = 2.4$ Hz, 1H), 6.30 (dd, $J = 8.4, 2.4$ Hz, 1H), 5.67 (s, 2H), 5.64 (s, 2H), 3.80 (s, 3H), 3.78 (s, 3H), 3.75 (s, 3H), 3.56 (s, 3H), 2.37 (s, 3H). ^{13}C NMR (150 MHz, CDCl_3) δ 160.7 (2C), 158.5, 157.4, 156.1, 153.4, 151.3, 138.5, 131.4, 130.5, 130.1, 128.50, 128.47, 128.4, 126.2, 118.6, 117.1, 116.7, 104.1, 104.0, 98.5, 98.3, 55.5, 55.34, 55.30, 55.0, 48.0, 45.9, 21.3. HRMS (ESI $^+$) m/z calcd for $\text{C}_{29}\text{H}_{30}\text{N}_5\text{O}_5$ $[\text{M}+\text{H}]^+$: 528.2241, found: 528.2243.

3,7-Bis(2,4-dimethoxybenzyl)-6-(*m*-tolyl)-3,7-dihydro-4*H*-imidazo[4,5-*d*][1,2,3]triazin-4-one (2c')



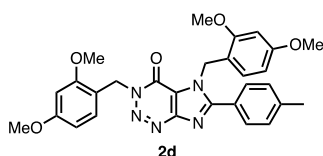
^1H NMR (600 MHz, CDCl_3) δ 7.59 (s, 1H), 7.46 (d, $J = 7.2$ Hz, 1H), 7.34–7.29 (m, 2H), 7.24 (d, $J = 8.4$ Hz, 1H), 6.82 (d, $J = 8.4$ Hz, 1H), 6.45 (d, $J = 2.4$ Hz, 1H), 6.42 (dd, $J = 8.7, 2.7$ Hz, 1H), 6.40 (d, $J = 2.4$ Hz, 1H), 6.35 (dd, $J = 8.4, 2.4$ Hz, 1H), 5.69 (s, 2H), 5.57 (s, 2H), 3.82 (s, 3H), 3.78 (s, 3H), 3.76 (s, 3H), 3.65 (s, 3H), 2.37 (s, 3H). ^{13}C NMR (150 MHz, CDCl_3) δ 160.9, 160.8, 158.6, 157.4, 154.5, 154.1, 146.7, 138.5, 131.3, 131.0, 130.2, 128.8, 128.6, 128.5, 126.4, 126.0, 116.9, 116.1, 104.12, 104.07, 98.5, 98.4, 55.5, 55.3 (2C), 55.1, 47.8, 43.7, 21.3. HRMS (ESI $^+$) m/z calcd for $\text{C}_{29}\text{H}_{29}\text{N}_5\text{O}_5\text{Na}$ $[\text{M}+\text{Na}]^+$: 550.2061, found: 550.2061.

2-9. Synthesis of DMB-protected *p*-tolyl-AHX (2d and 2d')



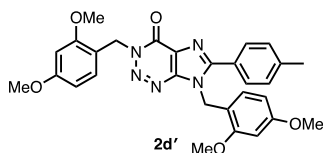
A Schlenk tube containing a magnetic stirring bar and K₃PO₄ (121mg, 0.57 mmol) was dried with a heat gun for 3 min *in vacuo* and refilled with N₂ after cooling to room temperature. To this vessel, were added the mixture of **1** and **1'** (100 mg, 0.23 mmol, **1/1'** = 4.2:1), CuI (87 mg, 0.46 mmol), Pd(OAc)₂ (2.6 mg, 0.011 mmol), 4-bromotoluene (56 μ L, 0.46 mmol) and DMF (1.0 mL). The resultant mixture was stirred at 140 °C for 12 h under N₂ atmosphere. The reaction mixture was then cooled to room temperature, passed through a pad of Celite[®] with CHCl₃ as the eluent. The filtrate was washed with saturated NH₄Cl aq., water and brine. The organic extracts were dried over Na₂SO₄. After filtration, solvent was removed by evaporation. The resulting residue was purified by MPLC (chloroform/EtOAc = chloroform only to 3:1) to afford mixture of **2d** and **2d'** as a pale yellow amorphous solid (83 mg, 69%, **2d/2d'** = 1.5:1). For the NMR analyses, analytical amount of each isomer was isolated by PTLC (hexane/EtOAc = 4:1).

3,5-Bis(2,4-dimethoxybenzyl)-6-(*p*-tolyl)-3,5-dihydro-4*H*-imidazo[4,5-*d*][1,2,3]triazin-4-one (**2d**)



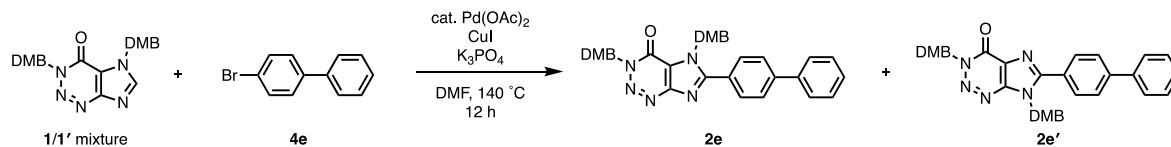
¹H NMR (600 MHz, CDCl₃) δ 7.55 (d, J = 8.4 Hz, 2H), 7.25 (d, J = 8.4 Hz, 2H), 7.13 (d, J = 8.4 Hz, 1H), 6.69 (d, J = 9.0 Hz, 1H), 6.44 (d, J = 2.4 Hz, 1H), 6.41 (dd, J = 9.0, 2.4 Hz, 1H), 6.36 (d, J = 2.4 Hz, 1H), 6.30 (dd, J = 9.0, 2.4 Hz, 1H), 5.66 (s, 2H), 5.63 (s, 2H), 3.79 (s, 3H), 3.77 (s, 3H), 3.75 (s, 3H), 3.59 (s, 3H), 2.41 (s, 3H). ¹³C NMR (150 MHz, CDCl₃) δ 160.71, 160.68, 158.4, 157.3, 156.1, 153.5, 151.2, 141.0, 130.4, 129.4, 129.2, 128.0, 125.7, 118.5, 117.1, 116.7, 104.1, 104.0, 98.5, 98.3, 55.5, 55.33, 55.30, 55.0, 47.9, 46.0, 21.5. HRMS (ESI⁺) m/z calcd for C₂₉H₃₀N₅O₅ [M+H]⁺: 528.2241, found: 528.2244.

3,7-Bis(2,4-dimethoxybenzyl)-6-(*p*-tolyl)-3,7-dihydro-4*H*-imidazo[4,5-*d*][1,2,3]triazin-4-one (2d')



¹H NMR (600 MHz, CDCl₃) δ 7.62 (d, *J* = 7.8 Hz, 2H), 7.28–7.22 (m, 3H), 6.78 (d, *J* = 9.0 Hz, 1H), 6.46–6.40 (m, 3H), 6.34 (dd, *J* = 9.0, 2.4 Hz, 1H), 5.68 (s, 2H), 5.56 (s, 2H), 3.81 (s, 3H), 3.78 (s, 3H), 3.76 (s, 3H), 3.67 (s, 3H), 2.41 (s, 3H). ¹³C NMR (150 MHz, CDCl₃) δ 160.8, 160.7, 158.6, 157.4, 154.5, 154.2, 146.7, 140.9, 131.0, 129.4, 129.1, 128.4, 126.4, 125.8, 116.9, 116.1, 104.11, 104.06, 98.51, 98.45, 55.5, 55.3 (2C), 55.2, 47.8, 43.8, 21.5. HRMS (ESI⁺) *m/z* calcd for C₂₉H₃₀N₅O₅ [M+H]⁺: 528.2241, found: 528.2244.

2-10. Synthesis of DMB-protected biphenyl-AHX (2e and 2e')

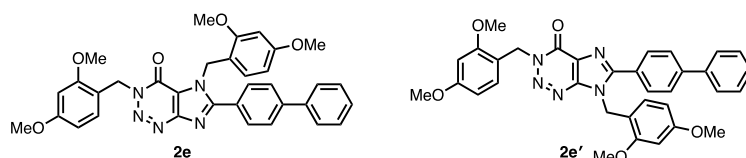


A Schlenk tube containing a magnetic stirring bar and K₃PO₄ (121mg, 0.57 mmol) was dried with a heat gun for 3 min *in vacuo* and refilled with N₂ after cooling to room temperature. To this vessel, were added the mixture of **1** and **1'** (100 mg, 0.23 mmol, **1/1'** = 4.2:1), CuI (87 mg, 0.46 mmol), Pd(OAc)₂ (2.6 mg, 0.011 mmol), 4-bromobiphenyl (107 mg, 0.46 mmol) and DMF (1.0 mL). The resultant mixture was stirred at 140 °C for 12 h under N₂ atmosphere. The reaction mixture was then cooled to room temperature, passed through a pad of Celite[®] with CHCl₃ as the eluent. The filtrate was washed with saturated NH₄Cl aq., water and brine. The organic extracts were dried over Na₂SO₄. After filtration, solvent was removed by evaporation. The resulting residue was purified by MPLC (chloroform/EtOAc = chloroform only to 3:1) to afford mixture of **2e** and **2e'** as a pale yellow amorphous solid (87 mg, 64%, **2e/2e'** = 1.0:0.63).

Mixture of

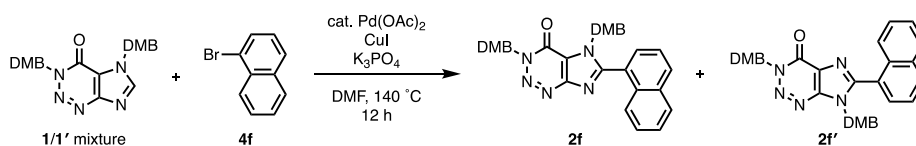
6-([1,1'-biphenyl]-4-yl)-3,5-bis(2,4-dimethoxybenzyl)-3,5-dihydro-4*H*-imidazo[4,5-*d*][1,2,3]triazin-4-one (**2e**)

and 6-([1,1'-biphenyl]-4-yl)-3,7-bis(2,4-dimethoxybenzyl)-3,7-dihydro-4*H*-imidazo[4,5-*d*][1,2,3]triazin-4-one (**2e'**) (**2e/2e'** = 1.0:0.63)



¹H NMR (600 MHz, CDCl₃) δ 7.82 (dd, *J* = 6.6, 1.8 Hz, 0.63×2H), 7.75 (dd, *J* = 6.6, 1.8 Hz, 2H), 7.69 (dd, *J* = 6.6, 1.8 Hz, 2H+0.63×2H), 7.62 (dd, *J* = 6.6, 1.2 Hz, 2H+0.63×2H), 7.49–7.44 (m, 2H+0.63×2H), 7.41–7.37 (m, 1H+0.63×1H), 7.25 (d, *J* = 7.8 Hz, 0.63×1H), 7.16 (d, *J* = 7.8 Hz, 1H), 6.84 (d, *J* = 8.4 Hz, 0.63×1H), 6.61 (d, *J* = 8.4 Hz, 1H), 6.46–6.40 (m, 2H+0.63×3H), 6.37–6.34 (m, 1H+0.63×1H), 6.32 (dd, *J* = 8.4, 2.4 Hz, 1H), 5.72 (s, 2H), 5.70 (s, 0.63×2H), 5.64 (s, 2H), 5.62 (s, 0.63×2H), 3.84–3.74 (m, 9H+0.63×9H), 3.66 (s, 0.63×3H), 3.58 (s, 3H). ¹³C NMR (150 MHz, CDCl₃) δ 160.9, 160.8 (2C), 160.7, 158.6, 158.5, 157.4, 157.3, 155.7, 154.1, 154.0, 153.5, 151.2, 146.8, 143.35, 143.27, 139.8, 131.0, 130.5, 129.8, 129.7, 128.9, 128.6, 128.2, 128.03, 128.01, 127.5, 127.4, 127.29, 127.27, 127.1, 126.5, 118.6, 117.0, 116.9, 116.7, 116.0, 104.11, 104.06, 98.51, 98.49, 98.46, 98.3, 55.54, 55.50, 55.34 (3C), 55.30, 55.2, 55.1, 48.0, 47.8, 46.0, 43.8 (five carbon peaks were overlapped between 115 ppm and 160 ppm). HRMS (ESI⁺) *m/z* calcd for C₃₄H₃₂N₅O₅ [M+H]⁺: 590.2398, found: 590.2402.

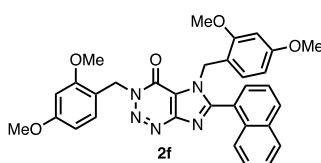
2-11. Synthesis of DMB-protected naphthyl-AHXs (**2f** and **2f'**)



A Schlenk tube containing a magnetic stirring bar and K₃PO₄ (121 mg, 0.57 mmol) was dried with a heat gun for 3 min *in vacuo* and refilled with N₂ after cooling to room temperature. To this vessel, were added the mixture of **1** and **1'** (100 mg, 0.23 mmol, **1/1'** = 4.2:1), CuI (87 mg, 0.46 mmol), Pd(OAc)₂ (2.6 mg, 0.011 mmol), 1-bromonaphthalene (64 μL, 0.46 mmol) and DMF (1.0 mL). The resultant mixture was stirred at 140 °C for 12 h under N₂ atmosphere. The reaction mixture was then cooled to room temperature, passed through a pad of Celite[®] with CHCl₃ as the

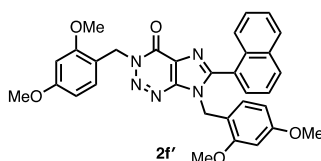
eluent. The filtrate was washed with saturated NH_4Cl aq., water and brine. The organic extracts were dried over Na_2SO_4 . After filtration, solvent was removed by evaporation. The resulting residue was purified by MPLC (chloroform/EtOAc = chloroform only to 3:1) to afford mixture of **2f** and **2f'** as a pale yellow amorphous solid (100 mg, 78%, **2f/2f'** = 2.8:1). For the NMR analyses, analytical amount of each isomer was separated by PTLC (hexane/EtOAc = 4:1).

3,5-Bis(2,4-dimethoxybenzyl)-6-(naphthalene-1-yl)-3,5-dihydro-4H-imidazo[4,5-*d*][1,2,3]triazin-4-one (2f)



^1H NMR (600 MHz, CDCl_3) δ 7.99 (d, $J = 9.0$ Hz, 1H), 7.90 (d, $J = 9.0$ Hz, 1H), 7.54–7.46 (m, 3H), 7.43–7.38 (m, 2H), 7.23 (d, $J = 8.4$ Hz, 1H), 6.50–6.44 (m, 3H), 6.06–6.02 (m, 2H), 5.72 (s, 2H), 5.50 (s, 2H), 3.85 (s, 3H), 3.80 (s, 3H), 3.64 (s, 3H), 3.12 (s, 3H). ^{13}C NMR (150 MHz, CDCl_3) δ 160.8, 160.7, 158.6, 157.6, 155.0, 153.3, 151.5, 133.4, 131.6, 130.8, 130.6, 129.9, 128.6, 128.2, 127.3, 126.40, 126.36, 124.9, 124.7, 118.3, 116.7, 116.2, 104.1, 103.6, 98.5, 97.8, 55.6, 55.4, 55.2, 54.6, 48.1, 45.6. HRMS (ESI $^+$) m/z calcd for $\text{C}_{32}\text{H}_{30}\text{N}_5\text{O}_5$ $[\text{M}+\text{H}]^+$: 564.2241, found: 564.2240.

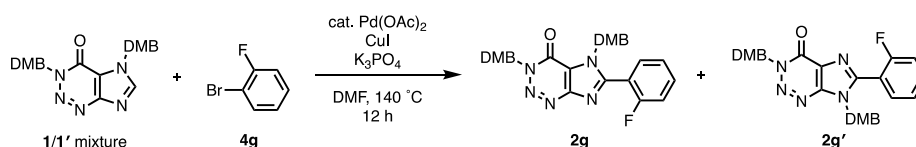
3,7-Bis(2,4-dimethoxybenzyl)-6-(naphthalene-1-yl)-3,7-dihydro-4H-imidazo[4,5-*d*][1,2,3]triazin-4-one (2f')



^1H NMR (600 MHz, CDCl_3) δ 8.00 (d, $J = 7.8$ Hz, 1H), 7.91 (d, $J = 8.4$ Hz, 1H), 7.62 (d, $J = 8.4$ Hz, 1H), 7.54–7.46 (m, 3H), 7.45–7.41 (m, 1H), 7.29 (d, $J = 8.4$ Hz, 1H), 6.76 (d, $J = 8.4$ Hz, 1H), 6.48 (d, $J = 2.4$ Hz, 1H), 6.45 (dd, $J = 8.4, 2.4$ Hz, 1H), 6.16 (dd, $J = 8.4, 2.4$ Hz, 1H), 6.11 (d, $J = 2.4$ Hz, 1H), 5.73 (s, 2H), 5.36 (s, 2H), 3.85 (s, 3H), 3.80 (s, 3H), 3.68 (s, 3H), 3.17 (s, 3H). ^{13}C NMR (150 MHz, CDCl_3) δ 160.9, 160.8, 158.6, 157.7, 154.1, 153.3, 146.3, 133.4, 131.8, 131.0, 130.8, 130.6, 128.7, 128.2, 127.2, 126.6, 126.4, 126.2, 125.2, 124.7, 116.9, 115.4, 104.1, 103.8, 98.5, 97.9, 55.6, 55.4, 55.3, 54.7, 47.9, 43.4. HRMS (ESI $^+$) m/z calcd for $\text{C}_{32}\text{H}_{30}\text{N}_5\text{O}_5$

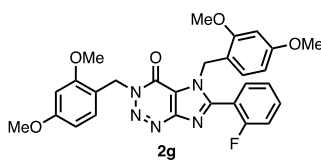
$[M+H]^+$: 564.2241, found: 564.2244.

2-12. Synthesis of DMB-protected *o*-fluorophenyl-AHXs (**2g** and **2g'**)



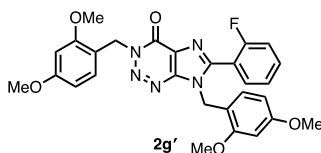
A Schlenk tube containing a magnetic stirring bar and K₃PO₄ (242 mg, 1.1 mmol) was dried with a heat gun for 3 min *in vacuo* and refilled with N₂ after cooling to room temperature. To this vessel, were added the mixture of **1** and **1'** (200 mg, 0.46 mmol, **1/1'** = 4.4:1), CuI (174 mg, 0.91 mmol), Pd(OAc)₂ (5.1 mg, 0.023 mmol), 2-bromofluorobenzene (99 μ L, 0.91 mmol) and DMF (1.0 mL). The resultant mixture was stirred at 140 °C for 12 h under N₂ atmosphere. The reaction mixture was then cooled to room temperature, passed through a pad of Celite[®] with CHCl₃ as the eluent. The filtrate was washed with saturated NH₄Cl aq., water and brine. The organic extracts were dried over Na₂SO₄. After filtration, solvent was removed by evaporation. The resulting residue was purified by MPLC (chloroform/EtOAc = 19:1 to 7:3) to afford **2g** (95 mg, 35%) and **2g'** (51 mg, 21%) as a pale yellow amorphous solid.

3,5-Bis(2,4-dimethoxybenzyl)-6-(*o*-fluorophenyl)-3,5-dihydro-4*H*-imidazo[4,5-*d*][1,2,3]triazin-4-one (**2g**)



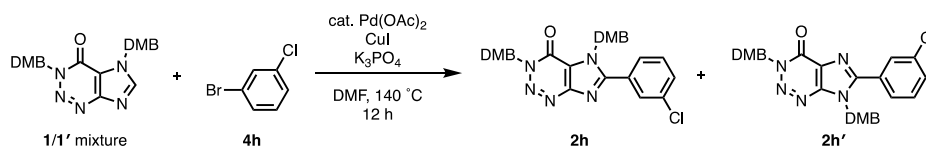
¹H NMR (600 MHz, CDCl₃) δ 7.54–7.49 (m, 1H), 7.43 (td, *J* = 7.5, 1.8 Hz, 1H), 7.24–7.19 (m, 2H), 7.17 (d, *J* = 8.4 Hz, 1H), 6.85 (d, *J* = 8.4 Hz, 1H), 6.46 (d, *J* = 2.4 Hz, 1H), 6.43 (dd, *J* = 8.4, 2.4 Hz, 1H), 6.21 (dd, *J* = 8.4, 2.4 Hz, 1H), 6.19 (d, *J* = 2.4 Hz, 1H), 5.67 (s, 2H), 5.61 (s, 2H), 3.82 (s, 3H), 3.79 (s, 3H), 3.71 (s, 3H), 3.34 (s, 3H). ¹³C NMR (150 MHz, CDCl₃) δ 161.0, 160.8, 159.1, 158.5, 158.0, 153.4, 151.4, 151.3, 132.63, 132.57, 132.1, 130.5, 130.4, 124.55, 124.53, 118.6, 117.8, 117.7, 116.7, 116.2, 116.0, 115.9, 104.1, 103.8, 98.5, 98.0, 55.6, 55.4, 55.3, 54.9, 48.1, 45.92, 45.88 (all observed peaks including splitting by ¹³C–⁹F couplings are shown). HRMS (ESI⁺) *m/z* calcd for C₂₈H₂₆FN₅O₅Na [M+Na]⁺: 554.1810, found: 554.1807.

3,7-Bis(2,4-dimethoxybenzyl)-6-(*o*-fluorophenyl)-3,7-dihydro-4*H*-imidazo[4,5-*d*][1,2,3]triazin-4-one (2g')



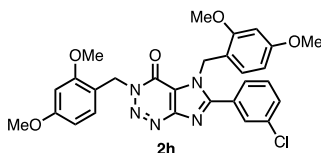
^1H NMR (600 MHz, CDCl_3) δ 7.55–7.49 (m, 2H), 7.25–7.20 (m, 3H), 7.05 (d, $J = 8.4$ Hz, 1H), 6.45 (d, $J = 2.4$ Hz, 1H), 6.42 (dd, $J = 9.0, 2.4$ Hz, 1H), 6.28 (dd, $J = 8.4, 2.4$ Hz, 1H), 6.23 (d, $J = 2.4$ Hz, 1H), 5.68 (s, 2H), 5.48 (s, 2H), 3.82 (s, 3H), 3.78 (s, 3H), 3.72 (s, 3H), 3.40 (s, 3H). ^{13}C NMR (150 MHz, CDCl_3) δ 161.1, 160.8, 159.1, 158.5, 158.0, 154.0, 149.7, 146.4, 132.53, 132.49, 132.3, 131.0, 130.9, 126.4, 124.5, 118.0, 117.9, 116.8, 115.9, 115.8, 115.3, 104.1, 103.9, 98.5, 98.0, 55.5, 55.33, 55.28, 54.9, 47.9, 43.80, 43.76 (all observed peaks including splitting by ^{13}C – ^{19}F couplings are shown). HRMS (ESI $^+$) m/z calcd for $\text{C}_{28}\text{H}_{26}\text{FN}_5\text{O}_5\text{Na}$ [$\text{M}+\text{Na}$] $^+$: 554.1810, found: 554.1806.

2-13. Synthesis of DMB-protected *m*-chlorophenyl-AHXas (2h and 2h')



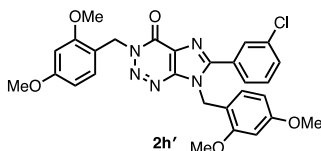
A Schlenk tube containing a magnetic stirring bar and K_3PO_4 (242 mg, 1.1 mmol) was dried with a heat gun for 3 min *in vacuo* and refilled with N_2 after cooling to room temperature. To this vessel, were added the mixture of **1** and **1'** (200 mg, 0.46 mmol, **1/1'** = 4.4:1), CuI (174 mg, 0.91 mmol), Pd(OAc)₂ (5.1 mg, 0.023 mmol), 3-bromochlorobenzene (107 μL , 0.91 mmol) and DMF (1.0 mL). The resultant mixture was stirred at 140 °C for 12 h under N_2 atmosphere. The reaction mixture was then cooled to room temperature, passed through a pad of Celite[®] with CHCl_3 as the eluent. The filtrate was washed with saturated NH_4Cl aq., water and brine. The organic extracts were dried over Na_2SO_4 . After filtration, solvent was removed by evaporation. The resulting residue was purified by MPLC (chloroform/EtOAc = chloroform only to 8:2) to afford mixture of **2h** and **2h'** as a pale yellow amorphous solid (87 mg, 35%, **2h/2h'** = 1.3:1). For the NMR analyses, analytical amount of each isomer was separated by PTLC (chloroform/EtOAc = 9:1).

3,5-Bis(2,4-dimethoxybenzyl)-6-(*m*-chlorophenyl)-3,5-dihydro-4*H*-imidazo[4,5-*d*][1,2,3]triazin-4-one (2h)



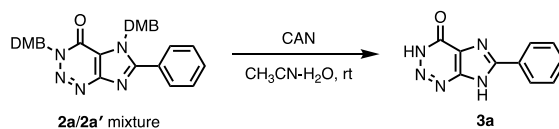
^1H NMR (600 MHz, CDCl_3) δ 7.64 (d, $J = 1.2$ Hz, 1H), 7.53 (d, $J = 7.2$ Hz, 1H), 7.48 (d, $J = 8.4$ Hz, 1H), 7.39 (t, $J = 8.1$ Hz, 1H), 7.16 (d, $J = 9.0$ Hz, 1H), 6.77 (d, $J = 8.4$ Hz, 1H), 6.45 (d, $J = 2.4$ Hz, 1H), 6.42 (dd, $J = 8.1, 2.7$ Hz, 1H), 6.35 (d, $J = 1.8$ Hz, 1H), 6.31 (dd, $J = 8.4, 1.8$ Hz, 1H), 5.68 (s, 2H), 5.65 (s, 2H), 3.81 (s, 3H), 3.78 (s, 3H), 3.75 (s, 3H), 3.56 (s, 3H). ^{13}C NMR (150 MHz, CDCl_3) δ 161.0, 160.8, 158.5, 157.4, 154.3, 153.3, 151.3, 134.7, 130.7, 130.6, 130.4, 129.9, 129.5, 128.8, 127.4, 118.8, 116.6, 116.5, 104.2, 104.1, 98.5, 98.3, 55.5, 55.4, 55.3, 55.1, 48.1, 45.9. HRMS (ESI $^+$) m/z calcd for $\text{C}_{28}\text{H}_{26}\text{ClN}_5\text{O}_5\text{Na}$ $[\text{M}+\text{Na}]^+$: 570.1515, found: 570.1512.

3,7-Bis(2,4-dimethoxybenzyl)-6-(*m*-chlorophenyl)-3,7-dihydro-4*H*-imidazo[4,5-*d*][1,2,3]triazin-4-one (2h')



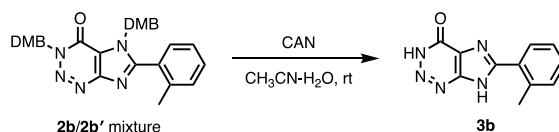
^1H NMR (600 MHz, CDCl_3) δ 7.73 (s, 1H), 7.60 (d, $J = 7.8$ Hz, 1H), 7.48 (d, $J = 8.4$ Hz, 1H), 7.39 (t, $J = 7.8$ Hz, 1H), 7.25 (d, $J = 9.6$ Hz, 1H), 6.87 (d, $J = 7.8$ Hz, 1H), 6.45 (s, 1H), 6.43 (d, $J = 8.4$ Hz, 1H), 6.40 (s, 1H), 6.35 (d, $J = 8.4$ Hz, 1H), 5.69 (s, 2H), 5.58 (s, 2H), 3.82 (s, 3H), 3.78 (s, 3H), 3.76 (s, 3H), 3.65 (s, 3H). ^{13}C NMR (150 MHz, CDCl_3) δ 161.1, 160.8, 158.6, 157.5, 154.0, 152.6, 146.8, 134.7, 131.1, 130.62, 130.55, 129.9, 129.4, 129.2, 127.3, 126.3, 116.8, 115.6, 104.3, 104.2, 98.6, 98.4, 55.6, 55.4 (2C), 55.2, 47.9, 43.6. HRMS (ESI $^+$) m/z calcd for $\text{C}_{28}\text{H}_{26}\text{ClN}_5\text{O}_5\text{Na}$ $[\text{M}+\text{Na}]^+$: 570.1515, found: 570.1514.

2-14. Synthesis of 6-phenyl-3,7-dihydro-4H-imidazo[4,5-d][1,2,3]triazin-4-one (**3a**)



The mixture of **2a** and **2a'** (620 mg, 1.2 mmol, **2a/2a'** = 3.6:1) and CH₃CN/H₂O = 10:1 solution (66 mL) was added to a round-bottom flask containing a magnetic stirring bar under open air. Then, ammonium cerium(IV) nitrate (CAN) (5.3 g, 9.7 mmol) was added and stirred at room temperature for 4 h. After reaction, solvent of the mixture was removed by reduced pressure. The resulting residue was dissolved with EtOAc and washed with water and brine. The organic extracts were then dried over Na₂SO₄. After filtration, solvent was removed by evaporation. The resulting residue was purified twice by MPLC (first: chloroform/MeOH = chloroform only to 9:1; second: EtOAc only). The obtained solid was further purified by recrystallization from EtOAc to afford **3a** as a white solid (109 mg, 42% yield). A single crystal of **3a** was obtained as a **3a**·H₂O complex from CH₃CN solution through slow evaporation at room temperature, and the structure of **3a**·H₂O complex was determined by X-ray crystallographic analysis (see Table 3 and Figure 11 for detail). ¹H NMR (600 MHz, CD₃OD) δ 8.18–8.14 (m, 2H), 7.59–7.55 (m, 3H). ¹³C NMR (150 MHz, CD₃OD) δ 155.3, 154.3 (br), 154.1 (br), 132.5, 130.3, 129.6, 128.4, 122.7 (br). HRMS (ESI⁺) *m/z* calcd for C₁₀H₇N₅O_nNa [M+Na]⁺: 236.0543, found: 236.0543.

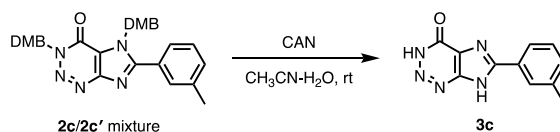
2-15. Synthesis of 6-(*o*-tolyl)-3,7-dihydro-4H-imidazo[4,5-d][1,2,3]triazin-4-one (**3b**)



The mixture of **2b** and **2b'** (622 mg, 1.2 mmol, **2b/2b'** = 3.8:1) and CH₃CN/H₂O = 10:1 solution (66 mL) were added to a round-bottom flask containing a magnetic stirring bar under open air. Then, CAN (5.2 g, 9.4 mmol) was added and stirred at room temperature for 4 h. After reaction, solvent of the mixture was removed by reduced pressure. The resulting residue was dissolved in EtOAc and washed with water and brine. The organic extracts were then dried over Na₂SO₄. After filtration, solvent was removed by evaporation. The resulting residue was purified twice by MPLC (first: chloroform/MeOH = chloroform only to 9:1; second: EtOAc only). The obtained solid was further purified by recrystallization from EtOAc to afford **3b** as a white solid (57 mg,

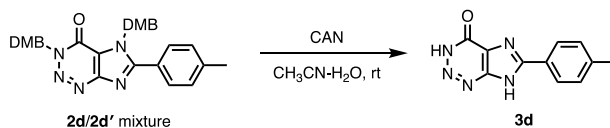
21% yield). ^1H NMR (600 MHz, CD_3OD) δ 7.66 (d, $J = 7.8$ Hz, 1H), 7.48–7.34 (m, 3H), 2.56 (s, 3H). ^{13}C NMR (150 MHz, CD_3OD) δ 155.9, 154.3 (br), 153.7 (br), 139.2, 132.5, 131.9, 131.0, 129.6, 127.3, 121.9 (br), 20.7. HRMS (ESI $^+$) m/z calcd for $\text{C}_{11}\text{H}_9\text{N}_5\text{ONa}$ $[\text{M}+\text{Na}]^+$: 250.0699, found: 250.0699.

2-16. Synthesis of 6-(*m*-tolyl)-3,7-dihydro-4*H*-imidazo[4,5-*d*][1,2,3]triazin-4-one (**3c**)



The mixture of **2c** and **2c'** (486 mg, 0.92 mmol, **2c/2c'** = 2.2:1) and $\text{CH}_3\text{CN}/\text{H}_2\text{O} = 10:1$ solution (66 mL) were added to a round-bottom flask containing a magnetic stirring bar under open air. Then, CAN (4.0 g, 7.4 mmol) was added and stirred at room temperature for 4 h. After reaction, solvent of the mixture was removed by reduced pressure. The resulting residue was dissolved in EtOAc and washed with water and brine. The organic extracts were then dried over Na_2SO_4 . After filtration, solvent was removed by evaporation. The resulting residue was purified twice by MPLC (first: chloroform/MeOH = chloroform only to 9:1; second: EtOAc only). The obtained solid was further purified by recrystallization from EtOAc to afford **3c** as a white solid (65 mg, 31% yield). ^1H NMR (600 MHz, CD_3OD) δ 7.99 (s, 1H), 7.94 (d, $J = 7.2$ Hz, 1H), 7.46 (t, $J = 7.2$ Hz, 1H), 7.41 (d, $J = 7.2$ Hz, 1H), 2.47 (s, 3H). ^{13}C NMR (150 MHz, CD_3OD) δ 155.3, 154.3 (br), 154.0 (br), 140.4, 133.3, 130.2, 129.4, 128.8, 125.5, 122.5 (br), 21.4. HRMS (ESI $^+$) m/z calcd for $\text{C}_{11}\text{H}_9\text{N}_5\text{ONa}$ $[\text{M}+\text{Na}]^+$: 250.0699, found: 250.0694.

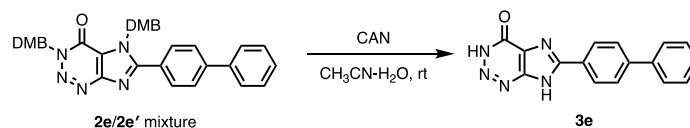
2-17. Synthesis of 6-(*p*-tolyl)-3,7-dihydro-4*H*-imidazo[4,5-*d*][1,2,3]triazin-4-one (**3d**)



The mixture of **2d** and **2d'** (707 mg, 1.3 mmol, **2d/2d'** = 2.5:1) and $\text{CH}_3\text{CN}/\text{H}_2\text{O} = 10:1$ solution (66 mL) was added to a round-bottom flask containing a magnetic stirring bar under open air. Then, CAN (5.9 g, 11 mmol) was added and stirred at room temperature for 5 h. After reaction, solvent of the mixture was removed by reduced pressure. The resulting residue was dissolved in EtOAc and washed with water and brine. The organic extracts were then dried over Na_2SO_4 . After

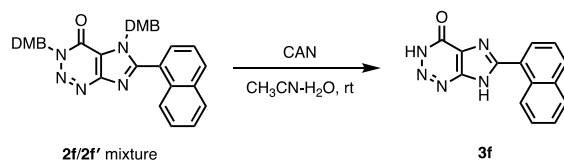
filtration, solvent was removed by evaporation. The resulting residue was purified twice by MPLC (first: chloroform/MeOH = chloroform only to 9:1; second: EtOAc only). The obtained solid was further purified by recrystallization from EtOAc to afford **3d** as a white solid (55 mg, 18% yield). ¹H NMR (600 MHz, CD₃OD) δ 8.05 (d, *J* = 7.8 Hz, 2H), 7.38 (d, *J* = 7.8 Hz, 2H), 2.44 (s, 3H). ¹³C NMR (150 MHz, CD₃OD) δ 155.8 (br), 154.4 (br), 143.3, 130.9, 128.3, 127.0 (br), 21.5 (two peaks were not observed because of the quite low solubility in CD₃OD). HRMS (ESI⁺) *m/z* calcd for C₁₁H₉N₅ONa [M+Na]⁺: 250.0699, found: 250.0696.

2-18. Synthesis of 6-([1,1'-biphenyl]-4-yl)-3,7-dihydro-4*H*-imidazo[4,5-*d*][1,2,3]triazin-4-one (**3e**)



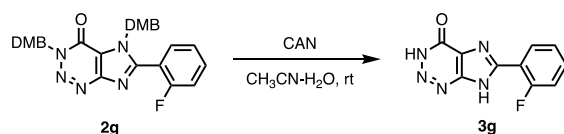
The mixture of **2e** and **2e'** (281 mg, 0.48 mmol, **2e/2e'** = 2.3:1) and CH₃CN/H₂O = 10:1 solution (33 mL) was added to a round-bottom flask containing a magnetic stirring bar under open air. Then, CAN (2.0 g, 3.8 mmol) was added and stirred at room temperature for 4 h. After reaction, solvent of the mixture was removed by reduced pressure. The resulting residue was dissolved in EtOAc and washed with water and brine. The organic extracts were then dried over Na₂SO₄. After filtration, solvent was removed by evaporation. The resulting residue was purified by MPLC (chloroform/MeOH = chloroform only to 9:1). The obtained solid was further purified by recrystallization from EtOAc to afford **3d** as a white solid (35 mg, 25% yield). ¹H NMR (600 MHz, DMSO) δ 8.32 (d, *J* = 8.4 Hz, 2H), 7.83 (d, *J* = 7.8 Hz, 2H), 7.77 (d, *J* = 7.8 Hz, 2H), 7.50 (t, *J* = 7.8 Hz, 2H), 7.40 (t, *J* = 7.2 Hz, 1H). ¹³C NMR (150 MHz, DMSO) δ 155.4 (br), 155.2 (br), 153.8, 141.0, 139.4, 130.6 (br), 129.0, 127.8, 127.3, 126.9, 126.7, 124.1 (br). HRMS (ESI⁺) *m/z* calcd for C₁₆H₁₁N₅ONa [M+Na]⁺: 312.0856, found: 312.0854.

2-19. Synthesis of 6-(naphthalen-1-yl)-3,7-dihydro-4*H*-imidazo[4,5-*d*][1,2,3]triazin-4-one (3f)



The mixture of **2f** and **2f'** (680 mg, 1.2 mmol, **2f/2f'** = 4.3:1) and CH₃CN/H₂O = 10:1 solution (66 mL) was added to a round-bottom flask containing a magnetic stirring bar under open air. Then, CAN (5.3 g, 9.7 mmol) was added and stirred at room temperature for 4 h. After reaction, solvent of the mixture was removed by reduced pressure. The resulting residue was dissolved in EtOAc and washed with water and brine. The organic extracts were then dried over Na₂SO₄. After filtration, solvent was removed by evaporation. The resulting residue was purified twice by MPLC (first: chloroform/MeOH = chloroform only to 9:1; second: EtOAc only). The obtained solid was further purified by recrystallization from EtOAc to afford **3f** as a white solid (27 mg, 8% yield). ¹H NMR (600 MHz, CD₃OD) δ 8.64 (d, *J* = 7.8 Hz, 1H), 8.11 (d, *J* = 8.4 Hz, 1H), 8.01 (dd, *J* = 7.2, 1.2 Hz, 2H), 7.95 (dd, *J* = 7.2, 1.2 Hz, 1H), 7.65–7.55 (m, 3H). ¹³C NMR (150 MHz, CD₃OD) δ 155.3, 154.4, 153.9 (br), 135.4, 132.8, 132.2, 129.9, 129.7, 128.7, 127.8, 127.3, 126.5, 126.2, 122.4 (br). HRMS (ESI⁺) *m/z* calcd for C₁₄H₉N₅ONa [M+Na]⁺: 286.0699, found: 286.0699.

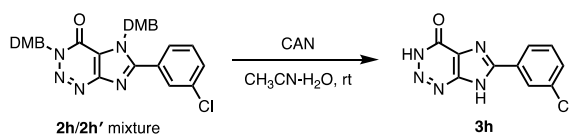
2-20. Synthesis of 6-(*o*-fluorophenyl)-3,7-dihydro-4*H*-imidazo[4,5-*d*][1,2,3]triazin-4-one (3g)



Compound **2g** (324 mg, 0.61 mmol) and CH₃CN/H₂O = 10:1 solution (33 mL) were added to a round-bottom flask containing a magnetic stirring bar under open air. Then, CAN (2.7 g, 4.9 mmol) was added and stirred at room temperature for 4 h. After reaction, solvent of the mixture was removed under reduced pressure. The resulting residue was dissolved in EtOAc and washed with water and brine. The organic extracts were then dried over Na₂SO₄. After filtration, solvent was removed by evaporation. The resulting residue was purified twice by MPLC (first: chloroform/MeOH = chloroform only to 9:1; second: EtOAc only). The obtained solid was further purified by recrystallization from EtOAc to afford **3g** as a white solid (35 mg, 25% yield). ¹H

NMR (600 MHz, CD₃OD) δ 8.16 (td, $J = 7.8, 1.8$ Hz, 1H), 7.64–7.58 (m, 1H), 7.41–7.33 (m, 2H). ¹³C NMR (150 MHz, CD₃OD) δ 161.6 (d, $J = 250$ Hz), 154.4, 153.3, 150.3, 134.5 (d, $J = 8.7$ Hz), 131.9, 126.3, 122.9 (br), 117.7 (d, $J = 11.4$ Hz), 117.6 (d, $J = 21.6$ Hz). HRMS (ESI⁺) m/z calcd for C₁₀H₆FN₅ONa [M+Na]⁺: 254.0449, found: 254.0446.

2-21. Synthesis of 6-(*m*-chlorophenyl)-3,7-dihydro-4*H*-imidazo[4,5-*d*][1,2,3]triazin-4-one (3h)



The mixture of **2h** and **2h'** (232 mg, 0.42 mmol, **2h/2h'** = 1.2:1) and CH₃CN/H₂O = 10:1 solution (33 mL) was added to a round-bottom flask containing a magnetic stirring bar under open air. Then, CAN (1.9 g, 3.4 mmol) was added and stirred at room temperature for 4 h. After reaction, solvent of the mixture was removed under reduced pressure. The resulting residue was dissolved in EtOAc and washed with water and brine. The organic extracts were then dried over Na₂SO₄. After filtration, solvent was removed by evaporation. The resulting residue was purified twice by MPLC (first: chloroform/MeOH = chloroform only to 9:1; second: EtOAc only). The obtained solid was further purified by recrystallization from EtOAc to afford **3h** as a white solid (20 mg, 19% yield). ¹H NMR (600 MHz, CD₃OD) δ 8.21 (s, 1H), 8.09 (d, $J = 7.2$ Hz, 1H), 7.59–7.54 (m, 2H). ¹³C NMR (150 MHz, CD₃OD) δ 154.6, 154.2 (br), 154.1, 136.3, 132.2, 131.9 (2C), 128.3, 126.6, 123.4 (br). HRMS (ESI⁺) m/z calcd for C₁₀H₆ClN₅ONa [M+Na]⁺: 270.0153, found: 270.0152.

3. Pd-catalyzed direct C–H arylation using isomerically pure **1** and **1'** with bromobenzene

Treatment of **1** (100 mg, 0.23 mmol) with bromobenzene (**4a**: 71 mg, 0.46 mmol) in the presence of Pd(OAc)₂ (2.6 mg, 5 mol %), CuI (87 mg, 0.46 mmol), and K₃PO₄ (121 mg, 0.57 mmol) in DMF (1.0 mL) at 140 °C for 12 h afforded the mixture of C₆-arylation products **2a** and **2a'** (**2a/2a'** = 1.4:1) in 56% combined yield (Scheme S1). The same reaction was also conducted using **1'** instead of **1**, which resulted in providing the mixture of **2a** and **2a'** (**2a/2a'** = 1.2:1) in 38% yield (Scheme S2). These results indicate that there is not stark difference in both isomers **1** and **1'** in terms of reactivity in C–H arylation, and the migration of DMB group between N7 and N9 positions occurs in **1a/1a'** or **2a/2a'** during the course of reaction.

4. Effect of AHX analogues and derivatives on shoot/root growth of rice

Rice seeds (*Oryza sativa* L. cv. Nipponbare) were sterilized in ethanol for 5 min and then 1% sodium hypochlorite for 30 min on a plastic container (18.5 × 14.5 × 4.5 cm). The seeds were washed completely in sterile water and germinated for 2 days at 30 °C with intensive light. The germinated seeds (n = 4–12) were planted onto test tube (ϕ 5.5 × 10 cm) containing samples, and incubated for a week at 30 °C with intensive light. The lengths of the root and shoot were measured to an accuracy of 0.01 mm with an absolute digimatic caliper (Mitutoyo Co., Kawasaki, Kanagawa, Japan).

5. X-ray crystallographic analysis of **6** and **3a**·H₂O

Details of the crystal data and a summary of the intensity data collection parameters for **6** and **3a**·H₂O are listed in Table S4. A suitable crystal, obtained by crystallization from corresponding solvents, was mounted with mineral oil on a MiTeGen MicroMounts and transferred to the goniometer of a Rigaku PILATUS diffractometer. Graphite-monochromated Mo K α radiation ($\lambda = 0.71075$ Å) was used. The structures were solved by direct methods with (SIR-97)¹⁸ and refined by full-matrix least-squares techniques against F^2 (SHELXL-2014/7)¹⁹ by using Yadokari-XG software package.²⁰ The intensities were corrected for Lorentz and polarization effects. The non-hydrogen atoms were refined anisotropically. Hydrogen atoms were placed using AFIX instructions.

Table 3. Crystallographic data and structure refinement detail for **6** and **3a**·H₂O

	6	3a ·H ₂ O
CCDC deposition No.	1845158	1845159
Formula	C ₁₁ H ₉ N ₅ O	C ₁₀ H ₇ N ₅ O ₂
F.W.	227.23	229.21
<i>T</i> (K)	123(2)	123 (2)
λ (Å)	0.71075	0.71073
cryst syst	Monoclinic	Monoclinic
space group	P2 ₁ /c	P2 ₁ /c
<i>a</i> , (Å)	12.6348(15)	13.0485(3)
<i>b</i> , (Å)	12.0277(13)	17.4172(4)
<i>c</i> , (Å)	13.3731(16)	9.0253(2)
α , (deg)	90	90
β , (deg)	90.447(3)	105.339(3)
γ , (deg)	90	90
<i>V</i> , (Å ³)	2032.2(4)	1978.10(8)
<i>Z</i>	8	8
<i>D</i> _{calc} , (g / cm ³)	1.485	1.539
μ (mm ⁻¹)	0.103	0.114
F(000)	944	944
cryst size (mm)	0.15 × 0.10 × 0.10	0.15 × 0.10 × 0.05
θ range, (deg)	3.047–25.372	1.618–24.997
reflns collected	22481	21505
indep reflns/ <i>R</i> _{int}	3726/0.0239	3495/0.0255
params	307	307
GOF on F^2	1.068	1.079
<i>R</i> ₁ , w <i>R</i> ₂ [I > 2 σ (I)]	0.0308, 0.0762	0.0595, 0.1731
<i>R</i> ₁ , w <i>R</i> ₂ (all data)	0.0354, 0.0794	0.0658, 0.1822

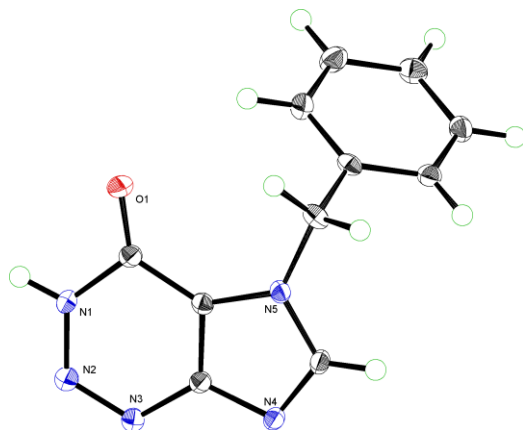


Figure 10. ORTEP drawing of **6** with 50% thermal ellipsoid.

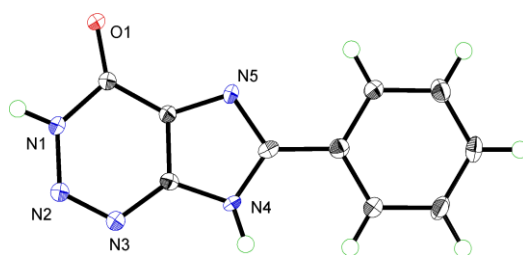


Figure 11. ORTEP drawing of **3a**·H₂O with 50% thermal ellipsoid (coordinated H₂O omitted for clarity).

References and notes

1. Makenzie, G. *Phil. Trans. R. Soc.* **1675**, *10*, 396–398.
2. (a) Couch, H. B. *Diseases of Turfgrasses*, 3rd ed.; Krieger: Malabar, FL, **1995**, 181–186. (b) Smith, J. D.; Jackson, N.; Woolhouse, A. R. *Fungal Diseases of Amenity Turf Grasses*, 3rd ed.; E. and F. N. Spon: London, **1989**, 339–353. (c) Shantz, H. L.; Piemeisel, R. L. *J. Agric. Res.* **1917**, *11*, 191–245. (d) Evershed, H. *Nature* **1884**, *29*, 384–385. (e) Ramsbottom, J. *Nature* **1926**, *117*, 158–159.
3. (a) Choi, J.; Fushimi, K.; Abe, N.; Tanaka, H.; Maeda, S.; Morita, A.; Hara, M.; Motohashi, R.; Matsunaga, J.; Eguchi, Y.; Ishigaki, N.; Hashizume, D.; Koshino, H.; Kawagishi, H. *ChemBioChem* **2010**, *11*, 1373–1377. (b) Choi, J.; Ohnishi, T.; Yamakawa, Y.; Takeda, S.; Sekiguchi, S.; Maruyama, W.; Yamashita, K.; Suzuki, T.; Morita, A.; Ikka, T.; Motohashi, R.; Kiriiwa, Y.; Tobina, H.; Asai, T.; Tokuyama, S.; Hirai, H.; Yasuda, N.; Noguchi, K.; Asakawa, T.; Sugiyama, S.; Kan, T.; Kawagishi, H. *Angew Chem Int Ed* **2014**, *53*, 1552–1555.
4. (a) Mitchinson, A. *Nature* **2014**, *505*, 298. (b) Kawagishi, H. *Bioscience, Biotechnology, and Biochemistry* **2018**, *82*, 752–758.
5. (a) Asai, T.; Choi, J.-H.; Ikka, T.; Fushimi, K.; Abe, N.; Tanaka, H.; Yamakawa, Y.; Kobori, H.; Kiriiwa, Y.; Motohashi, R.; Deo, V. K.; Asakawa, T.; Kan, T.; Morita, A.; Kawagishi, H. *JARQ* **2015**, *49*, 45–49. (b) Tobina, H.; Choi, J.-H.; Asai, T.; Kiriiwa, Y.; Asakawa, T.; Kan, T.; Morita, A.; Kawagishi, H. *Field Crops Research* **2014**, *162*, 6–11.
6. (a) Choi, J.-H.; Wu, J.; Sawada, A.; Takeda, S.; Takemura, H.; Yogosawa, K.; Hirai, H.; Kondo, M.; Sugimoto, K.; Asakawa, T.; Inai, M.; Kan, T.; Kawagishi, H. *Org. Lett.* **2018**, *20*, 312–314. (b) Choi, J.-H.; Kikuchi, A.; Pumkayo, P.; Hirai, H.; Tokuyama, S.; Kawagishi, H. *Bioscience, Biotechnology, and Biochemistry* **2016**, *80*, 2045–2050.
7. (a) Kende, H.; Zeevaart, J. *Plant Cell* **1997**, 1197–1210. (b) Santner, A.; Calderon-Villalobos, L. I. A.; Estelle, M. *Nat Chem Biol* **2009**, *5*, 301–307.
8. Bellina, F.; Cauteruccio, S.; Rossi, R. *Eur J Org Chem* **2006**, *2006*, 1379–1382.
9. Yang, Q.; Chang, J.; Wu, Q.; Zhang, B. *Res Chem Intermed* **2012**, *38*, 1335–1340.
10. Seiple, I. B.; Su, S.; Rodriguez, R. A.; Gianatassio, R.; Fujiwara, Y.; Sobel, A. L.; Baran, P. S. *J. Am. Chem. Soc.* **2010**, *132*, 13194–13196.
11. Sharma, D.; Narasimhan, B.; Kumar, P.; Judge, V.; Narang, R.; De Clercq, E.; Balzarini, J. *European Journal of Medicinal Chemistry* **2009**, *44*, 2347–2353.
12. (a) Lewis, J. C.; Wiedemann, S. H.; Bergman, R. G.; Ellman, J. A. *Org. Lett.* **2004**, *6*, 35–38. (b) Lewis, J. C.; Wu, J. Y.; Bergman, R. G.; Ellman, J. A. *Angew Chem Int Ed* **2006**, *45*, 1589–

1591. (c) Lewis, J. C.; Berman, A. M.; Bergman, R. G.; Ellman, J. A. *J. Am. Chem. Soc.* **2008**, *130*, 2493–2500. (d) Lewis, J. C.; Bergman, R. G.; Ellman, J. A. *Acc. Chem. Res.* **2008**, *41* (8), 1013–1025.
13. (a) Ziadi, A.; Uchida, N.; Kato, H.; Hisamatsu, R.; Sato, A.; Hagihara, S.; Itami, K.; Torii, K. *U. Chem. Commun.* **2017**, *53*, 9632–9635. (b) Ueda, A.; Amaike, K.; Shirotani, Y.; Warstat, R.; Ito, H.; Choi, J.-H.; Kawagishi, H.; Itami, K. *Can. J. Chem.* **2023**, *101*, 449–452.
14. Greene, T. W.; Wuts, P. G. M. *Protective Groups in Organic Synthesis*, 5th ed.; Wiley, **2014**.
15. Pivsa-Art, S.; Satoh, T.; Kawamura, Y.; Miura, M.; Nomura, M. *BCSJ* **1998**, *71*, 467–473.
16. Choi, J.-H.; Abe, N.; Tanaka, H.; Fushimi, K.; Nishina, Y.; Morita, A.; Kiriiwa, Y.; Motohashi, R.; Hashizume, D.; Koshino, H.; Kawagishi, H. *J. Agric. Food Chem.* **2010**, *58*, 9956–9959.
17. For selected reviews of C–H functionalization, see: (a) Yamaguchi, J.; Yamaguchi, A. D.; Itami, K. *Angew Chem Int Ed* **2012**, *51*, 8960–9009. (b) Segawa, Y.; Maekawa, T.; Itami, K. *Angew Chem Int Ed* **2015**, *54*, 66–81. (c) Wencel-Delord, J.; Glorius, F. *Nature Chem* **2013**, *5*, 369–375. (d) Rouquet, G.; Chatani, N. *Angew Chem Int Ed* **2013**, *52*, 11726–11743. (e) Engle, K. M.; Mei, T.-S.; Wasa, M.; Yu, J.-Q. *Acc. Chem. Res.* **2012**, *45*, 788–802. (f) Davies, H. M. L.; Manning, J. R. *Nature* **2008**, *451*, 417–424. (g) Ackermann, L.; Vicente, R.; Kapdi, A. R. *Angew Chem Int Ed* **2009**, *48*, 9792–9826. (h) Murakami, K.; Yamada, S.; Kaneda, T.; Itami, K. *Chem. Rev.* **2017**, *117*, 9302–9332. (i) Lyons, T. W.; Sanford, M. S. *Chem. Rev.* **2010**, *110*, 1147–1169. (j) Yi, H.; Zhang, G.; Wang, H.; Huang, Z.; Wang, J.; Singh, A. K.; Lei, A. *Chem. Rev.* **2017**, *117*, 9016–9085. (k) Gensch, T.; Hopkinson, M. N.; Glorius, F.; Wencel-Delord, J. *Chem. Soc. Rev.* **2016**, *45*, 2900–2936. (l) Chen, X.; Engle, K. M.; Wang, D.; Yu, J. *Angew Chem Int Ed* **2009**, *48*, 5094–5115. (m) Davies, H. M. L.; Morton, D. *J. Org. Chem.* **2016**, *81*, 343–350. (n) Hartwig, J. F.; Larsen, M. A. *ACS Cent. Sci.* **2016**, *2*, 281–292. (o) Santoro, S.; Ferlin, F.; Ackermann, L.; Vaccaro, L. *Chem. Soc. Rev.* **2019**, *48*, 2767–2782. (p) Guillemard, L.; Kaplaneris, N.; Ackermann, L.; Johansson, M. J. *Nat Rev Chem* **2021**, *5*, 522–545. (q) Holmberg-Douglas, N.; Nicewicz, D. A. *Chem. Rev.* **2022**, *122*, 1925–2016. (r) Sinha, S. K.; Guin, S.; Maiti, S.; Biswas, J. P.; Porey, S.; Maiti, D. *Chem. Rev.* **2022**, *122*, 5682–5841.
18. Altomare, A.; Burla, M. C.; Camalli, M.; Cascarano, G. L.; Giacovazzo, C.; Guagliardi, A.; Moliterni, G. Polidori, A. G. G.; Spagna, R. *J. Appl. Crystallogr.* **1999**, *32*, 115.
19. Sheldrick, G. M. *Acta Crystallogr. A* **2008**, *64*, 112.
- (a) Wakita, K. Yadokari-XG, Software for crystal structure analyses, **2001**. (b) Kabuto, C.; Akine,

S.; Nemoto, T.; Kwon, E. Release of Software (Yadokari-XG 2009) for Crystal Structure Analyses.
J. Cryst. Soc. Jpn. **2009**, *51*, 218.

**Annulative π -extension of indoles and pyrroles with diiodobiaryl
by palladium catalysis:
rapid synthesis of nitrogen-embedded polycyclic aromatic compounds**

Abstract

A palladium-catalyzed one-step annulative π -extension (APEX) reaction of indoles and pyrroles that allows rapid access to nitrogen-embedded polycyclic aromatic compounds is described. In the presence of palladium pivalate and silver carbonate, diverse indoles or pyrroles coupled with diiodobiaryls in a double direct C–H arylation manner to furnish the corresponding π -extended compounds in a single step. The newly developed catalytic system enables the use of various pyrroles and indoles as templates with a series of diiodobiaryls to provide structurally complicated and largely π -extended nitrogen-containing polycyclic aromatic compounds that are otherwise difficult to synthesize.

1. Introduction

With desirable electronic properties and diverse biological activities, nitrogen-embedded polycyclic aromatic compounds (N-PACs) have long been recognized as privileged structures in the fields of organic materials, pharmaceutical science and natural products (Figure 1).¹ As these properties can be readily tuned via skeletal modification of the core *N*-heteroarene structure, significant efforts have been devoted to develop new synthetic approaches for N-PACs.

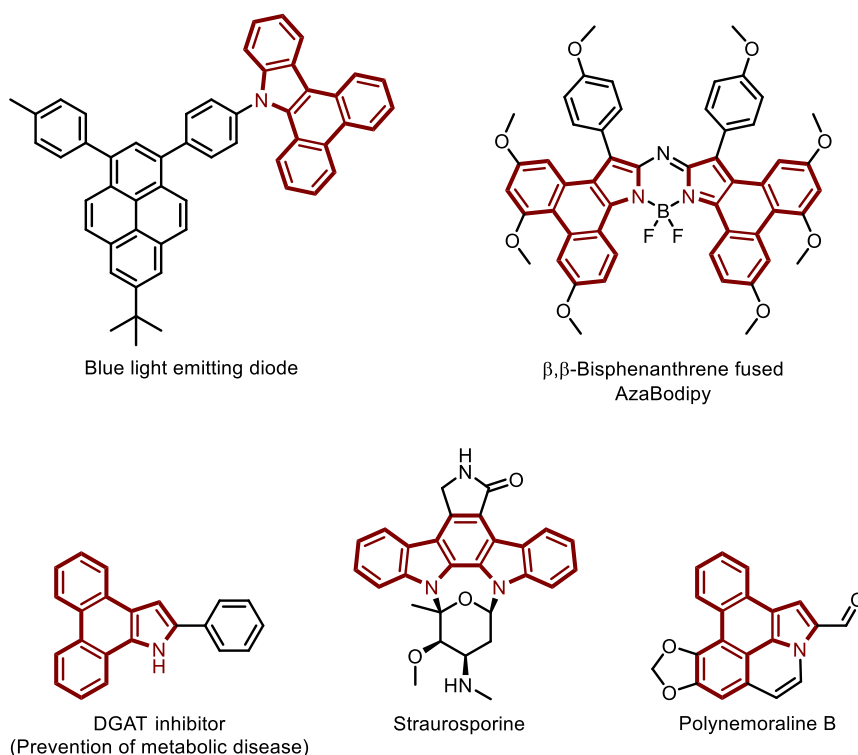


Figure 1. Widely used functional N-PACs.

Representative classical synthetic approaches for N-PACs include (i) intramolecular carbon–nitrogen bond formation of biaryl amines (Figure 2a),² (ii) intramolecular carbon–carbon bond formation of diaryl amines (Figure 2b),³ and (iii) stepwise functionalization and π -extension of indoles and pyrroles (Figures 2c).⁴ However, these methods require the use of prefunctionalized heteroaromatics such as halogenated pyrroles, anilines and indoles, and stepwise transformations from unfunctionalized (hetero)aromatics. To achieve maximum efficiency in synthesis of N-PAC, a more direct and ‘intuitive’ method for π -extension of unfunctionalized pyrroles and indoles is

demanded. Recently, Itami, Ito and co-workers have introduced several new one-step synthetic methods for fused heteroaromatics, namely annulative π -extension (APEX) reactions of unfunctionalized (hetero)aromatics (Figure 2d).⁵ APEX is a reaction concept that can directly transform easily available unfunctionalized (hetero)arenes to polycyclic aromatic hydrocarbons (PAHs), nanographenes and heteroatom-embedded polycyclic aromatic compounds (hetero-PACs) in a manner of direct C–H arylation. The APEX reactions offer large benefits in the context of cost, simplicity, step- and atom-economy.

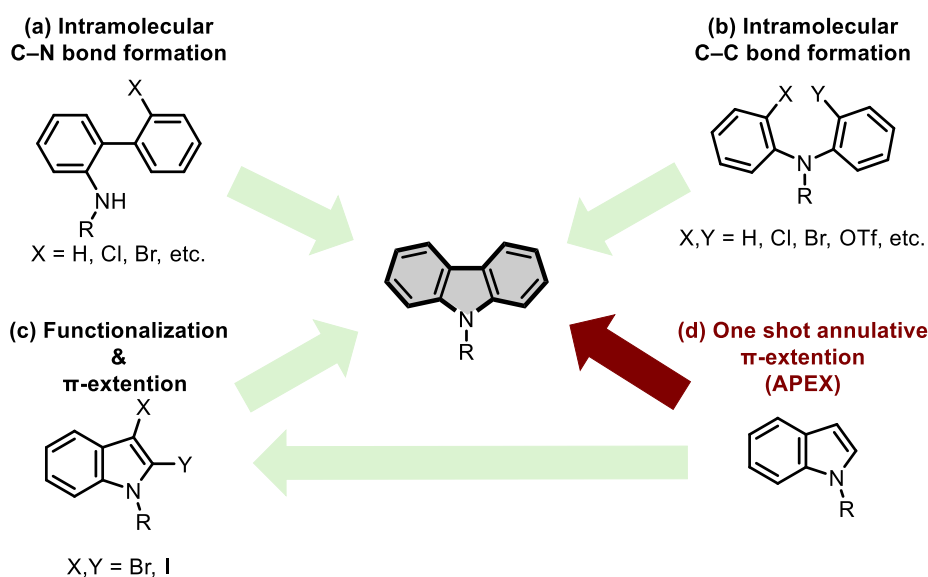
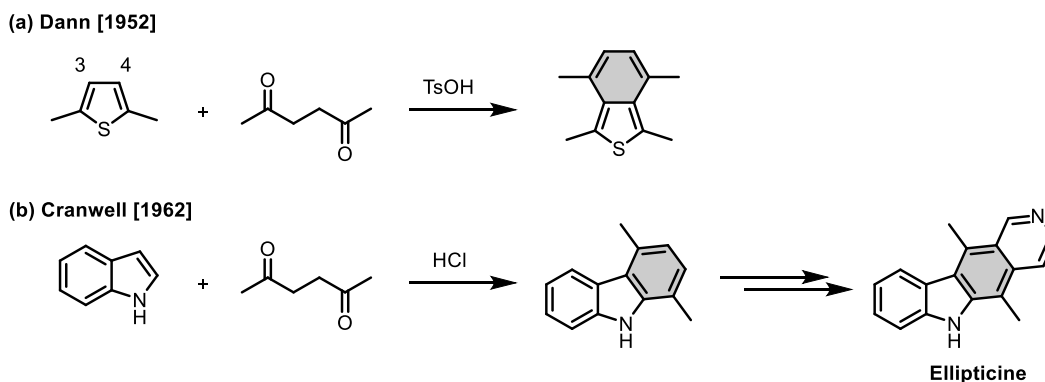


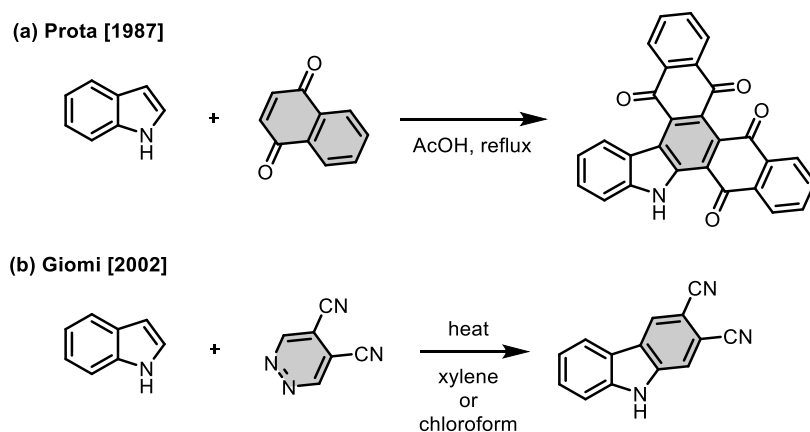
Figure 2. Synthesis of carbazole as a representative example of N-PACs by (a)(b)(c) classical approaches and (d) APEX reaction.

As early examples of APEX reaction of heteroarenes, Dann and co-workers reported the nucleophilic addition-type APEX reaction in 1954 (Scheme 1a).⁶ This reaction involves the addition of 2,5-hexadienone to the C3 and C4 positions of 2,5-dimethylthiophene, followed by acid-promoted dehydrative aromatization reaction. This classical reaction contributed the development of fundamental synthetic approach for indoles and carbazoles in the synthesis of natural products. Later, ellipticine,⁷ a significant natural product, was successfully synthesized using the APEX reaction by Cranwell in 1962 (Scheme 1b).⁸



Scheme 1. Nucleophilic addition-type APEX of indoles and pyrroles.

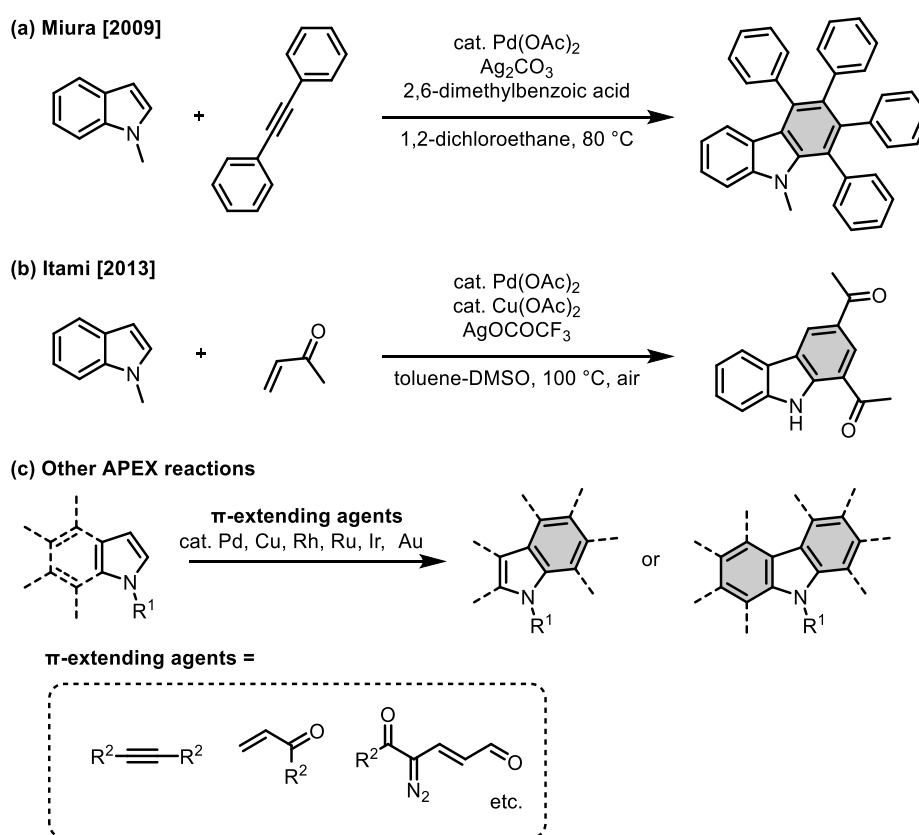
Afterwards, APEX reactions utilizing the [4+2] cycloaddition reaction were discovered (Scheme 2). In 1987, Prota and co-workers demonstrated the synthesis of carbazoles through a cascade reaction involving the Michael addition of indole with naphthoquinone, followed by a [4+2] cycloaddition (Scheme 2a).⁹ Additionally, in 2002, Giomi and co-workers discovered the indole-to-carbazole APEX reaction by utilizing inverse electron-demand Diels–Alder reaction between indole and 4,5-dicyanopyridazine followed by releasing nitrogen gas by retro-Diels–Alder reaction (Scheme 2b).¹⁰



Scheme 2. [4+2] cycloaddition-type APEX of indoles and pyrroles..

Recent advancements have led to the successful realization of the APEX reaction using transition metal catalysts for C–H functionalization. In 2009, Miura and co-workers reported a palladium-catalyzed indole-to-carbazole APEX reaction using alkyne as a π -extension unit (Scheme 3 a).¹¹ The reaction begins with the vinylation of the C3 position of indole, followed by

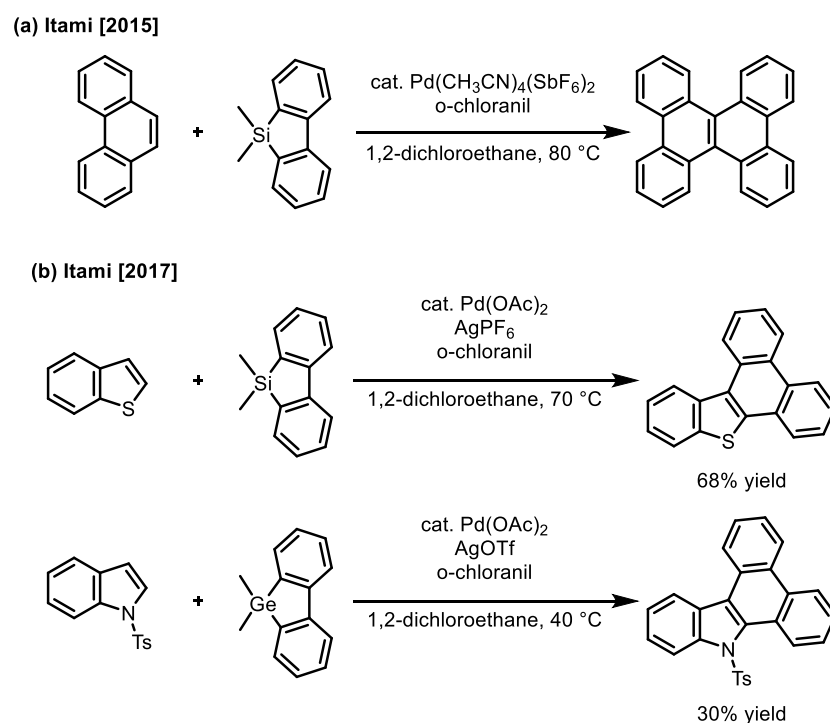
consecutive insertion of alkynes, resulting in π -extension. In 2013, Itami and co-workers developed similar APEX reaction with electron-deficient alkenes by a Pd/Ag/Cu-trimetallic system (Scheme 3 b).¹² With the advent of these reactions, a variety of transition metal-catalyzed APEX reactions of indoles and pyrroles using various π -extension units such as alkyne,^{11,13} alkene,^{12,14} 1-vinylpropargyl alcohols,¹⁵ α -diazocarbonyl compounds,¹⁶ α -bromoalcone,¹⁷ and α -bromocinnamate¹⁷ have been reported so far (Scheme 3c). However, the APEX products are generally limited to relatively small π -extended compounds such as substitute carbazoles and benzocarbazoles.



Scheme 3. Transition-metal-catalyzed APEX of indoles and pyrroles for synthesis of substituted carbazoles.

While creating larger π -extended polycyclic system has been challenging in previous APEX reaction of heteroles with small π -extending agents such as alkenes and alkynes, the double-arylation-type APEX reaction can be one of candidates for achieving the efficient synthesis of polycyclic aromatic structures. With regard to this, the double-arylation-type APEX reaction of polycyclic aromatic hydrocarbons (PAHs) using palladium catalyst, dibenzosilole and *o*-chloranil

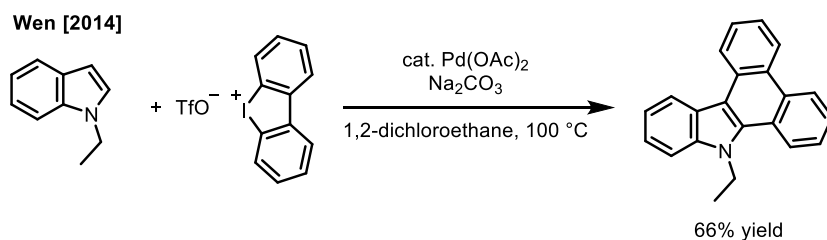
is a powerful method that can provide larger π -extended molecules (Scheme 4). Itami and co-workers first reported this APEX reaction in 2015, and demonstrated the synthesis of various nanographenes from simple PAHs such as phenanthrene (Scheme 4 a).¹⁸ Furthermore, this reaction can be applied to the APEX of benzothiophene, providing further π -extended molecules with good yields. However, this reaction could not be applied to electron-rich heteroarenes such as indoles and pyrroles, resulting in no formation of π -extended indoles nor carbazoles. Only successful example in this Pd-catalyzed APEX reaction system is the reaction of *N*-tosylindole with dibenzogermole as an alternative π -extending agent, whereas the yield of desired product remained in low yield (30%) (Scheme 4b).¹⁹ The reason for the low yield can be attributed to the presence of strong oxidants such as *o*-chloranil and the mismatched combination of electron-rich heteroles and strong oxidants, which leads to the undesired decomposition and deactivation of catalyst.



Scheme 4. Double-arylation-type APEX.

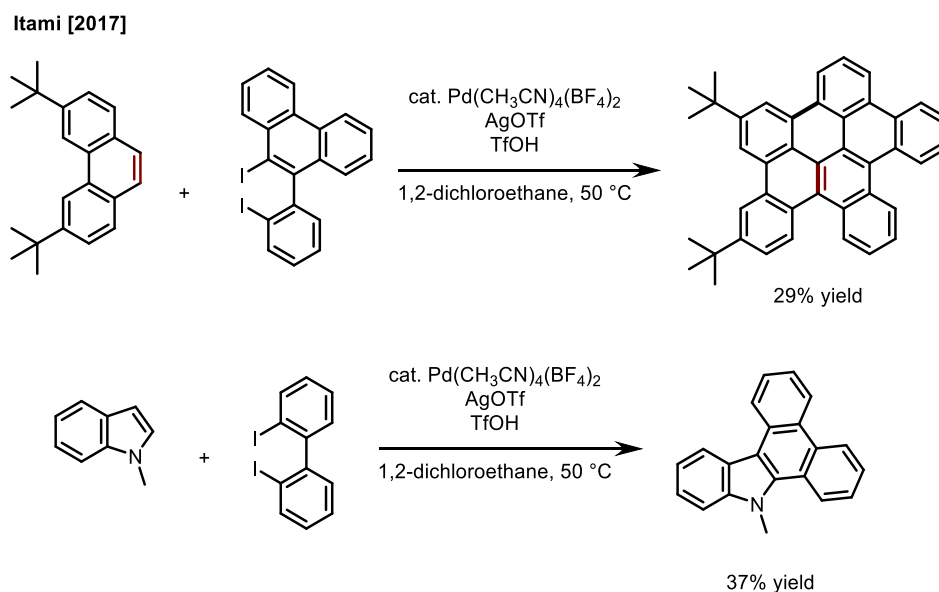
In 2014, Wen and co-workers discovered the APEX reaction of indoles, which avoids the use of additional oxidants.²⁰ This reaction utilizes cyclic hypervalent iodine reagents as a π -extension agent, allowing the π -extension of indole without the need for additional oxidants or special palladium ligands (Scheme 5). This reaction represents one of few useful methods as the one-step

preparation of dibenzocarbazoles from indoles. However, its potential application to larger N-PACs has not been demonstrated and remained unclear. In order to achieve efficient synthesis of larger N-PACs, there is a pressing need for the development of milder APEX reactions that are suitable for indoles and pyrroles.



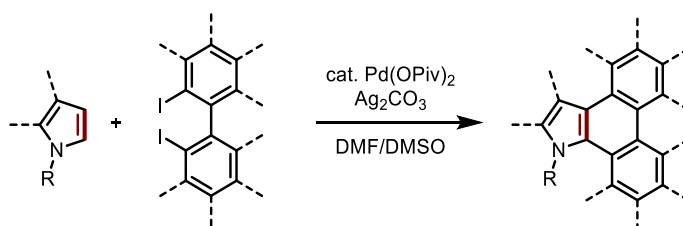
Scheme 5. Reported transition metal-catalyzed APEX reaction of indoles with cyclic diaryliodoniums.

Recently, Itami, Ito and co-workers have developed a catalytic system using Pd catalyst, AgOTf and TfOH that allows the use of diiodobiaryls as π -extension reagents, without the need of strong oxidizing agents such as *o*-chloranil (Scheme 6).²¹ The elimination of strong oxidizing agents resulted in an expanded range of π -extensible PAHs, and enables the utilization of even larger π -extension units. Actually, this reaction can be applied to electron-rich *N*-methylindoles, but the yield did not exceed over 37%. This is possibly due to the use of strong acids such as TfOH, which may decompose indole by protonation. Therefore, the APEX reaction of electron-rich heteroles is still challenging. Discovery of milder reaction conditions as well as appropriate π -extending agents is highly demanded for efficient synthesis of larger polycyclic aromatic systems from pyrrole- and indole-based molecules.



Scheme 6. Reported transition metal-catalyzed APEX reaction of substituted phenanthrene and *N*-methylindole with diiodobiaryls.

In this chapter, a new catalytic APEX reaction that allows efficient pyrrole-to-indole, pyrrole-to-carbazole and indole-to-carbazole π -extensions is described. The author newly established catalytic system featuring palladium pivalate and silver carbonate in a mixed DMF/DMSO solvent system that enables the rapid synthesis of structurally complicated N-PACs from readily available unfunctionalized pyrroles/indoles and various diiodobiaryls.



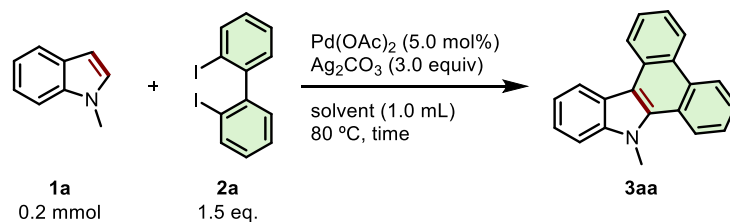
Scheme 7. Pd-catalyzed APEX reaction of indoles and pyrroles with various diiodobiaryls.

2. Results and Discussion

2-1. Screening of reaction conditions

First, optimization of the reaction conditions for indole-to-carbazole extension of *N*-methylindole (**1a**) was carried out using 2,2'-diido-1,1'-biphenyl (**2a**) as a π -extending agent (Table 1). After extensive screening, it is found that **1a** (1.0 equiv) coupled with **2a** (1.5 equiv) in the presence of Pd(OAc)₂ (5 mol%) and Ag₂CO₃ (3.0 equiv) at 80 °C in dimethylformamide (DMF) to provide *N*-methyldibenzo[*a,c*]carbazole (**3aa**) in 10% yield (entry 1). Then, the solvent effect was also investigated (entries 2–19). Other polar or apolar solvents such as dimethylacetamide (DMA), acetonitrile, 1,2-dichloroethane, tetrafluoroethanol (TFE), hexafluoroisopropanol (HFIP), 1,4-dioxane and toluene were not effective for this transformation (entries 2–9). Surprisingly, the use of mixed solvent system using dimethylsulfoxide (DMSO) with various solvents enhanced the reaction (entries 10–19). As a result of optimization study, APEX product was obtained in the highest yield when the DMF/DMSO mixed solvents were used at ratio of 7:3 (entry 10).

Table 1. Effect of solvents in the Pd-catalyzed APEX reaction of *N*-methylindole **1a** with diiodobiphenyl **2a**.

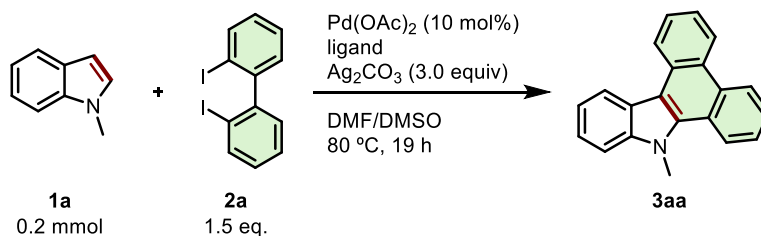


entry	solvent	time (h)	yield ^a	entry	solvent	time (h)	yield ^a
1	DMF	16	10%	11	DMA/DMSO (7:3)	21	47%
2	DMA	16	10%	12	1,2-dichloroethane/DMSO (7:3)	21	39%
3	DMSO	16	29%	13	1,4-dioxane/DMSO (7:3)	21	51%
4	CH ₃ CN	16	15%	14	CH ₃ CN/DMSO (7:3)	19	30%
5	1,2-dichloroethane	16	trace	15	DMF(1.0 mL), DMSO (1.0 eq.)	21	20%
6	TFE	16	trace	16	DMF/DMSO (9:1)	19	36%
7	HFIP	16	trace	17	DMF/DMSO (8:2)	19	41%
8	1,4-dioxane	16	trace	18	DMF/DMSO (5:5)	19	45%
9	toluene	16	trace	19	DMF/DMSO (2:8)	19	39%
10	DMF/DMSO (7:3)	21	54%				

^aDetermined by ¹H NMR using CH₂Br₂ as an internal standard.

Next, screening of ligands was conducted (Table 2). APEX reaction with bidentate nitrogen ligands such as 2,2'-bipyridyl and 1,10-phenanthroline shut down the reaction (entries 2 and 3). The use of phosphine ligands such as BINAP, PPh₃, Xanthphos, Brettphos, Sphos and Davephos afforded the desired product but was not effective compared to phosphine-free conditions (entries 4–9).

Table 2. Effect of ligands in the Pd-catalyzed APEX reaction of *N*-methylindole **1a** with diiodobiphenyl **2a**.

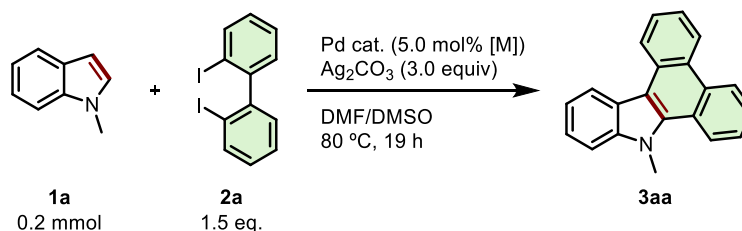


entry	ligand	yield ^a
1	none	43%
2	2,2'-bipyridyl (10 mol%)	trace
3	1,10-phenanthroline (10 mol%)	4%
4	<i>rac</i> -BINAP (10 mol%)	43%
5	PPh ₃ (20 mol%)	40%
6	Xanthphos (10 mol%)	29%
7	BrettPhos (20 mol%)	40%
8	SPhos (20 mol%)	46%
9	DavePhos (20 mol%)	36%

^aDetermined by ¹H NMR using CH₂Br₂ as an internal standard.

Then, a screening of palladium sources was conducted (Table 3). The use of palladium pivalate [Pd(OPiv)₂] instead of Pd(OAc)₂ improved the yield to 61% (entries 1 and 2), but other palladium sources such as PdCl₂, PdI₂, [PdCl(cinnamyl)]₂, Pd(PPh₃)₄, Pd(OCOCF₃)₂ and Pd(CH₃CN)₄(BF₄)₂ failed to give more than trace amounts of product (entries 3–8). In addition, the reaction did not proceed in the absence of Pd catalyst (entry 9).

Table 3. Effect of Pd-source in the Pd-catalyzed APEX reaction of *N*-methylindole **1a** with diiodobiphenyl **2a**.

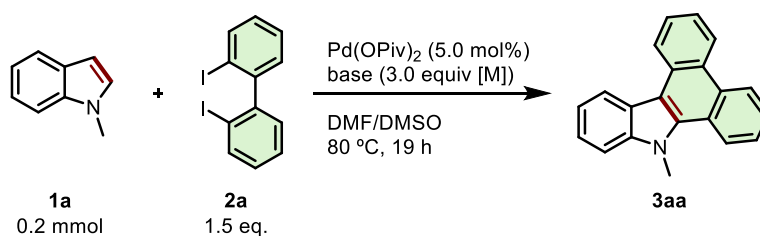


entry	Pd cat.	yield ^a
1	$\text{Pd}(\text{OAc})_2$	54%
2	$\text{Pd}(\text{OPiv})_2$	61%
3	PdCl_2	3%
4	PdI_2	2%
5	$[\text{PdCl}(\text{cinnamyl})]_2$	5%
6	$\text{Pd}(\text{PPh}_3)_4$	4%
7	$\text{Pd}(\text{OCOCF}_3)_2$	0%
8	$\text{Pd}(\text{CH}_3\text{CN})_4(\text{BF}_4)_2$	0%
9	none	0%

^aDetermined by ^1H NMR using CH_2Br_2 as an internal standard.

Setting $\text{Pd}(\text{OPiv})_2$ as the optimized catalyst, the effect of base was examined (Table 4). Decreasing the amount of Ag_2CO_3 to 1.5 equiv (relative to **1a**) further increased the yield of **3aa** to 78% (entry 2). The use of silver carboxylate salts (AgOAc , AgOPiv , AgOBz , AgOCOCF_3 , AgOTf or Ag_2O) instead of Ag_2CO_3 resulted in much lower yield (entries 2–8). The silver cation itself was essential for this reaction; the use of Na_2CO_3 , K_2CO_3 or Cs_2CO_3 instead of Ag_2CO_3 failed to give any product (entries 9–11). Finally, the reaction completely shut down without base (entry 12).

Table 4. Screening of base in the Pd-catalyzed APEX reaction of *N*-methylindole **1a** with diiodobiphenyl **2a**.

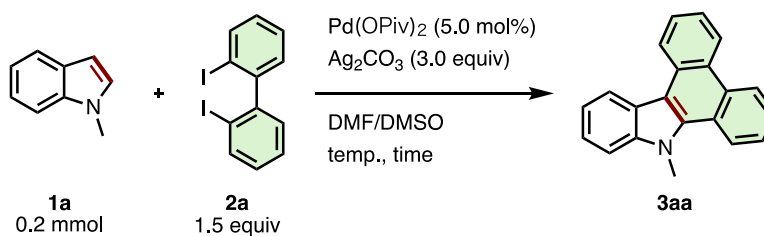


entry	base	yield ^a
1	Ag ₂ CO ₃	61%
2	Ag ₂ CO ₃ ^b	78%
3	AgOAc	33%
4	AgOPiv	0%
5	AgOBz	0%
6	AgTFA	0%
7	AgOTs	0%
8	Ag ₂ O	32%
9	Na ₂ CO ₃	0%
10	K ₂ CO ₃	0%
11	Cs ₂ CO ₃	0%
12	none	0%

^aDetermined by ¹H NMR using CH₂Br₂ as an internal standard. ^b1.5 equiv

Aiming to increase the product yield further, reaction temperature was examined (Table 5). Although higher reaction temperature accelerated the consumption of the starting material, the yield of **3aa** was decreased (entry 1 v.s. entries 2 and 3).

Table 5. Effect of reaction temperature in the Pd-catalyzed APEX reaction of *N*-methylindole **1a** with diiodobiphenyl **2a**.



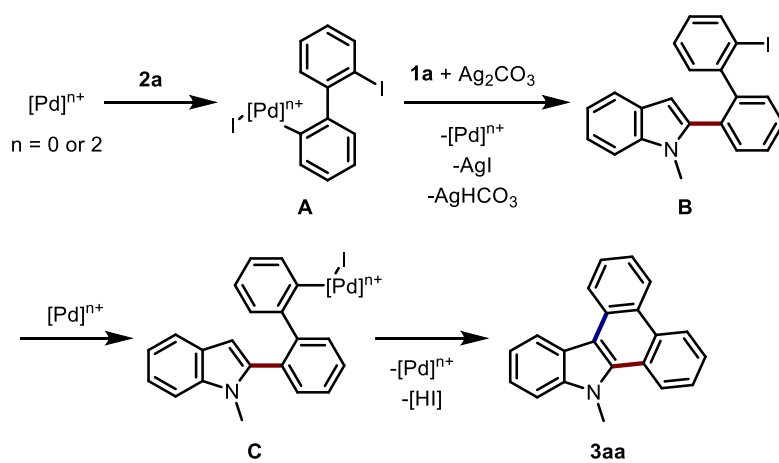
entry	temp. (°C)	time (h)	yield ^a
1	80	19	78%
2	100	19	57%
3	100	1	58%

^aDetermined by ¹H NMR using CH₂Br₂ as an internal standard.

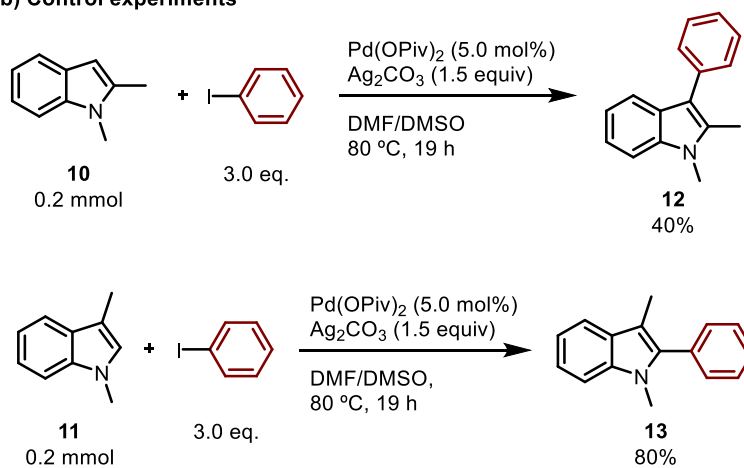
2-2. Plausible mechanism

A possible reaction mechanism of current indole-to-carbazole APEX reaction is shown in Scheme 8a. Oxidative addition of **2a** to palladium species (Pd(0) or Pd(II)) occurs to form biphenylylpalladium intermediate **A**.²² Then, the removal of iodide by silver salt may activate Pd complex **A**²³ to form electron-deficient aryl–Pd species²⁴, which then react with indole at the C2 position to afford intermediate **B**. Through the control experiments on the C–H arylations of 1,2-dimethylindole and 1,3-dimethylindole with iodobenzene, the present APEX reaction seems to occur through the C2-arylation of indole rather than C3-arylation in the first step (Scheme 8b). Final step would be well-established Pd-catalyzed intramolecular C–H/C–I coupling to afford the cyclized compound **3aa**.²⁵

(a) Proposed mechanism



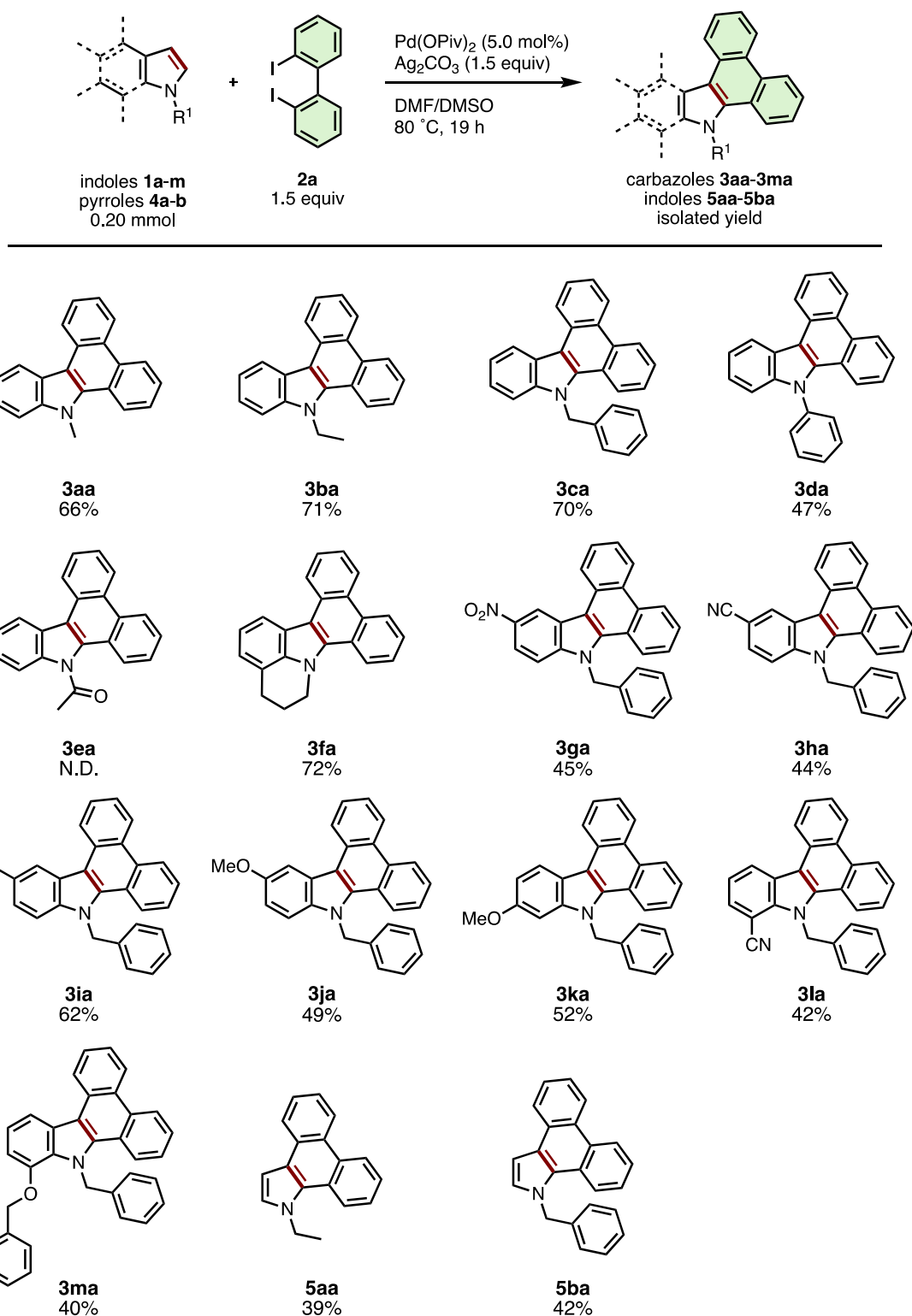
(b) Control experiments



Scheme 8. (a) Proposed reaction mechanism for the Pd-catalyzed APEX reaction of *N*-methylindole **1a** with diiodobiphenyl **2a**. (b) Control experiments on the C–H arylations of 1,2-dimethylindole and 1,3-dimethylindole with iodobenzene.

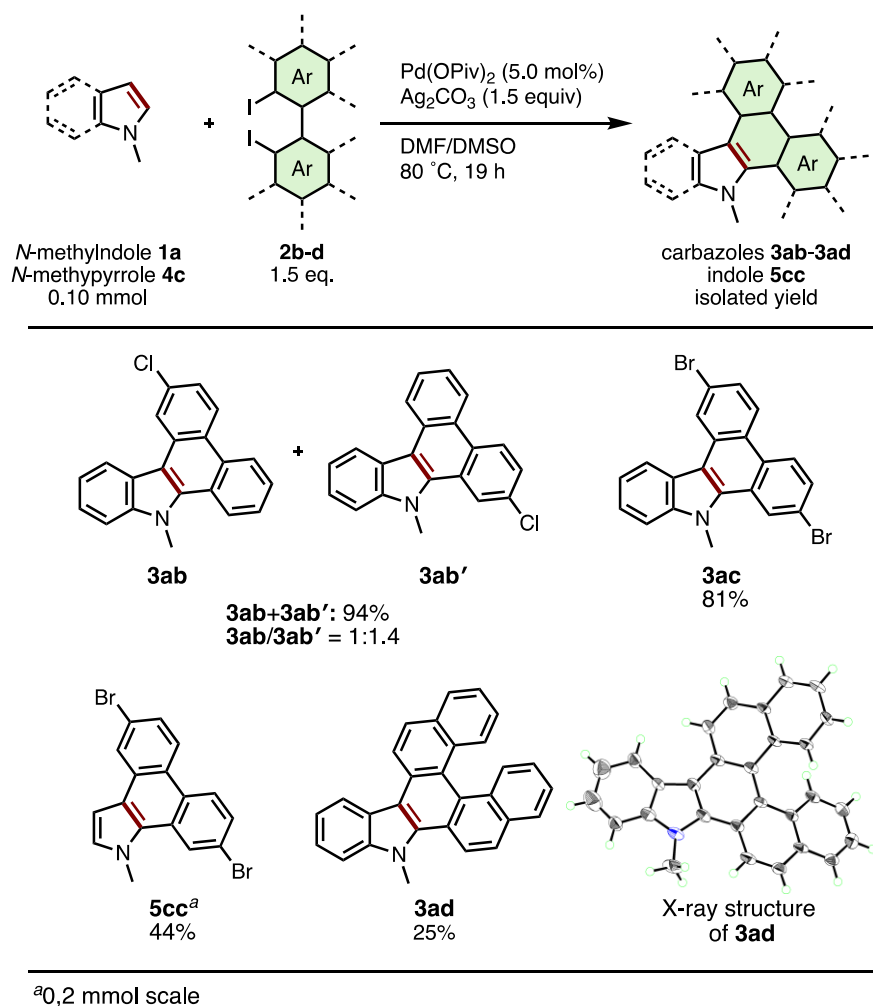
2-3. Substrate scope

Under the optimized conditions, various types of π -extended carbazoles/indoles **3**, **5** were prepared from the corresponding indole/pyrrole derivatives **1**, **4** and diiodobiaryls **2**. Scheme 9 illustrates the scope of applicable indole and pyrrole derivatives (**1a–1m**). *N*-Alkyl (**2a**, **2b**), *N*-benzyl (**2c**), *N*-phenyl (**2d**) indoles and cross-linked lilolidine (**2e**) were converted smoothly to the corresponding dibenzocarbazoles **3ba–3da** in good to moderate yield. However, the reaction of *N*-acetyl indole **2f** did not provide the expected π -extension product **3fa**. The presence of substituents at the 5-, 6-, or 7-positions of the indole ring was well-tolerated, giving various nitro- (**3ga**), cyano- (**3ha**, **3la**), bromo- (**3ia**), methoxy- (**3ja**, **3ka**), and benzyloxy-substituted (**3ma**) dibenzocarbazoles in moderate yields (40-62%). These results suggest that substituents on the benzene ring of indole do not critically affect the reaction progress. Interestingly, it was found that the current APEX reaction between *N*-substituted pyrroles and **2a** was mono-selective for the formation of dibenzoindoles **5aa** and **5ba** in 39% and 43% yields; only trace amounts of the di-APEX tetrabenzocarbazole products, the main products of our previous report,²¹ were observed. As synthetic methods to prepare the dibenzo[*e,g*]indole skeleton remain limited and inefficient,²⁵ the current APEX protocol provides a valuable, streamlined entry to this compound class.



Scheme 9. Substrate scope of indoles and pyrroles in the APEX reaction with diiodobiphenyl **2a**.

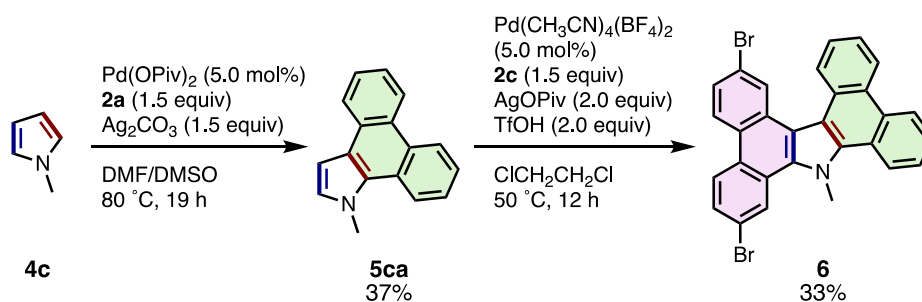
The scope of diiodobiaryls in the current APEX reaction is shown in Scheme 10. The reaction of *N*-methylindole (**2a**) with unsymmetrical 4-chloro-2,2'-diiodo-1,1'-biphenyl (**2b**) gave a 1:1.4 regioisomeric mixture of **3ab** and **3ab'** in 94% combined yield. APEX reactions of **1a** and **4a** with 4,4'-dibromo-2,2'-diiodo-1,1'-biphenyl (**2c**) smoothly occurred to give dibromodibenzocarbazole **3ac** and dibromodibenzoindole **5cc** in 81% and 44% yield, respectively. To our delight, the reaction of **1a** with 2,2'-diiodo-1,1'-binaphthalene (**2d**) gave dinaphthocarbazole **3ad** containing a [5]helicene moiety in 25% yield, whose helical structure was confirmed by X-ray crystallographic analysis. As this example clearly demonstrates, the late-stage attachment of complex, extended polyaromatic units is one of the most remarkable characteristics in the present APEX reaction.



Scheme 10. Substrate scope of diiodobiaryls.

2-4. Synthesis of unsymmetrical N-PACs

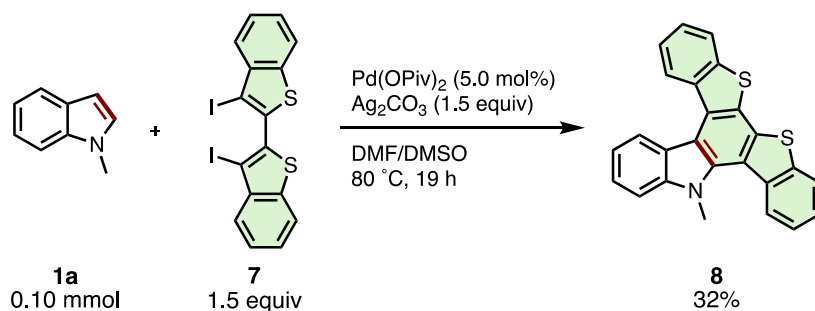
To demonstrate the power of the current APEX reaction to build complex, unsymmetrical N-PACs from simple starting materials, a two-step sequential synthesis was demonstrated to prepare tetrabenzocarbazole **6**, a compound that is difficult to prepare via known methods (Scheme 11). First, APEX reaction of *N*-methylpyrrole (**4c**) with **2a** was carried out to give the corresponding *N*-methylindole (**5ca**) in 37% yield. Notably, this reaction did not give double-APEX product which is the major product in the previously developed APEX reaction of *N*-phenylpyrrole.²¹ Then, **5ca** was further reacted with 4,4'-dibromo-2,2'-diiodo-1,1'-biphenyl (**2c**) by using Pd(CH₃CN)₄(BF₄)₂/AgOPiv/TfOH catalytic system²¹ to give the desired product **6** in 33% yield. Rapid access to a new class of unsymmetrically substituted tetrabenzocarbazole is notable and should contribute to the exploration of new compounds for organic electronics application.



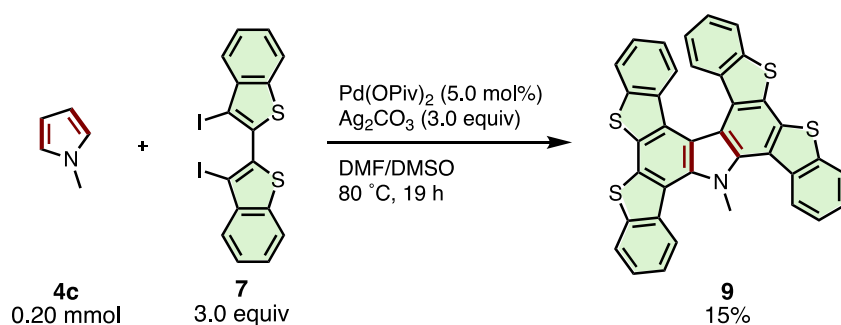
Scheme 11. Sequential APEX reactions of *N*-methylpyrrole **4c** for the synthesis of unsymmetrically substituted tetrabenzocarbazole **6**.

2-5. Synthesis of N-S-PACs

The current APEX reaction also provided a facile route to polycyclic aromatic compounds containing both nitrogen and sulfur (N-S-PACs) (Scheme 12). *N*-methylindole (**1a**) coupled with 3,3'-diiodo-2,2'-bibenzothiophene (**7**) to give di(benzothieno)carbazole **8** in 32%. The reaction of *N*-methylpyrrole (**4c**) with diiodo-2,2'-bibenzothiophene **7** afforded a double APEX product, tetra(benzothieno)carbazole **9**, in 15% yield (Scheme 13). While the yields were low, the generation of these novel N-S-PAC structures, which are highly interesting from the viewpoint of optoelectronic properties yet otherwise difficult to synthesize by conventional organic reactions, is notable.



Scheme 12. One-step APEX reactions for the synthesis of di(benzothieno)carbazole **8**



Scheme 13. One-step APEX reactions for the synthesis of tetra(benzothieno)carbazole **9**.

2-6. The structural and electronic properties of N-S-PACs **8** and **9**

The structural and electronic properties of **8** and **9** were elucidated via X-ray crystallography, UV–vis absorption and emission spectroscopies, and DFT/TD-DFT calculations at the B3LYP/6-31G(d) level of theory. Single crystal X-ray structures (Figures 3a, 3b) reveal that compound **8** adopts a relatively flattened structure in the solid state (Figure 2a), while compound **9** possesses a twisted structure owing to the embedded heterohelicene moiety. DFT calculations for **8** (Figure 4) reveal delocalization of the HOMO (−5.23 eV) over the entire molecule, while the LUMO (−1.49 eV) localizes on a benzothienocarbazole wing. On the other hand, the HOMO and LUMO of **9** are delocalized over entire molecule, and thus the energy level of LUMO (−1.72 eV) is slightly lower than that of **8**. The UV–vis absorption spectra of **8** and **9** in CH_2Cl_2 show that both compounds have broad absorption bands between 300 and 450 nm (Figure 5). Absorption maxima were found at 294, 317, 339, 357, 381 and 399 nm in **8**, and the corresponding peaks were also found in **9** at 305, 332, 348, 393 and 412 nm. The TD-DFT calculations revealed that the longest-wavelength absorptions in **8** and **9** (399 and 412 nm) are attributed to the allowed HOMO–LUMO transitions (see the experimental section for details). The fluorescence spectra of **8** and **9**

in CH₂Cl₂ display broad emissions with emission maxima of 427 and 437 nm, respectively (Figure 5).

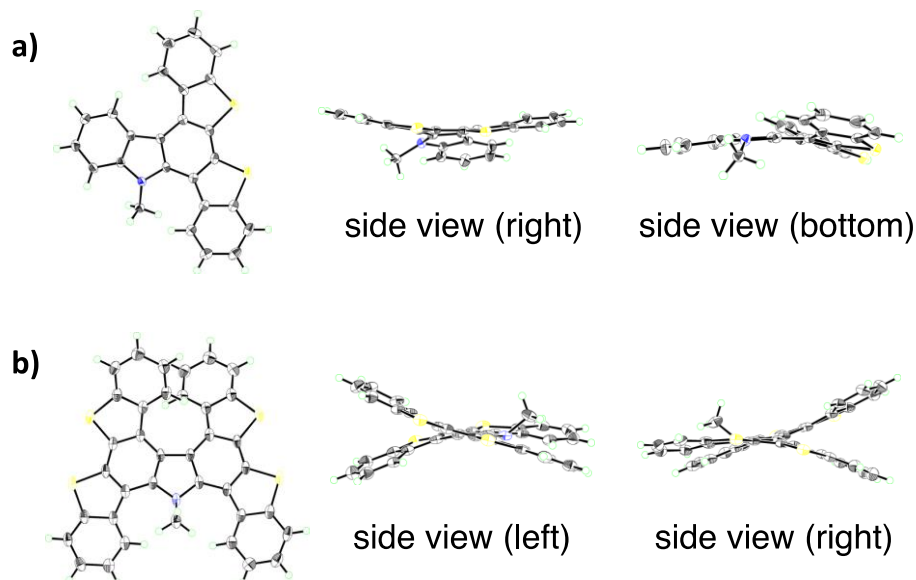


Figure 3. Top and side views of the X-ray crystal structures of (a) **8** and (b) **9**. Thermal ellipsoids are drawn at 50% probability.

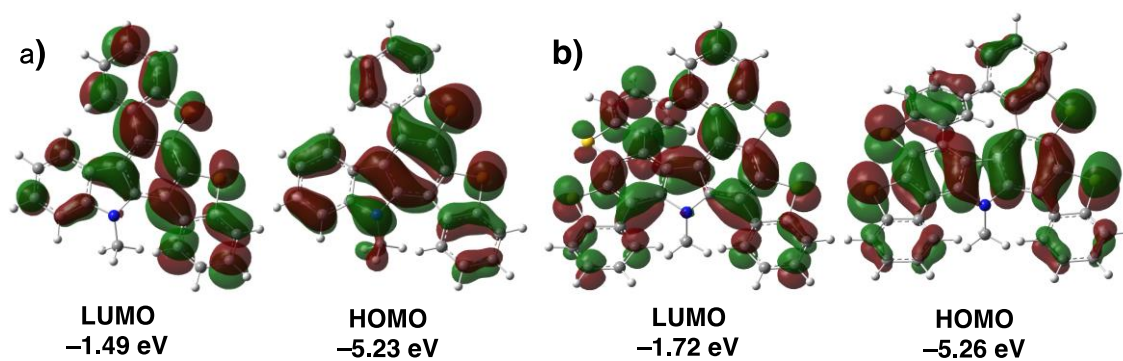


Figure 4. Pictorial frontier molecular orbitals and energy levels of (a) **8** and (b) **9** calculated using the B3LYP/6-31G(d) level of theory.

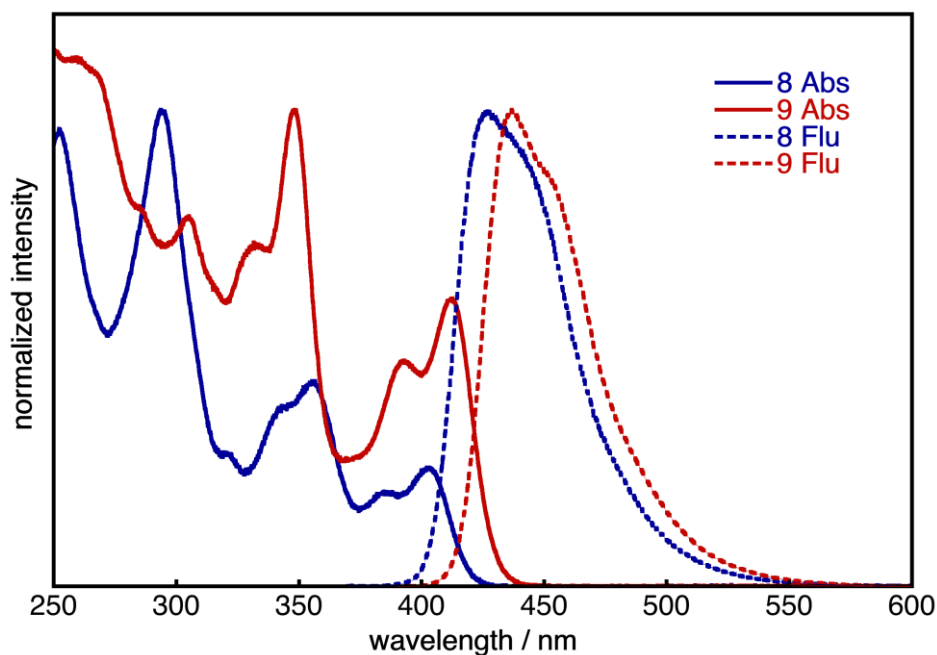


Figure 5. Normalized UV-vis absorption and fluorescence spectra of **8** and **9** in CH₂Cl₂ at rt.

3. Conclusion

In summary, the author has developed a novel palladium-catalyzed reaction to enable the APEX of indoles/pyrroles with diiodobiaryls. Use of the Pd(OPiv)₂/Ag₂CO₃ catalytic system in a mixed DMF/DMSO solvent allows the preparation of a diverse range of N-PACs in a single step, including several previously unsynthesized structures. Rapid access to exotic scaffolds such as complex, unsymmetrically substituted tetrabenzocarbazoles and extended N-heteroarenes featuring multiple helicene moieties is a particular highlight of the present APEX protocol. Developed APEX methodology also has great potential for the efficient and rapid synthesis of planar and non-planar π -extended N-PACs such as π -extended azacorannulenes, aza-buckybowls and pyrrolopyrroles which are regarded as one of promising materials for optoelectronics.²⁶ Further investigations into the reaction mechanism and applications of this APEX method towards the synthesis of larger π -extended heteroaromatics are currently underway.

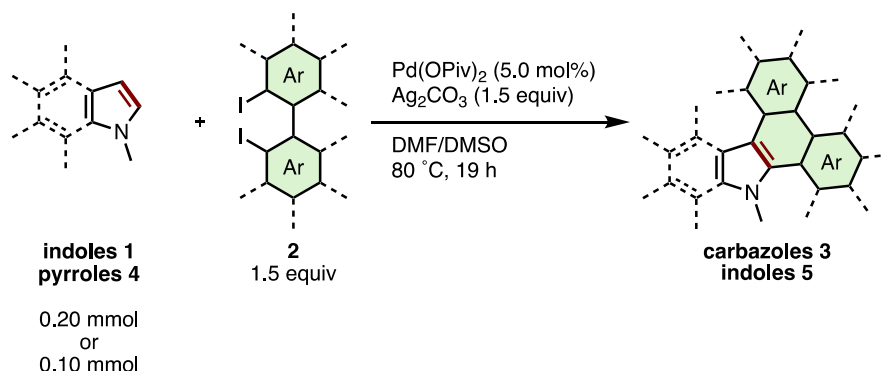
Experimental Section

1. General

Unless otherwise noted, all reactants or reagents including dry solvents were obtained from commercial suppliers and used as received. Pd(OPiv)₂ was obtained from Aldrich. Ag₂CO₃ was purchased from WAKO. 4,4'-Dibromo-2,2'-diiodo-1,1'-biphenyl (**2c**) was purchased from TCI. 2,2'-Diiodo-1,1'-biphenyl (**2a**),²⁷ 4-chloro-2,2'-diiodo-1,1'-biphenyl (**2b**),²⁸ 2,2'-diiodo-1,1'-binaphthalene (**2d**),²⁹ 3,3'-diiodo-2,2'-bibenzothiophene (**7**),³⁰ 2,2'-dibromo-1,1'-biphenyl (**2e**)²⁷, 1,2-dimethyl-1*H*-indole (**10**),³¹ and 1,3-dimethyl-1*H*-indole (**11**)³¹ were synthesized according to procedures reported in the literature. Unless otherwise noted, all reactions were performed with dry solvents under air. All work-up and purification procedures were carried out with reagent-grade solvents in air.

Analytical thin-layer chromatography (TLC) was performed using E. Merck silica gel 60 F₂₅₄ precoated plates (0.25 mm). The developed chromatogram was analyzed by UV lamp (254 nm). Medium pressure liquid chromatography (MPLC) was performed using Yamazen W-prep 2XY. Preparative thin-layer chromatography (PTLC) was performed using Wakogel B5-F silica coated plates (0.75 mm) prepared in our laboratory. Preparative gel permeation chromatography (GPC) was performed with a JAI LC-9204 instrument equipped with JAIGEL-1H/JAIGEL-2H columns using chloroform as an eluent. The high-resolution mass spectra (HRMS) were conducted on Thermo Fisher Scientific Exactive. Nuclear magnetic resonance (NMR) spectra were recorded on a JEOL JNM-ECA-600 (¹H 600 MHz, ¹³C 150 MHz) spectrometer and a JEOL JNM-ECA-600II with Ultra COOL™ probe (¹H 600 MHz, ¹³C 150 MHz) spectrometer. Chemical shifts for ¹H NMR are expressed in parts per million (ppm) relative to tetramethylsilane (δ 0.00 ppm). Chemical shifts for ¹³C NMR are expressed in ppm relative to CDCl₃ (δ 77.0 ppm). Data are reported as follows: chemical shift, multiplicity (s = singlet, d = doublet, dd = doublet of doublets, ddd = doublet of doublets of doublets, t = triplet, dt = doublet of triplets, td = triplet of doublets, q = quartet, m = multiplet), coupling constant (Hz), and integration.

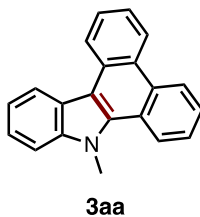
2. Palladium-catalyzed APEX reaction of indoles and pyrroles with diiodobiaryls



General procedure A: To a screw-capped glass tube containing a magnetic stirrer bar were added indole **1** or pyrrole **4** (0.20 mmol, 1.0 equiv), diiodobiaryl **2** (0.30 mmol, 1.5 equiv), Ag₂CO₃ (0.30 mmol, 1.5 equiv), Pd(OPiv)₂ (0.010 mmol, 5.0 mol%), DMF (0.70 mL) and DMSO (0.30 mL) under air. After stirring at 80 °C for 19 h, the reaction mixture was cooled to room temperature, and then passed through a short pad of Celite[®] (eluent: EtOAc or CHCl₃). After the organic solvent was removed under reduced pressure, the residue was purified by PTLC or MPLC to yield the corresponding π -extended carbazole **3** or indole **5**.

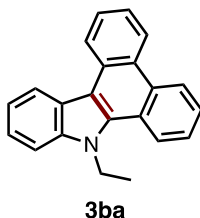
General procedure B: To a screw-capped glass tube containing a magnetic stirrer bar were added indole **1** or pyrrole **4** (0.10 mmol, 1.0 equiv), diiodobiaryl **2** (0.15 mmol, 1.5 equiv), Ag₂CO₃ (0.15 mmol, 1.5 equiv), Pd(OPiv)₂ (0.0050 mmol, 5.0 mol%), DMF (0.35 mL) and DMSO (0.15 mL) under air. After stirring at 80 °C for 19 h, the reaction mixture was cooled to room temperature, and then passed through a short pad of Celite[®] (eluent: EtOAc or CHCl₃). After the organic solvent was removed under reduced pressure, the residue was purified by PTLC or MPLC to yield the corresponding π -extended carbazole **3** or indole **5**.

9-Methyl-9H-dibenzo[*a,c*]carbazole (3aa)



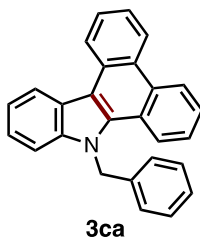
General procedure A: Purification by MPLC (hexane/CHCl₃ = hexane only to 9:1) afforded **3aa** as a white solid (37 mg, 66% yield). ¹H NMR (600 MHz, CDCl₃) δ 8.86–8.81 (m, 2H), 8.74 (d, *J* = 8.4 Hz, 1H), 8.68–8.64 (m, 1H), 8.59 (d, *J* = 8.4 Hz, 1H), 7.74 (ddd, *J* = 7.8, 6.9, 0.9 Hz, 1H), 7.67–7.62 (m, 2H), 7.59–7.54 (m, 2H), 7.49 (ddd, *J* = 8.4, 7.2, 1.2 Hz, 1H), 7.39 (ddd, *J* = 8.4, 7.2, 1.2 Hz, 1H), 4.35 (s, 3H). ¹³C NMR (150 MHz, CDCl₃) δ 140.8, 134.7, 130.9, 129.9, 127.3, 126.9, 126.1, 125.6, 124.1, 123.9, 123.7, 123.60, 123.56, 123.4, 122.9, 121.8, 120.3, 113.4, 109.5, 34.6 (one carbon peak was not observed because of overlapping). HRMS (ESI⁺) *m/z* calcd for C₂₁H₁₆N [M+H]⁺: 282.1277, found: 282.1277.

9-Ethyl-9H-dibenzo[*a,c*]carbazole (3ba)



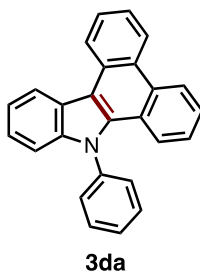
General procedure A: Purification by MPLC (hexane/CHCl₃ = hexane only to 9:1) afforded **3ba** as a white solid (42 mg, 71% yield). ¹H NMR (600 MHz, CDCl₃) δ 8.87 (t, *J* = 9.0 Hz, 2H), 8.76 (d, *J* = 8.4 Hz, 1H), 8.63 (d, *J* = 8.4 Hz, 1H), 8.53 (dd, *J* = 8.1, 1.5 Hz, 1H), 7.74 (ddd, *J* = 8.1, 7.2, 1.2 Hz, 1H), 7.71–7.65 (m, 2H), 7.62 (d, *J* = 8.4 Hz, 1H), 7.57 (ddd, *J* = 8.1, 7.5, 1.2 Hz, 1H), 7.50 (ddd, *J* = 8.1, 7.2, 1.2 Hz, 1H), 7.41 (ddd, *J* = 8.1, 6.9, 1.2 Hz, 1H), 4.85 (q, *J* = 7.2 Hz, 2H), 1.71 (t, *J* = 7.2 Hz, 3H). ¹³C NMR (150 MHz, CDCl₃) δ 140.1, 133.7, 130.9, 130.0, 127.3, 126.9, 126.5, 125.6, 124.2, 123.8, 123.63, 123.56, 123.4, 122.6, 122.0, 120.4, 113.6, 109.4, 41.0, 15.3 (two carbon peaks were not observed because of overlapping). HRMS (ESI⁺) *m/z* calcd for C₂₂H₁₈N [M+H]⁺: 296.1434, found: 296.1433.

9-Benzyl-9H-dibenzo[*a,c*]carbazole (3ca)



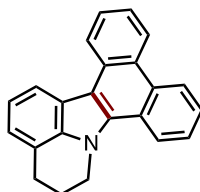
General procedure A: Purification by MPLC (hexane/CHCl₃ = hexane only to 9:1) afforded **3ca** as a white solid (50 mg, 70% yield). ¹H NMR (600 MHz, CDCl₃) δ 8.92 (d, *J* = 8.4 Hz, 1H), 8.82 (d, *J* = 8.4 Hz, 1H), 8.76 (d, *J* = 8.4 Hz, 1H), 8.68–8.64 (m, 1H), 8.23 (dd, *J* = 8.1, 0.9 Hz, 1H), 7.77 (ddd, *J* = 8.1, 6.9, 1.2 Hz, 1H), 7.59 (ddd, *J* = 8.4, 7.2, 1.2 Hz, 2H), 7.48–7.42 (m, 4H), 7.37–7.33 (m, 2H), 7.32–7.27 (m, 3H), 5.95 (s, 2H). ¹³C NMR (150 MHz, CDCl₃) δ 141.3, 137.4, 134.7, 130.9, 129.9, 129.1, 127.5, 127.4, 127.1, 126.4, 126.0, 125.7, 124.1, 124.0, 123.8, 123.7, 123.5, 123.2, 122.9, 121.9, 120.9, 113.9, 110.0, 50.2 (one carbon peak was not observed because of overlapping). HRMS (ESI⁺) *m/z* calcd for C₂₇H₂₀N [M+H]⁺: 358.1590, found: 358.1591.

9-Phenyl-9H-dibenzo[*a,c*]carbazole (3da)



General procedure A: Purification by MPLC (hexane/CHCl₃ = hexane only to 7:3) afforded **3da** as a white solid (32 mg, 47% yield). ¹H NMR (600 MHz, CDCl₃) δ 8.94 (d, *J* = 8.4 Hz, 1H), 8.80 (dd, *J* = 8.4, 4.8 Hz, 2H), 8.66 (d, *J* = 8.4 Hz, 1H), 7.79 (ddd, *J* = 8.1, 6.9, 0.9 Hz, 1H), 7.68–7.60 (m, 4H), 7.58–7.51 (m, 3H), 7.47 (dd, *J* = 8.4, 0.6 Hz, 1H), 7.43 (ddd, *J* = 8.1, 7.2, 1.2 Hz, 1H), 7.38 (ddd, *J* = 8.4, 7.2, 1.2 Hz, 1H), 7.27 (ddd, *J* = 8.1, 7.8, 0.6 Hz, 1H), 7.21 (d, *J* = 8.4 Hz, 1H). ¹³C NMR (150 MHz, CDCl₃) δ 142.1, 140.2, 134.5, 130.8, 130.2, 129.9, 129.1, 128.9, 127.4, 127.3, 125.9, 125.7, 124.0, 123.9, 123.81, 123.79, 123.5, 123.2, 121.7, 121.0, 114.2, 111.0 (two carbon peaks were not observed because of overlapping). HRMS (ESI⁺) *m/z* calcd for C₂₆H₁₈N [M+H]⁺: 344.1434, found: 344.1433.

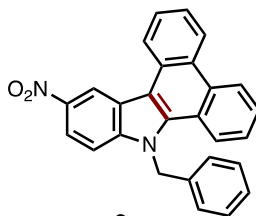
5,6-Dihydro-4*H*-dibenzo[*a,c*]pyrido[3,2,1-*jk*]carbazole (3ea)



3ea

General procedure A: Purification by MPLC (hexane/CHCl₃ = hexane only to 1:1) afforded **3ea** as a pale yellow solid (44 mg, 72% yield). ¹H NMR (600 MHz, CDCl₃) δ 8.89–8.83 (m, 2H), 8.78 (d, *J* = 8.4 Hz, 1H), 8.69–8.66 (m, 1H), 8.40 (d, *J* = 7.8 Hz, 1H), 7.75 (ddd, *J* = 8.1, 7.2, 1.2 Hz, 1H), 7.70–7.66 (m, 2H), 7.58 (ddd, *J* = 8.1, 6.9, 1.2 Hz, 1H) 7.31 (t, *J* = 7.5 Hz, 1H), 7.20 (dd, *J* = 6.9, 0.9 Hz, 1H), 4.99 (t, *J* = 6.0 Hz, 2H), 3.17 (t, *J* = 6.0 Hz, 2H), 2.42 (quintet, *J* = 6.0 Hz, 2H). ¹³C NMR (150 MHz, CDCl₃) δ 136.8, 133.6, 130.7, 130.4, 127.3, 126.6, 126.1, 125.5, 124.1, 123.7, 123.43, 123.38, 122.8, 122.4, 121.6, 121.0, 120.2, 119.4, 113.3, 46.7, 25.1, 23.7 (one carbon peak was not observed because of overlapping). HRMS (ESI⁺) *m/z* calcd for C₂₃H₁₈N [M+H]⁺: 308.1434, found: 308.1432.

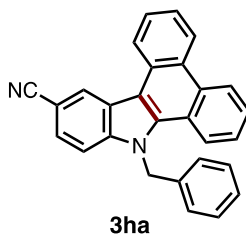
9-Benzyl-12-nitro-9*H*-dibenzo[*a,c*]carbazole (3ga)



3ga

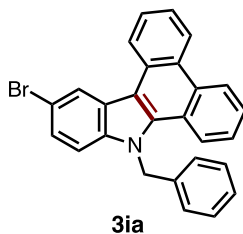
General procedure A: After purification by MPLC (CHCl₃ only), the obtained solid was washed with hexane and CH₂Cl₂ to afford **3ga** as a yellow solid (36 mg, 45% yield). ¹H NMR (600 MHz, CDCl₃) δ 9.62 (d, *J* = 1.8 Hz, 1H), 8.92 (d, *J* = 8.4 Hz, 1H), 8.88 (d, *J* = 8.4 Hz, 1H), 8.81 (d, *J* = 8.4 Hz, 1H), 8.36 (dd, *J* = 8.7, 2.1 Hz, 1H), 8.27 (d, *J* = 7.2 Hz, 1H), 7.87 (ddd, *J* = 8.1, 6.9, 1.5 Hz, 1H), 7.71–7.67 (m, 2H), 7.55–7.51 (m, 2H), 7.42–7.38 (m, 2H), 7.37–7.33 (m, 1H), 7.28 (d, *J* = 8.4 Hz, 1H), 6.08 (s, 2H). ¹³C NMR (150 MHz, CDCl₃) δ 143.9, 142.2, 136.7, 136.0, 131.6, 129.4, 128.8, 128.0, 127.6, 126.9, 126.8, 125.8, 125.0, 124.3, 123.7, 123.5, 123.1, 122.8, 122.5, 119.7, 118.7, 114.7, 109.7, 50.5 (one carbon peak was not observed because of overlapping). HRMS (ESI⁺) *m/z* calcd for C₂₇H₁₈N₂O₂Na [M+Na]⁺: 425.1260, found: 425.1260.

9-Benzyl-9H-dibenzo[*a,c*]carbazole-12-cyanitrile (**3ha**)



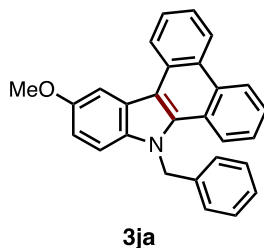
General procedure A: After purification by MPLC (CHCl₃ only), the obtained solid was washed with hexane to afford **3ha** as a pale yellow solid (34 mg, 44% yield). ¹H NMR (600 MHz, CDCl₃) δ 9.01 (d, *J* = 1.2 Hz, 1H), 8.88 (d, *J* = 8.4 Hz, 1H), 8.82 (dd, *J* = 8.1, 4.5 Hz, 2H), 8.27 (d, *J* = 8.4 Hz, 1H), 8.84 (ddd, *J* = 8.4, 7.2, 1.2 Hz, 1H), 7.71–7.66 (m, 3H), 7.56–7.51 (m, 2H) 7.41–7.37 (m, 2H), 7.36–7.33 (m, 1H), 7.30–7.26 (m, 2H), 6.06 (s, 2H). ¹³C NMR (150 MHz, CDCl₃) δ 142.5, 136.2, 135.8, 131.4, 129.3, 128.9, 127.92, 127.86, 127.4, 126.9, 126.8, 126.6, 125.7, 124.8, 124.1, 123.64, 123.60, 123.4, 122.8, 122.5, 120.6, 113.5, 110.6, 103.8, 50.2 (one carbon peak was not observed because of overlapping). HRMS (ESI⁺) *m/z* calcd for C₂₈H₁₉N₂ [M+H]⁺: 383.1543, found: 383.1547.

9-Benzyl-12-bromo-9H-dibenzo[*a,c*]carbazole (**3ia**)



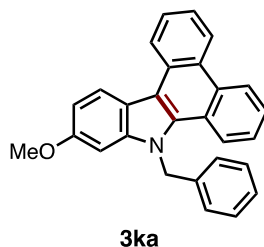
General procedure A: After purification by MPLC (hexane/CHCl₃ = hexane only to 1:1), the obtained solid was washed with hexane to afford **3ia** as a pale yellow solid (54 mg, 62% yield). ¹H NMR (600 MHz, CDCl₃) δ 8.85 (d, *J* = 8.4 Hz, 1H), 8.81–8.77 (m, 3H), 8.25 (d, *J* = 8.4 Hz, 1H), 7.80 (ddd, *J* = 8.1, 7.2, 1.2 Hz, 1H), 7.64 (ddd, *J* = 9.6, 7.2, 1.2 Hz, 2H), 7.53 (dd, *J* = 9.0, 1.8 Hz, 1H), 7.49 (ddd, *J* = 8.4, 7.2, 1.2 Hz, 1H), 7.39–7.35 (m, 3H), 7.34–7.30 (m, 1H), 7.28 (d, *J* = 7.2 Hz, 2H), 5.99 (s, 2H). ¹³C NMR (150 MHz, CDCl₃) δ 139.9, 136.9, 135.3, 131.2, 129.5, 129.2, 127.73, 127.66, 127.2, 126.8, 126.6, 126.2, 125.9, 125.4, 124.5, 124.3, 124.1, 123.6, 123.5, 123.0, 122.9, 114.0, 113.2, 111.4, 50.3. HRMS (ESI⁺) *m/z* calcd for C₂₇H₁₉BrN [M+H]⁺: 436.0695, found: 436.0696.

9-Benzyl-12-methoxy-9H-dibenzo[*a,c*]carbazole (3ja)



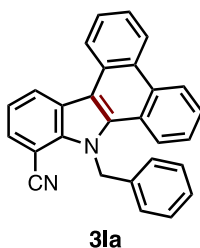
General procedure A: After purification by MPLC (hexane/CHCl₃ = 7:3 to 1:1), the obtained solid was washed with hexane to afford **3ja** as a white solid (38 mg, 49% yield). ¹H NMR (600 MHz, CDCl₃) δ 8.85 (dd, *J* = 7.8, 3.0 Hz, 2H), 8.79 (d, *J* = 7.8 Hz, 1H), 8.25 (d, *J* = 7.8 Hz, 1H), 8.13 (d, *J* = 2.4 Hz, 1H), 7.79 (ddd, *J* = 8.1, 6.9, 1.2 Hz, 1H), 7.64–7.59 (m, 2H), 7.48 (ddd, *J* = 8.4, 7.2, 1.2 Hz, 1H), 7.42–7.35 (m, 3H), 7.33–7.28 (m, 3H), 7.12 (dd, *J* = 8.4, 2.4 Hz, 1H), 5.99 (s, 2H), 4.05 (s, 3H). ¹³C NMR (150 MHz, CDCl₃) δ 154.9, 137.5, 136.5, 135.2, 130.9, 130.0, 129.1, 127.5, 127.4, 127.0, 126.4, 126.0, 125.7, 124.1, 124.0, 123.7, 123.5, 123.3, 122.8, 113.5, 113.2, 110.5, 105.0, 56.2, 50.3 (one carbon peak was not observed because of overlapping). HRMS (ESI⁺) *m/z* calcd for C₂₈H₂₂NO [M+H]⁺: 388.1696, found: 388.1700.

9-Benzyl-11-methoxy-9H-dibenzo[*a,c*]carbazole (3ka)



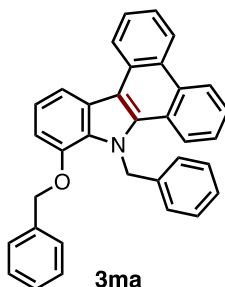
General procedure A: After purification by MPLC (hexane/CHCl₃ = 7:3 to 1:1), the obtained solid was washed with hexane to afford **3ka** as a yellow solid (41 mg, 52% yield). ¹H NMR (600 MHz, CDCl₃) δ 8.87 (d, *J* = 7.8 Hz, 1H), 8.85 (d, *J* = 7.8 Hz, 1H), 8.79 (d, *J* = 8.4 Hz, 1H), 8.55 (d, *J* = 9.0 Hz, 1H), 8.24 (d, *J* = 8.4 Hz, 1H), 7.77 (ddd, *J* = 8.4, 7.2, 1.2 Hz, 1H), 7.62–7.57 (m, 2H), 7.47 (ddd, *J* = 8.4, 7.2, 1.2 Hz, 1H), 7.40–7.31 (m, 5H), 7.08 (dd, *J* = 8.7, 2.1 Hz, 1H), 6.95 (d, *J* = 2.4 Hz, 1H), 5.97 (s, 2H), 3.90 (s, 3H). ¹³C NMR (150 MHz, CDCl₃) δ 157.9, 142.7, 137.4, 134.2, 130.3, 129.6, 129.2, 127.5, 127.3, 127.1, 126.4, 126.0, 125.2, 124.0, 123.8, 123.54, 123.49, 123.3, 122.7, 122.4, 118.1, 114.2, 109.7, 94.0, 55.7, 50.4. HRMS (ESI⁺) *m/z* calcd for C₂₈H₂₂NO [M+H]⁺: 388.1696, found: 388.1696.

9-Benzyl-9H-dibenzo[*a,c*]carbazole-10-carbonitrile (3la)



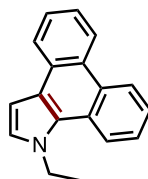
General procedure A: After purification by MPLC (CHCl₃ only), the obtained solid was washed with hexane to afford **3la** as a pale yellow solid (32 mg, 42% yield). ¹H NMR (600 MHz, CDCl₃) δ 8.86 (t, *J* = 9.0 Hz, 2H), 8.89 (d, *J* = 7.8 Hz, 1H), 8.73 (d, *J* = 8.4 Hz, 1H), 8.28 (d, *J* = 8.4 Hz, 1H), 7.83–7.79 (m, 2H), 7.72–7.64 (m, 3H), 7.54 (ddd, *J* = 8.4, 7.2, 1.2 Hz, 1H), 7.42–7.34 (m, 3H), 7.29 (d, *J* = 7.2 Hz, 2H), 6.04 (s, 2H). ¹³C NMR (150 MHz, CDCl₃) δ 139.9, 137.0, 136.2, 131.7, 129.4, 129.2, 128.0, 127.8, 127.4, 127.0, 126.8, 126.7, 125.7, 124.7, 124.2, 123.70, 123.67, 123.4, 123.2, 122.5, 122.3, 120.2, 114.2, 113.5, 106.3, 50.2. HRMS (ESI⁺) *m/z* calcd for C₂₈H₁₉N₂ [M+H]⁺: 383.1543, found: 383.1546.

9-Benzyl-10-(benzyloxy)-9H-dibenzo[*a,c*]carbazole (3ma)



General procedure A: After purification by MPLC (hexane/CHCl₃ = 7:3 to 1:1), the obtained solid was washed with hexane/CH₂Cl₂ solution to afford **3ma** as a pale yellow solid (37 mg, 40% yield). ¹H NMR (600 MHz, CDCl₃) δ 8.93 (d, *J* = 8.4 Hz, 1H), 8.84 (d, *J* = 7.8 Hz, 1H), 8.78 (d, *J* = 9.0 Hz, 1H), 8.32 (d, *J* = 8.4 Hz, 1H), 8.26 (d, *J* = 9.0 Hz, 1H), 7.77 (ddd, *J* = 8.4, 6.9, 1.5 Hz, 1H), 7.62–7.58 (m, 2H), 7.44–7.40 (m, 1H), 7.35–7.21 (m, 7H), 7.19 (d, *J* = 6.6 Hz, 2H), 7.03 (d, *J* = 7.2 Hz, 2H), 7.00 (d, *J* = 7.8 Hz, 1H), 6.30 (br s, 2H), 5.06 (s, 2H). ¹³C NMR (150 MHz, CDCl₃) δ 146.9, 139.8, 136.4, 135.6, 131.0, 130.9, 129.8, 128.7, 128.4, 127.7, 127.6, 127.3, 126.7, 126.33, 126.28, 125.9, 125.6, 124.0, 123.8, 123.6, 123.4, 123.32, 123.26, 121.2, 114.9, 114.2, 106.6, 70.7, 52.3 (one carbon peak was not observed because of overlapping). HRMS (ESI⁺) *m/z* calcd for C₃₄H₂₆NO [M+H]⁺: 464.2009, found: 464.2011.

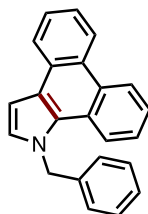
1-Ethyl-1*H*-dibenzo[*e,g*]indole (5aa)



5aa

General procedure A: Purification by MPLC (hexane/CHCl₃ = hexane only to 7:3) and GPC afforded **5aa** as a white solid (19 mg, 39% yield). ¹H NMR (600 MHz, CDCl₃) δ 8.78 (dt, *J* = 7.8, 0.6 Hz, 1H), 8.65 (d, *J* = 8.4 Hz, 1H), 8.29 (dd, *J* = 9.0, 1.2 Hz, 1H), 8.22 (d, *J* = 8.1, 0.9 Hz, 1H), 7.64–7.57 (m, 2H), 7.54 (ddd, *J* = 8.1, 6.9, 1.2 Hz, 1H), 7.50 (ddd, *J* = 8.4, 6.9, 1.2 Hz, 1H), 7.11 (d, *J* = 2.4 Hz, 1H), 7.02 (d, *J* = 3.0 Hz, 1H), 4.61 (q, *J* = 7.2 Hz, 2H), 1.60 (t, *J* = 7.5 Hz, 3H). ¹³C NMR (150 MHz, CDCl₃) δ 128.9, 128.8, 127.1, 126.8, 126.7, 126.4, 124.5, 124.2, 124.0, 123.8, 123.2, 123.1, 121.0, 100.9, 45.4, 16.4 (two carbon peaks were not observed because of overlapping). HRMS (ESI⁺) *m/z* calcd for C₁₈H₁₆N [M+H]⁺: 246.1277, found: 246.1278.

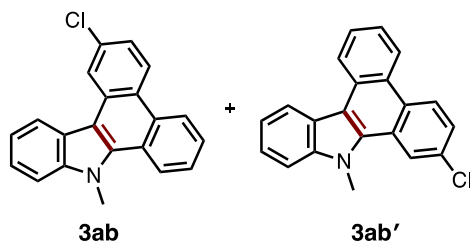
1-Benzyl-1*H*-dibenzo[*e,g*]indole (5ba)



5ba

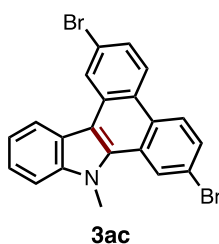
General procedure A: Purification by MPLC (hexane/CHCl₃ = hexane only to 4:1) and PTLC (hexane/CHCl₃ = 7:3) afforded **5ba** as a white solid (26 mg, 41% yield). ¹H NMR (600 MHz, CDCl₃) δ 8.72 (d, *J* = 8.4 Hz, 1H), 8.64 (d, *J* = 9.0 Hz, 1H), 8.26 (d, *J* = 8.4 Hz, 1H), 8.05 (d, *J* = 8.4 Hz, 1H), 7.64–7.60 (m, 1H), 7.54–7.50 (m, 1H), 7.47–7.44 (m, 1H), 7.41–7.37 (m, 1H), 7.30–7.26 (m, 2H), 7.25–7.21 (m, 1H), 7.16 (d, *J* = 3.6 Hz, 1H), 7.13 (dd, *J* = 9.3, 0.9 Hz, 1H), 7.09 (s, 1H), 7.08 (s, 1H), 5.81 (s, 2H). ¹³C NMR (150 MHz, CDCl₃) δ 137.7, 129.0, 128.9, 128.71, 128.67, 127.6, 127.5, 127.0, 126.8, 126.3, 125.9, 124.2, 124.1, 124.0, 123.9, 123.3, 123.14, 123.11, 121.3, 101.5, 53.9. HRMS (ESI⁺) *m/z* calcd for C₂₃H₁₈N [M+H]⁺: 308.1434, found: 308.1433.

1:1.4 Mixture of 2-Chloro-9-methyl-9H-dibenzo[*a,c*]carbazole (3ab) and 7-Chloro-9-methyl-9H-dibenzo[*a,c*]carbazole (3ab')



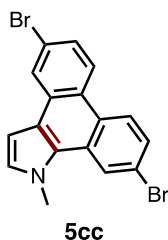
General procedure B: Purification by MPLC (hexane/CHCl₃ = hexane only to 1:1) afforded a regioisomeric mixture of **3ab** and **3ab'** as a yellow powder (30 mg, 94% yield, **3ab/3ab'** = 1:1.4). ¹H NMR (600 MHz, CDCl₃) δ 8.75 (d, *J* = 8.4 Hz, 1.4×1H), 8.67–8.61 (m, 2H + 1.4×1H), 8.60–8.50 (m, 2H + 1.4×2H), 8.47 (d, *J* = 2.4 Hz, 1.4×1H), 8.44 (d, *J* = 8.4 Hz, 1H), 7.71 (ddd, *J* = 8.1, 6.6, 1.2 Hz, 1.4×1H), 7.63–7.59 (m, 2H), 7.55–7.47 (m, 2H + 1.4×4H), 7.44 (dd, *J* = 8.7, 2.1 Hz, 1H), 7.41–7.36 (m, 1H + 1.4×1H), 4.25 (s, 3H), 4.21 (s, 1.4×3H). ¹³C NMR (100 MHz, CDCl₃) δ 140.7, 140.6, 135.0, 133.22, 133.18, 132.0, 130.8, 130.3, 129.7, 129.0, 127.5, 126.30, 126.25, 125.8, 125.7, 125.5, 125.0, 124.9, 124.6, 124.1, 123.92, 123.89, 123.8, 123.7, 123.61, 123.58, 123.3, 123.1, 123.0, 122.9, 122.7, 122.1, 121.9, 121.5, 120.5, 120.4, 114.2, 112.3, 109.6 (2C), 34.4, 34.2. HRMS (ESI⁺) *m/z* calcd for C₂₁H₁₅ClN [M+H]⁺: 316.0888, found: 316.0892.

2,7-Dibromo-9-methyl-9H-dibenzo[*a,c*]carbazole (3ac)



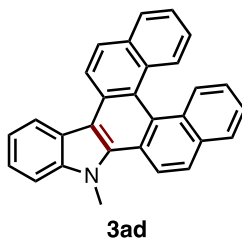
General procedure B: Purification by MPLC (hexane/CHCl₃ = hexane only to 1:1) afforded **3ac** as a white solid (36 mg, 81% yield). ¹H NMR (600 MHz, CDCl₃) δ 8.68 (d, *J* = 1.8 Hz, 1H), 8.54 (d, *J* = 2.4 Hz, 1H), 8.42 (d, *J* = 9.0 Hz, 1H), 8.34 (d, *J* = 8.4 Hz, 1H), 8.33 (d, *J* = 9.0 Hz, 1H), 7.65 (dd, *J* = 8.7, 2.1 Hz, 1H), 7.55 (dd, *J* = 9.0, 1.8 Hz, 1H), 7.54–7.52 (m, 2H), 7.42–7.38 (m, 1H), 4.13 (s, 3H). ¹³C NMR (150 MHz, CDCl₃) δ 140.6, 133.4, 130.9, 128.72, 128.65, 126.7, 125.9, 125.4, 125.2, 124.8, 124.7, 124.4, 122.6, 121.9, 121.6, 120.8, 120.5, 112.9, 109.6, 34.2 (one carbon peak was not observed because of overlapping). HRMS (APCI⁺) *m/z* calcd for C₂₁H₁₄Br₂N [M+H]⁺: 439.9467, found: 439.9468.

5,10-Dibromo-1-methyl-1*H*-dibenzo[*e,g*]indole (**5cc**)



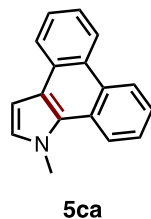
General procedure A: Purification by MPLC (hexane/CHCl₃ = 7:3 to 1:1) and GPC afforded **5cc** as a white solid (35 mg, 44% yield). ¹H NMR (600 MHz, CDCl₃) δ 8.56–8.53 (m, 2H), 8.43 (d, *J* = 8.4 Hz, 1H), 8.32 (d, *J* = 1.8 Hz, 1H), 7.64 (dd, *J* = 9.0, 1.8 Hz, 1H), 7.59 (dd, *J* = 8.7, 2.1 Hz, 1H), 7.10 (d, *J* = 3.0 Hz, 1H), 6.96 (d, *J* = 2.4 Hz, 1H), 4.30 (s, 3H). ¹³C NMR (150 MHz, CDCl₃) δ 130.1, 129.5, 127.3, 127.1, 127.0, 126.9, 125.9, 125.7, 125.6, 124.94, 124.88, 123.5, 122.5, 121.3, 120.8, 100.8, 38.8. HRMS (ESI⁺) *m/z* calcd for C₁₇H₁₂Br₂N [M+H]⁺: 389.9311, found: 389.9312.

11-Methyl-11*H*-dinaphtho[2,1-*a*:1',2'-*c*]carbazole (**3ad**)



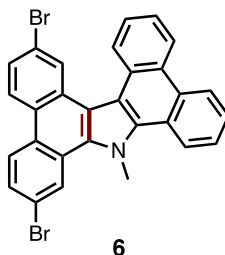
General procedure B: Purification by MPLC (hexane/CHCl₃ = hexane only to 3:2) afforded **3ad** as a yellow solid (9.7 mg, 25% yield). A single crystal of **3ad** was obtained by recrystallization from a CHCl₃ solution through vapor diffusion of pentane at room temperature, and the structure was determined by X-ray crystallography (see Table 6 and Figure 6). ¹H NMR (600 MHz, CDCl₃) δ 8.95 (d, *J* = 9.0 Hz, 1H), 8.79 (d, *J* = 9.0 Hz, 1H), 8.68 (d, *J* = 8.4 Hz, 1H), 8.32 (d, *J* = 8.4 Hz, 1H), 8.21 (d, *J* = 9.0 Hz, 1H), 8.12 (d, *J* = 9.0 Hz, 1H), 8.03 (d, *J* = 9.0 Hz, 1H), 7.97 (d, *J* = 7.8 Hz, 2H), 7.64 (d, *J* = 8.4 Hz, 1H), 7.54 (ddd, *J* = 8.1, 7.2, 1.2 Hz, 1H), 7.50 (ddd, *J* = 8.1, 6.9, 1.2 Hz, 1H), 7.45–7.41 (m, 2H), 7.26–7.19 (m, 2H), 4.48 (s, 3H). ¹³C NMR (150 MHz, CDCl₃) δ 141.8, 135.9, 131.8, 131.6, 131.1, 130.5, 130.4, 129.2, 129.1, 128.3, 127.8, 127.4, 126.9, 126.8, 125.9, 124.8, 124.7, 124.5, 124.2, 123.2, 122.1, 121.9, 121.5, 120.4, 120.2, 115.4, 109.6, 34.7 (one carbon peak was not observed because of overlapping). HRMS (ESI⁺) *m/z* calcd for C₂₉H₂₀N [M+H]⁺: 382.1590, found: 382.1592.

1-Methyl-1*H*-dibenzo[*e,g*]indole (**5ca**)



To a screw-capped glass tube containing a magnetic stirrer bar were added 1-methylpyrrole (**4c**) (2.0 mmol, 1.0 equiv), 2,2'-diiodo-1,1'-biphenyl (**2a**) (3.0 mmol, 1.5 equiv), Ag₂CO₃ (3.0 mmol, 1.5 equiv), Pd(OPiv)₂ (0.10 mmol, 5.0 mol%), DMF (7.0 mL) and DMSO (3.0 mL) under air. After stirring at 80 °C for 19 h, the reaction mixture was cooled to room temperature, and then passed through a short pad of Celite[®] (eluent: CHCl₃). After the organic solvent was removed under reduced pressure, the residue was purified by MPLC (hexane/CHCl₃ = hexane only to 7:3) to afford **5ca** as a white solid (171 mg, 37% yield). ¹H NMR (600 MHz, CDCl₃) δ 8.77 (dt, *J* = 8.4, 0.6 Hz, 1H), 8.65 (dd, *J* = 7.8, 0.6 Hz, 1H), 8.47 (dd, *J* = 8.4, 0.6 Hz, 1H), 8.22 (dd, *J* = 8.1, 0.9 Hz, 1H), 7.62–7.58 (m, 2H), 7.55 (ddd, *J* = 8.4, 7.2, 1.2 Hz, 1H), 7.51 (ddd, *J* = 8.4, 6.9, 1.5 Hz, 1H), 7.05 (d, *J* = 3.0 Hz, 1H), 7.00 (d, *J* = 2.4 Hz, 1H), 4.30 (s, 3H). ¹³C NMR (150 MHz, CDCl₃) δ 128.9, 128.7, 128.6, 127.9, 126.83, 126.76, 126.3, 124.9, 124.1, 124.0, 123.9, 123.3, 123.1, 122.7, 121.0, 100.6, 38.9. HRMS (ESI⁺) *m/z* calcd for C₁₇H₁₄N [M+H]⁺: 232.1121, found: 232.1123.

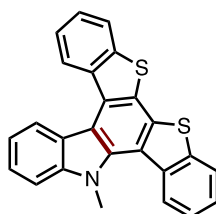
2,7-Dibromo-9-methyl-9*H*-tetrabenzo[*a,c,g,i*]carbazole (**6**)



To a screw-capped glass tube containing a magnetic stirrer bar were added *N*-methyl-dibenzoindole (**5ca**) (0.20 mmol, 1.0 equiv), 4,4'-dibromo-2,2'-diiodo-1,1'-biphenyl (**2a**) (0.30 mmol, 1.5 equiv), AgOPiv (0.40 mmol, 2.0 equiv), Pd(CH₃CN)₂(BF₄)₂ (0.010 mmol, 5.0 mol%), 1,2-dichloroethane (2.0 mL) and TfOH (0.40 mmol, 2.0 equiv) under air. After stirring at 50 °C for 12 h, the reaction mixture was cooled to room temperature, and then passed through a short pad of Celite[®] (eluent: CHCl₃). After the organic solvent was removed under reduced

pressure, the residue was purified by MPLC (hexane/CHCl₃ = hexane only to 7:3), and then the obtained solid was washed with hexane to afford **6** as a white solid (36 mg, 33% yield). ¹H NMR (600 MHz, CDCl₃) δ 9.13 (d, *J* = 1.8 Hz, 1H), 8.87 (dd, *J* = 8.1, 1.5 Hz, 1H), 8.84 (dd, *J* = 8.1, 1.5 Hz, 1H), 8.76 (dd, *J* = 8.1, 1.5 Hz, 1H), 8.61 (d, *J* = 1.8 Hz, 1H), 8.59 (d, *J* = 9.0 Hz, 1H), 8.51–8.48 (m, 2H), 7.74–7.62 (m, 6H), 4.59 (s, 3H). ¹³C NMR (150 MHz, CDCl₃) δ 137.9, 136.5, 131.0, 130.1, 128.8, 128.34, 128.3, 128.13, 128.08, 127.6, 126.4, 126.2, 126.0, 125.8, 125.6, 125.33, 125.28, 125.2, 124.9, 124.1, 123.9, 123.3, 123.0, 120.7, 120.3, 117.1, 116.8, 41.2 (one carbon peak was not observed because of overlapping). HRMS (APCI⁺) *m/z* calcd for C₂₉H₁₈Br₂N [M+H]⁺: 539.9780, found: 539.9781.

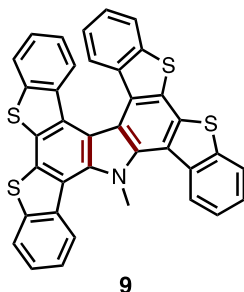
11-Methyl-11*H*-benzo[4,5]thieno[3,2-*a*]benzo[4,5]thieno[2,3-*c*]carbazole (**8**)



8

General procedure B: Purification by MPLC (hexane/CHCl₃ = hexane only to 4:1) and GPC afforded **8** as a yellow solid (13 mg, 32% yield). A single crystal of **8** was obtained by recrystallization from a CHCl₃ solution through vapor diffusion of pentane at room temperature, and the structure was determined by X-ray crystallography (see Table 6 and Figure 7). ¹H NMR (600 MHz, CDCl₃) δ 9.16 (d, *J* = 8.4 Hz, 1H), 8.92 (d, *J* = 8.4 Hz, 1H), 8.49 (d, *J* = 7.8 Hz, 1H), 8.01 (dd, *J* = 7.5, 5.1 Hz, 2H), 7.68 (d, *J* = 8.4 Hz, 1H), 7.65–7.52 (m, 4H), 7.50 (ddd, *J* = 8.4, 7.2, 1.2 Hz, 1H), 7.45 (ddd, *J* = 8.4, 6.9, 1.2 Hz, 1H), 4.23 (s, 3H). ¹³C NMR (150 MHz, CDCl₃) δ 144.3, 139.8, 139.3, 138.8, 136.3, 134.7, 133.1, 129.8, 126.8, 126.1, 125.5, 125.4, 125.3, 125.2, 124.4, 124.2, 123.9, 123.22, 123.15, 122.8, 120.24, 120.21, 117.8, 111.0, 37.4. HRMS (ESI⁺) *m/z* calcd for C₂₅H₁₆NS₂ [M+H]⁺: 394.0719, found: 394.0720.

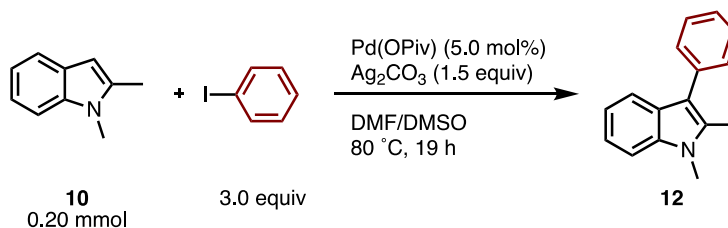
21-Methyl-21H-benzo[4,5]thieno[3,2-a]benzo[4,5]thieno[2,3-c]benzo[4,5]thieno[3,2-g]benzo[4,5]thieno[2,3-i]carbazole (9)



To a screw-capped glass tube containing a magnetic stirrer bar were added *N*-methylpyrrole (**4c**) (0.20 mmol, 1.0 equiv), 2,2'-diiodo-1,1'-biaryl (**7**) (0.60 mmol, 3.0 equiv), Ag₂CO₃ (0.60 mmol, 3.0 equiv), Pd(OPiv)₂ (0.010 mmol, 5.0 mol%), DMF (0.7 mL) and DMSO (0.3 mL) under air. After stirring at 80 °C for 19 h, the reaction mixture was cooled to room temperature, and then passed through a short pad of Celite® (eluent: CHCl₃). After the organic solvent was removed under reduced pressure, the residue was purified by MPLC (hexane/CHCl₃ = 19:1 to 3:2) and GPC to afford **9** as a yellow solid (18 mg, 15% yield). A single crystal of **9** was obtained by recrystallization from a THF solution through vapor diffusion of pentane at room temperature, and the structure was determined by X-ray crystallography (see Table 6 and Figure 8). ¹H NMR (600 MHz, CDCl₃) δ 8.83 (d, *J* = 7.8 Hz, 2H), 8.09 (d, *J* = 7.8 Hz, 2H), 7.95 (d, *J* = 7.8 Hz, 2H), 7.80 (ddd, *J* = 8.4, 7.2, 1.2 Hz, 2H), 7.69 (d, *J* = 8.4 Hz, 2H), 7.62 (ddd, *J* = 8.1, 7.2, 1.2 Hz, 2H), 7.29 (ddd, *J* = 8.1, 7.2, 0.9 Hz, 2H), 6.78 (ddd, *J* = 8.1, 7.2, 0.9 Hz, 2H), 3.98 (s, 3H). ¹³C NMR (150 MHz, CDCl₃) δ 144.7, 139.7, 139.2, 136.6, 134.4, 133.0, 129.2, 129.1, 127.7, 126.1, 125.3, 125.1, 123.2, 122.7, 122.3, 122.2, 120.0, 41.4 (one carbon peak was not observed because of overlapping). HRMS (APCI⁺) *m/z* calcd for C₃₇H₂₀NS₄ [M+H]⁺: 606.0473, found: 606.0473.

3. Experiments for mechanistic considerations

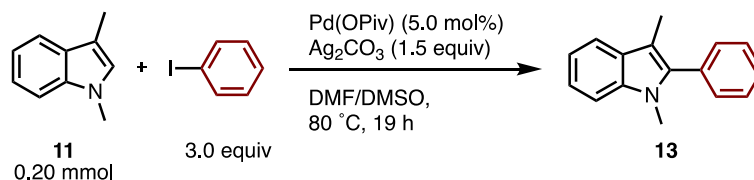
Palladium-catalyzed C–H phenylation of 1,2-dimethylindole (**10**)



To a screw-capped glass tube containing a magnetic stirrer bar were added 1,2-dimethylindole (**10**) (0.20 mmol, 1.0 equiv), iodobenzene (0.60 mmol, 3.0 equiv), Ag₂CO₃ (0.30 mmol, 1.5 equiv),

Pd(OPiv)₂ (0.010 mmol, 5.0 mol%), DMF (0.7 mL) and DMSO (0.3 mL) under air. After stirring at 80 °C for 19 h, the reaction mixture was cooled to room temperature, and then passed through a short pad of Celite[®] (eluent: EtOAc or CHCl₃). After the organic solvent was removed under reduced pressure, the residue was purified by PTLC (hexane/AcOEt = 10:1) to afford 1,2-dimethyl-3-phenyl-1*H*-indole (**12**) as a white solid (18 mg, 40% yield). ¹H NMR (600 MHz, CDCl₃) δ 7.66 (d, *J* = 7.8 Hz, 1H), 7.51–7.43 (m, 4H), 7.33–7.27 (m, 2H), 7.21 (ddd, *J* = 8.1, 7.2, 0.9 Hz, 1H), 7.11 (ddd, *J* = 8.1, 7.2, 1.2 Hz, 1H), 3.74 (s, 3H), 2.49 (s, 3H). ¹³C NMR (150 MHz, CDCl₃) δ 136.6, 135.8, 133.3, 129.7, 128.4, 126.9, 125.6, 121.1, 119.6, 118.7, 114.0, 108.7, 29.6, 11.1. HRMS (ESI⁺) *m/z* calcd for C₁₆H₁₆N [M+H]⁺: 222.1277, found: 222.1278.

Palladium-catalyzed C–H phenylation of 1,3-dimethylindole (**11**)



To a screw-capped glass tube containing a magnetic stirrer bar were added 1,3-dimethylindole (**11**) (0.20 mmol, 1.0 equiv), iodobenzene (0.60 mmol, 3.0 equiv), Ag₂CO₃ (0.30 mmol, 1.5 equiv), Pd(OPiv)₂ (0.010 mmol, 5.0 mol%), DMF (0.7 mL) and DMSO (0.3 mL) under air. After stirring at 80 °C for 19 h, the reaction mixture was cooled to room temperature, and then passed through a short pad of Celite[®] (eluent: EtOAc or CHCl₃). After the organic solvent was removed under reduced pressure, the residue was purified by PTLC (hexane/AcOEt = 10:1) to afford 1,3-dimethyl-2-phenyl-1*H*-indole (**13**) as a white solid (36 mg, 80% yield). ¹H NMR (600 MHz, CDCl₃) δ 7.60 (dt, *J* = 7.8, 1.2 Hz, 1H), 7.50–7.46 (m, 2H), 7.42–7.38 (m, 3H), 7.33 (d, *J* = 7.8 Hz, 1H), 7.25 (ddd, *J* = 8.4, 7.2, 1.2 Hz, 1H), 7.15 (ddd, *J* = 8.1, 7.2, 1.2 Hz, 1H), 3.61 (s, 3H), 2.29 (s, 3H). ¹³C NMR (150 MHz, CDCl₃) δ 137.6, 137.2, 132.1, 130.6, 128.4, 128.3, 127.7, 121.7, 119.1, 118.8, 109.2, 108.5, 30.9, 9.3. HRMS (ESI⁺) *m/z* calcd for C₁₆H₁₆N [M+H]⁺: 222.1277, found: 222.1278.

5. X-ray crystallographic analysis of **3ad**, **8** and **9**

Each single crystal of **3ad**, **8** and **9** was obtained by the recrystallizations from CHCl₃/pentane, CHCl₃/pentane and THF/pentane, respectively. Details of the crystal data and a summary of the intensity data collection parameters for **3ad**, **8**, and **9** are listed in Table S1. A suitable crystal, obtained by crystallization from appropriate solution, was mounted with mineral oil on a MiTeGen MicroMounts and transferred to the goniometer of a Rigaku PILATUS diffractometer. Graphite-monochromated Mo K α radiation ($\lambda = 0.71075 \text{ \AA}$) was used. The structures were solved by direct methods with (SIR-97)³² and refined by full-matrix least-squares techniques against F^2 (SHELXL-2014/7)³³ by using Yadokari-XG software package.³⁴ The intensities were corrected for Lorentz and polarization effects. The non-hydrogen atoms were refined anisotropically. Hydrogen atoms were placed using AFIX instructions.

Table 6. Crystallographic data and structure refinement detail for **3ad**, **8** and **9**.

	3ad	8	9
CCDC deposition No.	1848311	1848309	1848310
Formula	C ₂₉ H ₁₉ N	C ₂₅ H ₁₅ NS ₂	C ₄₁ H ₂₇ NOS ₄
Fw	381.45	393.50	677.87
<i>T</i> (K)	123(2)	123(2)	123(2)
λ (Å)	0.71073	0.71073	0.71073
cryst syst	Monoclinic	Orthorhombic	Monoclinic
space group	P2 ₁ /n	Pbca	P2 ₁ /c
<i>a</i> , (Å)	10.6434(15)	18.7793(2)	16.1846(6)
<i>b</i> , (Å)	9.1028(13)	7.45210(10)	27.2713(9)
<i>c</i> , (Å)	20.109(3)	50.3987(6)	7.6092(3)
α , (deg)	90	90	90
β , (deg)	102.565(15)	90	97.890(3)
γ , (deg)	90	90	90
<i>V</i> , (Å ³)	1901.6(5)	7053.06(15)	3326.7(2)
<i>Z</i>	4	16	4
D _{calc} , (g / cm ³)	1.332	1.482	1.353
μ (mm ⁻¹)	0.077	0.313	0.321
F(000)	800	3264	1408
cryst size (mm)	0.20 × 0.05 × 0.05	0.25 × 0.10 × 0.10	0.20 × 0.10 × 0.02
θ range, (deg)	2.009–24.998	1.946–24.999	1.961–24.999
reflns collected	13195	68569	30329
indep reflns/ <i>R</i> _{int}	3357/0.1713	6212/0.0227	5832/0.0434
params	272	507	469
GOF on <i>F</i> ²	1.010	1.278	1.086
<i>R</i> ₁ , w <i>R</i> ₂ [I>2σ(I)]	0.1013, 0.2480	0.0410, 0.0917	0.0653, 0.2172
<i>R</i> ₁ , w <i>R</i> ₂ (all data)	0.1869, 0.3280	0.0419, 0.0921	0.0871, 0.2336

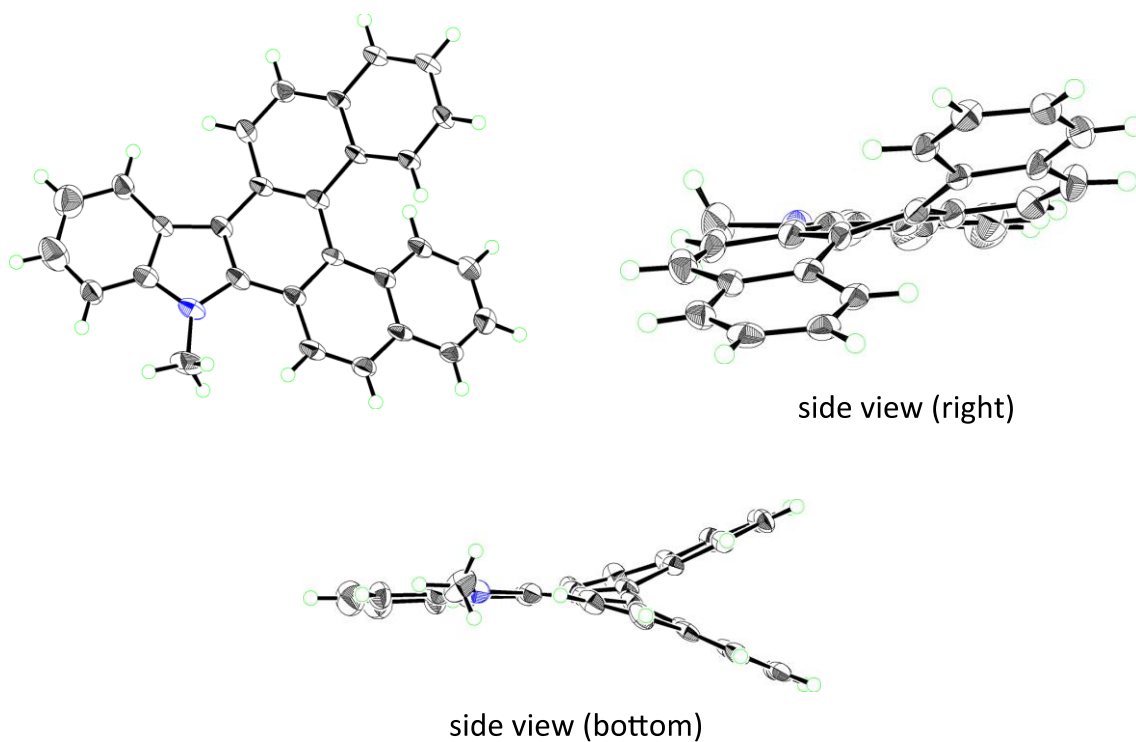


Figure 6. ORTEP drawings of **3ad** with 50% thermal ellipsoid

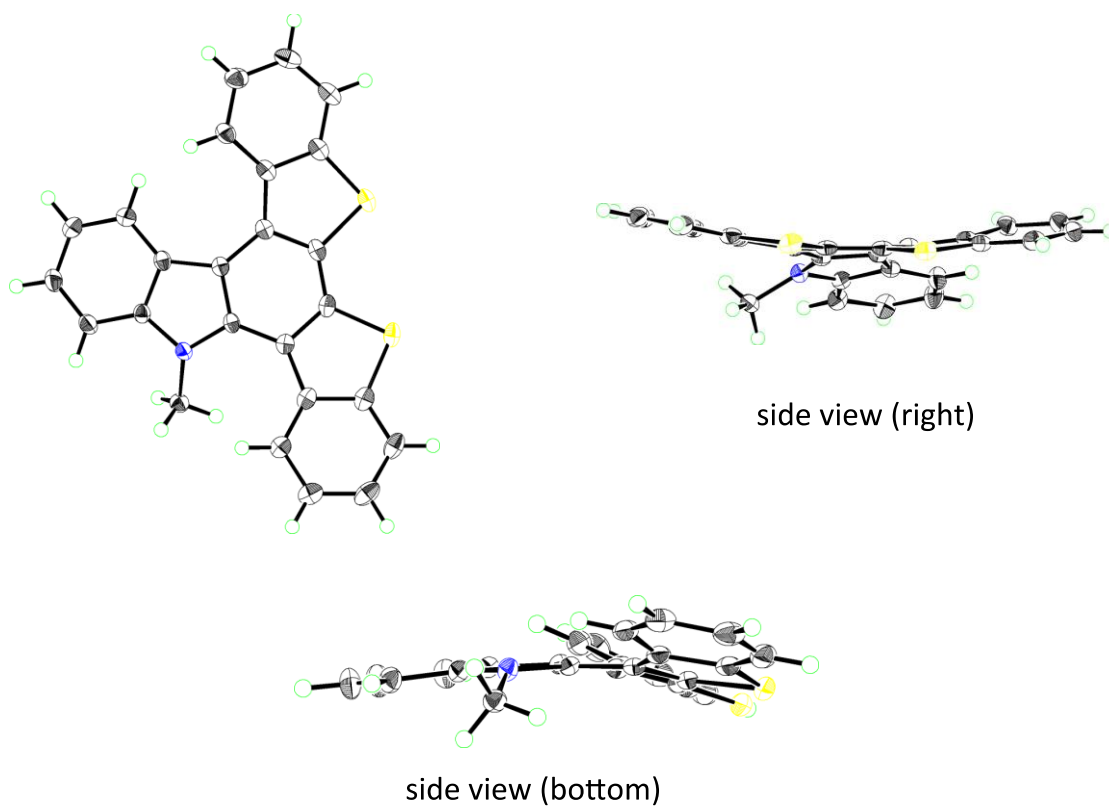
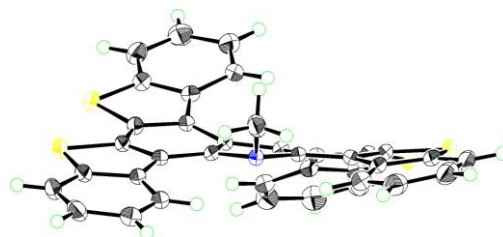
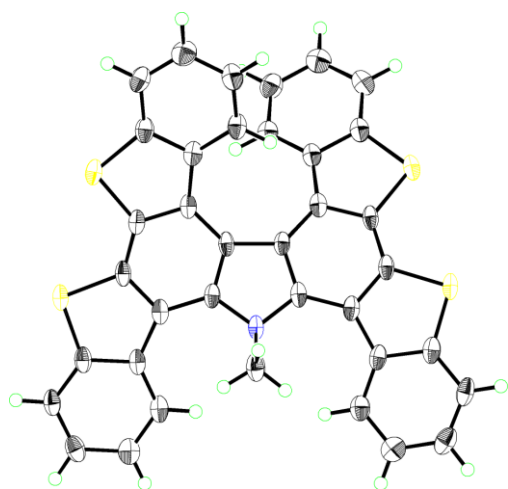
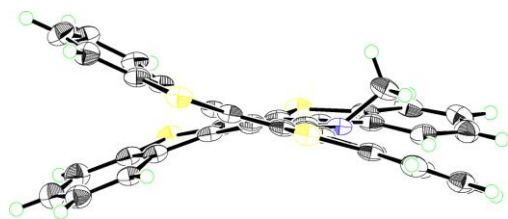


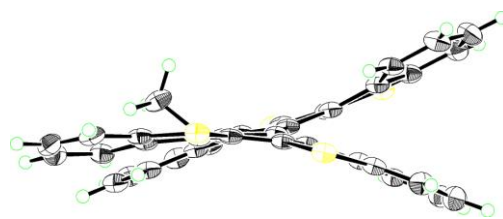
Figure 7. ORTEP drawings of **8** with 50% thermal ellipsoid.



side view (bottom)



side view (left)



side view (right)

Figure 8. ORTEP drawings of **9** with 50% thermal ellipsoid.

6. DFT calculations of **8** and **9**

The Gaussian 09 program³⁵ running on a SGI Altix4700 system was used for geometry optimization (B3LYP/6-31G(d)).³⁶ All structures were optimized without any symmetry assumptions. Zero-point energy, enthalpy, and Gibbs free energy at 298.15 K and 1 atm were estimated from the gas-phase unless otherwise noted. Calculations of harmonic vibration frequencies, molecular orbitals and their energies at the same level were performed to verify all stationary points as local minima (with no imaginary frequency) or transition states (with one imaginary frequency). Visualization of the results was performed by use of GaussView 5.0 software.

Table 7. Uncorrected and thermal-corrected (298 K) energies of stationary points (Hartree).^a

structure	E	$E + ZPE$	H	G
8	-1812.87556461	-1812.548257	-1812.526842	-1812.596592
9	-3068.96648317	-3068.518491	-3068.486765	-3068.578818

E : electronic energy; ZPE : zero-point energy; $H (= E + ZPE + E_{\text{vib}} + E_{\text{rot}} + E_{\text{trans}} + RT)$: sum of electronic and thermal enthalpies; $G (= H - TS)$: sum of electronic and thermal free energies.

Cartesian coordinates of optimized structures

Compound 8

C	0.30925000	3.07541200	-0.03921000
C	1.38308400	2.14870300	-0.01702900
C	-0.62860900	1.02499200	-0.02130600
C	0.78038800	0.82391700	0.01443300
C	1.29834600	-0.50406700	-0.01707800
C	2.64489300	-1.03108400	0.18441300
C	0.39110800	-1.54644200	-0.29883100
C	2.72615800	-2.41759700	-0.10076600
C	3.79662000	-0.40943600	0.70175900
C	3.91844000	-3.13451600	0.01369800
C	4.98360900	-1.12109700	0.83387700
H	3.75047600	0.61477400	1.04575700
C	5.05470100	-2.47295200	0.46851400
H	3.95058700	-4.19350500	-0.22578600
H	5.86102100	-0.62462000	1.23858200
H	5.99021200	-3.01602300	0.56865900
C	-1.54565100	-0.05914900	-0.04256100
C	-2.98636400	-0.14607600	0.18512200
C	-0.99168000	-1.33055600	-0.30137500
C	-3.48404300	-1.44918400	-0.06790500
C	-3.88788200	0.80156700	0.70634500
C	-4.83259300	-1.77479600	0.08382700
C	-5.22965500	0.47807200	0.87607000
H	-3.53438800	1.77717700	1.01541700
C	-5.70907600	-0.79685100	0.54432900
H	-5.18497900	-2.77968400	-0.13017000
H	-5.90973300	1.22093300	1.28331500
H	-6.76099200	-1.03429900	0.67465800
N	-0.90352500	2.39448100	-0.05035300
S	1.16439300	-3.11595600	-0.51354300
S	-2.20876200	-2.59016300	-0.48529900
C	-2.07644800	3.01688700	-0.65645400
H	-2.65129200	3.60277400	0.06996100
H	-1.75399700	3.68550400	-1.46180900
H	-2.72317100	2.25308800	-1.08438100
C	0.50644000	4.45683900	-0.11642800
H	-0.33349900	5.14483800	-0.11644500
C	1.81370900	4.92696700	-0.19301500
H	1.99644000	5.99663300	-0.24600700
C	2.89326300	4.03092600	-0.22190400
H	3.90594200	4.41233900	-0.31732700
C	2.68765100	2.65668200	-0.14411300
H	3.53801700	1.99364200	-0.22695600

Compound 9

C	1.19279800	-0.93227300	-0.22681400
C	0.68985400	0.37957000	-0.04310700
C	-1.04833700	-1.11128300	-0.09180600
C	-0.76794300	0.27152000	-0.10768200
C	-1.85720600	1.17594600	-0.29888000
C	-1.88991900	2.54534700	-0.80334400
C	-3.16747400	0.66746100	-0.14498800
C	-3.20604800	3.06613900	-0.86005000

C	-0.85077500	3.33080200	-1.33525900
C	-3.47726300	4.35116400	-1.33282100
C	-1.11777900	4.60216200	-1.82859300
C	-2.42027900	5.12174700	-1.80797300
C	-2.34847100	-1.62310100	0.09856700
C	-2.81471300	-2.97083900	0.39018500
C	-3.40578900	-0.69003300	0.09324000
C	-4.22397000	-3.02480100	0.51882400
C	-2.08105900	-4.14737500	0.62662700
C	-4.89398700	-4.21428700	0.80758200
C	-2.74480600	-5.33334000	0.92246000
H	-0.99718900	-4.11798000	0.61482500
C	-4.14456000	-5.37252100	0.99761000
H	-5.97640300	-4.23349500	0.89510700
H	-2.17021000	-6.23672900	1.10631900
H	-4.64988100	-6.30712900	1.22384100
N	0.13412700	-1.86384700	-0.29886000
S	-4.42086600	1.88528300	-0.37717600
S	-4.98038600	-1.44040100	0.33926800
C	0.08118100	-2.69515800	-1.52859000
H	1.03113800	-3.20588500	-1.67434100
H	-0.70948800	-3.44041700	-1.44145000
H	-0.11934800	-2.06583500	-2.40523000
C	2.57469800	-1.21252800	-0.29481600
C	3.31370200	-2.46949700	-0.31192900
C	3.44568600	-0.10056200	-0.29547900
C	4.70593800	-2.26196400	-0.47139600
C	2.86477400	-3.78802900	-0.11074800
C	2.97776800	1.18269800	0.00719400
S	5.13481300	-0.55137700	-0.50969000
C	5.61209700	-3.32179400	-0.52469900
C	3.76649000	-4.84655800	-0.14561000
H	1.82140400	-3.97588500	0.11479200
C	1.60910500	1.42730700	0.25784500
S	4.00458500	2.58073300	0.32792400
C	5.13104600	-4.61957800	-0.37328300
H	6.67362200	-3.13592000	-0.65995500
H	3.40817500	-5.85917700	0.01637900
C	1.42274400	2.71824700	0.91030900
C	2.62501800	3.46325600	0.98057000
H	5.82307700	-5.45620500	-0.40637500
C	2.68396100	4.72184300	1.58133100
C	1.53048300	5.23137900	2.17066200
H	-4.49525700	4.72924700	-1.35496700
H	3.61675500	5.27732600	1.61310400
H	-2.61288500	6.12091500	-2.18863300
C	0.28462200	3.24223600	1.54977500
C	0.34378700	4.48354500	2.17142500
H	1.55948300	6.20418900	2.65348700
H	-0.63471200	2.67019900	1.57256400
H	-0.54078900	4.87608100	2.66441000
H	-0.30583600	5.19703900	-2.23663800
H	0.15689300	2.93771000	-1.37847100

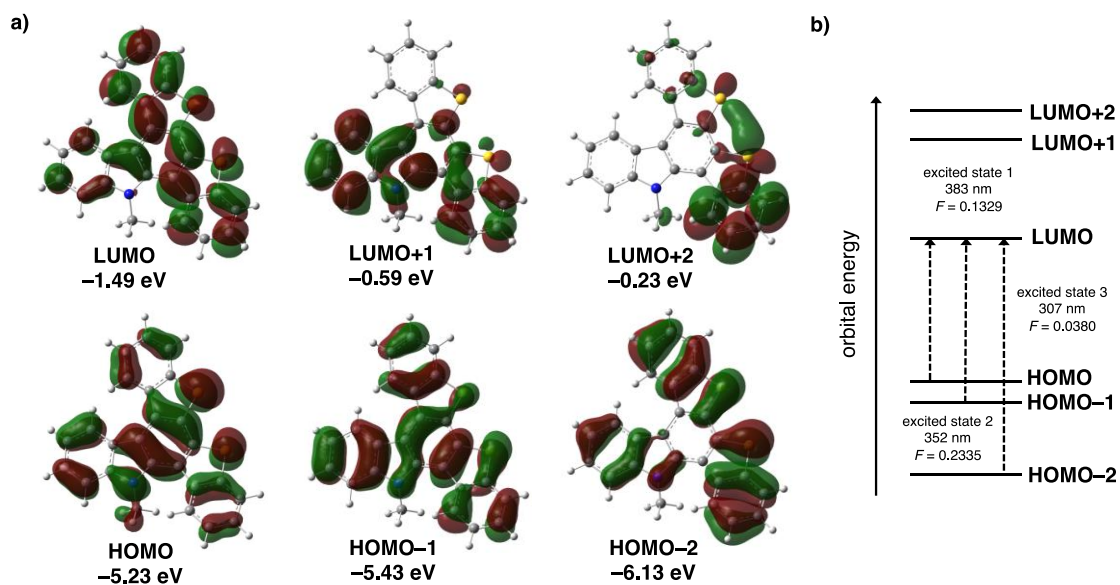


Figure 9. Pictorial representations of the frontier MOs of **8** and energy diagrams and, calculated at the B3LYP/6-31G(d) level of theory.

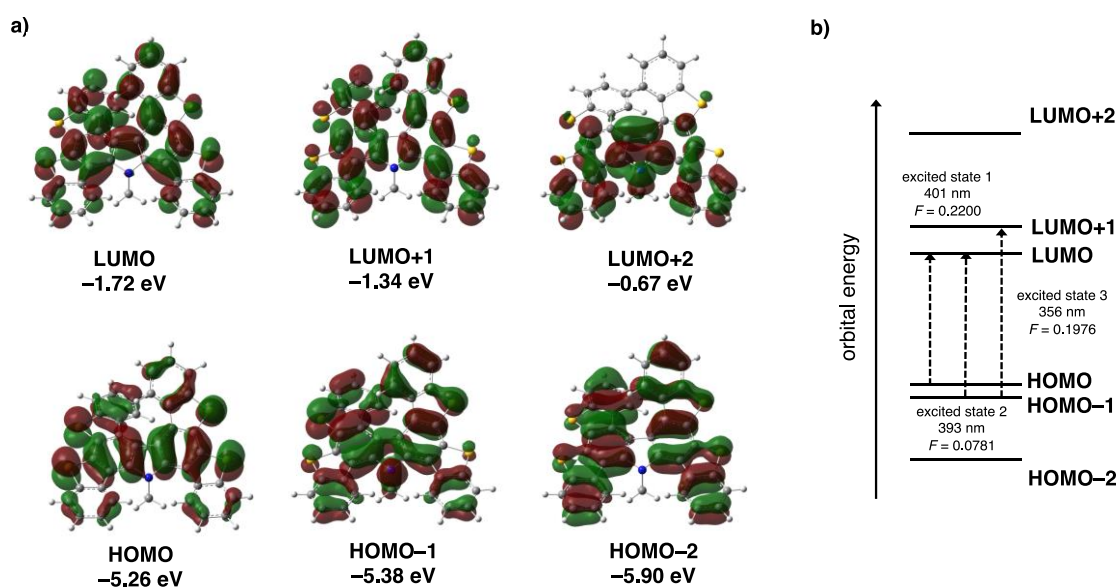


Figure 10. Pictorial representations of the frontier MOs of **9** and energy diagrams and, calculated at the B3LYP/6-31G(d) level of theory.

Table 8. TD-DFT vertical one-electron excitations (3 states) calculated for the conformation of optimized **8**.

excited state	energy	wavelength	oscillator strength (<i>f</i>)	description
1	3.2338 eV	383.41 nm	0.1329	HOMO → LUMO (0.68377) HOMO-1 → LUMO+1 (0.13101)
2	3.5204 eV	352.19 nm	0.2335	HOMO-1 → LUMO (0.67894) HOMO → LUMO+1 (-0.12685)
3	4.0345 eV	307.31 nm	0.0380	HOMO-2 → LUMO (0.63711) HOMO-1 → LUMO+1 (0.10179) HOMO → LUMO+1 (-0.19606)

Table 9. TD-DFT vertical one-electron excitations (5 states) calculated for the conformation of optimized **9**.

excited state	energy	wavelength	oscillator strength (<i>f</i>)	description
1	3.0922 eV	400.96 nm	0.2200	HOMO → LUMO (0.67912) HOMO-1 → LUMO (0.12453)
2	3.1538 eV	393.13 nm	0.0781	HOMO-1 → LUMO (0.62281) HOMO → LUMO (-0.13802) HOMO → LUMO+1 (0.27352) HOMO-3 → LUMO (0.10794)
3	3.4845 eV	355.82 nm	0.1976	HOMO-1 → LUMO (-0.27528) HOMO → LUMO+1 (0.62304)
4	3.5461 eV	349.63 nm	0.1649	HOMO-1 → LUMO+1 (0.68477) HOMO → LUMO+2 (0.12258)
5	3.6880 eV	336.19 nm	0.0296	HOMO-2 → LUMO (0.66399) HOMO → LUMO+2 (0.19397)

References and notes

1. For examples of natural products, see: (a) Knölker, H.-J.; Reddy, K. R. *Chem. Rev.* **2002**, *102*, 4303–4428. (b) Somei, M.; Yamada, F. *Nat. Prod. Rep.* **2003**, *20*, 216–242. (c) Deslandes, S.; Chassaing, S.; Delfourne, E. Marine Pyrrolocarbazoles and Analogues: Synthesis and Kinase Inhibition. *Marine Drugs* **2009**, *7*, 754–786. (d) Schmidt, A. W.; Reddy, K. R.; Knölker, H.-J. *Chem. Rev.* **2012**, *112*, 3193–3328. For examples of organic materials, see: (e) Blouin, N.; Leclerc, M. *Acc. Chem. Res.* **2008**, *41*, 1110–1119. (f) Beaujuge, P. M.; Reynolds, J. R. *Chem. Rev.* **2010**, *110*, 268–320. (g) Wang, C.; Dong, H.; Hu, W.; Liu, Y.; Zhu, D. *Chem. Rev.* **2012**, *112*, 2208–2267. (h) Karon, K.; Lapkowski, M. *J. Solid State Electrochem* **2015**, *19*, 2601–2610. (i) Ledwon, P. *Organic Electronics* **2019**, *75*, 105422. (j) Yin, J.; Ma, Y.; Li, G.; Peng, M.; Lin, W. *Coordination Chemistry Reviews* **2020**, *412*, 213257. (k) Dumur, F. *European Polymer Journal* **2020**, *125*, 109503. (l) Oner, S.; Bryce, M. R. *Mater. Chem. Front.* **2023**, *7*, 4304–4338. For examples of pharmaceuticals; see (m) Bashir, M.; Bano, A.; Ijaz, A.; Chaudhary, B. *Molecules* **2015**, *20*, 13496–13517. (n) Thomas, S. M.; Purmal, A.; Pollastri, M.; Mensa-Wilmot, K. *Sci Rep* **2016**, *6*, 32083. (o) Huang, L.; Feng, Z.-L.; Wang, Y.-T.; Lin, L.-G. *Chinese Journal of Natural Medicines* **2017**, *15*, 881–888. (p) Wang, G.; Sun, S.; Guo, H. *European Journal of Medicinal Chemistry* **2022**, *229*, 113999. (q) Ding, Y.-Y.; Zhou, H.; Peng-Deng; Zhang, B.-Q.; Zhang, Z.-J.; Wang, G.-H.; Zhang, S.-Y.; Wu, Z.-R.; Wang, Y.-R.; Liu, Y.-Q. *European Journal of Medicinal Chemistry* **2023**, *259*, 115627. (r) Patil, S. A.; Patil, S. A.; Ble-González, E. A.; Isabel, S. R.; Hampton, S. M.; Bugarin, A. *Molecules* **2022**, *27*, 6575. (s) Issa, S.; Prandina, A.; Bedel, N.; Rongved, P.; Yous, S.; Le Borgne, M.; Bouaziz, Z. *Journal of Enzyme Inhibition and Medicinal Chemistry* **2019**, *34*, 1321–1346.
2. (a) Chen, Z.; Wang, B.; Zhang, J.; Yu, W.; Liu, Z.; Zhang, Y. *Org. Chem. Front.* **2015**, *2*, 1107–1295. (b) Song, G.; Wang, F.; Li, X. *Chem. Soc. Rev.* **2012**, *41*, 3651. (c) Yuan, J.; Liu, C.; Lei, A. *Chem. Commun.* **2015**, *51*, 1394–1409. (d) Zhang, M.; Zhang, Y.; Jie, X.; Zhao, H.; Li, G.; Su, W. *Org. Chem. Front.* **2014**, *1*, 843. (e) Bariwal, J.; Van der Eycken, E. *Chem. Soc. Rev.* **2013**, *42*, 9283. (f) Louillat, M.-L.; Patureau, F. W. *Chem. Soc. Rev.* **2014**, *43*, 901–910. (g) Thirunavukkarasu, V. S.; Kozhushkov, S. I.; Ackermann, L. *Chem. Commun.* **2014**, *50*, 29–39. (h) Thansandote, P.; Lautens, M. *Chemistry A European J* **2009**, *15*, 5874–5883. (i) Bjørsvik, H.; Elumalai, V. *Eur J Org Chem* **2016**, *2016*, 5474–5479.
3. (a) Yamaguchi, J.; Yamaguchi, A. D.; Itami, K. *Angew Chem Int Ed* **2012**, *51*, 8960–9009. (b)

- Yeung, C. S.; Dong, V. M. Catalytic Dehydrogenative Cross-Coupling: Forming Carbon–Carbon Bonds by Oxidizing Two Carbon–Hydrogen Bonds. *Chem. Rev.* **2011**, *111*, 1215–1292. (c) McGlacken, G. P.; Bateman, L. M. *Chem. Soc. Rev.* **2009**, *38*, 2447. (d) Ackermann, L.; Vicente, R.; Kapdi, A. R. *Angew Chem Int Ed* **2009**, *48*, 9792–9826.
4. (a) T. Eicher, S. Hauptmann and A. Speicher, Five-Membered Heterocycles, in *The Chemistry of Heterocycles: Structure, Reactions, Syntheses, and Applications*, Wiley-VCH Verlag GmbH & Co. KGaA, Weinheim, 2nd edn, **2003**, ch. 5.1–5.21, 52–121. (b) Toguem, S. T.; Knepper, I.; Ehlers, P.; Dang, T. T.; Patonay, T.; Langer, P. *Adv Synth Catal* **2012**, *354*, 1819–1826.
5. For selected reviews of APEX, see: (a) Ito, H.; Ozaki, K.; Itami, K. *Angew Chem Int Ed* **2017**, *56*, 11144–11164. (b) Ito, H.; Segawa, Y.; Murakami, K.; Itami, K. *J. Am. Chem. Soc.* **2019**, *141*, 3–10. (c) Ito, H.; Kawahara, K. P.; Itami, K. *Synthesis* **2023**, a-2169-4078.
6. Dann, O.; Kokorudz, M.; Gropper, R. *Chem. Ber.* **1954**, *87*, 140–145.
7. (a) Goodwin, S.; Smith, A. F.; Horning, E. C. *J. Am. Chem. Soc.* **1959**, *81*, 1903–1908. (b) Miller, C. M.; McCarthy, F. O. *RSC Adv.* **2012**, *2*, 8883.
8. Cranwell, P. A.; Saxton, J. E. *J. Chem. Soc.* **1962**, 3482.
9. Napolitano, A.; Corradini, M. G.; Protà, G. *Tetrahedron* **1987**, *43*, 2749–2754.
10. Giomi, D.; Cecchi, M. *Tetrahedron* **2002**, *58*, 8067–8071.
11. Yamashita, M.; Horiguchi, H.; Hirano, K.; Satoh, T.; Miura, M. *J. Org. Chem.* **2009**, *74*, 7481–7488.
12. Ozaki, K.; Zhang, H.; Ito, H.; Lei, A.; Itami, K. *Chem. Sci.* **2013**, *4*, 3416.
13. (a) Matsuda, Y.; Naoe, S.; Oishi, S.; Fujii, N.; Ohno, H. *Chemistry A European J* **2015**, *21*, 1463–1467. (b) Shi, Z.; Zhang, B.; Cui, Y.; Jiao, N. *Angew Chem Int Ed* **2010**, *49*, 4036–4041. (c) Shi, L.; Zhong, X.; She, H.; Lei, Z.; Li, F. *Chem. Commun.* **2015**, *51*, 7136–7139. (e) Jia, J.; Shi, J.; Zhou, J.; Liu, X.; Song, Y.; Xu, H. E.; Yi, W. *Chem. Commun.* **2015**, *51*, 2925–2928. (f) Kawada, Y.; Ohmura, S.; Kobayashi, M.; Nojo, W.; Kondo, M.; Matsuda, Y.; Matsuoka, J.; Inuki, S.; Oishi, S.; Wang, C.; Saito, T.; Uchiyama, M.; Suzuki, T.; Ohno, H. *Chem. Sci.* **2018**, *9*, 8416–8425. (f) Yi, X.; Chen, K.; Chen, W. *Adv Synth Catal* **2018**, *360*, 4497–4501. (g) Li, Q.; Wang, Y.; Li, B.; Wang, B. *Org. Lett.* **2018**, *20*, 7884–7887. (h) Das, D.; Bhosle, A. A.; Panjekar, P. C.; Chatterjee, A.; Banerjee, M. *ACS Sustainable Chem. Eng.* **2020**, *8*, 19105–19116. (i) Prusty, N.; Banjare, S. K.; Mohanty, S. R.; Nanda, T.; Yadav, K.; Ravikumar, P. C. *Org. Lett.* **2021**, *23*, 9041–9046. (j) Yin, H.; Wu, Y.; Jiang, Y.; Wang, M.; Wang, S. *Org. Lett.* **2023**, *25*, 3078–3082. (k) Yao, M.-L.; Wang, X.-Y.; Feng, G.-C.; Liu,

- J.-K.; Wu, B.; Yang, J.-M. *Org. Lett.* **2023**, *25*, 4615–4620. (l) Yadav, S. K.; Jeganmohan, M. *J. Org. Chem.* **2023**, *88*, 14454–14469.
14. (a) Guo, T.; Jiang, Q.; Huang, F.; Chen, J.; Yu, Z. *Org. Chem. Front.* **2014**, *1*, 707–711. (b) Verma, A. K.; Danodia, A. K.; Saunthwal, R. K.; Patel, M.; Choudhary, D. *Org. Lett.* **2015**, *17*, 3658–3661. (c) Laha, J. K.; Dayal, N. *Org. Lett.* **2015**, *17*, 4742–4745. (d) Lin, K.; Jian, Y.; Zhao, P.; Zhao, C.; Pan, W.; Liu, S. *Org. Chem. Front.* **2018**, *5*, 590–594. (e) Saunthwal, R. K.; Saini, K. M.; Patel, M.; Verma, A. K. *Tetrahedron* **2017**, *73*, 2415–2431. (f) Qiao, Y.; Wu, X.; Zhao, Y.; Sun, Y.; Li, B.; Chen, S. *Adv Synth Catal* **2018**, *360*, 2138–2143. (g) Wu, X.-R.; Peng, H.-L.; Wei, L.-Q.; Li, L.-P.; Yao, S.-Y.; Ye, B.-H. *Catalysis Communications* **2019**, *124*, 12–18.
15. (a) Thies, N.; Hrib, C. G.; Haak, E. *Chemistry A European J* **2012**, *18*, 6302–6308. (b) Kaufmann, J.; Jäckel, E.; Haak, E. *Angew Chem Int Ed* **2018**, *57*, 5908–5911.
16. (a) Dawande, S. G.; Kanchupalli, V.; Kalepu, J.; Chennamsetti, H.; Lad, B. S.; Katukojvala, S. *Angew Chem Int Ed* **2014**, *53*, 4076–4080. (b) Rathore, K. S.; Harode, M.; Katukojvala, S. *Org. Biomol. Chem.* **2014**, *12*, 8641–8645. (c) Wu, J.-Q.; Yang, Z.; Zhang, S.-S.; Jiang, C.-Y.; Li, Q.; Huang, Z.-S.; Wang, H. *ACS Catal.* **2015**, *5*, 6453–6457.
17. Paria, S.; Reiser, O. *Adv Synth Catal* **2014**, *356*, 557–562.
18. Ozaki, K.; Kawasumi, K.; Shibata, M.; Ito, H.; Itami, K. *Nat Commun* **2015**, *6*, 6251.
19. Ozaki, K.; Matsuoka, W.; Ito, H.; Itami, K. *Org. Lett.* **2017**, *19*, 1930–1933.
20. Wu, Y.; Peng, X.; Luo, B.; Wu, F.; Liu, B.; Song, F.; Huang, P.; Wen, S. *Org. Biomol. Chem.* **2014**, *12*, 9777–9780.
21. Matsuoka, W.; Ito, H.; Itami, K. *Angew Chem Int Ed* **2017**, *56*, 12224–12228.
22. (a) Qin, C.; Lu, W. Phosphine-Free Palladium(II)-Catalyzed Arylation of Naphthalene and Benzene with Aryl Iodides. *J. Org. Chem.* **2008**, *73*, 7424–7427. (b) Hickman, A. J.; Sanford, M. S. *ACS Catal.* **2011**, *1*, 170–174. (c) Collins, K. D.; Honeker, R.; Vásquez-Céspedes, S.; Tang, D.-T. D.; Glorius, F. *Chem. Sci.* **2015**, *6*, 1816–1824. (d) Kawai, H.; Kobayashi, Y.; Oi, S.; Inoue, Y. *Chem. Commun.* **2008**, *12*, 1464–1466. (e) Funaki, K.; Kawai, H.; Sato, T.; Oi, S. *Chem. Lett.* **2011**, *40*, 1050–1052.
23. (a) Lebrasseur, N.; Larrosa, I. *J. Am. Chem. Soc.* **2008**, *130*, 2926–2927. (b) Liston, D. J.; Lee, Y. J.; Scheidt, W. R.; Reed, C. A. *J. Am. Chem. Soc.* **1989**, *111*, 6643–6648. (c) Albano, V. G.; Di Serio, M.; Monari, M.; Orabona, I.; Panunzi, A.; Ruffo, F. *Inorg. Chem.* **2002**, *41*, 2672–2677.
24. (a) Shibata, M.; Ito, H.; Itami, K. *J. Am. Chem. Soc.* **2018**, *140*, 2196–2205. (b) Nova, A.;

- Ujaque, G.; Maseras, F.; Lledós, A.; Espinet, P. *J. Am. Chem. Soc.* **2006**, *128*, 14571–14578.
Also see ref. 18 and 23
25. (a) Jones, G. B.; Mathews, J. E. *Tetrahedron* **1997**, *53*, 14599–14614. (b) Hyun, S. Y.; Jung, S. O.; Oh, H. J. KR Pat. 20150121626A, 2015
26. (a) Ito, S.; Tokimaru, Y.; Nozaki, K. *Angew Chem Int Ed* **2015**, *54*, 7256–7260. (b) Yokoi, H.; Hiraoka, Y.; Hiroto, S.; Sakamaki, D.; Seki, S.; Shinokubo, H. *Nat Commun* **2015**, *6*, 8215. (c) Tokimaru, Y.; Ito, S.; Nozaki, K. *Angew Chem Int Ed* **2018**, *57*, 9818–9822. (d) Krzeszewski, M.; Kodama, T.; Espinoza, E. M.; Vullev, V. I.; Kubo, T.; Gryko, D. T. *Chemistry A European J* **2016**, *22*, 16478–16488. (e) Mishra, S.; Krzeszewski, M.; Pignedoli, C. A.; Ruffieux, P.; Fasel, R.; Gryko, D. T. *Nat Commun* **2018**, *9*, 1714. (f) Krzeszewski, M.; Gryko, D.; Gryko, D. T. *Acc. Chem. Res.* **2017**, *50*, 2334–2345.
27. Shi, G.; Chen, D.; Jiang, H.; Zhang, Y.; Zhang, Y. S. *Org. Lett.* **2016**, *18*, 2958–2961.
28. Wu, B.; Yoshikai, N. *Angew Chem Int Ed* **2015**, *54*, 8736–8739.
29. Li, X.; Han, J.; Wong, H. N. C. *Asian J Org Chem* **2016**, *5*, 74–81.
30. Miura, M.; Sato, T.; Tsurugi, H.; Kumagai, A.; Ueda, M. Jpn Pat., 2009190999, 2009.
31. Xu, X.-H.; Liu, G.-K.; Azuma, A.; Tokunaga, E.; Shibata, N. *Org. Lett.* **2011**, *13*, 4854–4857.
32. Altomare, A.; Burla, M. C.; Camalli, M.; Cascarano, G. L.; Giacovazzo, C.; Guagliardi, A.; Moliterni, A. G. G.; Polidori, G.; Spagna, R. *J Appl Crystallogr* **1999**, *32*, 115–119.
33. Sheldrick, G. M. *Acta Crystallogr A Found Crystallogr* **2008**, *64*, 112–122.
34. (a) Wakita, K. Yadokari-XG, Software for crystal structure analyses, **2001**. (b) Kabuto, C.; Akine, S.; Nemoto, T.; Kwon, E.; *J. Cryst. Soc. Jpn.* **2009**, *51*, 218–224.
35. Frisch, M. J.; Trucks, G. W.; Schlegel, H. B.; Scuseria, G. E.; Robb, M. A.; Cheeseman, J. R.; Scalmani, G.; Barone, V.; Mennucci, B.; Petersson, G. A.; Nakatsuji, H.; Caricato, M.; Li, X.; Hratchian, H. P.; Izmaylov, A. F.; Bloino, J.; Zheng, G.; Sonnenberg, J. L.; Hada, M.; Ehara, M.; Toyota, K.; Fukuda, R.; Hasegawa, J.; Ishida, M.; Nakajima, T.; Honda, Y.; Kitao, O.; Nakai, H.; Vreven, T.; Montgomery, J. A.; Jr., Peralta, J. E.; Ogliaro, Jr. F.; Bearpark, M.; Heyd, J. J.; Brothers, E.; Kudin, K. N.; Staroverov, V. N.; Keith, T.; Kobayashi, R.; Normand, J.; Raghavachari, K.; Rendell, A.; Burant, J. C.; Iyengar, S. S.; Tomasi, J.; Cossi, M.; Rega, N.; Millam, J. M.; Klene, M.; Knox, J. E.; Cross, J. B.; Bakken, V.; Adamo, C.; Jaramillo, J.; Gomperts, R.; Stratmann, R. E.; Yazyev, O.; Austin, A. J.; Cammi, R.; Pomelli, C.; Ochterski, J. W.; Martin, R. L.; Morokuma, K.; Zakrzewski, V. G.; Voth, G. A.; Salvador, P.; Dannenberg, J. J.; Dapprich, S.; Daniels, A. D.; Farkas, O.; Foresman, J. B.; Ortiz, J. V.; Cioslowski, J.; Fox, D. J. Gaussian 09, Revision D.01, Gaussian, Inc., Wallingford CT, **2013**.

36. (a) Becke, A. D. *J. Chem. Phys.*, **1993**, *98*, 5648–5652. (b) Lee, C.; Yang, W.; Parr, R. G. *Phys. Rev. B*, **1988**, *37*, 785–789.

Palladium-Catalyzed Esterification of Carboxylic Acids with Aryl Iodides

Abstract

The first palladium-catalyzed esterification of carboxylic acids with aryl iodides is described. A palladium-based catalytic system consisting of 1,3-bis((pentafluorophenyl)methyl)imidazole-2-ylidene (IBn^F) ligand was found to significantly accelerate aryl–O bond-forming esterification reaction. A series of aryl iodides and carboxylic acids undergoes a palladium-catalyzed coupling reaction to provide the corresponding aryl esters in moderate to good yields. In addition, sterically hindered aryl iodides and carboxylic acids were well tolerated yielding the corresponding aryl esters.

1. Introduction

Since aryl esters have biological functions and tunable reactivity to nucleophiles, they are fundamental subunits found often in pharmaceuticals, agrochemicals, polymers, natural products and also in variety of synthetic intermediates.¹ A group of compounds that frequently contain esters in pharmaceuticals are prodrugs, also shown below. Prodrugs are designed to allow bioactive drugs with poor pharmacokinetics to be efficiently absorbed and distributed in the body.² When an ester prodrug is administered to the body, the ester bond is hydrolyzed by carboxyesterase in the body to generate the original drug. This transformation improves drug solubility and membrane permeability, and enables effective drug concentrations to be achieved *in vivo*.

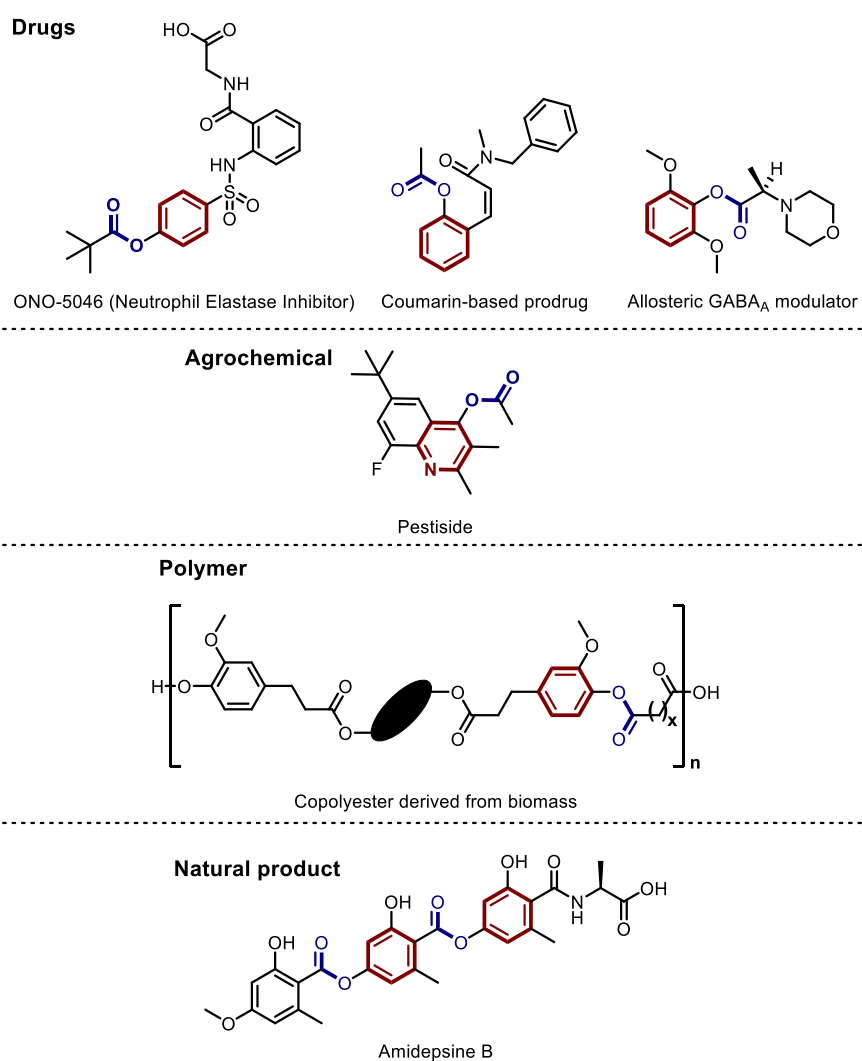
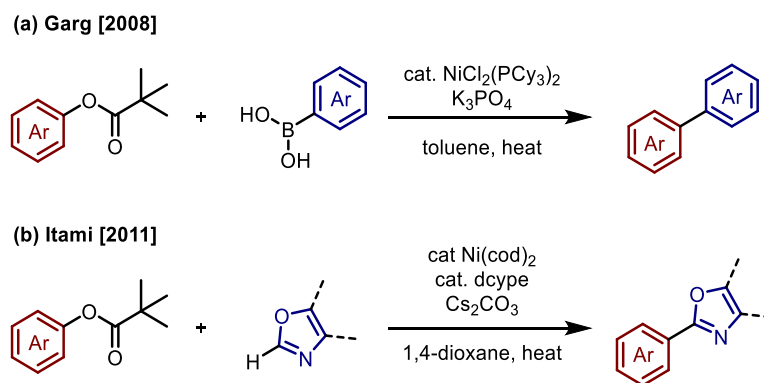


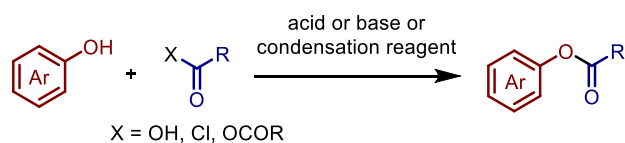
Figure 1. Widely used or found functional aryl esters.

Recently, aryl esters have also attracted much interests as green and low-cost arylating agents via C–O activation in metal-catalyzed coupling reactions.³ One of representative examples would be a cross-coupling reaction of aryl pivalates with boronic acids developed by Garg and co-workers in 2008 (Scheme 1a).⁴ They achieved the cross-coupling by using Ni catalyst to activate typically unreactive C_{aryl}–O_{acyl} bond of low-cost and readily available *O*-acylated phenols. Since then, aryl pivalates have attracted attention as new electrophiles and have been applied not only to coupling with boronic acids but also to C–H arylation reactions. In 2011, Itami, Yamaguchi, and co-workers reported nickel-catalyzed C–H/C–O couplings using aryl pivalates (Scheme 1b). This catalytic system using Ni(cod)₂, dcype and Cs₂CO₃ is applicable to direct arylation of various thiazoles and has been adapted to the synthesis of complex natural product derivatives (Scheme 1b).⁵

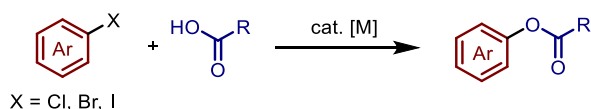


Scheme 1. Ni-catalyzed cross-coupling reactions of aryl pivalates with electrophiles.

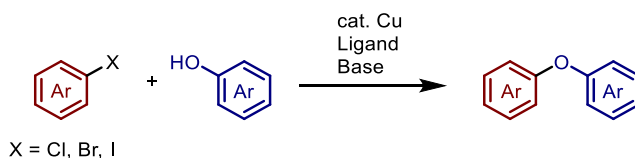
Among various synthetic routes for aryl esters, condensation of phenols and carboxylic acids or their derivatives, *i.e.* C_{acyl}–O_{aryl} bond formations, undoubtedly represents one of most conventional and established transformations (Scheme 2).⁶ On the other hand, less attention has been paid to the synthesis of aryl esters *via* C_{aryl}–O_{acyl} bond formations such as the cross-coupling between aryl halides and carboxylic acids (Scheme 3), while a number of useful metal-catalyzed C_{aryl}–O bond forming reactions using aryl halides/metals with alcohols such as Ullmann reaction have been developed for the synthesis of aryl ethers (Scheme 4).⁷



Scheme 2. Most conventional and established preparation method of aryl esters through C_{aryl}–O_{aryl} bond formation.

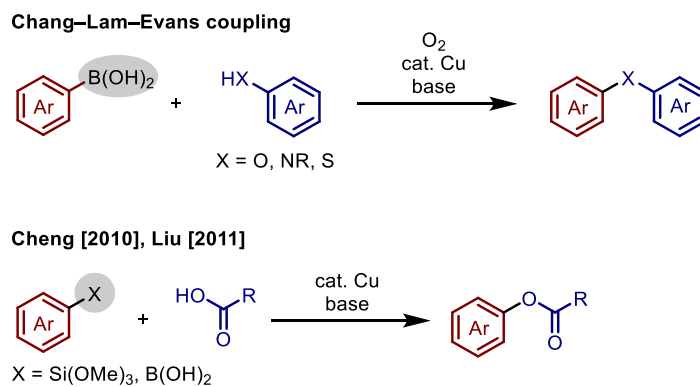


Scheme 3. Undeveloped cross-coupling of aryl halides with carboxylic acids through C_{aryl}–O_{acyl} bond formation.

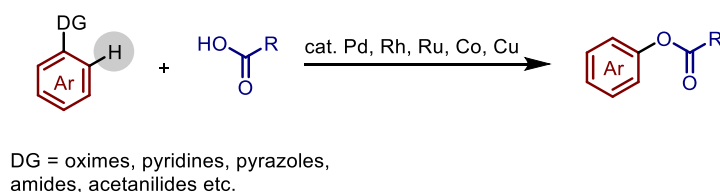


Scheme 4. Ullman reaction of aryl halides with aryl alcohols.

Based on the findings that have been reported to date, the use of carboxylic acids as an *O*-nucleophile in metal-catalyzed C_{aryl}–O_{acyl} bond formation has been limited to three types of esterifications. In 2010, Cheng and coworkers established an esterification of arenecarboxylic acids with aryl- and alkenyl-substituted trimethoxysilanes by copper(II) catalyst (Scheme 5).⁸ This catalytic system is similar to Chan–Lam–Evans coupling which affords diaryl ether from phenols and arylboronic acids, and the Cheng’s reaction allowed a series of aryltrimethoxysilanes to react with arene carboxylic acids in the presence of copper(II) catalyst, smoothly giving aryl esters in good yields. In the same year, they also reported copper(II)-catalyzed esterification of arenecarboxylic acid with arylboronic acids. Liu also developed Cu-mediated *O*-arylation of arenecarboxylic acids independently in 2011.⁹ Directing group-assisted catalytic C–H activation is also known as another example for C_{aryl}–O_{acyl} bond formation. Because of its synthetic advantages in terms of step- and atom-economy, huge efforts have been devoted to establish efficient acyloxylation of arenes from many groups. As one of extensive studies, C–H activation by the use of variety of transition metals can achieve the cross coupling of arenes with carboxylic acids (Scheme 6).¹⁰



Scheme 5. Chang–Lam–Evans-type Cu-catalyzed cross-coupling reactions between arylsilanes/arylboronic acids and carboxylic acids.



Scheme 6. Synthesis of aryl esters by directing group-assisted C–H activation.

When the author started the present study, there has been no report on cross-couplings using aryl halide as an electrophile and carboxylic acid as a nucleophile. Two assumptions can be made to explain why $\text{C}_{\text{aryl}}\text{-O}_{\text{acyl}}$ bond formations has not been reported. Firstly, carboxylate have weak coordinating ability due to the delocalization of the negative charge over the oxygen atoms, so they tend to deviate from Pd even if its coordinated. Secondly, reductive elimination is less likely to occur in the cationic counter metal coordinated κ^1 -binding (monodentate) mode which is predominant in the presence of Lewis acidic metals such as alkali metal ions (Figure 2).¹¹ Furthermore, the aryl–palladium–carboxylate (Ar-Pd-OCOR) intermediate is well known to show an ability of C–H activation *via* concerted metalation-deprotonation (CMD) pathway rather than the reductive elimination of aryl carboxylate (Ar-OCOR) (Figure 3a). In related metal-catalyzed reactions where aryl metal carboxylates (Ar-M-OCOR) are formed *in situ*, the Ar-OCOR bond is easily cleaved through the oxidative addition of electron-rich low-valent metals like nickel(0) (Figure 3b).³ In addition, phenoxy esters can easily undergo decomposition in the presence of nucleophiles due to the high leaving ability of the phenoxy group (Figure 3c).¹²

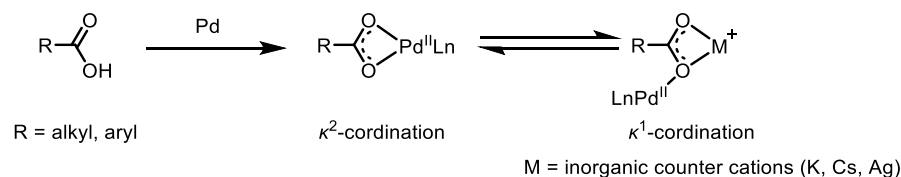


Figure 2. Coordination patterns of carboxylate to palladium.

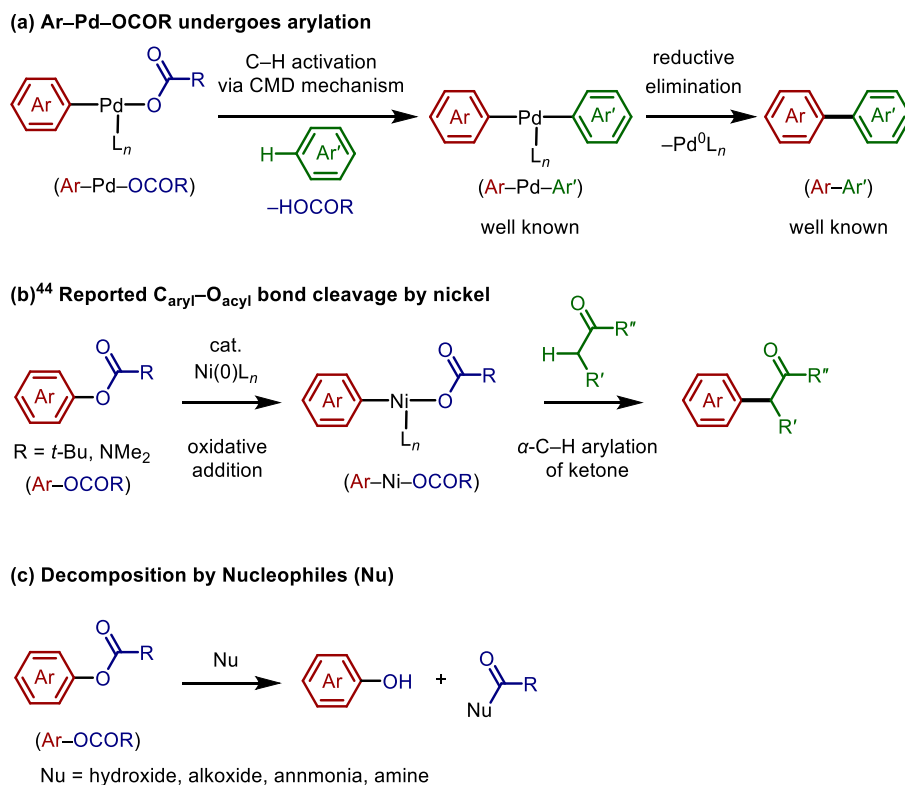
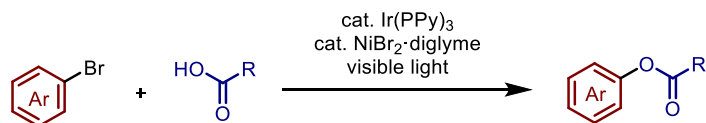
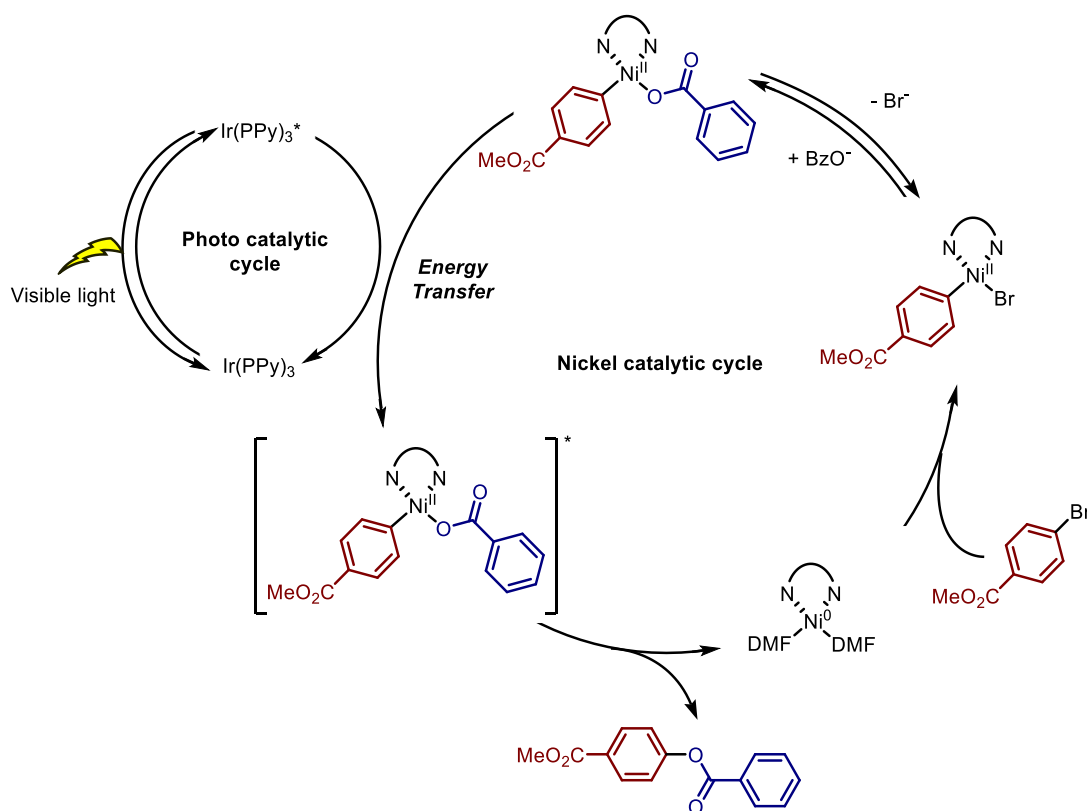


Figure 3. Possible bypass reactions in C_{aryl}–O_{acyl} bond forming cross-coupling reactions.

With this background, in 2017, McCusker and MacMillan achieved a first cross-coupling between aryl bromides and carboxylic acids by energy transfer-driven organometallic catalysis (Scheme 7).¹³ They found Ir(ppy)₃ photosensitizer can transfer excitation energy to aryl–Ni(II) carboxylate under visible light irradiation, thus achieving challenging reductive elimination of C_{aryl}–O_{acyl} bond to give the corresponding aryl esters (Scheme 8). The achievement of this photoredox reaction can be attributed not only to the photoredox catalyst, but also the mild reaction temperature around 40 °C and the use of organic bases with low nucleophilicity.



Scheme 7. Cross-coupling between aryl bromides and carboxylic acids by energy transfer-driven organometallic catalysis.

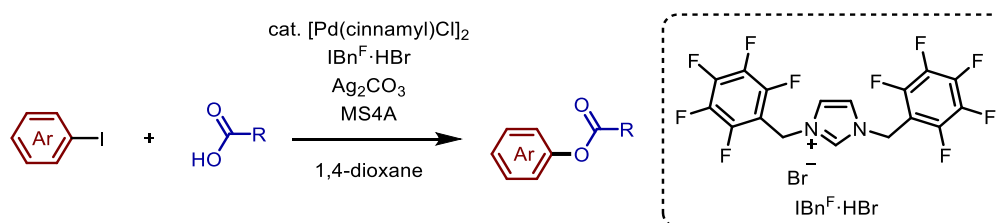


Scheme 8. Synthesis of aryl esters by energy transfer-driven coupling.

As mentioned above, the substrate generality of metal-catalyzed C_{aryl}-O_{acyl} bond forming reactions has been increased along with their development. However, there is no report on transition metal-catalyzed cross-coupling between aryl halides and carboxylic acids in 2016 when the author started the research on related projects, whereas McCusker and MacMillan's report the first example by Ni-photoredox system in 2017. As already introduced, there are obvious difficulties in producing an aryl ester through reductive elimination from an Ar-Pd-OCOR, and the low stability of aryl esters themselves under conditions with low valent transition metal catalysts makes this reaction much more difficult. From the viewpoints of fundamental understanding of undeveloped elementary reaction in organometallic chemistry as well as achieving challenging

organic transformation, screening a new catalytic system with appropriate metal, ligand and conditions is highly important for achieving C_{aryl}-O_{acyl} bond formation.

In this chapter, the first palladium-catalyzed esterification of carboxylic acids with aryl iodides is described. In the presence of a unique palladium catalyst, prepared *in situ* from [Pd(cinnamyl)Cl]₂, HBr salt of 1,3-bis((pentafluorophenyl)methyl)imidazole-2-ylidene (IBn^F), and Ag₂CO₃, series of aryl iodides and carboxylic acids undergoes a cross-coupling reaction to provide the corresponding aryl esters in moderate to good yields (Scheme 9).



Scheme 9. Pd-catalyzed esterification of aryl iodides with carboxylic acids.

2. Results and Discussion

2-1. Screening of reaction conditions

First, the optimization of reaction conditions using 4-iodoanisole (**1a**) and pivalic acid (**2a**) as model substrates was performed (Table 1). Through extensive screening of metal catalysts, ligands, bases and so on, it was found that the combination of Pd(OAc)₂ (5 mol %) and Ag₂CO₃ (3.0 equiv) promoted the desired esterification in the presence of MS4A in 1,4-dioxane at 100 °C, providing aryl ester **3aa** in 32% GC yield (entry 1). The screening of phosphine ligands such as PCy₃, PPh₃, SPhos, BINAP and dppbz was conducted but the yield of **3aa** was not improved (entries 2–6). The use of nitrogen-based ligand such as 2,2'-bipyridyl (bipy) dramatically lowered the yield (entry 7, 3% yield). To our delight, *N*-heterocyclic carbene (NHC) ligands such as 1,3-bis(2,4,6-trimethylphenyl)imidazole-2-ylidene (IMes) and 1,3-bis(2,6-diisopropylphenyl)imidazole-2-ylidene (IPr) effectively facilitated the esterification reaction (entry 8, 9). Especially, hydrogen bromide salt of (1,3-bis((perfluorophenyl)methyl)imidazole-2-ylidene) (IBn^F)⁸ showed further increase of yield (entry 10, 78% yield). The reaction with more electron-rich dibenzyl NHC ligand (IBn) was also tested for comparison, but the yield of **3aa** dropped to 55% (entry 11).⁹

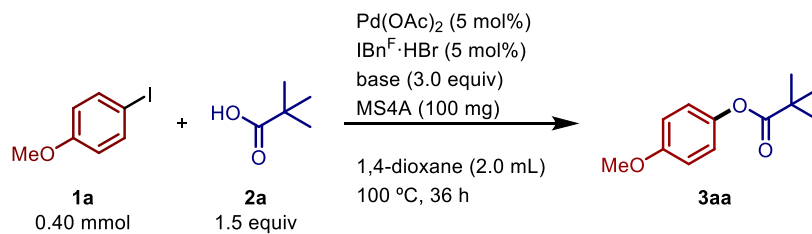
Table 1. Ligand screening in the Pd-catalyzed esterification of aryl iodide **1a** with carboxylic acid **2a**.

entry	ligand	yield ^a
1	none	32%
2	PCy ₃ ·HBF ₄ ^b	37%
3	PPh ₃ ^b	25%
4	SPhos	32%
5	BINAP	32%
6	dppbz	26%
7	bipy	3%
8	IMes·HCl	50%
9	IPr·HCl	66%
10	IBn ^F ·HBr	78% (75%) ^c
11	IBn·HBr	51%

^aDetermined by gas chromatography by using dodecane as an internal standard. ^b10 mol%. ^cIsolated yield.

Setting IBn^F·HBr as an optimal ligand precursor, further investigation on the effect of base was carried out (Table 2). The use of Ag₂O resulted in lower yield (entry 2, 34% yield). Silver salts are essential for this reaction; the use of K₂CO₃, Na₂CO₃ and Cs₂CO₃ instead of Ag₂CO₃ or the absence of silver salt completely shuts down the reaction (entries 3–6). Interestingly, the employment of silver pivalate instead of the combination of pivalic acid (**2a**) and Ag₂CO₃ also gave the product **3aa** in 55% yield (entry 7). This result implies that mixing **2a** and Ag₂CO₃ would also give AgOPiv *in situ*, and it works as effective transmetalation or ligand exchanging agents in the present catalytic reaction.

Table 2. Screening of base in the Pd-catalyzed esterification of aryl iodide **1a** with carboxylic acid **2a**.

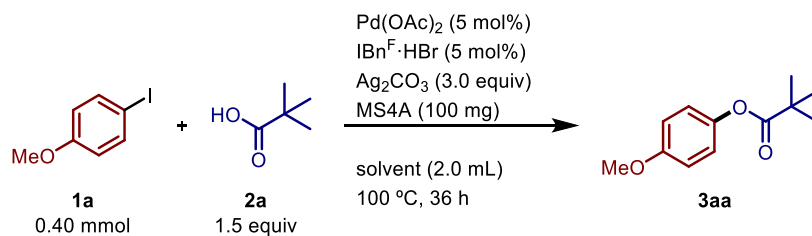


entry	base	yield ^a
1	Ag_2CO_3	78%
2	Ag_2O	34%
3	K_2CO_3	0%
4	Na_2CO_3	0%
5	Cs_2CO_3	0%
6	none	0%
7 ^b	AgOPiv^{c}	55%

^aDetermined by gas chromatography by using dodecane as an internal standard. ^bReaction without pivalic acid. ^c1.5 equiv. ^dIsolated yield.

Then, the reaction solvents were examined (Table 3). As the solvent, 1,4-dioxane gave the best result (entry 1). Low polar solvents such as toluene and 1,2-dichloroethane decreased the yield (entries 2 and 3) in terms of yield, while highly polar solvents such as acetonitrile, dimethylformamide (DMF) and 1,1,1,3,3,3-hexafluoroisopropyl alcohol (HFIP) completely suppressed the reaction progress (entries 4–6).

Table 3. Solvent screening in the Pd-catalyzed esterification of aryl iodide **1a** with carboxylic acid **2a**.

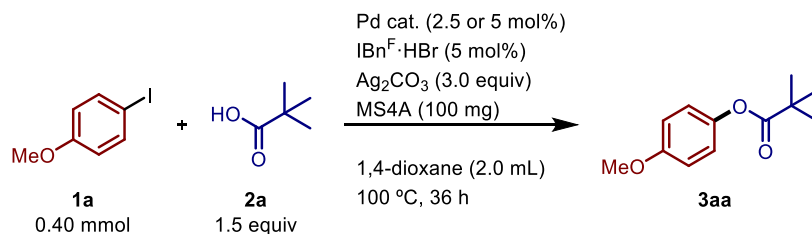


entry	solvent	yield ^a
1	1,4-dioxane	78%
2	toluene	34%
3	ClCH ₂ CH ₂ Cl	57%
4	CH ₃ CN	0%
5	DMF	0%
6	HFIP	0%

^aDetermined by gas chromatography by using dodecane as an internal standard.

Next, the effect of Pd source was investigated (Table 4). While PdCl₂, PdI₂ and Pd(PPh₃)₄ showed lower activity than Pd(OAc)₂ (entries 1–4), the use of [Pd(allyl)Cl]₂ or [Pd(cinnamyl)Cl]₂ gave the almost comparable results to Pd(OAc)₂ in terms of yield (entries 6 and 7). Due to higher solubility and reproducibility, using [Pd(cinnamyl)Cl]₂, IBn^F·HBr and the conditions in entry 7 as optimal catalyst, ligand and reaction conditions, respectively. The use of MS4A further increased the reproducibility of yield.

Table 4. Screening of Pd source in the Pd-catalyzed esterification of aryl iodide **1a** with carboxylic acid **2a**.



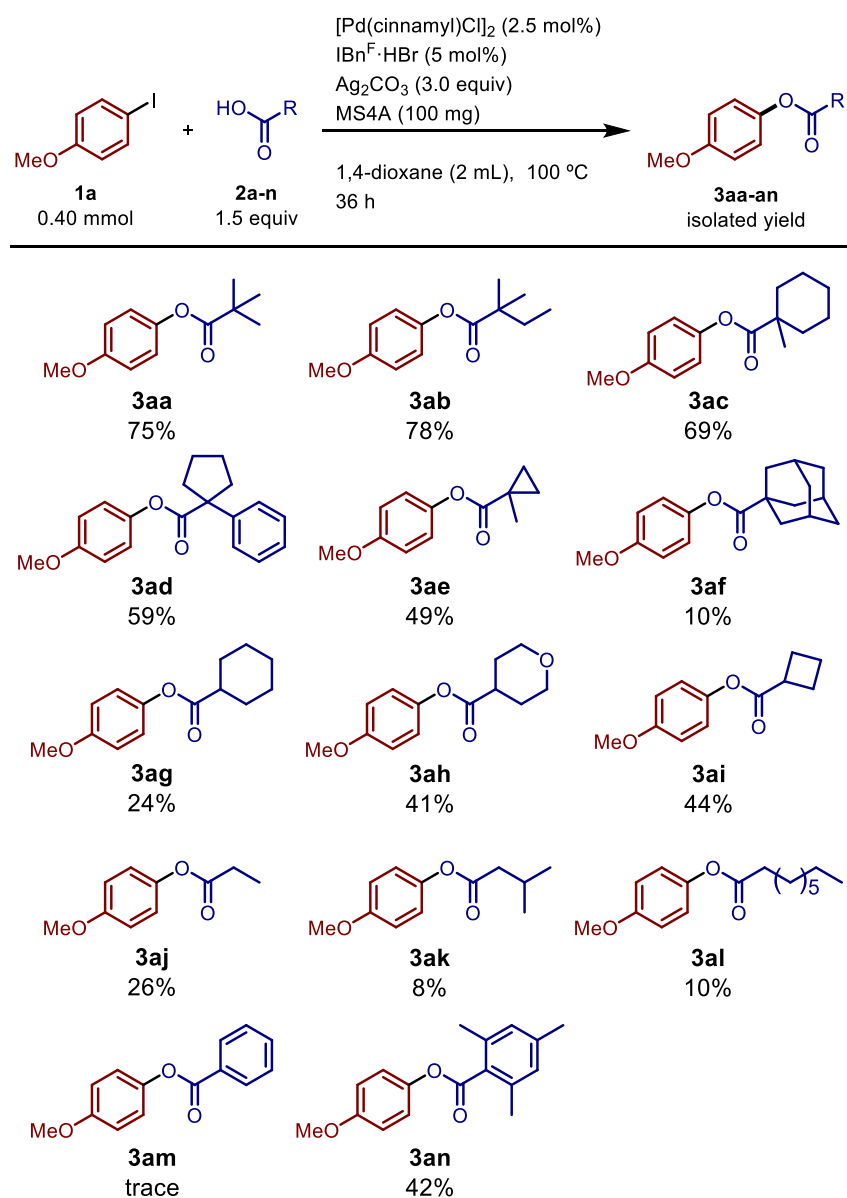
entry	Pd cat.	yield ^a
1	PdCl ₂ (5 mol%)	5%
2	PdI ₂ (5 mol%)	66%
3	Pd(OAc) ₂ (5 mol%)	78% (75%) ^d
4	Pd(PPh ₃) ₄ (5 mol%)	49%
5	Pd ₂ (dba) ₃ (2.5 mol%)	7%
6	[Pd(allyl)Cl] ₂ (2.5 mol%)	67%
7 ^c	[Pd(cinnamyl)Cl] ₂ (2.5 mol%)	77% ^b (77%) ^d

^aDetermined by gas chromatography by using dodecane as an internal standard. ^bDetermined by ¹H NMR using CH₂Br₂ as an internal standard. ^cReaction time: 42 h. ^dIsolated yield

2-2. Substrate scope

With the optimal conditions in hand, the substrate scope of the carboxylic acid by employing 4-iodoanisole (**1a**) was examined in the presence of catalytic amount of [Pd(cinnamyl)Cl]₂ and IBn^F·HBr (Scheme 10). Except pivalic acid (**2a**), tertiary alkyl carboxylic acids such as *tert*-amyl carboxylic acid (**2b**) and 1-methyl-cyclohexane-1-carboxylic acid (**2c**) gave the corresponding products **3ab** and **3ac** in 79% and 69% yields, respectively. The reactions with other tertiary carboxylic acids such as 1-phenylcyclopentane-1-carboxylic acid (**2d**) and 1-methylcyclopropane-1-carboxylic acid (**2e**) afforded esters **3ad** and **3ae** in moderate yields. The bulkiness around carboxylic acid seems to be important for the reaction progress. However, the reaction with 1-adamantanecarboxylic acid (**2f**) somehow dropped the yield of **3af** (10%). The reaction efficiency also decreased when secondary alkyl carboxylic acids were used. Cyclohexanecarboxylic acid (**2g**), tetrahydro-2*H*-pyran-4-carboxylic acid (**2h**) and cyclobutanecarboxylic acid (**2i**) provided the aryl esters **3ag**, **3ah** and **3ai** in low to moderate yields. Less bulky primary alkyl carboxylic acids such as propionic acid (**2j**), isopentanoic acid

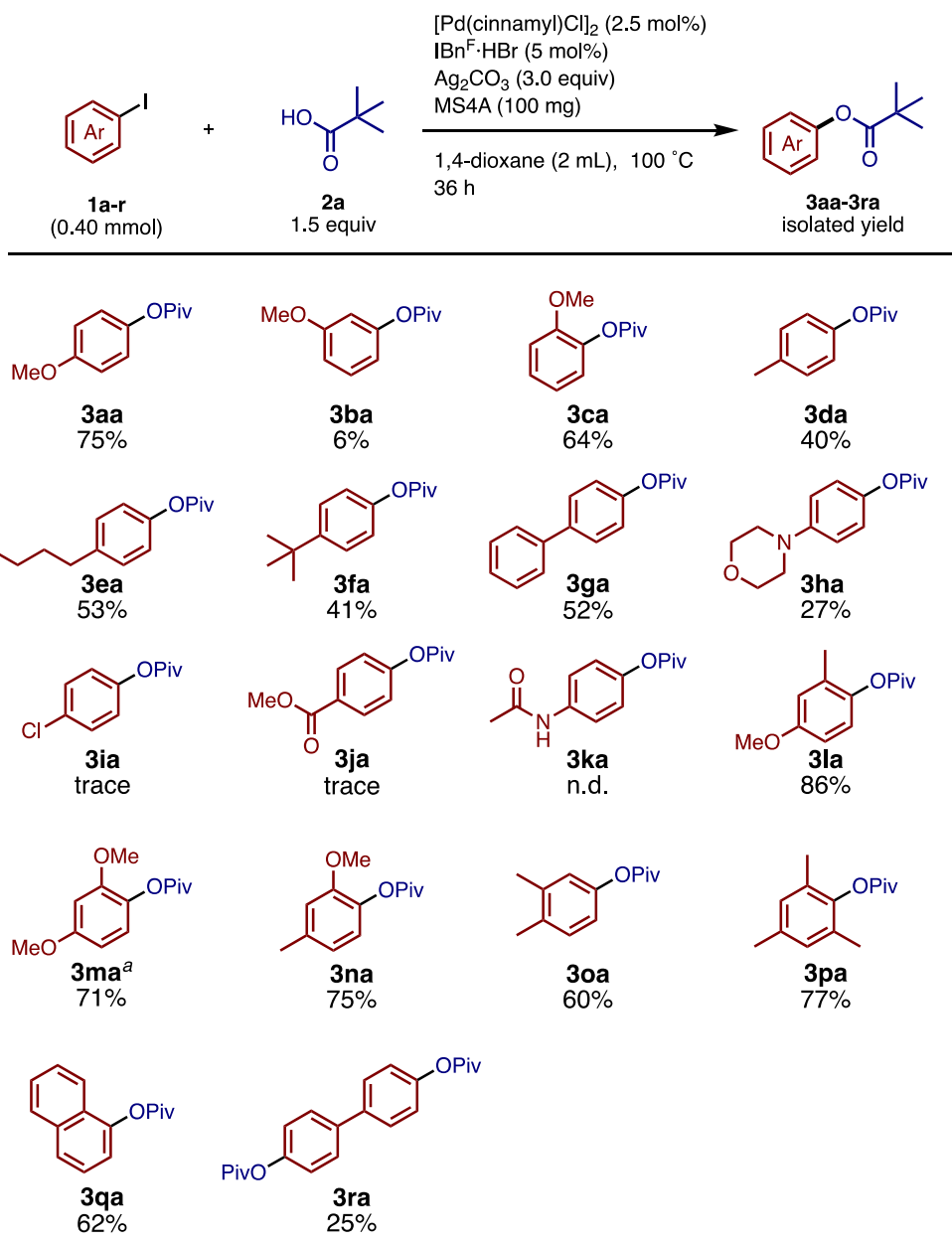
(**2k**) and nonanoic acid (**2l**) carboxylic acids resulted in low yields of product **3aj**, **3ak** and **3al** (8–26%). While benzoic acid (**2m**) did not furnish the ester **3am**, the use of 2,4,6-trimethyl benzoic acid (**2n**) gave the corresponding ester **3an** in moderate yield. These results also suggest that the steric hinderance around the carboxylic acid facilitated the esterification reaction. Notably, over 71% conversions of **1a** were observed in the reaction using **2a–2l** and **2n**, while the reaction with **2m** resulted in the only 14% conversion of **1a**. In addition, the stabilities of bulkier ester **3aa** and less bulky **3aj** were also evaluated by estimating the conversions under the standard reaction conditions in the absence of iodoarenes. As a result, almost no conversion of esters was observed. These results suggest that the reason for high/low yield of esters is not mainly attributed to their stabilities under the present reaction conditions.



Scheme 10. Substrate scope of carboxylic acids **2** in esterification with 4-iodoanisole **1a**.

The substrate scope of aryl iodides was also investigated (Scheme 11). *p*-Methoxy (**1a**) and *o*-methoxy (**1c**) substituted phenyl iodides can participate in the present coupling reaction, but *m*-methoxyphenyl iodide (**1b**) gave the corresponding product **3ba** in quite low yield albeit the almost all **1b** was consumed, likely owing to the inductive effect of *meta*-methoxyl group. The reactions with other *para*-substituted iodobenzenes such as 1-iodo-4-methylbenzene (**1d**), 1-*n*-butyl-4-iodobenzene (**1e**), 1-*tert*-butyl-4-iodobenzene (**1f**), and 4-iodo-1,1'-biphenyl (**1g**) afforded the corresponding esters **3da**, **3ea**, **3fa** and **3ga** in moderate yields. The reaction with 4-

(4-iodophenyl)morpholine (**1h**) resulted in low yield of the product **3ha** (27%). However, iodobenzenes having electron deficient *para*-substituents such as chloro, methoxycarbonyl and acetoamido groups (**1i**, **1j** and **1k**) did not provide the products. In these reactions, 14%, 70% and 77% of **1i**, **1j** and **1k** remained unreacted after reactions, respectively. Multi-substituted and electron-rich aryl iodides such as 1-iodo-4-methoxy-2-methylbenzene (**1l**), 1-iodo-2,4-dimethoxybenzene (**1m**), 1-iodo-2-methoxy-4-methylbenzene (**1n**), 1-iodo-3,4-dimethyliodobenzene (**1o**) and mesityl iodide (**1p**) worked well to afford the corresponding products **3la**, **3ma**, **3na**, **3oa**, and **3pa** (60–86%). These results suggest that both electron density of the benzene ring and the steric hindrance around an iodine atom are the key factors for the reaction efficacy. Indeed, the reaction with 1-iodonaphthalene (**1q**), whose iodine atom is hindered by a hydrogen atom on the *peri*-position, afforded the ester **3qa** in a good yield (62%). Furthermore, double esterification with 4,4'-diiodobiphenyl (**1r**) gave the corresponding ester **3ra** in 25%, whose value is comparable to the yield found in the single esterification forming **3ga**.

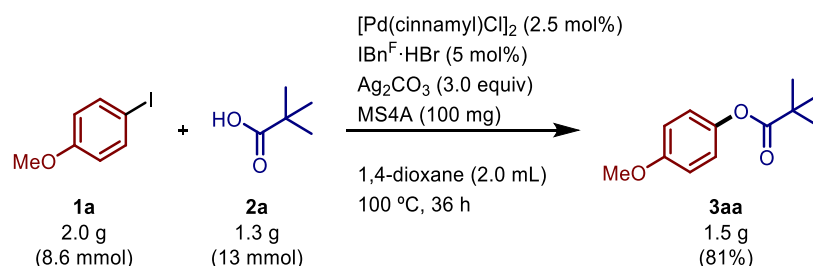


^aReaction time 42 h

Scheme 11. Substrate scope of Aryl iodides **1** in esterification with pivalic acid **2a**.

2-3. Gram-scale synthesis

A gram-scale synthesis was examined using 2.0 g (8.6 mmol) of 4-iodoanisole (**1a**) and 1.3 g (13 mmol) of pivalic acid (**2a**) under optimal reaction conditions (Scheme 12). As a result, the esterification reaction successfully worked to afford 4-methoxyphenyl pivalate (**3aa**) in 81% yield (1.5 g of product).



Scheme 12. Gram-scale synthesis of aryl ester **3aa**.

The proposed reaction mechanism is shown in Figure 4. First, $[\text{PdCl}(\text{cinnamyl})]_2$ and $\text{IBn}^{\text{F}}\cdot\text{HBr}$ would easily form $[\text{Pd}^{\text{II}}\text{Cl}(\text{cinnamyl})(\text{IBn}^{\text{F}})]$ by Ag_2CO_3 or *in situ*-generated AgOPiv , and then $\text{Pd}^0\text{-IBn}^{\text{F}}$ complex **4** can form through the formal reductive elimination of cinnamyl chloride.¹⁴ Next, the oxidative addition of 4-iodoanisole (**1a**) to **4** can occur to form a aryl-Pd(II) complex **5**, which undergoes the anion exchanging with *in situ*-generated AgOPiv to form aryl palladium(II) pivalate **6**. Finally, the reductive elimination of aryl pivalate **3aa** can occur along with the regeneration of $\text{Pd}^0\text{-IBn}^{\text{F}}$ complex **4**. The higher reactivities found in the reaction of electron-rich iodoarenes (**1a**, **1c**, **1l**, **1m** and **1p**) and carboxylic acids (**2a-2e** and **2n**) support that the reductive elimination step can be possible rate-determining step in the current catalytic system. While the ligand effect by IBn^{F} was not unclear at this stage, the author envisages that the electron-deficient NHC ligand can facilitate the rate-limiting reductive elimination step which includes the difficult $\text{C}_{\text{aryl}}\text{-O}_{\text{acyl}}$ bond formation.

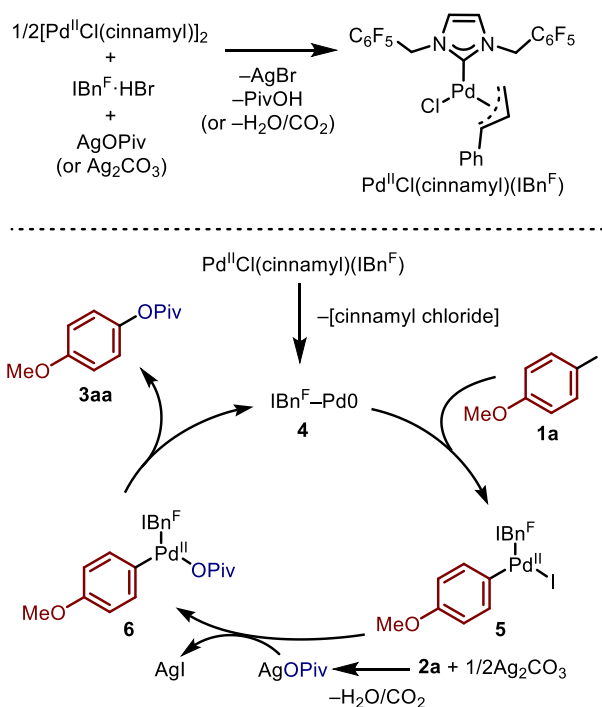


Figure 4. Proposed catalytic mechanism on esterification of 4-iodoanisole **1a** with pivalic acid **2a**.

3. Conclusion

In summary, the palladium-catalyzed esterification reaction of carboxylic acids with aryl iodides was developed for the first time as a palladium catalytic system. Electron-rich aryl iodides showed good reactivity to this reaction even in the gram-scale synthesis. Sterically hindered aryl iodides and carboxylic acids were well tolerated to furnish the corresponding aryl esters in good yields. The discovery demonstrated the potential of palladium/electron deficient NHC catalysis in $\text{C}_{\text{aryl}}\text{-O}$ bond formation, and thus contributed to the development of palladium-based chemical transformation.¹⁵

Experimental Section

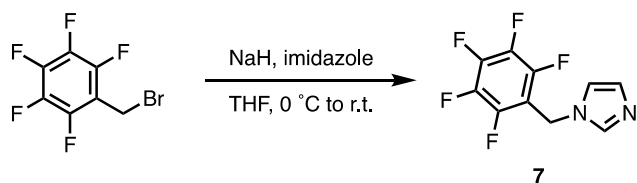
1. General

Unless otherwise noted, all reactants or reagents including dry solvents were obtained from commercial suppliers and used as received. $[\text{Pd}(\text{cinnamyl})\text{Cl}]_2$ was obtained from Aldrich. Pivalic acid was purchased from TCI. Ag_2CO_3 was purchased from WAKO. MS4A was purchased from Nakalai Chemicals. AgOPiv^{16} , 1-iodo-4-methoxy-2-methylbenzene (**2i**)¹⁷, 1-iodo-2-methoxy-4-methylbenzene (**2n**)¹⁷ and $\text{IBn}\cdot\text{HBr}^{18}$ were synthesized according to procedures reported in the literature. Unless otherwise noted, all reactions were performed with dry solvents under air. All work-up and purification procedures were carried out with reagent-grade solvents in air.

Analytical thin-layer chromatography (TLC) was performed using E. Merck silica gel 60 F₂₅₄ precoated plates (0.25 mm). The developed chromatogram was analyzed by UV lamp (254 nm). Medium Pressure liquid chromatography (MPLC) was performed using Yamazen W-prep 2XY. Preparative thin-layer chromatography (PTLC) was performed using Wakogel B5-F silica coated plates (0.75 mm) prepared in our laboratory. Preparative gel permeation chromatography (GPC) was performed with a JAI LC-9204 instrument equipped with JAIGEL-1H/JAIGEL-2H columns using chloroform as an eluent. Gas chromatography (GC) analysis was conducted on a Shimadzu GC-2010 instrument equipped with a HP-5 column (30 m × 0.25 mm, Hewlett-Packard) with dodecane as an internal standard. The high-resolution mass spectra (HRMS) were conducted on Thermo Fisher Scientific Exactive. Nuclear magnetic resonance (NMR) spectra were recorded on a JEOL JNM-ECA-600 (¹H 600 MHz, ¹³C 150 MHz) spectrometer and a JEOL JNM-ECA-400 (¹H 400 MHz, ¹³C 100 MHz) spectrometer. Chemical shifts for ¹H NMR are expressed in parts per million (ppm) relative to tetramethylsilane (δ 0.00 ppm) or residual peak of acetone-*d*₆ (δ 2.05 ppm). Chemical shifts for ¹³C NMR are expressed in ppm relative to CDCl_3 (δ 77.0 ppm) or acetone-*d*₆ (δ 29.84 ppm). Data are reported as follows: chemical shift, multiplicity (s = singlet, d = doublet, dd = doublet of doublets, ddd = doublet of doublets of doublets, t = triplet, dt = doublet of triplets, td = triplet of doublets, q = quartet, p = quintet, m = multiplet, br d = broad doublet), coupling constant (Hz), and integration.

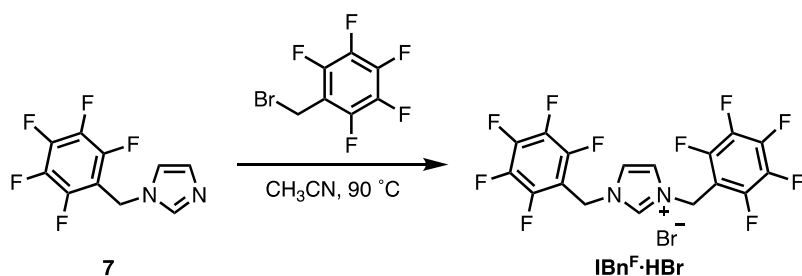
2. Synthesis of 1,3-Bis((pentafluorophenyl)methyl)-1*H*-imidazol-3-ium bromide (IBn^F·HBr)

2-1. Synthesis of 1-((pentafluorophenyl)methyl)-1*H*-imidazole (7)



Imidazole (2.9 g, 42 mmol, 1.1 equiv) was placed in a 200-mL round-bottomed flask under a stream of N₂, and THF (40 mL) was added to the flask. After cooled to 0 °C, NaH (60% dispersion in paraffin liquid: 1.6 g, 40 mmol, 1.1 equiv) was added, and then the mixture was warmed to room temperature and stirred for 1 h. To this mixture, pentafluorobenzyl bromide (10 g, 38 mmol, 1.0 equiv) was added dropwise, and then the mixture was stirred for additional 4 h. The reaction was quenched by the addition of water. The organic layer was extracted with EtOAc, washed with water and brine, dried over Na₂SO₄, and then filtered. The filtrate was concentrated *in vacuo*. The crude residue was purified by MPLC (chloroform/EtOAc = 1:0 to 1:1) to afford **7** as a colorless liquid (7.2 g, 76% yield). ¹H NMR (600 MHz, CDCl₃) δ 7.59 (s, 1 H), 7.04 (s, 1H), 6.98 (s, 1H), 5.23 (s, 2H). ¹³C NMR (150 MHz, CDCl₃) δ 145.0 (d, *J* = 253 Hz), 141.7 (d, *J* = 252 Hz), 137.5 (d, *J* = 255 Hz), 137.0, 130.0, 118.7, 109.9 (t, *J* = 18 Hz), 37.2. HRMS (ESI⁺) *m/z* calcd for C₁₀H₆F₅N₂ [M+H]⁺: 249.0446, found: 249.0441.

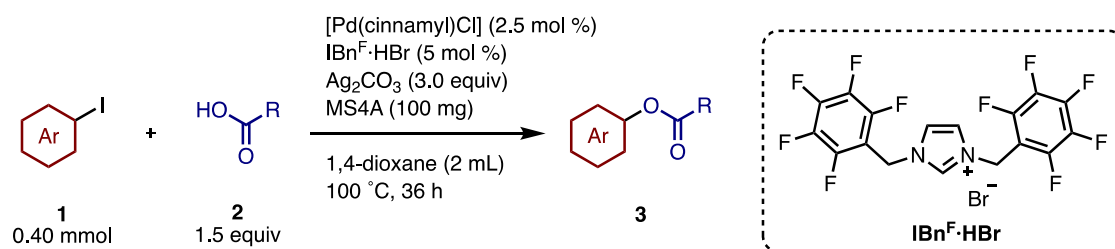
2-2. Synthesis of 1,3-Bis((pentafluorophenyl)methyl)-1*H*-imidazol-3-ium bromide (IBn^F·HBr)



To a 200-mL glass vessel equipped with a J. Young[®] O-ring tap containing a magnetic stirring bar were added 1-((pentafluorophenyl)methyl)-1*H*-imidazole **7** (6.0 g, 24 mmol, 1.0 equiv) and acetonitrile (24 mL). To this mixture, pentafluorobenzyl bromide (8.2 g, 31 mmol, 1.3 equiv) was added. Then the mixture was heated at 90 °C and stirred for 20 h. After cooled to room temperature, the mixture was concentrated and the residue was purified by recrystallization from acetonitrile to afford IBn^F·HBr as a white solid (8.7 g, 71% yield). ¹H NMR (600 MHz, acetone-

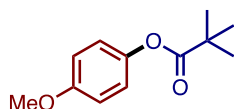
d_6) δ 10.74 (s, 1H), 8.02 (s, 2H), 5.99 (s, 4H). ^{13}C NMR (150 MHz, acetone- d_6) δ 146.8 (d, J = 248 Hz), 143.1 (d, J = 249 Hz), 139.5, 138.8 (d, J = 237 Hz), 123.8, 108.8, 41.6. HRMS (ESI $^+$) m/z calcd for $\text{C}_{17}\text{H}_7\text{F}_{10}\text{N}_2$ $[\text{M}]^+$: 429.0444, found: 429.0443.

3. Pd-Catalyzed Esterification of Carboxylic acids with Aryl iodides



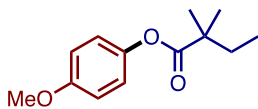
General Procedure: To a screw-capped glass tube containing a magnetic stirrer bar were added iodoarene **1a–1r** (0.40 mmol, 1.0 equiv), carboxylic acid **2a–2n** (0.60 mmol, 1.5 equiv), Ag_2CO_3 (1.2 mmol, 3.0 equiv), MS4A (0.10 g), $[\text{Pd}(\text{cinnamyl})\text{Cl}]_2$ (0.010 mmol, 2.5 mol%), 1,3-bis((pentafluorophenyl)methyl)-1*H*-imidazol-3-ium bromide ($\text{IBn}^{\text{F}}\cdot\text{HBr}$) (0.020 mmol, 5.0 mol%) and 1,4-dioxane (2.0 mL) under air. After stirring at 100 °C for 36 h, the reaction mixture was cooled to room temperature, and then passed through a short pad of Celite $^{\text{®}}$ (eluent: EtOAc or CHCl_3). After the organic solvent was removed under reduced pressure, the residue was purified by PTLC or MPLC to yield aryl ester **3aa–3ra**.

4-Methoxyphenyl pivalate (**3aa**)



Purification by MPLC (hexane/EtOAc = 99:1 to 4:1) afforded **3aa** as a pale yellow oil (62 mg, 75% yield). ^1H NMR (600 MHz, CDCl_3) δ 6.96 (d, J = 9.0 Hz, 2H), 6.88 (d, J = 9.0 Hz, 2H), 3.79 (s, 3H), 1.34 (s, 9H). ^{13}C NMR (150 MHz, CDCl_3) δ 177.4, 157.1, 144.6, 122.2, 114.4, 55.8, 39.0, 27.1. HRMS (ESI $^+$) m/z calcd for $\text{C}_{12}\text{H}_{17}\text{O}_3$ $[\text{M}+\text{H}]^+$: 209.1172, found: 209.1172.

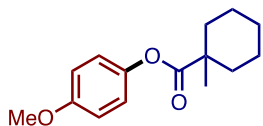
4-Methoxyphenyl 2,2-dimethylbutanoate (**3ab**)



Purification by MPLC (hexane/EtOAc = 49:1 to 4:1) afforded **3ab** as a colorless oil (69 mg, 78% yield). ^1H NMR (600 MHz, CDCl_3) δ 6.96 (d, J = 9.6 Hz, 2H), 6.88 (d, J = 9.6 Hz, 2H), 3.79

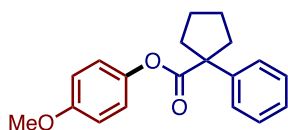
(s, 3H), 1.71 (q, $J = 7.8$ Hz, 2H), 1.29 (s, 6H), 0.96 (t, $J = 7.8$ Hz, 3H). ^{13}C NMR (150 MHz, CDCl_3) δ 176.8, 157.0, 144.5, 122.2, 114.3, 55.5, 42.9, 33.4, 24.6, 9.3. HRMS (ESI⁺) m/z calcd for $\text{C}_{13}\text{H}_{19}\text{O}_3$ [M+H]⁺: 223.1329, found: 223.1329.

4-Methoxyphenyl 1-methylcyclohexane-1-carboxylate (**3ac**)



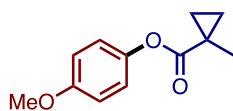
Purification by MPLC (hexane/EtOAc = 49:1 to 4:1) afforded **3ac** as a colorless oil (68 mg, 69% yield). ^1H NMR (600 MHz, CDCl_3) δ 6.96 (d, $J = 9.0$ Hz, 2H), 6.88 (d, $J = 9.0$ Hz, 2H), 3.79 (s, 3H), 2.17 (br d, $J = 7.2$ Hz, 2H), 1.67–1.55 (m, 3H), 1.52–1.43 (m, 2H), 1.36–1.29 (m, 6H). ^{13}C NMR (150 MHz, CDCl_3) δ 176.7, 157.0, 144.5, 122.3, 114.4, 55.6, 43.4, 35.6, 26.4, 25.7, 23.2. HRMS (ESI⁺) m/z calcd for $\text{C}_{15}\text{H}_{21}\text{O}_3$ [M+H]⁺: 249.1485, found: 249.1484.

4-Methoxyphenyl 1-phenylcyclopentane-1-carboxylate (**3ad**)



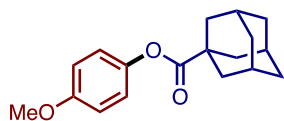
Purification by MPLC (hexane/EtOAc = 49:1 to 4:1) afforded **3ad** as a colorless oil (70 mg, 59% yield). ^1H NMR (600 MHz, CDCl_3) δ 7.49–7.45 (m, 2H), 7.38–7.33 (m, 2H), 7.29–7.25 (m, 1H), 6.81 (s, 4H), 3.75 (s, 3H), 2.82–2.76 (m, 2H), 2.06–1.99 (m, 2H), 1.86–1.80 (m, 4H). ^{13}C NMR (150 MHz, CDCl_3) δ 174.9, 157.1, 144.6, 142.8, 128.4, 126.9, 126.8, 122.0, 114.3, 59.3, 55.5, 36.1, 23.6. HRMS (ESI⁺) m/z calcd for $\text{C}_{19}\text{H}_{21}\text{O}_3$ [M+H]⁺: 297.1485, found: 297.1484.

4-Methoxyphenyl 1-methylcyclopropane-1-carboxylate (**3ae**)



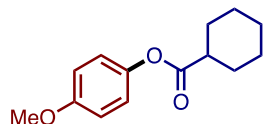
Purification by MPLC (hexane/EtOAc = 49:1 to 4:1) afforded **3ae** as a colorless oil (40 mg, 49% yield). ^1H NMR (600 MHz, CDCl_3) δ 6.97 (d, $J = 9.0$ Hz, 2H), 6.86 (d, $J = 9.0$ Hz, 2H), 3.78 (s, 3H), 1.43–1.38 (m, 5H), 0.83–0.79 (m, 2H). ^{13}C NMR (150 MHz, CDCl_3) δ 174.9, 157.0, 144.4, 122.2, 114.3, 55.5, 19.4, 18.7, 17.3. HRMS (ESI⁺) m/z calcd for $\text{C}_{12}\text{H}_{15}\text{O}_3$ [M+H]⁺: 207.1016, found: 207.1017.

4-Methoxyphenyl (3*r*,5*r*,7*r*)-adamantane-1-carboxylate (**3af**)



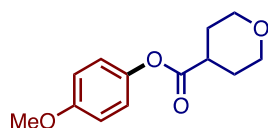
Purification by MPLC (hexane/EtOAc = 49:1 to 4:1) and PTLC (hexane/chloroform = 1:1) afforded **3af** as a colorless oil (11 mg, 10% yield). ¹H NMR (600 MHz, CDCl₃) δ 6.95 (d, *J* = 9.0 Hz, 2H), 6.87 (d, *J* = 9.0 Hz, 2H), 3.79 (s, 3H), 2.15–2.02 (m, 9H), 1.85–1.73 (m, 6H). ¹³C NMR (150 MHz, CDCl₃) δ 176.5, 157.0, 144.5, 122.3, 114.3, 55.6, 40.9, 38.8, 36.5, 27.9. HRMS (ESI⁺) *m/z* calcd for C₁₈H₂₃O₃ [M+H]⁺: 287.1642, found: 287.1641.

4-Methoxyphenyl cyclohexanecarboxylate (**3ag**)



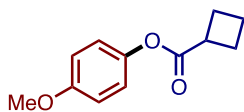
Purification by MPLC (hexane/EtOAc = 49:1 to 4:1) and PTLC (hexane/chloroform = 1:1) afforded **3ag** as a colorless oil (23 mg, 24% yield). ¹H NMR (600 MHz, CDCl₃) δ 6.97 (d, *J* = 9.0 Hz, 2H), 6.87 (d, *J* = 9.0 Hz, 2H), 3.79 (s, 3H), 2.55–2.50 (m, 1H), 2.08–2.02 (m, 2H), 1.84–1.78 (m, 2H), 1.71–1.65 (m, 1H), 1.62–1.53 (m, 2H), 1.39–1.23 (m, 3H). ¹³C NMR (150 MHz, CDCl₃) δ 174.9, 157.1, 144.3, 122.2, 114.3, 55.5, 43.1, 28.9, 25.7, 25.3. HRMS (ESI⁺) *m/z* calcd for C₁₄H₁₉O₃ [M+H]⁺: 235.1329, found: 235.1329.

4-Methoxyphenyl tetrahydro-2*H*-pyran-4-carboxylate (**3ah**)



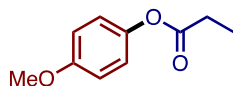
Purification by MPLC (hexane/EtOAc = 49:1 to 2:1) afforded **3ah** as a yellow oil (39 mg, 41% yield). ¹H NMR (600 MHz, CDCl₃) δ 6.98 (d, *J* = 9.0 Hz, 2H), 6.89 (d, *J* = 9.0 Hz, 2H), 4.02 (dt, *J* = 12.0, 3.6 Hz, 2H), 3.80 (s, 3H), 3.50 (td, *J* = 11.4, 2.4 Hz, 2H), 2.82–2.75 (m, 1H), 2.02–1.87 (m, 4H). ¹³C NMR (150 MHz, CDCl₃) δ 173.3, 157.2, 144.1, 122.1, 114.4, 67.0, 55.6, 40.1, 28.6. HRMS (ESI⁺) *m/z* calcd for C₁₃H₁₆O₄Na [M+Na]⁺: 259.0941, found: 259.0940.

4-Methoxyphenyl cyclobutanecarboxylate (**3ai**)



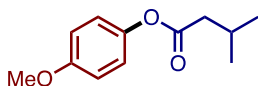
Purification by MPLC (hexane/EtOAc = 49:1 to 4:1) afforded **3ai** as a colorless oil (36 mg, 44% yield). ¹H NMR (600 MHz, CDCl₃) δ 6.99 (d, *J* = 9.0 Hz, 2H), 6.88 (d, *J* = 9.0 Hz, 2H), 3.79 (s, 3H), 3.36 (quint, *J* = 9.0 Hz, 1H), 2.46–2.38 (m, 2H), 2.34–2.27 (m, 2H), 2.09–1.93 (m, 2H). ¹³C NMR (150 MHz, CDCl₃) δ 174.3, 157.1, 144.3, 122.2, 114.3, 55.5, 38.0, 25.3, 18.4. HRMS (ESI⁺) *m/z* calcd for C₁₂H₁₅O₃ [M+H]⁺: 207.1016, found: 207.1016.

4-Methoxyphenyl propionate (**3aj**)



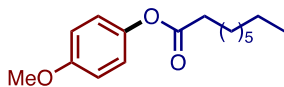
Purification by MPLC (hexane/EtOAc = 49:1 to 4:1) afforded **3aj** as a colorless oil (19 mg, 26% yield). ¹H NMR (600 MHz, CDCl₃) δ 6.99 (d, *J* = 9.0 Hz, 2H), 6.88 (d, *J* = 9.0 Hz, 2H), 3.79 (s, 3H), 2.57 (q, *J* = 7.8 Hz, 2H), 1.26 (t, *J* = 7.8 Hz, 3H). ¹³C NMR (150 MHz, CDCl₃) δ 173.4, 157.1, 144.2, 122.3, 114.4, 55.6, 27.7, 9.1. HRMS (ESI⁺) *m/z* calcd for C₁₀H₁₂O₃Na [M+Na]⁺: 203.0679, found: 203.0679.

4-Methoxyphenyl 3-methylbutanoate (**3ak**)



Purification by MPLC (hexane/EtOAc = 49:1 to 4:1) and PTLC (hexane/chloroform = 1:1) afforded **3ak** as a colorless oil (7 mg, 8% yield). ¹H NMR (600 MHz, CDCl₃) δ 6.99 (d, *J* = 9.0 Hz, 2H), 6.88 (d, *J* = 9.0 Hz, 2H), 3.80 (s, 3H), 2.41 (d, *J* = 7.2 Hz, 2H), 2.28–2.22 (m, 1H), 1.05 (d, *J* = 6.6 Hz, 6H). ¹³C NMR (150 MHz, CDCl₃) δ 172.0, 157.2, 144.2, 122.3, 114.4, 55.6, 43.3, 25.9, 22.4. HRMS (ESI⁺) *m/z* calcd for C₁₂H₁₇O₃ [M+H]⁺: 209.1172, found: 209.1173.

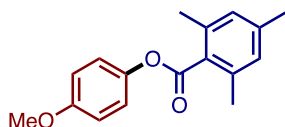
4-Methoxyphenyl nonanoate (**3al**)



Purification by MPLC (hexane/EtOAc = 49:1 to 4:1) and PTLC (hexane/chloroform = 1:1) afforded **3al** as a colorless oil (11 mg, 10% yield). ¹H NMR (600 MHz, CDCl₃) δ 6.99 (d, *J* = 9.0

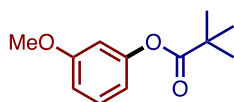
Hz, 2H), 6.88 (d, $J = 9.0$ Hz, 2H), 3.80 (s, 3H), 2.53 (t, $J = 7.8$ Hz, 2H), 1.77–1.71 (m, 2H), 1.43–1.23 (m, 10H), 0.89 (t, $J = 7.2$ Hz, 3H). ^{13}C NMR (150 MHz, CDCl_3) δ 172.7, 157.1, 144.2, 122.3, 114.4, 55.6, 34.3, 31.8, 29.2, 29.1 (2C), 25.0, 22.6, 14.1. HRMS (ESI $^+$) m/z calcd for $\text{C}_{16}\text{H}_{25}\text{O}_3$ $[\text{M}+\text{H}]^+$: 265.1798, found: 265.1799.

4-Methoxyphenyl 2,4,6-trimethylbenzoate (**3an**)



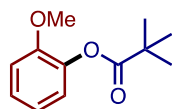
Purification by MPLC (hexane/EtOAc = 49:1 to 2:1) afforded **3an** as a white solid (45 mg, 42% yield). ^1H NMR (600 MHz, CDCl_3) δ 7.14 (d, $J = 9.0$ Hz, 2H), 6.94 (d, $J = 9.0$ Hz, 2H), 6.91 (s, 2H), 3.81 (s, 3H), 2.44 (s, 6H), 2.31 (s, 3H). ^{13}C NMR (150 MHz, CDCl_3) δ 168.8, 157.4, 144.2, 139.8, 135.5, 130.1, 128.6, 122.3, 114.6, 55.6, 21.1, 19.9. HRMS (ESI $^+$) m/z calcd for $\text{C}_{17}\text{H}_{19}\text{O}_3$ $[\text{M}+\text{H}]^+$: 271.1329, found: 271.1329.

3-Methoxyphenyl pivalate (**3ba**)



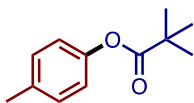
Purification by PTLC (hexane/EtOAc = 49:1 to 4:1) and GPC afforded **3ba** as a colorless oil (5 mg, 6% yield). ^1H NMR (600 MHz, CDCl_3) δ 7.25 (t, $J = 8.4$ Hz, 1H), 6.76 (ddd, $J = 8.4, 2.4, 0.6$ Hz, 1H), 6.64 (ddd, $J = 8.4, 2.4, 0.6$ Hz, 1H), 6.59 (t, $J = 2.4$ Hz, 1H), 3.79 (s, 3H), 1.34 (s, 9H). ^{13}C NMR (100 MHz, CDCl_3) δ 177.0, 160.5, 152.1, 129.7, 113.7, 111.5, 107.4, 55.4, 39.1, 27.1. HRMS (ESI $^+$) m/z calcd for $\text{C}_{12}\text{H}_{17}\text{O}_3$ $[\text{M}+\text{H}]^+$: 209.1172, found: 209.1173.

2-Methoxyphenyl pivalate (**3ca**)



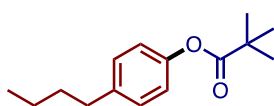
Purification by MPLC (hexane/EtOAc = 49:1 to 4:1) afforded **3ca** as a colorless oil (53 mg, 64% yield). ^1H NMR (600 MHz, CDCl_3) δ 7.18 (ddd, $J = 8.4, 7.8, 1.8$ Hz, 1H), 7.00 (dd, $J = 7.8, 1.8$ Hz), 6.97–6.91 (m, 2H), 3.80 (s, 3H), 1.37 (s, 9H). ^{13}C NMR (150 MHz, CDCl_3) δ 176.7, 151.2, 140.2, 126.5, 122.7, 120.7, 112.4, 55.9, 39.0, 27.2. HRMS (ESI $^+$) m/z calcd for $\text{C}_{12}\text{H}_{17}\text{O}_3$ $[\text{M}+\text{H}]^+$: 209.1172, found: 209.1173.

p-Tolyl pivalate (**3da**)



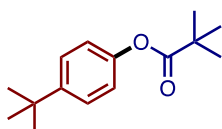
Purification by MPLC (hexane/EtOAc = 49:1 to 4:1) afforded **3da** as a pale yellow oil (31 mg, 40% yield). ¹H NMR (400 MHz, CDCl₃) δ 7.16 (d, *J* = 8.8 Hz, 2H), 6.93 (d, *J* = 8.8 Hz, 2H), 2.34 (s, 3H), 1.35 (s, 9H). ¹³C NMR (150 MHz, CDCl₃) δ 177.3, 148.8, 135.1, 129.8, 121.1, 39.0, 27.1, 20.8. HRMS (ESI⁺) *m/z* calcd for C₁₂H₁₆O₂Na [M+Na]⁺: 215.1043, found: 215.1042.

4-Butylphenyl pivalate (**3ea**)



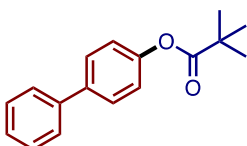
Purification by MPLC (hexane/EtOAc = 49:1 to 4:1) afforded **3ea** as a pale yellow oil (50 mg, 53% yield). ¹H NMR (400 MHz, CDCl₃) δ 7.16 (d, *J* = 8.4 Hz, 2H), 6.95 (d, *J* = 8.4 Hz, 2H), 2.59 (t, *J* = 8.0 Hz, 2H), 1.63–1.53 (m, 2H), 1.40–1.29 (m, 11H), 0.92 (t, *J* = 8.0 Hz, 3H). ¹³C NMR (150 MHz, CDCl₃) δ 177.2, 148.9, 140.1, 129.2, 121.0, 39.0, 35.0, 33.6, 27.1, 22.3, 13.9. HRMS (ESI⁺) *m/z* calcd for C₁₅H₂₃O₂ [M+H]⁺: 235.1693, found: 235.1693.

4-(*tert*-Butyl)phenyl pivalate (**3fa**)



Purification by MPLC (hexane/EtOAc = 49:1 to 4:1) afforded **3fa** as a pale yellow solid (39 mg, 41% yield). ¹H NMR (400 MHz, CDCl₃) δ 7.37 (d, *J* = 8.8 Hz, 2H), 6.97 (d, *J* = 8.8 Hz, 2H), 1.35 (s, 9H), 1.31 (s, 9H). ¹³C NMR (150 MHz, CDCl₃) δ 177.2, 148.7, 148.3, 126.2, 120.7, 39.0, 34.4, 31.4, 27.1. HRMS (ESI⁺) *m/z* calcd for C₁₅H₂₃O₂ [M+H]⁺: 235.1693, found: 235.1693.

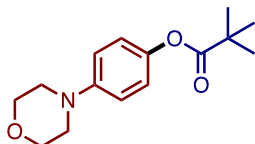
(1,1'-Biphenyl)-4-yl pivalate (**3ga**)



Purification by MPLC (hexane/EtOAc = 9:1 to 6:1) afforded **3ga** as a white solid (53 mg, 52% yield). ¹H NMR (600 MHz, CDCl₃) δ 7.62–7.54 (m, 4H), 7.43 (t, *J* = 7.8 Hz, 2H), 7.36–7.32 (m, 1H), 7.13 (d, *J* = 7.8 Hz, 2H), 1.38 (s, 9H). ¹³C NMR (150 MHz, CDCl₃) δ 177.1, 150.5, 140.4,

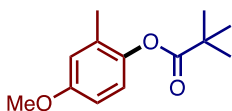
138.7, 128.7, 128.1, 127.3, 127.1, 121.7, 39.1, 27.1. HRMS (ESI⁺) *m/z* calcd for C₁₇H₁₉O₂ [M+H]⁺: 255.1380, found: 255.1380.

4-Morpholinophenyl pivalate (**3ha**)



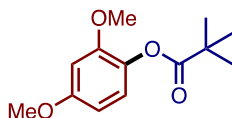
Purification by MPLC (hexane/EtOAc = 49:1 to 4:1) afforded **3ha** as a yellow solid (28 mg, 27% yield). ¹H NMR (600 MHz, CDCl₃) δ 6.96 (d, *J* = 9.6 Hz, 2H), 6.90 (d, *J* = 9.6 Hz, 2H), 3.86 (t, *J* = 4.8 Hz, 4H), 3.12 (t, *J* = 4.8 Hz, 4H), 1.34 (s, 9H). ¹³C NMR (150 MHz, CDCl₃) δ 177.4, 149.1, 144.4, 121.9, 116.6, 66.9, 49.8, 39.0, 27.1. HRMS (ESI⁺) *m/z* calcd for C₁₅H₂₂NO₃ [M+H]⁺: 264.1594, found: 264.1592.

4-Methoxy-2-methylphenyl pivalate (**3la**)



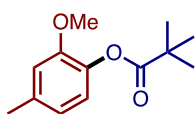
Purification by MPLC (hexane/EtOAc = 49:1 to 4:1) afforded **3la** as a colorless oil (77 mg, 86% yield). ¹H NMR (600 MHz, CDCl₃) δ 6.87 (d, *J* = 9.0 Hz, 1H), 6.74 (d, *J* = 3.0 Hz, 1H), 6.71 (dd, *J* = 9.0, 3.0 Hz, 1H), 3.77 (s, 3H), 2.13 (s, 3H), 1.37 (s, 9H). ¹³C NMR (150 MHz, CDCl₃) δ 177.0, 157.1, 143.1, 131.0, 122.3, 116.2, 111.8, 55.5, 39.1, 27.2, 16.4. HRMS (ESI⁺) *m/z* calcd for C₁₃H₁₉O₃ [M+H]⁺: 223.1329, found: 223.1329.

2,4-Dimethoxyphenyl pivalate (**3ma**)



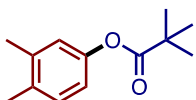
Reaction time: 42 h. Purification by MPLC (chloroform) afforded **3ma** as pale yellow solid (67 mg, 71% yield). ¹H NMR (600 MHz, CDCl₃) δ 6.89 (d, *J* = 8.4 Hz, 1H), 6.52 (d, *J* = 2.4 Hz, 1H), 6.43 (dd, *J* = 8.7, 2.7 Hz, 1H), 3.79 (s, 3H), 3.77 (s, 3H), 1.35 (s, 9H). ¹³C NMR (150 MHz, CDCl₃) δ 177.1, 158.2, 151.8, 134.0, 122.6, 103.8, 100.2, 55.8, 55.6, 39.0, 27.2. HRMS (ESI⁺) *m/z* calcd for C₁₃H₁₉O₄ [M+H]⁺: 239.1278, found: 239.1277.

2-Methoxy-4-methylphenyl pivalate (**3na**)



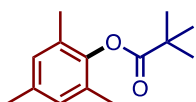
Purification by MPLC (hexane/EtOAc = 49:1 to 4:1) afforded **3na** as a colorless crystal (67 mg, 75% yield). ¹H NMR (600 MHz, CDCl₃) δ 6.86 (d, *J* = 8.4 Hz, 1H), 6.75 (s, 1H), 6.72 (d, *J* = 8.4 Hz, 1H), 3.77 (s, 3H), 2.33 (s, 3H), 1.36 (s, 9H). ¹³C NMR (150 MHz, CDCl₃) δ 176.8, 150.8, 137.9, 136.4, 122.2, 121.1, 113.3, 55.8, 39.0, 27.2, 21.4. HRMS (ESI⁺) *m/z* calcd for C₁₃H₁₉O₃ [M+H]⁺: 223.1329, found: 223.1329.

3,4-Dimethylphenyl pivalate (**3oa**)



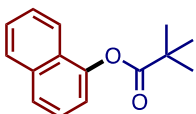
Purification by MPLC (hexane/EtOAc = 49:1 to 4:1) afforded **3oa** as a colorless crystal (50 mg, 60% yield). ¹H NMR (600 MHz, CDCl₃) δ 7.10 (d, *J* = 8.4 Hz, 1H), 6.82 (d, *J* = 2.4 Hz, 1H), 6.77 (dd, *J* = 8.4, 2.4 Hz, 1H), 2.24 (s, 3H), 2.23 (s, 3H), 1.34 (s, 9H). ¹³C NMR (150 MHz, CDCl₃) δ 177.3, 149.0, 137.8, 133.8, 130.2, 122.4, 118.5, 39.0, 27.1, 19.8, 19.1. HRMS (ESI⁺) *m/z* calcd for C₁₃H₁₉O₂ [M+H]⁺: 207.1380, found: 207.1381.

Mesityl pivalate (**3pa**)



Purification by MPLC (hexane/EtOAc = 49:1 to 4:1) afforded **3pa** as a colorless oil (68 mg, 77% yield). ¹H NMR (600 MHz, CDCl₃) δ 6.85 (s, 2H), 2.25 (s, 3H), 2.08 (s, 6H), 1.39 (s, 9H). ¹³C NMR (150 MHz, CDCl₃) δ 176.1, 145.9, 134.9, 129.6, 129.2, 39.2, 27.3, 20.7, 16.2. HRMS (ESI⁺) *m/z* calcd for C₁₄H₂₁O₂ [M+H]⁺: 221.1536, found: 221.1536.

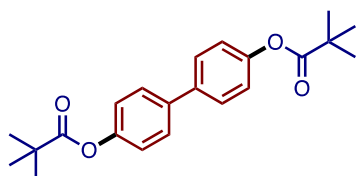
Naphthalen-1-yl pivalate (**3qa**)



Purification by MPLC (hexane/EtOAc = 9:1 to 6:1) afforded **3qa** as a pale yellow oil (56 mg, 62% yield). ¹H NMR (600 MHz, CDCl₃) δ 7.87–7.84 (m, 2H), 7.72 (d, *J* = 8.4 Hz, 1H), 7.53–

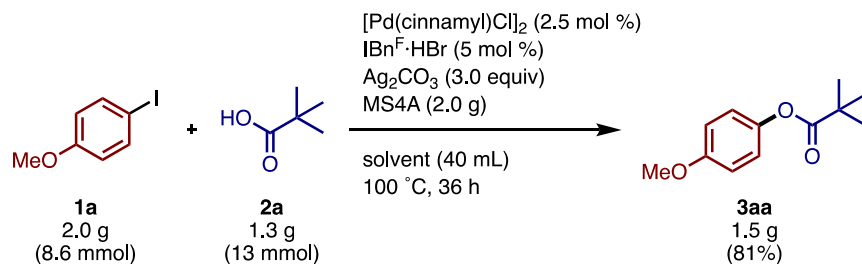
7.43 (m, 3H), 7.20 (dd, $J = 7.2, 1.2$ Hz, 1H), 1.49 (s, 9H). ^{13}C NMR (150 MHz, CDCl_3) δ 177.0, 146.9, 134.6, 128.0, 127.0, 126.35, 126.31, 125.7, 125.4, 121.0, 117.9, 39.5, 27.4. HRMS (ESI⁺) m/z calcd for $\text{C}_{15}\text{H}_{17}\text{O}_2$ $[\text{M}+\text{H}]^+$: 229.1223, found: 229.1223.

(1,1'-Biphenyl)-4,4'-diyl bis(2,2-dimethylpropanoate) (**3ra**)



Purification by MPLC (hexane/EtOAc = 49:1 to 4:1) and PTLC (hexane/EtOAc = 3:1) afforded **3ra** as a white solid (18 mg, 25% yield). ^1H NMR (600 MHz, CDCl_3) δ 7.55 (d, $J = 8.4$ Hz, 4H), 7.12 (d, $J = 8.4$ Hz, 4H), 1.38 (s, 18H). ^{13}C NMR (150 MHz, CDCl_3) δ 177.1, 150.5, 137.9, 128.0, 121.8, 39.1, 27.1. HRMS (ESI⁺) m/z calcd for $\text{C}_{22}\text{H}_{27}\text{O}_4$ $[\text{M}+\text{H}]^+$: 355.1904, found: 355.1904.

4. Gram-scale synthesis of 4-methoxyphenyl pivalate



To a 300-mL round bottom flask containing a magnetic stirrer bar was added MS4A (2.0 g) and dried with a heat gun and filled with N_2 after cooling to room temperature. Then to this vessel were added 4-iodoanisole (**1a**) (2.0 g, 8.6 mmol, 1.0 equiv), pivalic acid (**2a**) (1.3 g, 13 mmol, 1.5 equiv), Ag_2CO_3 (7.1 g, 26 mmol, 3.0 equiv), $[\text{Pd}(\text{cinnamyl})\text{Cl}]_2$ (0.11 g, 0.21 mmol, 2.5 mol%), 1,3-bis((pentafluorophenyl)methyl)-1*H*-imidazol-3-ium bromide (IBn^F·HBr) (0.22 g, 0.43 mmol, 5.0 mol%) and 1,4-dioxane (40 mL). After stirring at 100 °C for 36 h, the reaction mixture was cooled to room temperature, and then passed through a short pad of Celite[®] (eluent: EtOAc). After the organic solvent was removed under reduced pressure, the residue was purified by MPLC (hexane/EtOAc = 1:0 to 4:1) to afford 4-methoxyphenyl pivalate (**3aa**) as a pale yellow oil (1.5 g, 81%).

References and notes

1. (a) Kawabata, K.; Suzuki, M.; Sugitani, M.; Imaki, K.; Toda, M.; Miyamoto, T. *Biochemical and Biophysical Research Communications* **1991**, *177*, 814–820. (b) Binghe Wang; Huijuan Zhang; Wei Wang. *Bioorganic & Medicinal Chemistry Letters* **1996**, *6*, 945–950. (c) Anderson, A.; Belelli, D.; Bennett, D. J.; Buchanan, K. I.; Casula, A.; Cooke, A.; Feilden, H.; Gemmell, D. K.; Hamilton, N. M.; Hutchinson, E. J.; Lambert, J. J.; Maidment, M. S.; McGuire, R.; McPhail, P.; Miller, S.; Muntoni, A.; Peters, J. A.; Sansbury, F. H.; Stevenson, D.; Sundaram, H. *J. Med. Chem.* **2001**, *44*, 3582–3591. (d) Hulsman, N.; Medema, J. P.; Bos, C.; Jongejan, A.; Leurs, R.; Smit, M. J.; de Esch, I. J. P.; Richel, D.; Wijtmans, M. *J. Med. Chem.* **2007**, *50*, 2424–2431. (e) Fang, Y.; Zhang, R.; Shen, Z.; Wu, H.; Tan, C.; Weng, J.; Xu, T.; Liu, X. *Journal of Heterocyclic Chem* **2018**, *55*, 240–245. (f) Warren, J. D.; Miller, J. S.; Keding, S. J.; Danishefsky, S. J. *J. Am. Chem. Soc.* **2004**, *126*, 6576–6578. (g) Li, X.; Lam, H. Y.; Zhang, Y.; Chan, C. K. *Org. Lett.* **2010**, *12*, 1724–1727. (h) Haddleton, D. M.; Waterson, C. *Macromolecules* **1999**, *32*, 8732–8739. (i) Pion, F.; Ducrot, P.; Allais, F. *Macro Chemistry & Physics* **2014**, *215*, 431–439. (j) Nagamitsu, T.; Marumoto, K.; Nagayasu, A.; Fukuda, T.; Arima, S.; Uchida, R.; Ohshiro, T.; Harigaya, Y.; Tomoda, H.; Ōmura, S. *J. Antibiot* **2009**, *62*, 69–74.
2. Selected reviews for prodrugs, see: (a) Liederer, B. M.; Borchardt, R. T. *Journal of Pharmaceutical Sciences* **2006**, *95*, 1177–1195. (b) Rautio, J.; Kumpulainen, H.; Heimbach, T.; Oliyai, R.; Oh, D.; Järvinen, T.; Savolainen, J. *Nat Rev Drug Discov* **2008**, *7*, 255–270. (c) Ferriz, J. M.; Vinsova, J. *Current Pharmaceutical Design* **2010**, *16*, 2033–2052.
3. (a) Campeau, L.-C.; Hazari, N. *Organometallics* **2019**, *38*, 3–35. (b) Yamaguchi, J.; Muto, K.; Itami, K. *Eur J Org Chem* **2013**, *2013*, 19–30. (c) Yu, D.-G.; Li, B.-J.; Shi, Z.-J. *Acc. Chem. Res.* **2010**, *43*, 1486–1495.
4. Quasdorf, K. W.; Tian, X.; Garg, N. K. *J. Am. Chem. Soc.* **2008**, *130*, 14422–14423.
5. Muto, K.; Yamaguchi, J.; Itami, K. *J. Am. Chem. Soc.* **2012**, *134*, 169–172.
6. Selected reviews for conventional ester preparation, see: (a) Otera, Junzo. *Chem. Rev.* **1993**, *93*, 1449–1470. (b) Ishihara, K. *Tetrahedron* **2009**, *65*, 1085–1109. For examples, see: (c) Chakraborti, A. K.; Shivani. *J. Org. Chem.* **2006**, *71*, 5785–5788. (d) Carle, M. S.; Shimokura, G. K.; Murphy, G. K. *Eur J Org Chem* **2016**, *2016* (23), 3930–3933. (e) Tandon, N.; Patil, S. M.; Tandon, R.; Kumar, P. *RSC Adv.* **2021**, *11*, 21291–21300. (f) Yu, W.; Zhou, M.; Wang, T.; He, Z.; Shi, B.; Xu, Y.; Huang, K. *Org. Lett.* **2017**, *19*, 5776–5779
7. For selected review, see: (a) Evano, G.; Blanchard, N.; Toumi, M. *Chem. Rev.* **2008**, *108* (8),

- 3054–3131. (b) Ley, S. V.; Thomas, A. W. *Angew Chem Int Ed* **2003**, *42*, 5400–5449. (c) Ma, D.; Cai, Q. *Acc. Chem. Res.* **2008**, *41* (11), 1450–1460. (d) Zhang, R.; Song, C.; Sui, Z.; Yuan, Y.; Gu, Y.; Chen, C. *The Chemical Record* **2023**, *23*, e202300020 (e) Yang, Q.; Zhao, Y.; Ma, D. *Org. Process Res. Dev.* **2022**, *26*, 1690–1750.
8. (a) Luo, F.; Pan, C.; Qian, P.; Cheng, J. *Synthesis* **2010**, *2010*, 2005–2010. (b) Zhang, L.; Zhang, G.; Zhang, M.; Cheng, J. *J. Org. Chem.* **2010**, *75*, 7472–7474.
9. Dai, J.-J.; Liu, J.-H.; Luo, D.-F.; Liu, L. *Chem. Commun.* **2011**, *47*, 677–679.
10. (a) Krylov, I. B.; Vil', V. A.; Terent'ev, A. O. *Beilstein J. Org. Chem.* **2015**, *11*, 92–146. (b) Moghimi, S.; Mahdavi, M.; Shafiee, A.; Foroumadi, A. *Eur J Org Chem* **2016**, *2016* (20), 3282–3299.
11. (a) Shi, G.; Zhang, Y. *Adv Synth Catal* **2014**, *356*, 1419–1442. (b) Dutta, S.; Bhattacharya, T.; Geffers, F. J.; Bürger, M.; Maiti, D.; Werz, D. B. *Chem. Sci.* **2022**, *13*, 2551–2573.
12. For examples of decomposition of pivalic esters in transition-metal-catalyzed reactions, see: Shimasaki, T.; Tobisu, M.; Chatani, N. *Angew Chem Int Ed* **2010**, *49*, 2929–2932.
13. Welin, E. R.; Le, C.; Arias-Rotondo, D. M.; McCusker, J. K.; MacMillan, D. W. C. *Science* **2017**, *355*, 380–385.
14. For selected review, see: (a) Garrison, J. C.; Youngs, W. J. *Chem. Rev.* **2005**, *105* (11), 3978–4008. (b) Lin, I. J. B.; Vasam, C. S. *Coordination Chemistry Reviews* **2007**, *251*, 642–670. For selected examples, see: (c) Viciu, M. S.; Germaneau, R. F.; Navarro-Fernandez, O.; Stevens, E. D.; Nolan, S. P. *Organometallics* **2002**, *21*, 5470–5472. (d) Simons, R. S.; Custer, P.; Tessier, C. A.; Youngs, W. J. *Organometallics* **2003**, *22*, 1979–1982. (e) Viciu, M. S.; Navarro, O.; Germaneau, R. F.; Kelly, R. A.; Sommer, W.; Marion, N.; Stevens, E. D.; Cavallo, L.; Nolan, S. P. *Organometallics* **2004**, *23*, 1629–1635. (f) Marion, N.; Navarro, O.; Mei, J.; Stevens, E. D.; Scott, N. M.; Nolan, S. P. *J. Am. Chem. Soc.* **2006**, *128*, 4101–4111. (g) Peng, H. M.; Song, G.; Li, Y.; Li, X. *Inorg. Chem.* **2008**, *47*, 8031–8043.
15. (a) Liang, J.-Y.; Shen, S.-J.; Xu, X.-H.; Fu, Y.-L. *Org. Lett.* **2018**, *20*, 6627–6631. (b) Toriumi, N.; Inoue, T.; Iwasawa, N. *J. Am. Chem. Soc.* **2022**, *144*, 19592–19602. (c) Li, L.; Song, F.; Zhong, X.; Wu, Y.; Zhang, X.; Chen, J.; Huang, Y. *Adv Synth Catal* **2020**, *362*, 126–132.
16. Zhu, R.-Y.; He, J.; Wang, X.-C.; Yu, J.-Q. *J. Am. Chem. Soc.* **2014**, *136*, 13194–13197.
17. Perry, G. J. P.; Quibell, J. M.; Panigrahi, A.; Larrosa, I. *J. Am. Chem. Soc.* **2017**, *139*, 11527–11536.
- Chapman, M. R.; Shafi, Y. M.; Kapur, N.; Nguyen, B. N.; Willans, C. E. *Chem. Commun.* **2015**, *51*, 1282–1284.

Conclusion

This thesis describes the development of palladium-catalyzed arylation of C–H and O–H bonds with aryl halides. By exploring the effects of reaction conditions, such as temperature, solvents, ligands, and catalysts, optimal conditions have been identified which allows efficient and selective arylation of C–H and O–H bonds. Furthermore, several synthesized compounds were subjected to analysis to determine their electronic properties or potential physiological activities.

In Chapter 1, palladium-catalyzed C–H arylation reaction of DMB-protected AHX that enables the synthesis of arylated AHX has been developed. Through the developed method and deprotection of DMB groups, a series of non-protected aryl AHXs were synthesized for the first time. Furthermore, some of synthesized arylated AHX derivatives showed stronger growth-promoting activity toward the root of rice compared to mother AHX, the natural plant growth promoter. The discovery of these compounds opens up immense possibilities for their application in agriculture. Understanding the target proteins and a structure activity relationship of these compounds would provide valuable insights into their mode of action, potentially leading to the development of more effective plant growth regulators.

In Chapter 2, palladium-catalyzed one-step annulative π -extension (APEX) reaction of indoles and pyrroles that allows rapid access to N-PACs and N-S-PACs has been developed. By using diiodobiaryl, Ag_2CO_3 and a DMF/DMSO mixed solvent, APEX reaction under milder conditions than the previously reported oxidative conditions was achieved. The developed method allows the convenient and streamlined synthesis of both planar and non-planar π -extended indoles and pyrroles, which are promising candidates for various optoelectronic applications.

In Chapter 3, the first palladium-catalyzed esterification of carboxylic acids with aryl iodides is described. A palladium catalytic system using IBn^{F} , novel NHC ligand, was discovered to significantly enhance the typically challenging aryl–O bond-forming esterification reaction. This discovery highlights the potential of palladium/electron-deficient NHC catalysis in $\text{C}_{\text{aryl}}\text{–O}$ bond formation.

The aryl group is extensively utilized in countless reported molecules. This is largely attributed to the remarkable developments in aryl group introducing reactions. The reactions and transformations discovered by the author had been considered challenging. Similar to the impact brought about by previous innovative reactions, the author has high expectations that these discoveries will contribute to further advancements in the development of related reactions and the exploration of new functional molecules.

List of Publications

(副論文)

1. Discovery of Plant Growth Stimulants by C–H Arylation of 2-Azahypoxanthine
Kitano, H.; Choi, J.-H.; Ueda, A.; Ito, H.; Hagihara, S.; Kan, T.; Kawagishi, H.; Itami, K.
Org. Lett. **2018**, *20*, 5684–5687
2. Annulative π -Extension of Indoles and Pyrroles with Diiodobiaryls by Pd Catalysis: Rapid Synthesis of Nitrogen-Containing Polycyclic Aromatic Compounds
Kitano, H.; Matsuoka, W.; Ito, H.; Itami, K.
Chem. Sci. **2018**, *9*, 7556–7561
3. Palladium-Catalyzed Esterification of Carboxylic Acids with Aryl Iodides
Kitano, H.; Ito, H.; Itami, K.
Org. Lett. **2018**, *20*, 2428–2432

(参考論文)

1. Total Synthesis of Myceliothermophins A–E
Shionozaki, N.; Yamaguchi, T.; Kitano, H.; Tomizawa, M.; Makino, K.; Uchiro, H.
Tetrahedron Letters **2012**, *53*, 5167–5170
2. First Total Synthesis of Oteromycin Utilizing One-Pot Four-Step Cascade Reaction Strategy
Uchiro, H.; Shionozaki, N.; Tanaka, R.; Kitano, H.; Iwamura, N.; Makino, K.
Tetrahedron Letters **2013**, *54*, 506–511
3. Discover of 2,6-Dihalopurines as Stomata Opening Inhibitors: Implication of an LRX-Mediated H⁺-ATPase Phosphorylation Pathway
Ueda, A.; Aihara, Y.; Sato, S.; Kano, K.; Mishiro-Sato, E.; Kitano, H.; Sato, A.; Fujimoto, K. J.; Yanai, T.; Amaike, K.; Kinoshita, T.; Itami, K.
ACS Chem. Biol. **2023**, *18*, 347–355